Vol. 55 • No. 10

October 2012

Microwave Journal

MONITORING RF INTERFERENCE

horizon house®

Founded in 1958

mwjournal.com

MVP
Aeroflex Synthetic ATE

RUGGED & RELIABLE
MADE IN THE USA FOR 50 YEARS!
M*E*C*A* – MICROWAVE ELECTRONIC COMPONENTS OF AMERICA
Aviation
Earth Station
Instrumentation
L, S, C, X, and Ku Bands
Microwave Radio
Mobile Satellite
Radar
Telemetry
MOST MODELS AVAILABLE FROM STOCK - 4 WEEKS ARO
POWER DIVIDERS/ COMBINERS
2-way through 16-way in N, SMA, BNC, TNC and 7/16 DIN connector styles from 0.4 to 18.0 GHz.
ATTENUATORS
Most available in 1 dB increments from 0 - 40dB. Power ratings from 2 to 150 Watts.
RF LOADS
Power ratings from 1 to 500 watts and frequency ranges up to 18 GHz.
DIRECTIONAL & HYBRID COUPLERS
Average power handling from 50W to 1kW. Standard coupling values of 3, 6, 10, 20, 30 and 40 dB.
DC BLOCKS
Available in N, BNC, TNC, SMA & 7/16 DIN configurations . Power ratings to 500 watts (2.5 kW peak).
INTEGRATED ASSEMBLIES
Let MECA create an integrated assembly with any of our standard RF/Microwave products on 19" panels, shelves or enclosures.
BIAS TEES
Covering bands from 0.5 – 2.5 GHz and 0.7 to 2.7 GHz in 7/16 DIN, SMA, N, BNC & TNC configurations with RF power ratings to 300 watts (3 kW peak).
CIRCULATORS & ISOLATORS
In both N & SMA-Female connectors with average power ratings from 2 to 250 watts. "Popular" frequency bands between 0.7 - 18.0 GHz.
MECA
MECA ELECTRONICS, INC.
459 East Main Street Denville, NJ 07834
To learn more, please call 866-444-6322 or visit our website at www.e-MECA.com
MECA
1961-2011

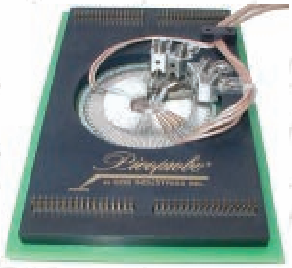

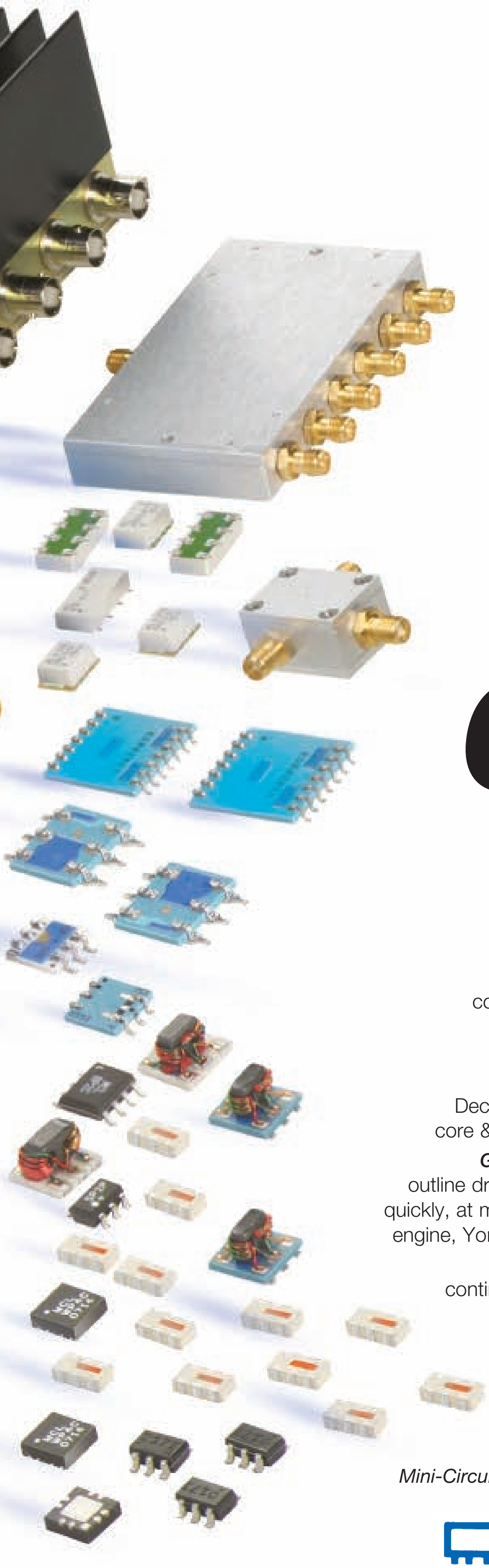

Technology On the Move™

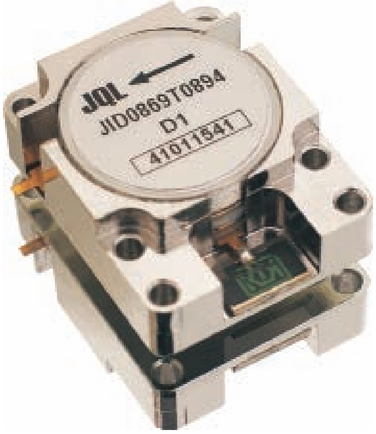

Drop-in Isolators

Cavity Filters

Surface Mount Circulators

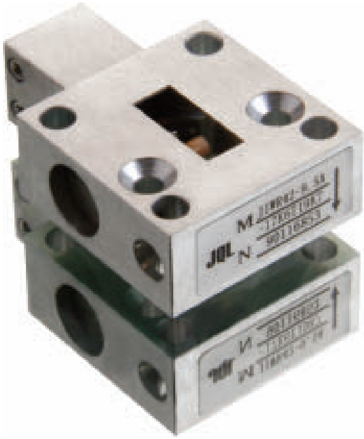

Waveguide Isolators

Power Combiners

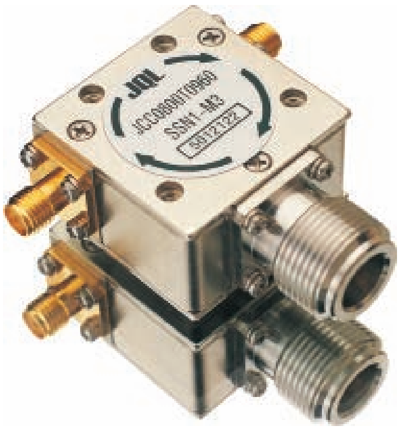

Coaxial Circulators

JQL

Tel:1(888)236-9828(US&Canada)
1(630)930-9917(Worldwide)
www.jqlelectronics.com sales@jqlelectronics.com


“Shut-Up”
is Not a Viable ConOps.
Warfighters must be able to communicate whenever necessary.
The more radios and the closer together they are, the greater the self-generated cosite interference, which drastically reduces communication range.
Pole/Zero purifies each transmission and protects each receiver, allowing your radios to deliver the clarity and range for which they are designed.
Don’t shut-up. Talk to Pole/Zero.
Defeat cosite interference, before it defeats our warfighters.
1.513.870.4087
POLE ZERO
CMP
A DOVER COMPANY
www.polezero.com

Microwave Journal

OCTOBER 2012 VOL. 55 • NO. 10

NOTE FROM THE EDITOR

COVER FEATURE

MVP: MOST VALUABLE PRODUCT

TECHNICAL FEATURES

55 Years of Publishing Excellence

Microwave Journal (USPS 396-250) (ISSN 0192-6225) is published monthly by Horizon House Publications Inc., 685 Canton St., Norwood, MA 02062. Periodicals postage paid at Norwood, MA 02062 and additional mailing offices.

POSTMASTER: Send address corrections to *Microwave Journal*, PO Box 3256, Northbrook, IL 60065-3256 or e-mail mwj@omeda.com. Subscription information: (847) 291-5216. This journal is issued without charge upon written request to qualified persons working in the RF & microwave industry. Other subscriptions are: domestic, $120.00 per year, two-year subscriptions, $185.00; foreign, $200.00 per year, two-year subscriptions, $370.00; back issues (if available) and single copies, $10.00 domestic and $20.00 foreign. Claims for missing issues must be filed within 90 days of date of issue for complimentary replacement.

Posted under Canadian international publications mail agreement #PM40612608

Microwave Journal

Departments

STAFF

Executive Editorial Office:
685 Canton Street, Norwood, MA 02062
Tel: (781) 769-9750
FAX: (781) 769-5037
e-mail: mwj@mwjournal.com

European Editorial Office:
16 Sussex Street, London SW1V 4RW, England
Tel: Editorial: +44 207 596 8730 Sales: +44 207 596 8740
FAX: +44 207 596 8749

www.mwjournal.com

Printed in the USA

Microwave Journal Online

Visit us @ mwjournal.com

Free Webinars

Innovations in EDA
Presented by: Agilent Technologies
Integrated Electro-Thermal Solution Delivers Thermally Aware Circuit Simulation — Available On Demand after 10/4

Agilent in Aerospace/Defense
Using RF Recording Techniques to Resolve Interference Problems — Live webcast: 10/18, 1:00 PM ET

FieldFox Handheld Analyzers
Presented by: Agilent Technologies
Techniques for Precise Cable and Antenna Measurements in the Field — Live webcast: 10/24, 1:00 PM ET

Agilent in LTE
3GPP LTE Standards Update: Release 11, 12 and Beyond — Live webcast: 10/25, 1:00 PM ET

CST Webinar Series 2012
TSV and Interposer: Modeling, Design and Characterization — Available On Demand after 10/4

Combined 3D Electromagnetic and Spin Response Simulation of MRI Systems — Live Webcast: 10/11, 11:00 AM ET

Advanced RCS Analysis of Airborne Vehicles — Live webcast: 10/17, 11:00 AM ET

Automotive PCBs: Efficient Signal and Power Integrity Analysis — Live webcast: 10/25, 11:00 AM ET

Technical Education Training Series
Presented by: Dr. Joey Bray
Sponsored by: Rohde & Schwarz
Radar Fundamentals II – Pulse Doppler Radar — Live webcast: 10/16, 11:00 AM ET

Web Survey

What had the biggest impact on the development of microwave technology?

Look for our multiple choice survey online at mwjournal.com

August Survey

"The Most Important Book on Microwave Engineering is..."

Time-Harmonic Electromagnetic Fields
by Rogers [7 votes] (11%)

Microwave Engineering: Passive Circuits
by Peter Rizzi [6 votes] (10%)

Stripline Circuit Design
by Harlan Howe [4 votes] (7%)

Microwave Circuit Design Using Linear and Non Linear Techniques
by Vendelin, Pavio and Rohde [7 votes] (11%)

Microwave Engineering
by David Pozar [18 votes] (30%)

Microwave Filters, Impedance-Matching, and Coupling Structure
by Matthaei, Young and Jones [19 votes] (31%)

Executive Interview

Barry Phelps, Chairman and CEO of **Empower RF Systems** discusses his company's new products and industry perspective.

White Papers

Signal Integrity: Frequency Range Matters!
Anritsu

What is a Vector Signal Transceiver?
National Instruments

Selecting RF Chip Capacitors for Wireless Applications
Richardson RFPD

Optimize Your RF/Microwave Coaxial Connection
Dave McReynolds, RF Industries

Amplifier Fundamentals Chart
AR RF/Microwave Instrumentation

EuMW Online Show Coverage

MWJ's coverage of the conference and exhibition at this year's European Microwave Week starts October 15th. View the latest new products, demo and interview videos and more at mwjournal.com/eumw2012

COM

NOVEMBER 2012

SUNDAY	MONDAY	TUESDAY	WEDNESDAY	THURSDAY	FRIDAY	SATURDAY
28	29 Coming this month: **Webinar: Networks Analysis** Sponsored by Agilent Technologies	30	31	1	2	3
4	5 **Call for Papers Deadline** PSATS 2013	6 IME2012 November 5-7 China, Shanghai, China	7	8 **Webinar: Synthesis and Tuning of Modern Microwave Filters** (CST)	9	10
11	12	13 electronica 2012, Munich, Germany	14	15 **Webinar: EMC Simulation of Consumer Electronic Devices** (CST); **Webinar: RF Module Design Using Amalfi CMOS PA** Sponsored by Agilent Technologies	16	17
18	19	20 **Besser Webinar: Dividers and Combiners** Sponsored by Mini-Circuits; **Webinar: Multiphysics Approach for a Magnetron and Microwave Oven Design** (CST)	21	22	23	24
25	26	27 **Call for Papers Deadline** SPACOMM 2013	28 **Webinar: Calibration and Alignment Techniques for Precise Field Measurements** Sponsored by Agilent Technologies	29 **Webinar: Simulation of Wearable Antennas for Wireless Communication** (CST)	30	1

Go to: mwjournal.com/events

Coming Events

CALL FOR PAPERS

PSATS 2013
November 5, 2012

SPACOMM 2013
November 27, 2012

IMS 2013
December 10, 2012

WAMICON 2013
December 26, 2012

mwjournal.com

OCTOBER

AMTA 2012
34TH ANNUAL SYMPOSIUM OF THE ANTENNA MEASUREMENT TECHNIQUES ASSOCIATION
October 21–26, 2012 • Bellevue, WA
www.amta.org

RADAR 2012
INTERNATIONAL CONFERENCE ON RADAR
October 22–25, 2012 • Glasgow, UK
www.radar2012.org

EUMW 2012
EUROPEAN MICROWAVE WEEK
October 28–November 2, 2012
Amsterdam, The Netherlands
www.eumweek.com

MILCOM 2012
MILITARY COMMUNICATIONS CONFERENCE
October 29–November 1, 2012 • Orlando, FL
www.milcom.org

4G WORLD 2012
October 29–November 1, 2012 • Chicago, IL
www.4gworld.com

NOVEMBER

IME 2012
7TH INTERNATIONAL CONFERENCE AND EXHIBITION ON MICROWAVE AND ANTENNA
November 5–7, 2012 • Shanghai, China
www.imwexpo.com

ELECTRONICA 2012
November 13–16, 2012 • Munich, Germany
www.electronica.de

DECEMBER

APMC 2012
ASIA PACIFIC MICROWAVE CONFERENCE
December 4–7, 2012 • Kaohsiung, Taiwan
www.apmc2012.com

JANUARY

IEEE RWS 2013
RADIO AND WIRELESS SYMPOSIUM
January 20–23, 2013 • Austin, TX
www.radiowirelessweek.org

IEEE MEMS 2013
26TH IEEE INTERNATIONAL CONFERENCE ON MICRO ELECTRO MECHANICAL SYSTEMS
January 20–24, 2013 • Taipei, Taiwan
www.mems2013.org

FEBRUARY

ISSCC 2013
IEEE INTERNATIONAL SOLID-STATE CIRCUITS CONFERENCE
February 17–21, 2013 • San Francisco, CA
http://isscc.org

NATE 2013
18TH ANNUAL CONFERENCE & EXPOSITION FOR THE NATIONAL ASSOCIATION OF TOWER ERECTORS
February 18–21, 2013 • Fort Worth, TX
http://natehome.com/annual-conference

MWC 2013
MOBILE WORLD CONGRESS
February 25–28, 2013
Barcelona, Spain
www.mobileworldcongress.com

MARCH

ISQED
INTERNATIONAL SYMPOSIUM ON QUALITY ELECTRONIC DESIGN
March 4–6, 2013 • Santa Clara, CA
www.isqed.org

IWCE 2013
INTERNATIONAL WIRELESS COMMUNICATIONS EXPO
March 11–15, 2013 • Las Vegas, NV
www.iwceexpo.com

EDI CON 2013
ELECTRONIC DESIGN INNOVATION CONFERENCE
March 12–14, 2013 • Beijing, China
www.ediconchina.com

SATELLITE 2013
March 18–21, 2013 • Washington D.C.
www.satellitetoday.com/satellite2013

PSATS 2013
5TH INTERNATIONAL CONFERENCE ON PERSONAL SATELLITE SERVICES
March 28–29, 2013 • Toulouse, France
www.psats.eu

APRIL

WAMICON 2013
IEEE WIRELESS AND MICROWAVE TECHNICAL CONFERENCE
April 7–9, 2013 • Orlando, FL
www.wamicon.org

IWS 2013
IEEE INTERNATIONAL WIRELESS SYMPOSIUM
April 13–18, 2013 • Beijing, China
www.iws-ieee.org

SPACOMM 2013
5TH INTERNATIONAL CONFERENCE ON ADVANCES IN SATELLITE AND SPACE COMMUNICATIONS
April 22–26, 2013 • Venice, Italy
www.iaria.org/conferences2013

EDI CON Electronic Design Innovation Conference 电子设计创新会议 2013

EDI CON Technology Matters

In the global marketplace for microwave ideas, technical developments in a few key areas are of particular interest thanks to their potential to transform the status quo. Semiconductor technology is one such area where the higher power densities and wide bandwidth properties of GaN have been creating new opportunities for system integrators from wireless communications to aerospace applications and beyond. Another such area is MIMO and its promise to greatly enhance over-the-air connectivity by enabling true 4G data rates. The adoption of either GaN or MIMO also presents a number of challenges for system integrators, including the accurate characterization of GaN-based power devices and the proper representation of the multi-path channel when testing mobile devices. Such information is necessary for designers to unlock the potential offered by these technologies. In addition to the measurement and simulation tools that will help designers implement and verify such technology, advances in circuit architectures, use of high-speed FPGAs for real-time signal processing, spectrum monitoring and re-use, carrier aggregation, cognitive radio and a host of other research areas will play a significant supporting role in expanding the capabilities of high-frequency based networks.

Many of our field's most exciting technologies were well represented in the paper proposals submitted to the EDI CON technical committee as the deadline approached on August 31st for the first Call for Papers. While the technical committee is currently ranking the proposals for quality, impact, originality, and relevance, the conference organizers sorted the proposals according to subject matter, revealing a few interesting trends. While the bulk of papers came from Chinese engineers working for multi-national companies, individual authors from companies/academia inside and outside China were also among the contributors. Within the design track, papers could be grouped among several sub-categories including: power amplifier design (and most commonly GaN-based Doherty PAs), high-speed oscillators, patch antennas, high-speed interconnects, on- and off-chip (PCB-based) passive components and receivers. Apart from the high-speed, signal- and power-integrity papers, most papers covered areas often represented in *Microwave Journal* throughout the year.

The modeling track received proposals for a range of topics from new methodologies to practical techniques on subjects such as noise figure measurements for microwave and millimeter-wave active devices (frequency- and non-frequency – converting), simulating structures with EM-based software, GaN device modeling, improving VNA measurements for RF and high-speed applications, load-pull for ultra-low impedance devices, high-speed backplane analysis, calibration methodologies and compensation for probes and fixtures used in measurements. Achieving greater accuracy and verification of results were among the themes in a number of proposals. Papers submitted on time- and mixed-domain measurements, over-the-air testing and system-level performance testing, correlation and verification demonstrate the industry's shift toward more complex, higher-level analysis tools.

The system track papers reflect a broad range of topics including wideband 802.11, spectral re-use and cognitive radio, receiver and RF front-end architectures, SATCOM, satellite navigation systems, localization technology, near-field and low power communication, multilane MIPI, high-speed display, MIMO and of course, LTE/LTE-A/TD-LTE.

With this first round of proposals received, the technical committee will complete their review of the submitted abstracts and recommend papers for the conference, authors will be notified and the schedule will begin to fill out. In parallel, we will continue to develop workshops and panels with input from the event's sponsors and commercial organizations interested in participating.

David Vye,
Microwave Journal Editor

RFHIC means Affordable GaN

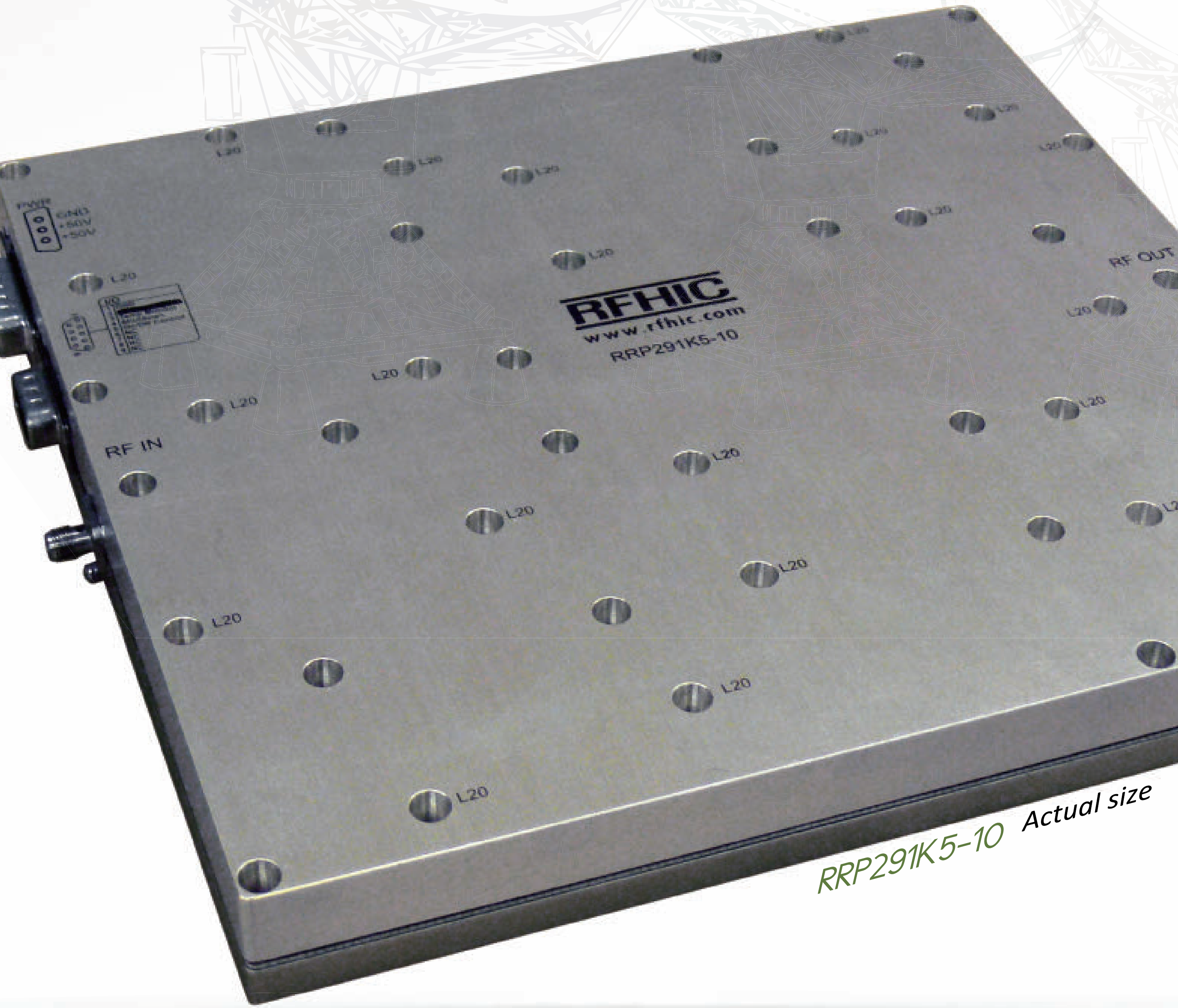

RRP291K5-10 Actual size

COVER FEATURE
INVITED PAPER

Accelerating the Response to RF Interference

In a perfect world, receivers would use brick wall filters, amplifiers and mixers would never distort, command centers would always coordinate their spectrum operations and the term "jam" would have meaning only at breakfast and during musical gatherings. Until then, there will be interference. Interference may be either unintentional or intentional. Whatever the form, the most significant effect is reduced sensitivity in the receiver, potentially disrupting or completely blocking reception of desired signals.

Unintentional interference is often caused by the ever-increasing number of emitters in the RF environment: cell phones, wireless links, cordless phones, terrestrial television and medical electronics are among the many contributors. In addition, some military systems have the potential to cause unintentional interference that disrupts civilian systems ranging from garage door openers and automobile key fobs to Wi-Fi links and the cellular infrastructure. The effects of unintentional interference range from merely annoying in residential settings, to potentially costly in business or medical environments. This type of interference can often be detected, characterized and mitigated through susceptibility and interoperability testing.

In contrast, intentional interference has been created to disrupt the operation of a "victim" receiver. This is undesirable in a wide range of aerospace, defense and public-safety applications: radio communications, radar scans, electronic countermeasures, telemetry links, flight-range operations, spectrum monitoring, signal intelligence and more. On the other hand, intentional interference is a desirable asset when used to block transmissions to improvised electronic devices (IED) or otherwise disrupt enemy tracking, navigation and communication systems. The need to understand and either create or defeat intentional interference is typically exponentially more urgent than interoperability or susceptibility testing.

This article focuses on intentional interference and the ultimate goal of countering undesired signals. The proposed process has four steps: capture the signal in the field, analyze it in the lab, simulate and playback the signal and develop ways to defeat it.

JOHN S. HANSEN
Agilent Technologies, Santa Clara, CA
JIM TABER
X-COM Systems, Reston, VA

COAXIAL AND WAVEGUIDE SWITCHES

RLC has the exact solution you're looking for.

RLC Electronics manufactures a complete range of RF switches including coaxial in the frequency range from DC to 65 GHz and rectangular or double ridge waveguide. The operating modes on all designs are failsafe, latching and manual.

Control options are DC voltages as low as 5V, TTL, BCD, RS232, and RS422. All switches have excellent repeatability and lifetimes in excess of one million operations. Many types are QPL listed per MIL-DTL-3928.

- **SPDT to SP12T**
- **Transfer**
- **Low VSWR**
- **High Isolation**
- **Low Insertion Loss**
- **High Power**
- **Low Passive Intermodulation**
- **Surface Mount Options**

For more detailed information on coaxial and waveguide switches, visit our web site.

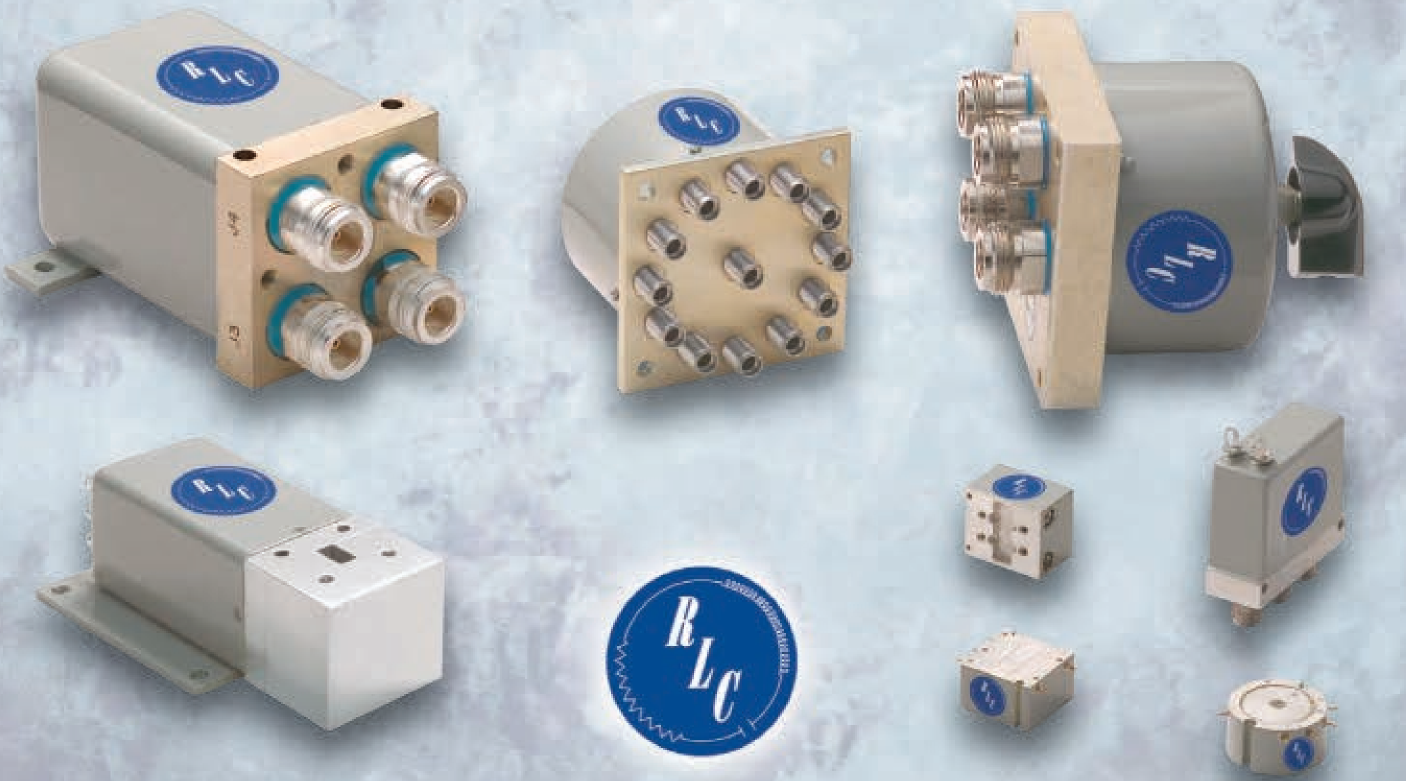

RLC ELECTRONICS, INC.

83 Radio Circle, Mount Kisco, New York 10549 • Tel: 914.241.1334 • Fax: 914.241.1753
E-mail: sales@rlcelectronics.com • www.rlcelectronics.com

ISO 9001:2000 CERTIFIED

VISA MasterCard

RLC is your complete microwave component source...
Switches, Filters, Power Dividers, Terminations, Attenuators, DC Blocks, Bias Tees & Detectors.

Sketching the Goals of Interference Testing

Unintentional interference from "friendly" systems can be understood by testing for interoperability and susceptibility. Interoperability testing centers on verifying the compliance of a design relative to published standards. It is important to understand how well a system meets its design criteria in the presence of real-world signal levels.

Susceptibility testing focuses on unintended interactions between the system-under-test and other RF systems. In aerospace, military and public-safety, this includes receiver performance in the presence of other mission-critical RF assets. One key goal is to avoid unwanted effects that reduce or block receiver sensitivity during any type of operating scenario.

OUTLINING THE NEED FOR INTERFERENCE TESTING

Various types of "culprit" emitters can affect a victim receiver, and the culprit may be producing out-of-band or in-band interference.

Out-of-band interference is most severe when the culprit is a high-power transmitter operating near the victim (see ***Figure 1a***). The most common problems are passive intermodulation (PIM), RF overload and spurious signals. PIM occurs when dissimilar or corroded metals near large broadcast antennas act as non-linear junctions (that is diodes). These create intermodulation products that fall within the passband of the victim receiver, reducing its sensitivity. Similarly, harmonics and spurs from a high-power out-of-band transmitter can fall within the passband of the victim and desensitize the receiver. RF overload occurs when electromagnetic energy, regardless of frequency, couples into the receiver's antenna and front end, thereby desensitizing the victim. As an example, dense RF congestion in a shipboard environment can cause coupling strong enough to physically destroy RF front-end circuitry.

In-band interference comes from other systems that are operating in the same frequency range as the receiver. This type of interference will pass through the victim receiver's channel filter and, if the signal amplitude is large relative to the expected signal, that signal will be corrupted. Two

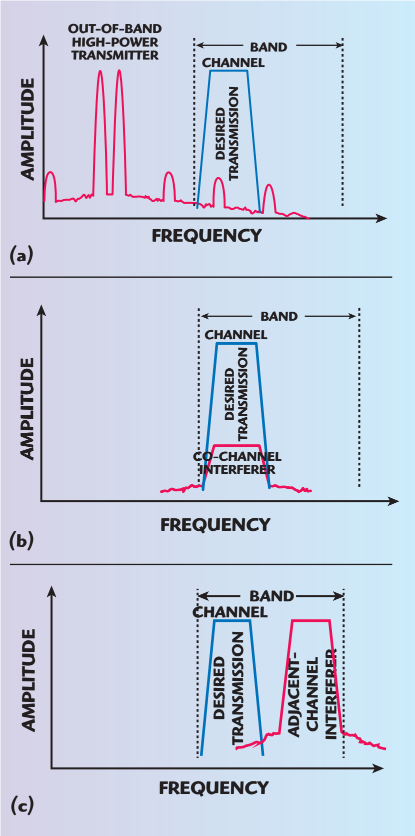

▲ *Fig. 1 Intermodulation products that fall within the passband (a), co-channel interference (b) and adjacent channel interference (c).*

forms of in-band interference are especially prevalent: co-channel and adjacent-channel. Co-channel interference comes from another transmitter operating in the same spectrum occupied by the victim receiver (see ***Figure 1b***). Although this is common in the cellular industry due to frequency reuse plans, military systems also can experience the same problem, especially in-theater where it may be more difficult to coordinate frequency planning prior to an operation.

Adjacent-channel interference is the result of in-band transmissions that produce unwanted energy or "energy splatter" in channels at higher and lower frequencies (see ***Figure 1c***). This energy splatter, often called intermodulation distortion or spectral regrowth, is created by nonlinear effects in the transmitter's high-power amplifier.

FOCUSING ON INTENTIONAL INTERFERENCE

Intentional interference is being transmitted for a specific purpose: disrupting communication, jamming

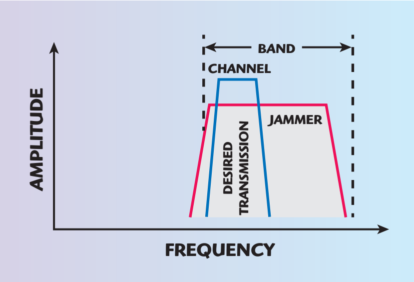

Fig. 2 Intentional interference.

a radar system, and otherwise deceiving or disrupting a victim receiver (see ***Figure 2***). Because such signals are intermittent and transient, it is often difficult to pinpoint the culprit.

Within this scenario, the specific problem is capturing and analyzing a complete set of spectrum data that contains an offending signal. This often requires the acquisition of seconds, minutes or hours of spectrum data — and this can consume gigabytes or terabytes of disk space. To provide a complete picture during analysis, the captured data must be gap-free. In most cases, storage capacity is perhaps the easiest part of the problem. More difficult is the continuous acquisition of high-fidelity RF data. Once the mountain of gap-free data has been acquired and stored, the next challenge is pinpointing one or more interference events. True understanding comes with the extraction of meaningful signal information — in the time, frequency and modulation domains — from each event.

LEVERAGING RECENT INNOVATIONS

Advances in commercial off-the-shelf (COTS) technologies are providing the levels of performance needed for effective interference analysis in radar and EW applications. This is true for both the capture and playback of possible interferers.

Driving the Evolution of Signal Analysis

Accurate, gap-free analysis of the RF spectrum requires one or more fast digitizers coupled with excellent front-end circuitry. In a signal analyzer, this equates to exceptional performance that reduces measurement uncertainty and reveals new levels of signal detail. Several key specifications enable the level of performance needed for interference analysis. First is a spurious-free dynamic range of up to 75 dB at a 160 MHz analysis bandwidth. Next are –129 dBc/Hz phase noise (room temperature) at 10 kHz offset (1 GHz), ±0.19 dB absolute amplitude accuracy and sensitivity of –172 dBm displayed average noise level (DANL) at 2 GHz, with a preamplifier and noise floor extension (NFE) technology.

NFE provides a dramatic improvement in a signal analyzer's ability to accurately measure low-level signals approaching the theoretical "kTB" noise floor. This method compensates for the noise contribution from active microcircuits in the analyzer's RF and IF chain. With increased averaging, the analyzer's effective noise floor can be extended by up to 10 dB because 90 percent or more of the contributed noise power is predictable. As a result, that noise is modeled, measured and calibrated during the manufacturing

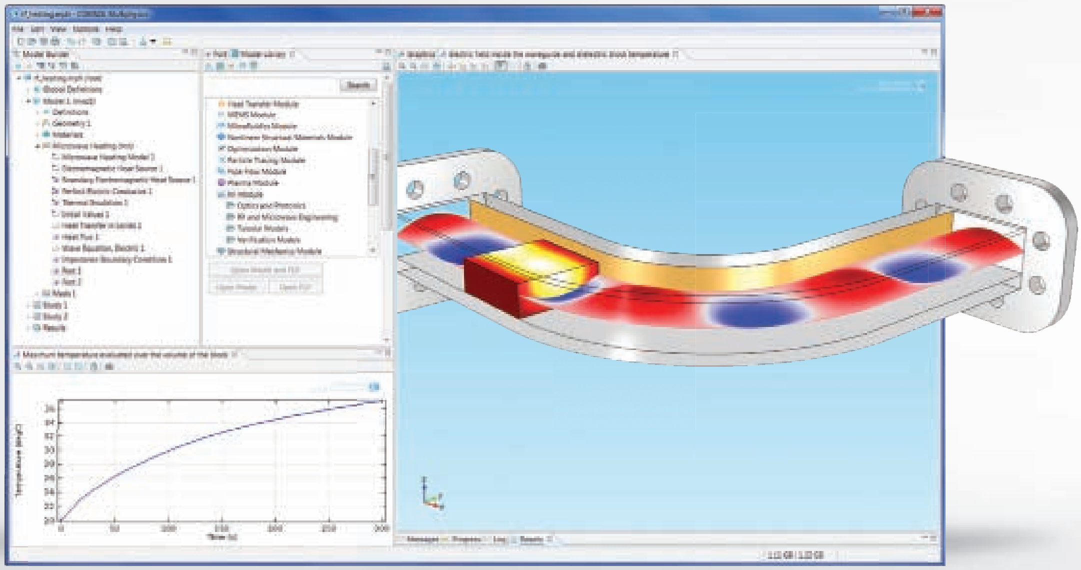

process for all allowed operating conditions the analyzer may face and then eliminated automatically during normal measurements.

Enabling Highly Accurate Signal Scenarios

For playback of captured or simulated signals, the critical attributes of an arbitrary waveform generator (AWG) are bandwidth, accuracy and dynamic range (resolution). These characteristics are especially important in radar and EW applications because today's typical signals have fast transition times, short on/off intervals and widely divergent power levels. Most typical AWGs require a tradeoff between units that offer either wide bandwidth with low dynamic range or limited bandwidth with high dynamic range. The respective levels of performance in bandwidth and dynamic range depend on the digital-to-analog converter (DAC) used within the AWG. Bandwidth is limited by the DAC sample rate and accuracy is limited by the quality and performance of the analog components used within the device.

A poorly designed DAC may produce glitches that corrupt the spectral content of the output signal, potentially causing inaccurate results. In a typical DAC, nonlinear slewing of the output signals is one possible cause of unwanted signal distortion. This problem is often caused by switched current sources within the DAC. Filtering is typically used to reduce the effect, but this can have an adverse effect on bandwidth.

Interference analysis requires signal generation that is free from the spurs and distortion produced by typical DACs. This is possible with state-of-the-art devices recently developed by Agilent's Measurement Research Lab. These DACs have two key attributes. First, the device allows switched current sources to settle within the DAC. Second, the DAC re-samples the signal with a special low-noise clock before outputting the simulated signal. This innovation makes it possible to deliver excellent spurious-free dynamic range at wide bandwidths.

Using this type of DAC in an advanced AWG makes it possible to provide high resolution and wide bandwidth simultaneously. For example, Agilent has an RF-quality DAC that provides 14-bit resolution at 8 GSa/s or a 12-bit resolution at 12 GSa/s. Spurious-free dynamic range of less than –75 dBc gives developers confidence that they are testing the radar or EW system, not the signal source.

STRUCTURING THE SOLUTION

The driving idea behind the proposed solution is "captured interference equals information." Quick and accurate extraction of meaningful signal information enables rapid understanding of the interference, its impact on the victim system and possible mitigating countermeasures. All this can be accomplished with a configuration based on COTS hardware and software elements. The system accelerates the process of sifting through terabytes of data and performing detailed analysis. It also retains the original signal fidelity throughout the entire process — capture, analysis, simulation and playback. Because all elements are COTS, the solution offers traceable performance and enables easy redeployment as a conventional test system. An overall block diagram is shown in ***Figure 3***.

Capturing and Analyzing Interference Signals

Signal capture and analysis utilizes three hardware elements: a signal analyzer, a data recorder and an external data pack. These are shown in the left and center sections of ***Figure 4***.

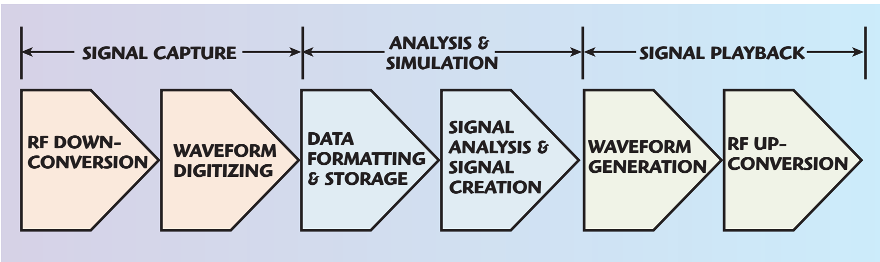

Fig. 3 Block diagram of the conversion process of captured interference into useful information.

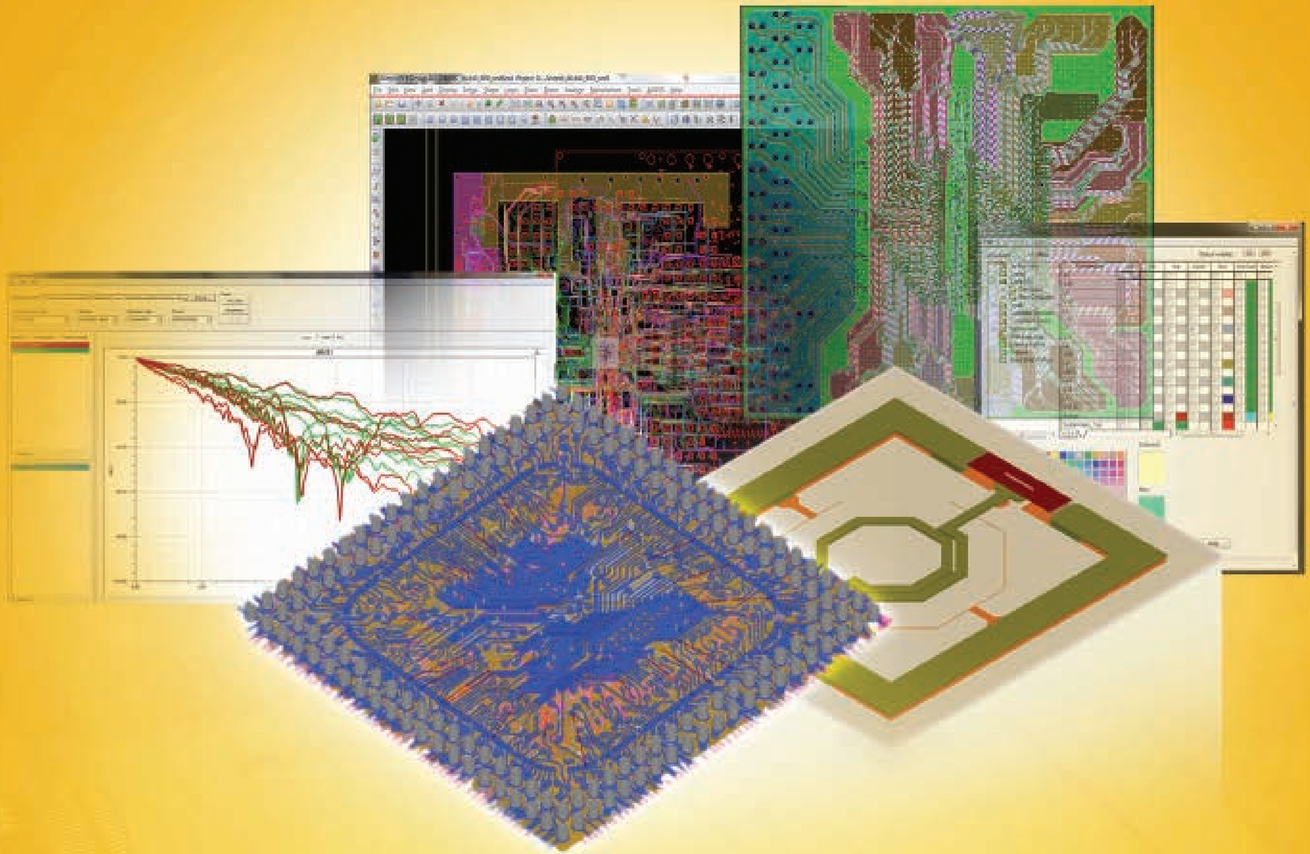

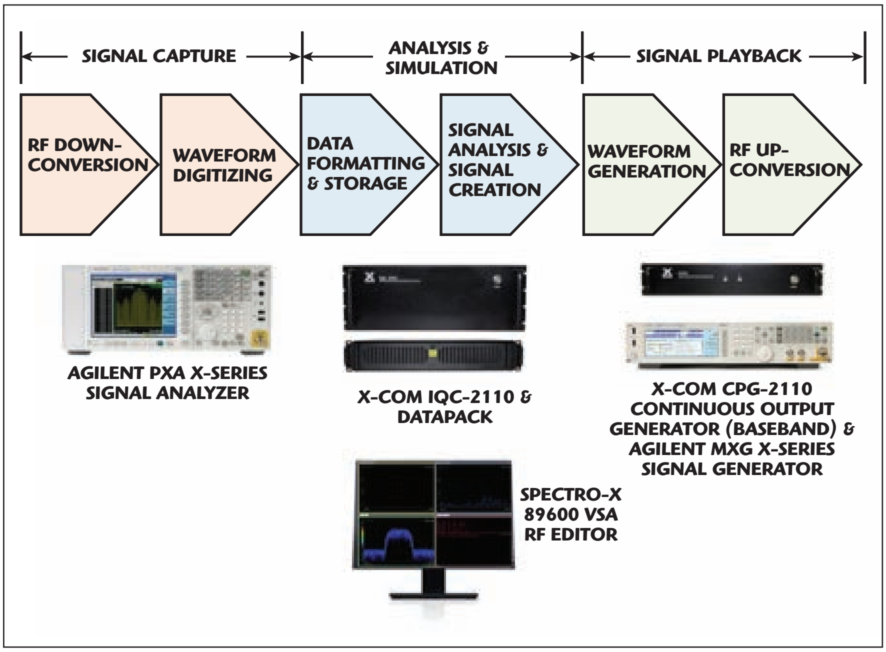

▲ *Fig. 4 A combination of COTS hardware and software elements enables high-fidelity capture, analysis, simulation and playback of interference signals.*

Signal analyzer: A high quality signal analyzer is used as the front-end downconverter and IF digitizer. Maximizing signal fidelity at the beginning of the process helps ensure high fidelity through the remaining stages.

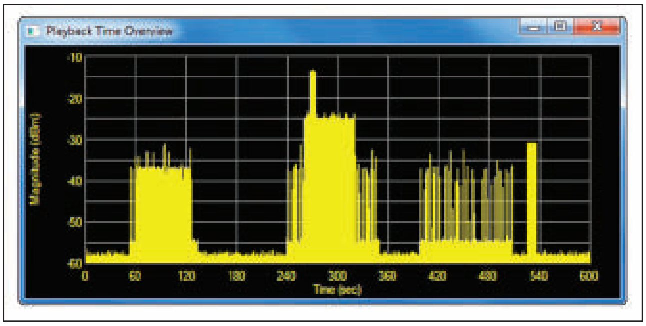

▲ *Fig. 5 Visual inspection of the captured spectrum data revealed four regions of interest.*

High-capacity data recorder: The input to the recorder is a stream of digital I/Q samples from the signal analyzer. The data recorder formats the I/Q data, tags it with external marker events and adds time and GPS stamps before sending to the data pack.

Data pack: The unit used here can be configured with a capacity of 2, 4, 8, 12 or 16 TB.

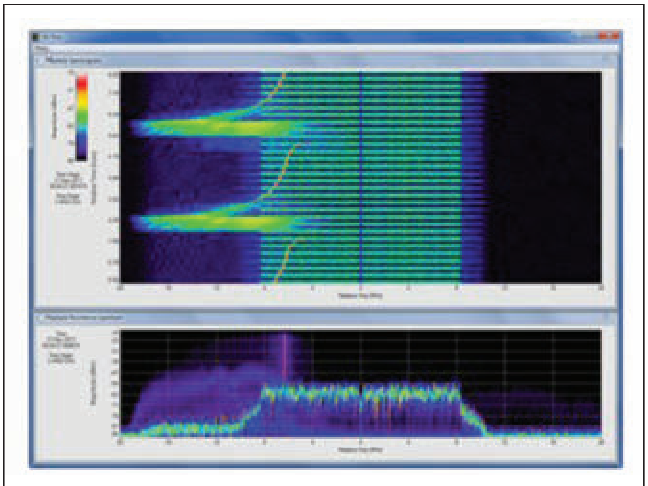

▲ *Fig. 6 Spectrogram display shows two bursts of the interferer.*

A variety of post-processing activities can be performed with the software elements of the solution.

Signal analysis software: Key capabilities include pre-processing of large data sets and location of suspect signals. Useful features include built-in search engines to identify and "fingerprint" waveforms as well as "clip and save" capability for replay into vector signal analysis (VSA) software.


AMPLIFIERS
HIGH PERFORMANCE
100 kHz to 50 GHz
• To Your Specification
• Reasonable Prices
Most can be delivered in one week!
+15V
B&Z
IN
SN: 3837
OUT
+15V
B&Z
IN
SN: 1966
OUT
Visit our Web Site at www.bnztech.com
Fill Out the Custom Specification form
Receive a Quotation within 24 hours!
B&Z TECHNOLOGIES
INNOVATING TO EXCEL
Ph: +1 (631) 444-8827
Fax: +1 (631) 444-8825
E-Mail: info@bnztech.com
Web: www.bnztech.com
Made in USA
Year 3 Warranty

Vector signal analysis software: This application should provide multiple views into highly complex signals. In addition, built-in capabilities should enable bit-level modulation analysis of established, emerging and evolving standards and signal types.

SIMULATING AND GENERATING INTERFERENCE SIGNALS

For simulation and playback, the system includes signal-creation software, a baseband generator and a vector signal generator. These are shown at the bottom and right of Figure 4.

Signal-editing software: This application can be used to create signal scenarios that include the recorded files. Capabilities include clipping, stitching, translating, filtering and looping of waveforms. The resulting waveforms can be downloaded to the continuous playback generator.

Continuous playback generator: This baseband generator is used to drive the I and Q modulation inputs of the vector signal generator.

Vector signal generator: This instrument upconverts the I/Q modulation and serves as the over-the-air signal source. Suitable models provide sufficient analog and vector performance to ensure excellent signal fidelity during playback.

FINDING AND IDENTIFYING AN INTERFERENCE SIGNAL

A brief case study based on an actual interference scenario will illustrate the capabilities of the system. The initial signal acquisition was performed using a signal analyzer that streamed a 40 MHz-wide capture into a data recorder and its 2 TB external data pack. The gap-free capture ran for 10 minutes and generated 120 GB

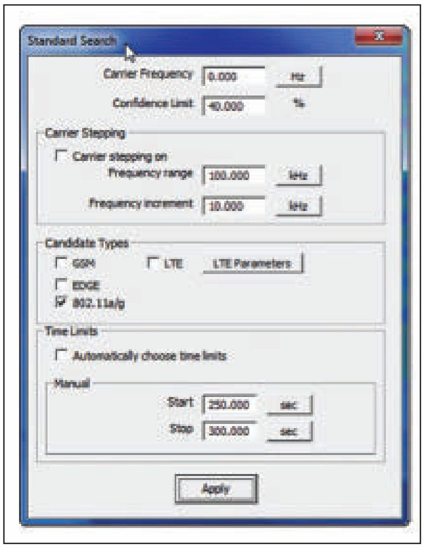

▲ *Fig. 7 "Standard search" dialogue box used to select parameters.*

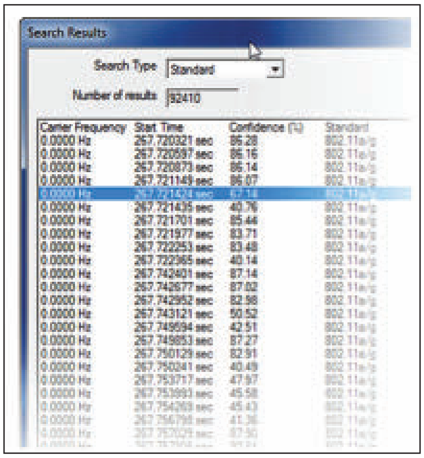

▲ *Fig. 8 The search results summary reveals areas of high and low confidence.*

of data, which was copied to a laptop running the signal-analysis and VSA software.

Extracting Information from Interference

The signal-analysis software was used to visually inspect the captured data for signs of suspicious interferers. An overview measurement of magnitude versus time for the full 600-second capture revealed four distinct periods of potentially interesting activity (see ***Figure 5***). In the region between approximately 230 and 350 seconds, a large spike appeared around the 270 second mark. Focusing on this area provided informative views in the spectrogram and persistence spectrum formats, as shown in ***Figure 6***. In the spectrogram display (top), two bursts of the interferer intrude into the spectrum of an orderly carrier signal.

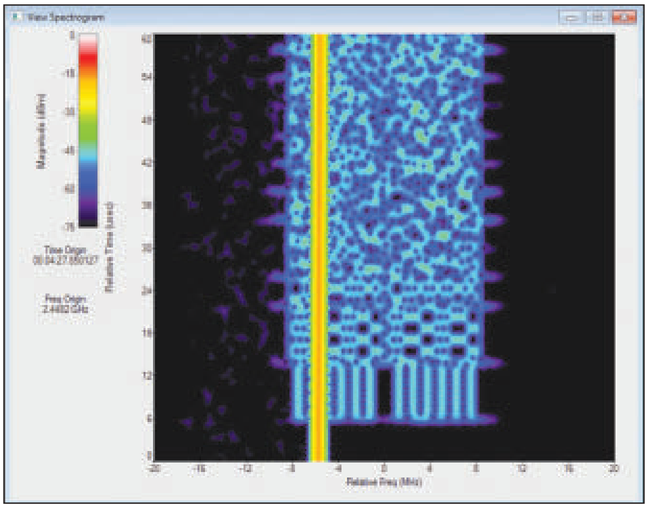

Fig. 9 Spectrogram display showing the interferer.

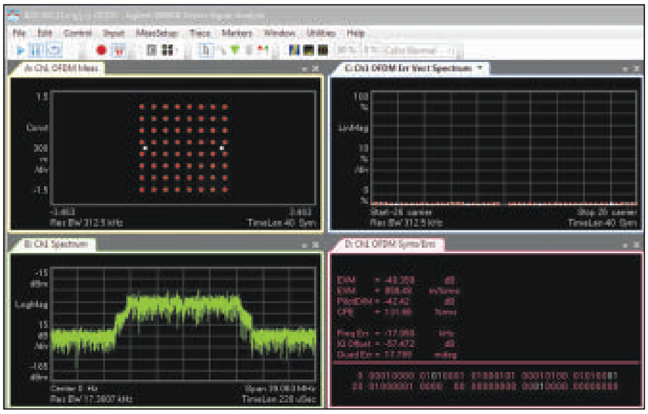

Fig. 10 Key indicator of modulation quality when interferer is dormant.

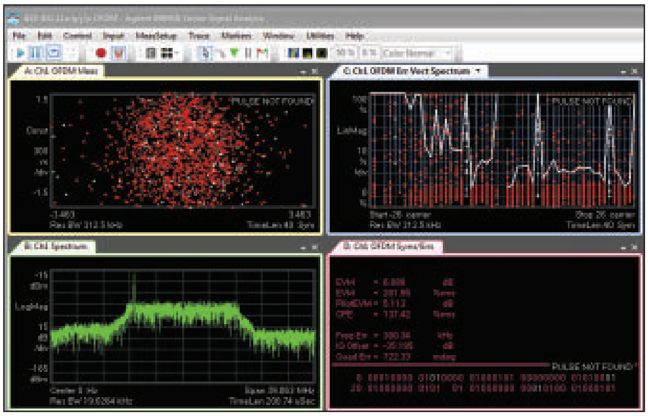

Fig. 11 Key indicator of modulation quality with interferer present.

The "standard search" capability in the software was used to identify the orderly carrier, which was believed to be an 802.11g signal. As shown in ***Figure 7***, the search parameters include a confidence limit (set to 40 percent in this case), a candidate type of standard (here set to 802.11a/g) and the time range of interest within the captured data (set to 250 to 300 seconds). The confidence limit helps reveal signals that look similar to an ideal wireless standard. This value defines the desired level of correlation between the reference and a captured signal. Using a value of less than 100 percent provides clues into how severely the interference is affecting the victim signal.

In this case, the search found more than 92,000 instances of signals that resembled the 802.11g reference. As expected, there were regions of severe degradation that occurred when the interference signal appeared: as shown in ***Figure 8***, correlation dropped from 80-plus percent to less than 50 percent. For each region of poor correlation, the results were examined using a spectrogram display (***Figure 9***). This 60 µs (top to bottom) spectrogram display shows the interferer disrupting the reference sequence (3 to 11 µs) and payload (11 µs and above) of the 802.11g signal. This pinpointed the five-second span during which the interferer was operating.

The associated I/Q data was then exported to the VSA software for detailed analysis. In the time prior to the interference, the key indicators of modulation quality were all good, as shown in ***Figure 10***. The OFDM constellation (upper left), EVM (upper right) and spectrum (lower left) are normal. When the interference was active, the impact was catastrophic: the pilots and payload carriers were completely disrupted as the interfering signal walked through the transmission (see ***Figure 11***). The OFDM constellation (upper left) is shattered, EVM (upper right) is erratic and a large spike is present in the frequency spectrum (lower left).

Revealing the Scenario

This incident occurred in an Internet café. The unintentional jammer was a microwave oven and it disrupted the Wi-Fi connectivity every time the staff warmed a pastry or sandwich. Even though this was a relatively benign situation, the suggested procedure works equally well in scenarios that involve interference that affects radio communications, telemetry links, flight range operations, signal intelligence (SIGINT), system interoperability, and so on. It also supports the three most common usage scenarios: record in theater and playback in the lab, record in the lab and playback in the lab, and create in the lab and playback on the range.

DEPLOYING EFFECTIVE TOOLS

Various types of interference can impact critical defense systems. When that interference is an intentional threat, it is important for designers and researchers to have effective "RF forensic tools" — such as those shown here — that can unravel what actually happened in the electromagnetic spectrum. Extracting useful RF information is the first step in developing effective mitigation strategies and solutions. ■

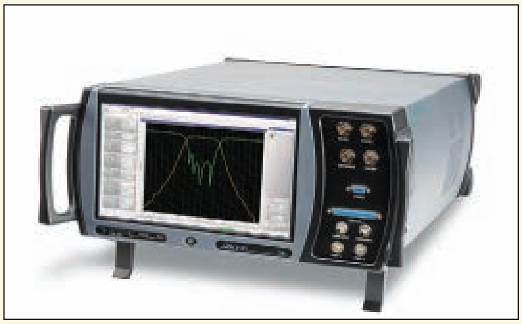

Integrated Microwave Test Solution

The challenges of microwave verification and manufacturing testing have never been greater, as managers and engineers are continually asked to do more with less. The ever increasing demands of speed to market mean that by the time the test manager receives the test requirements, the program is usually behind schedule. At this point a suitable test solution needs to be selected, acquired and implemented.

This traditional approach to Automatic Test Equipment (ATE) development involves selecting appropriate instruments and then integrating these assets to form a complete test solution for the Device Under Test (DUT). The integration typically involves creation of software to control the test system, environment and possibly the DUT. This effort can take months of system and software engineering time that the program cannot afford.

The Aeroflex 7700 Integrated Microwave Test Solution addresses this problem by turning the traditional ATE approach upside down. The 7700 is not a single instrument or even a group of instruments; it is a complete test system. Built around a full-featured test executive software called the Aeroflex Measurement Console (AMC), the 7700 contains measurement sequences that control all aspects of the test, including signal generation, measurement, switching, power handling, temperature and DUT control. By accelerating the time between requirements and testing, the 7700 helps put programs back on schedule.

A TRUE SYNTHETIC ATE IN A BOX

Over the past decade, Aeroflex has been a pioneer in the development of synthetic test systems targeted specifically at reducing the cost of test of complex ATE environments. The 7700 is the next stage of this measurement evolution. By combining modular PXI hardware, the Aeroflex common platform modules, and the AMC test executive, the 7700 provides a capable, flexible and scalable synthetic test instrumentation with the lowest cost of ownership in the industry.

The system utilizes a common set of hardware for stimulus and response functions (see

Aeroflex
Wichita, KS

Figure 1). This common utilization reduces hardware costs, results in a smaller footprint than conventional systems and allows for a system-level calibration scheme that provides superior performance as compared to a traditional rack and stack approach. Using the production test sequences in AMC, the 7700 includes the capability to emulate the functionality of the following instrumentation:

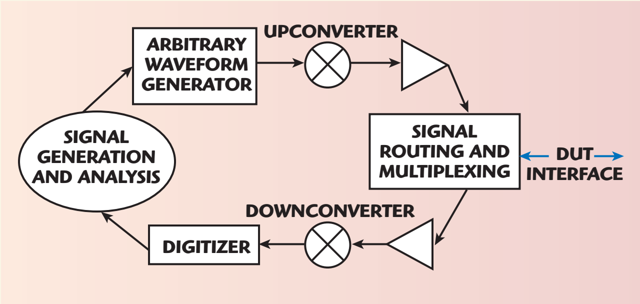

Fig. 1 System architecture.

- Vector signal generator
- Spectrum analyzer
- Vector network analyzer
- Oscilloscope
- Power meter
- Frequency counter
- Noise figure meter
- Phase noise analyzer

The system can also meet or exceed most standard instruments when it comes to RF performance.

- Frequency Range: 1 MHz to 6 GHz (expandable to 32 GHz)
- RF Modulation BW: 90 MHz
- Frequency Switching Times: < 1 msec
- Output Power Range: > 100 dB
- Phase Noise (2 GHz, 20 kHz offset): −115 dBc/Hz
- Residual Noise Floor: < −120 dBm
- Total Dynamic Range: > 100 dB
- DANL (1 Hz res bandwidth)
- 1 MHz to 1 GHz: −164 dBm/Hz
- 1 to 3 GHz: −159 dBm/Hz
- 3 to 6 GHz: −154 dBm/Hz

Figure 2 shows some common measurements controlled by the test executive software AMC. This mature software package provides a complete measurement and development environment, including test execution, sequencing of multiple tests, and reporting of test data as well as test development and debug.

FUTURE PROOF DESIGN

The 7700's true synthetic flexible architecture ensures that today's system can meet tomorrow's requirements. With traditional instrumentation, new measurements or increased performance requires the system engineer to replace individual instruments used in the test system. Measurement software developed using these instruments will need to be modified or completely rewritten. It is often more

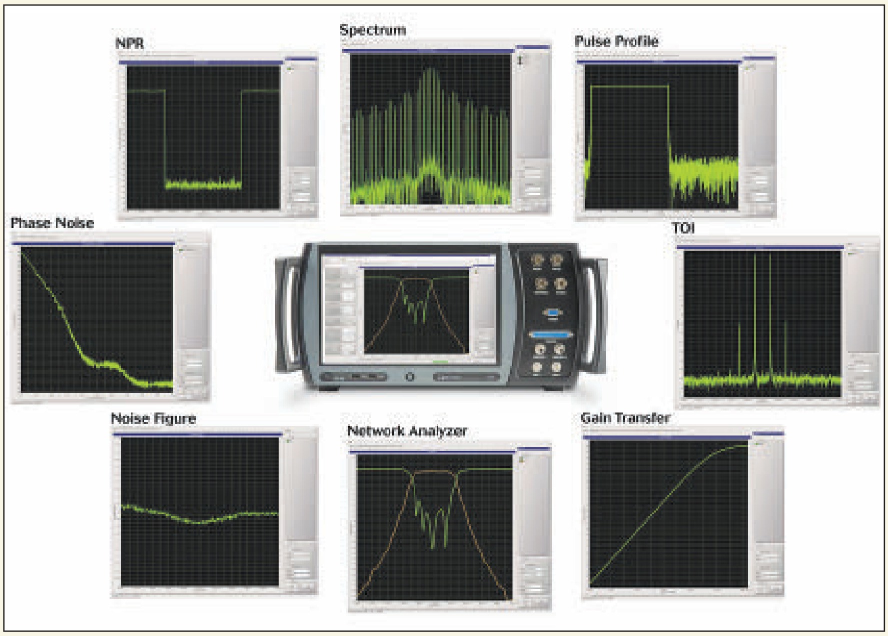

Fig. 2 The 7700 includes a complete measurement suite that would normally require a full rack of instrumentation.

Most Valuable Product

economical to simply replace the entire system rather than upgrade to new capability. With the 7700's modular synthetic approach, most new measurements require only a new software sequence. When new hardware is needed to meet new requirements, such as higher instantaneous bandwidth, possibly only a single PXI card will need to be replaced. Since the 7700 measurement sequences utilize a synthetic hardware driver layer, none of the existing measurement sequences will be affected with the addition of the new hardware. It is even possible to add hardware to configure the 7700 to cover RF frequencies up to 32 GHz.

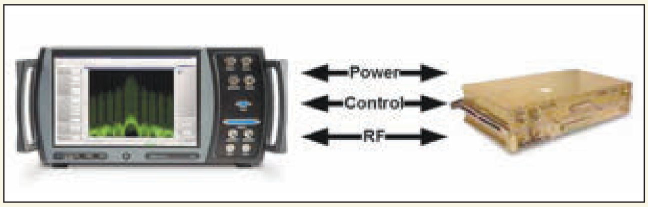

▲ *Fig. 3 The 7700 removes the need to make independent calls to several instruments and the DUT.*

WORLD CLASS MEASUREMENT SPEED

With traditional instrumentation, system engineers are often forced to develop independent instrument, power, environmental and DUT control schemes. This usually requires additional hardware and software to be added to the system architecture, compromising efficiency and reducing throughput. By providing tight coupling of all test aspects, the 7700 removes the additional software overhead and measurement processing necessary to make independent calls to several instruments and the DUT when executing a test (see ***Figure 3***).

In the 10+ years of delivering similar synthetic solutions, Aeroflex has received customer feedback that this approach has consistently yielded a better than 4× improvement in measurement throughput over traditional methods.

CONFIGURATIONS AND MEASUREMENTS FOR MANY APPLICATIONS

The 7700 is delivered with measurement sequences that provide basic measurement capability including the emulation of signal generators, spectrum analyzers and vector network analyzers. In addition to the basic sequences, comprehensive libraries are available that provide many measurements typically performed during the characterization and test of RF devices. These measurement sequences provide the ability to generate complex stimulus signals, receive the response signals from the DUT, and process the data to derive the required data product, all while providing tightly synchronized control of the DUT. ***Table 1*** shows some of the measurement personalities that are available for the 7700.

TABLE I

LISTING OF SOME OF THE MEASUREMENT CAPABILITIES OF THE AEROFLEX 7700

Pulse Amplifier Measurements
S-Parameter (CW and Pulsed)
P_{out} versus P_{in}
Time Domain Measurements and Pulse Characterization
Total Absorbed Power
Noise Figure (Y-Factor)
Hot S_{22}
CW and Frequency Translated Measurements
P_{out} versus P_{in}
Frequency Response/Conversion
Spectrum, Spurs, Harmonics
Third Order Intercept
AM/PM
Channel Isolation
Noise Figure (Cold Source)
Group Delay
Absolute Time Delay
Phase Noise
Multi-Tone Measurements
Noise Power Ratio
Passive Intermodulation (PIM)
Multi-Carrier Relative Amplitude and Phase

The next generation of synthetic-based instrumentation has been developed and released. To date, the 7700 provides the most complete "ATE in a Box" solution.

Aeroflex,
Wichita, KS (316) 522-4981,
www.aeroflex.com.
info-test@aeroflex.com

Defense News

Dan Massé, Associate Technical Editor

Boeing Receives 10th WGS Satellite Order from U.S. Air Force

Boeing has received a $338.7 million contract modification from the U.S. Air Force to produce and launch a tenth Wideband Global SATCOM (WGS) satellite. The authorization includes production, launch site activities, initial orbital operations and checkout.

Boeing is working with the Air Force on potential cost-effective upgrades that would further increase the WGS satellites' capacity and operational flexibility. In June, Boeing was contracted to implement an enhanced Wideband Digital Channelizer upgrade that provides a 90 percent improvement in satellite bandwidth – with no additional cost to the government. The new channelizer will be included on satellites WGS-8 and beyond.

"We are continuously looking for ways to realize cost savings on the WGS program, whether through product upgrades or improvements in the acquisition process," said Craig Cooning, vice president and general manager of Boeing Space & Intelligence Systems. "Unlike previous annual authorizations of single satellites, the Air Force recently acquired three satellites – WGS-8, -9 and -10 – within a six-month window. This enabled us to generate significant savings by combining procurements for materials and by maintaining an active production line across the vehicles."

The WGS payload architecture can accept the Wideband Digital Channelizer upgrade with minimal impact. Boeing will continue to work with the Air Force to develop WGS enhancements that can unlock additional bandwidth and capacity. The contract announcement comes six months after Congress provided funding for the Air Force in fiscal year 2012 to purchase WGS-10. This additional order is part of the WGS Block II follow-on contract, under which Boeing had previously been authorized for production and launch of WGS-7 through WGS-9. The state-of-the-art WGS satellites are built on the proven Boeing 702 platform that leverages decades of industry-leading, space-proven technologies. All three Block I satellites have been delivered and are in operation.

In June, Boeing was contracted to implement an enhanced Wideband Digital Channelizer upgrade that provides a 90 percent improvement in satellite bandwidth – with no additional cost to the government.

"The Block I satellites, which are meeting or exceeding all mission requirements, provide unique capabilities such as on-station reconfigurable X-Band coverage and X/Ka cross-banding, which enable communication in contested theaters around the globe," said Cooning.

The Block II program also is proceeding well. WGS-4, the first in the Block II series, was launched on January 19 and handed over to the Air Force on April 11. The launches of WGS-5 and WGS-6 are scheduled for 2013.

Fabrication of Northrop Grumman-Built Spacecraft for NASA's James Webb Space Telescope Moves Forward

The spacecraft that will carry NASA's James Webb Space Telescope to its orbit nearly a million miles from Earth has completed a Critical Design Review for the structure that supports Webb's data link to NASA's ground station. Northrop Grumman Corp. is under contract to NASA's Goddard Space Flight Center in Greenbelt, MD for the design and development of the telescope, sunshield and spacecraft.

Now ready for fabrication, the Webb spacecraft's communications support structure stows and holds the communications antenna when folded for launch. When the telescope unfurls in space, the antenna is released and points to NASA's Deep Space Network, transmitting data to the world's scientists. Another spacecraft structure, the solar array, has completed its preliminary design audit and moves into the detailed design phase. The spacecraft's solar array supplies all electrical power to the science instruments, communications equipment and computers for the entire telescope. The solar array is the first component that deploys once the telescope separates from the launch vehicle and its performance is critical. Without power, there is no science mission.

Successor to the Hubble Space Telescope, the James Webb Space Telescope is the world's next-generation space observatory. It will be the most powerful space telescope ever built.

"This progress represents a steady path forward on spacecraft subsystems," said Andy Cohen, Webb spacecraft manager, Northrop Grumman Aerospace Systems. "We have accelerated the structural build of the spacecraft by four and a half months and have completed qualification testing for the engineering model of the command and telemetry processor, our main onboard computer, responsible for all spacecraft operations and fine guidance of the telescope."

Successor to the Hubble Space Telescope, the James Webb Space Telescope is the world's next-generation space observatory. It will be the most powerful space telescope ever built. Webb will observe the most distant objects in the universe, provide images of the very first galaxies ever formed and study planets around distant stars. The Webb Telescope is a joint project of NASA, the European Space Agency and the Canadian Space Agency.

Go to mwjournal.com for more defense news items

U.S. Army's JLENS Will Protect Sailors, Critical Waterways

Soldiers will soon have a system that enables them to protect sailors and safeguard commercial and military navigation in strategic waterways. In June, a series of tests demonstrated that Raytheon Co.'s JLENS is capable of detecting and tracking swarming boats from hundreds of miles away. During the tests, JLENS simultaneously detected and tracked multiple speedboats on the Great Salt Lake. The boats, similar to swarming boats in the inventories of hostile navies in high-threat regions, simulated a real-world scenario with a series of tactical maneuvers at low and high speeds.

"JLENS is affordable because during a 30-day period, one system provides the warfighter the same around-the-clock coverage that it would normally take four or five fixed-wing surveillance aircraft to provide," said David Gulla, vice president of Global Integrated Sensors for Raytheon's Integrated Defense Systems business. "JLENS is significantly less expensive to operate than a fixed-wing surveillance aircraft because it takes less than half the manpower to operate and has a negligible maintenance and fuel cost."

U.S. Air Force Awards Lockheed Martin $152 M Sniper ATP Sustainment Contract

Lockheed Martin has received a $152 million contract from the U.S. Air Force for Sniper® Advanced Targeting Pod (ATP) sustainment support over a five-year period, beginning September 2012. The contract transitions legacy Sniper pod sustainment support from Wright Patterson Air Force Base, OH, to Warner Robins Air Force Base, GA. Additional scope includes engineering support, initial line replaceable unit spares, support equipment and pod containers. Specific tasks will be covered under a series of delivery orders to be awarded incrementally over the five-year period.

"Receiving this contract is critical to preserving Sniper pod sustainment for the U.S. Air Force without incurring a gap in support to the warfighter," said Ashlie Payne, Sniper program manager in Lockheed Martin's Missiles and Fire Control business. "Through collaboration with Warner Robins, legacy Sniper ATP pods will continue to excel in providing aircrews with unmatched targeting capability."

The Sniper pod provides precision targeting and non-traditional intelligence, surveillance and reconnaissance information for multiple U.S. Air Force and international aircraft, with testing ongoing on additional platforms.

Reactel, Incorporated
Reacting First to All Your Filter Needs.
REACTEL, INC.
REACTEL, INC.
REACTEL, INC
Let our Engineers show you what we can do in tight spaces!
High Performance, Rugged Packaging, Small Size and Weight
Great things can come in small packages. Reactel filters are ideally suited for the demanding environments that unmanned vehicles encounter.
Many manufacturers rely on Reactel to provide units which are:
• High performance
• Lightweight
• Low profile
Contact a Reactel engineer with your filter or multiplexer requirements. We can create a unit which will be the perfect fit for your applications.
Reactel is happy to introduce our Filter RFQ App available for Apple and Android devices.
8031 Cessna Avenue • Gaithersburg, Maryland 20879 • Phone: (301) 519-3660 • Fax: (301) 519-2447
For general inquiries, please email reactel@reactel.com • Follow us on Twitter: @reacteljim
Go online to www.reactel.com to download your Reactel catalog today.
FM Approvals
ISO 9001-2008 Registered
@reacteljim

QinetiQ Contracted to Lead ISTAR Research

QinetiQ has been awarded a prime contract worth £6.4 million by UK Ministry of Defence scientists, following an open competition to deliver key aspects of a four-year programme of Intelligence, Surveillance, Target Acquisition and Reconnaissance (ISTAR) research.

The ISTAR Concepts and Solutions (ICS) programme is driving the next generation of ISTAR developments. This is achieved by applying the best science and technology to demonstrate cost-effective system solutions that will significantly improve the information and intelligence available to UK Armed Forces.

The ICS research programme, which includes the industry-led collaborative environment known colloquially as the ICS Engine Room, is managed by MoD staff at the Defence Science and Technology Laboratory (Dstl), working closely with colleagues in industry and academia. QinetiQ has been selected to lead the ICS Engine Room, the purpose of which is to provide a collaborative interface to draw on innovative solutions from a wide supply base (MoD, industry and academia) to address the most difficult challenges in ISTAR across the whole of defence.

> *"The team will provide the MoD with access to world leading innovation in C4ISTAR technology..."*

Jeremy Ward, MD of QinetiQ C4ISR Division said: "QinetiQ is delighted to have the opportunity to work with Dstl on the ICS project. We will lead a strong, pan-industry and academia team, which includes some of the UK's most respected scientists, engineers and academics. The team will provide the MoD with access to world leading innovation in C4ISTAR technology and will explore novel ISTAR technologies and processes, which will really make a difference to front line troops in the future."

Dstl's Dr. Steven Meers, ICS Technical Lead, said: "Awarding this contract is a major landmark in the delivery of the ICS programme and is a model for how Dstl, industry and academic partners will be working together in the future. This project will improve the MoD's ISTAR capability, for example by combining the best information technologies emerging from the civil sector with some of the defence specific capabilities which we have access to. A technically excellent group of scientists and engineers drawn from small and medium sized enterprises (SME), prime contractors, world-class universities and Dstl, working together in a collaborative environment, is the best way to deliver this complex, fast paced, challenging programme and provide real impact for MoD."

ESA and EIB Launch Space for Mediterranean Countries Initiative

The European Space agency (ESA) and the European Investment Bank (EIB) have signed the Space for Mediterranean Countries Initiative agreement. The two organisations will work together towards satellite-based services bridging the digital divide and aiming at bringing economic growth to the Mediterranean region.

The EIB assists the economic and social development of partner countries in the South and East Mediterranean. It has invested €13 billion through its operations in this region since 2002, supported 2300 small and medium sized enterprises, which created 30,000 jobs, and mobilised about €35 billion of additional capital together with international financing institutions, bilateral agencies and the private sector in order to advance the development of the region.

> *"...dialogue and coordination between ESA and EIB is of mutual interest..."*

The EIB has also granted more than €102 million for technical assistance operations to build knowledge and capacity. In particular, the current initiative received the support of the Facility for Euro-Mediterranean Investment and Partnership (FEMIP) Trust Fund, the main objective of which is to support private sector development in the Mediterranean partner countries.

On ESA's side, the Integrated Applications Promotion (IAP) programme aims to provide new, sustainable services in close partnership with end users, through the development of applications that rely on a combination of existing space and terrestrial systems.

"I am convinced that an increased dialogue and coordination between ESA and EIB is of mutual interest to our organisations," said Magali Vaissière, ESA Director of Telecommunications and Integrated Applications. "It will allow the expansion of the use of satellite-based applications for the benefit of people and of the economy."

68 Projects Funded for 8th Eurostars Cut-Off

The funding synchronisation phase of the 8th Eurostars Cut-Off was concluded with 68 project applications funded from the 112 applications ranked above the quality threshold. The R&D-performing SMEs and SMEs targeted by the programme continue to benefit, representing around 70 percent of the participants. They also carry 77 percent of the projects' total costs, proving that the Programme truly responds to this crucial sector's needs and expectation.

The funded projects include participants from 23 Eurostars participating countries, with the main technologies

Go to mwjournal.com for more international news items

represented in the pool of funded projects being electronics, IT and telecoms technologies (32 percent); biological sciences and technologies (24 percent) and industrial manufacturing, material and transport (14 percent). The total public funding estimates amount to €40 million from the participating countries, with a further €6.5 million from the European community.

Eurostars aims to stimulate SMEs to lead international collaborative research and innovation projects by easing access to support and funding. It is fine-tuned to focus on the needs of SMEs, and specifically targets the development of new products, processes and services and the access to transnational and international markets.

Eurostars aims to stimulate SMEs to lead international collaborative research and innovation…

The commitment of the Member States to the programme continues to be assured, with national public funds being increased substantially in order to better support the innovations being carried out by SME-led project consortia under the auspices of Eurostars.

EC Consultation on Research Infrastructures

The European Commission has launched a consultation to prepare future EU activities in order to achieve further integration and the opening-up of national research infrastructures. These activities come as a follow-up to successful initiatives supported by the Seventh Framework Programme (FP7) and are entitled Integrating Activities. The aim is to provide wider and more efficient access to, and use of, research infrastructures existing in EU Member States, FP7-associated countries and, occasionally, at the international level.

The consultation is a call for suggestions on topics that should be proposed by research infrastructures stakeholders, e.g., operators of research infrastructures and user communities. This will help identify potential topics for future Integrating Activities.

The received proposals will be reviewed by a panel of high-level independent experts. A report mapping the needs and providing recommendations will be produced by the panel, which will then be made available on the Internet.

TINY

Wideband Transformers

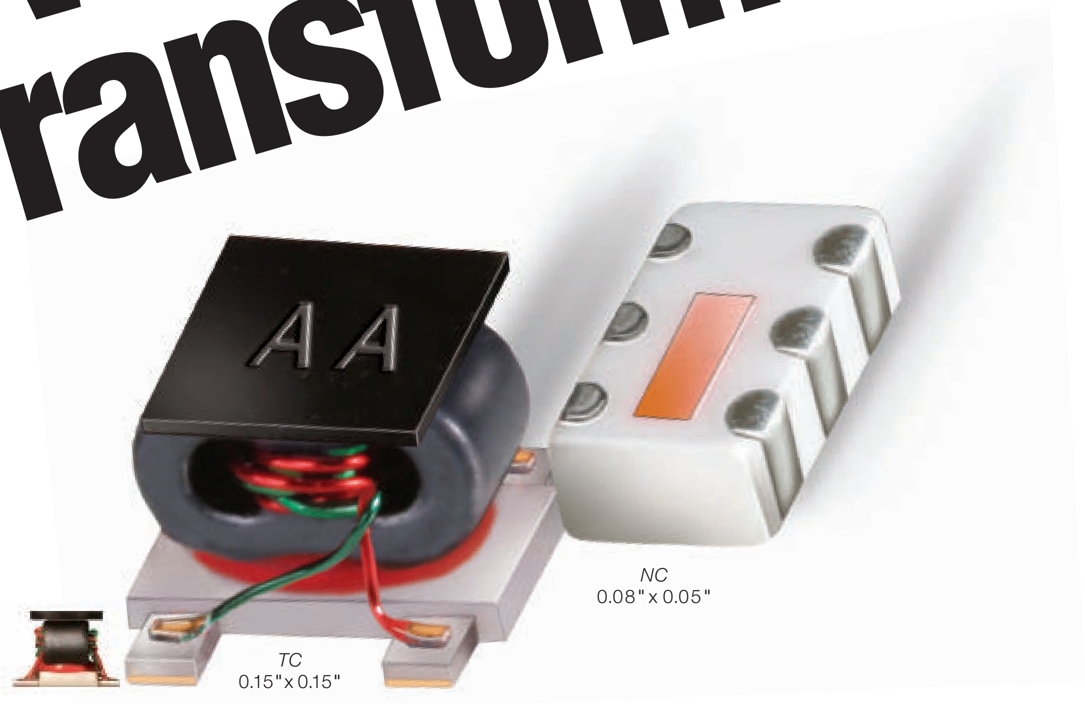

0.15-6200 MHz as low as 99¢ each (qty. 1000) RoHS compliant.

Rugged, repeatable performance.
At Mini-Circuits, we're passionate about transformers. We even make own transmission line wire under tight manufacturing control, and utilize all-welded connections to maximize performance, reliability, and repeatability. And for signals up to 6 GHz, our rugged LTCC ceramic models feature wrap-around terminations for your visual solder inspection, and they are even offered in packages as small as 0805!

Continued innovation: Top Hat.
A Mini-Circuits exclusive, this new feature is now available on every open-core transformer we sell. Top Hat speeds customer pick-and-place throughput in four distinct ways: (1) faster set-up times, (2) fewer missed components, (3) better placement accuracy and consistency, and (4) high-visibility markings for quicker visual identification and inspection.

More models, to meet more needs
Mini-Circuits has over 200 different SMT models in stock. So for RF or microwave baluns and transformers, with or without center taps or DC isolation, you can probably find what you need at minicircuits.com. Enter your requirements, and Yoni2, our patented search engine, can identify a match in seconds. And new custom designs are just a phone call away, with surprisingly quick turnaround times gained from over 40 years of manufacturing and design experience!

See minicircuits.com for technical specifications, performance data, pricing, and real-time, in-stock availability!
Mini-Circuits...we're redefining what Value is all about!

Mini-Circuits®
ISO 9001 ISO 14001 AS 9100
P.O. Box 350166, Brooklyn, New York 11235-0003 (718) 934-4500 Fax (718) 332-4661

Yoni2® **The Design Engineers Search Engine** *finds the model you need, Instantly* • For detailed performance specs & shopping online see **minicircuits.com**
U.S. Patents 7739260, 7761442

IF/RF MICROWAVE COMPONENTS

377 rev Y

Turn USB Power Sensors into

Smart RF POWER METERS

from -35 up to +20 dBm 9 kHz to 8 GHz

• ***True RMS model now available!*** • *Lightning-fast measurement, as quick as 10 ms**
• *Compatible with most test software†* • *Up to 55 dB dynamic range* • *Measurement averaging*

Don't break your bank with expensive conventional power meters. Mini-Circuits USB Power Sensors turn almost any Linux® or Windows® based computer into a low-cost testing platform for all kinds of RF components. Reference calibration is built in, and your USB port supplies required power. Our GUI offers a full range of watt or dB measurements, including averaging, frequency sweeps, and multi-sensor support.

Our power sensors can be carried in your pocket, or mounted remotely for manual or automated system monitoring (internet connectivity required). Data can be viewed on-screen or exported to Excel® spreadsheets for reporting and analytic tools. Mini-Circuits Power Sensors cost half as much as you might expect, so why do without? Place an order today, and we can have it in your hands as early as tomorrow.

All Power Sensor models include:

- *Power Sensor Unit*
- *Power Data Analysis Software*
- *SMA Adaptor (50Ω only)*
- *USB Cable*

Model	Frequency	Price $ ea. (Qty 1-4)
PWR-4GHS	9 kHz-4 GHz	795.00
PWR-2GHS-75	100 kHz-2 GHz	795.00
PWR-2.5GHS-75	100 kHz-2.5 GHz	895.00
PWR-6GHS	1 MHz-6 GHz	695.00
PWR-8GHS	1 MHz-8 GHz	869.00
PWR-8FS	1 MHz-8 GHz	969.00
NEW! PWR-4RMS	50 MHz-4 GHz	1169.00

** Measurement speed as fast as 10 ms with PWR 8 FS. All other models as fast as 30 ms.*

† See datasheets for an extensive list of compatible software.

Windows and Excel are registered trademarks of Microsoft Corporation in the US and other countries. Linux is a registered trademark of Linus Torvalds. Neither Mini-Circuits nor Mini-Circuits Power Sensors are affiliated with or endorsed by the owners of the above-referenced trademarks.

Mini-Circuits...we're redefining what VALUE is all about!

RoHS compliant

Mini-Circuits®
ISO 9001 ISO 14001 AS 9100

P.O. Box 350166, Brooklyn, New York 11235-0003 (718) 934-4500 Fax (718) 332-4661

Yoni2® ***The Design Engineers Search Engine*** *finds the model you need, Instantly* • For detailed performance specs & shopping online see **minicircuits.com**

U.S. Patents 7739260, 7761442

IF/RF MICROWAVE COMPONENTS

488 rev M

Active DAS Equipment Market for In-Building Wireless to Cross $1 B

Active distributed antenna systems (DAS) equipment revenues are estimated to cross $1 billion by 2013. Active DAS equipment is mostly made up of head-end and remote units, which are used to distribute cellular signals throughout a building.

The global market for in-building wireless equipment is estimated to reach $2 billion by 2013, with Active DAS contributing 50 percent of the total revenues. The other half includes passive DAS, repeaters, cabling and antennas. The overall market for in-building wireless, which includes equipment and service revenues, also known as labor costs, is estimated to reach $3.6 billion by the end of 2013.

Aditya Kaul, practice director, mobile networks at ABI Research says, "Active DAS is the fastest growing segment of the market today, as large public and commercial buildings need highly scalable, flexible, high-capacity, multi-technology and multi-operator solutions. While active DAS is where the action is, traditional passive DAS and repeaters will continue to see demand, especially in Asia Pacific and some parts of Europe because of their cost-effectiveness and operator familiarity."

The Active DAS equipment market has an overall CAGR of 15 percent, with the North American region being the strongest, where the market is growing at 20 percent annually. Passive DAS equipment revenue on the other hand is expected to show a modest CAGR of 6 percent in North America. The market data mainly covers DAS and repeater equipment, but does account for the impact of small cells on DAS systems. Small cells and DAS intersect mostly in small and medium-sized buildings where small cells could be deployed independently in place of DAS, complement DAS as a hotpot fill-in, or more importantly, feed into DAS replacing the need of large expensive macro base stations, repeaters or even remote radio heads.

In-Building Wireless Equipment Overview,
Equipment Revenue by Component
World Market, 2011 – 2017

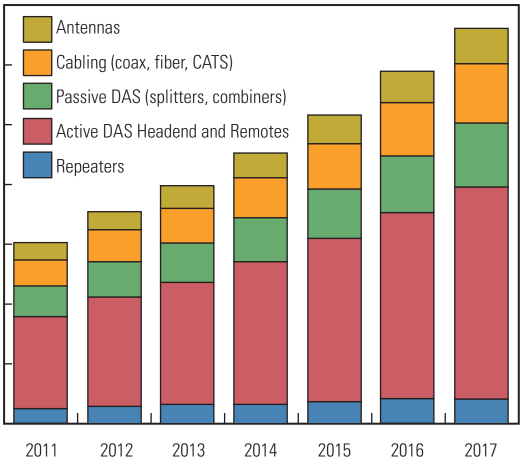

Source: ABI Research

Plextek a Key Part of European Project to Reduce Household Carbon Footprint

Plextek is developing a pioneering solution to the growing energy demands of household appliances – starting with the humble microwave. Research from the Energy Saving Trust shows that one third of household energy bills and well over a quarter of household carbon dioxide emissions, comes from electrical appliances. Plextek, in conjunction with the ENIAC Joint Undertaking, set up to encourage collaboration within Europe's largest organizations, SMEs and academic institutions, aims to achieve the goal to enhance the miniaturization of devices and their functionality, while improving overall energy efficiency.

Experts estimate that microwaves account for 12.8 tera watt-hours per year, the equivalent of boiling more than 400 billion cups of tea.

The collaboration has set the target of reducing household consumption by 25 percent through technological advancements. Gareth Williams, director of Plextek's Digital Engineering Group, believes that it is an aggressive target, but one Plextek must strive to achieve.

"The footprint of our household appliances is constantly on the rise, correlating with the huge growth in the amount of household appliances that we each use. There is already some great work being done to encourage behavior change in our society in the way that we manage these appliances, but we aim to revolutionize the products right from blueprint stage."

Over 190 million households in Europe possess a microwave oven, adding to the plethora of cold and hot appliances contributing to homeowner electricity bills. Experts estimate that microwaves account for 12.8 tera watt-hours per year, the equivalent of boiling more than 400 billion cups of tea.

The joint undertaking has refined its research into the way that radio frequency (RF) energy is used in everyday appliances such as microwaves. Plextek has completed the first stage of a three-year project, in conjunction with its partners and is currently in the process of constructing prototype microwaves to be tested for study and the results could make a significant impact on household bills.

Gareth Williams continued, "Clearly the food preparation sector is likely to benefit from this program, but other industries outside domestic cooking are also likely to benefit: Areas such as microwave drying, mobile basestation design, and radar technology to name a few. It's exciting to have so many different organizations coming together as part of this aspiring venture."

The other companies collaborating with Plextek as part of this project are Whirlpool, NXP, Comheat, Bergh Hybrid Circuits and the Universities of Warsaw, Chalmers, Padova and TU Delft.

Go to mwjournal.com for more commercial market news items

The ENIAC Joint Undertaking, set up in February 2008, has allocated grants for projects selected for funding until December 31, 2017. The total value of the research and development activities generated through this partnership upon its conclusion is estimated at €3 billion.

Microwave Small Cell Backhaul Equipment Market Will Reach $6.4 B in 2017

ABI Research expects the market for small cell microwave backhaul equipment to grow to over $6.4 billion in 2017, up from a forecast $1.5 billion for 2012 which represents a 35 percent compound annual growth rate. Millimeter wave line-of-sight (MMW LoS) will accumulate 44 percent of revenue, or over $2.8 billion, with 23 percent of microwave links in 2017, Orthogonal Frequency-Division Multiplexing Non Line-of-Sight (OFDM NLoS) will capture 31 percent of small cell microwave backhaul equipment revenue, or $1.9 billion, with 48 percent of links in 2017, and Wi-Fi will capture almost 19 percent of revenue or $784 million, with 12 percent of small cell backhaul links.

"Thanks to its NLoS properties and Point-to-Multipoint (PMP) hub-and-spoke architecture OFDM NLoS becomes the most popular backhaul technology for small cells in 2017," says Nick Marshall, principal analyst at ABI Research. ABI Research believes that the millimeter wave bands from 60 to 80 GHz (MMW LoS) will also prove compelling for small cell backhaul in many situations. Traditional microwave LoS (6 to 38 GHz) equipment for small cell applications is overtaken by these technologies and will represent only 13 percent of revenue and 10 percent of links in 2017. ABI Research also expects fiber backhaul solutions to experience a healthy growth between 2012 and 2017 with small cell backhaul over fiber reaching almost 24 percent in 2017, up from 7 percent in 2012, with regions like China and North America favoring fiber as a backhaul solution in many circumstances. "We believe that 4G/LTE small cell solutions will again drive most of the microwave and fiber backhaul growth in metropolitan, urban and suburban areas," continues Marshall.

Traditional microwave LoS (6 to 38 GHz) equipment for small cell applications is overtaken by these technologies and will represent only 13 percent of revenue and 10 percent of links in 2017.

Around the Circuit

Laura Glazer, Staff Editor

INDUSTRY NEWS

Agilent Technologies Inc. announced an agreement to collaborate with **China Mobile Communications Co. Ltd. Research Institute** (CMRI). China Mobile is the world's largest mobile network operator and a market leader in 3G and next-generation wireless network development. The two companies signed a memorandum of understanding in Beijing to initiate a collaboration that will focus on developing technology and test methods for a next-generation cloud-based radio access network, or C-RAN, a new approach to network design aimed at building an environmentally friendly, cost-effective, intelligent network.

The boards of **Navratna1 Public Sector Co.**, **Bharat Electronics Ltd.** (BEL) and **Thales** have approved the formation of a joint venture company (JVC) subject to statutory approvals of the Government of India and the French Government. The JVC will be dedicated to the design, development, marketing, supply and support of civilian and select defense radars for Indian and global markets. The parent companies aim to make the JVC a center of excellence with the ability to offer solutions specifically aimed at meeting the needs of both Indian and export customers.

Teledyne Technologies Inc. and **LeCroy Corp.** announced the successful completion of the acquisition of LeCroy. At a special meeting of stockholders, LeCroy stockholders approved and adopted the Agreement and Plan of Merger, dated as of May 28, 2012, by and among LeCroy, Teledyne and a wholly-owned subsidiary of Teledyne. Pursuant to the transaction, effective August 3, 2012, Teledyne acquired all of the outstanding common shares of LeCroy for $14.30 per share payable in cash. The aggregate value for the transaction, excluding transaction costs, was approximately $291 million, taking into account LeCroy's stock options, stock appreciation rights and net debt as of March 31, 2012.

Tektronix Component Solutions announced an agreement with leading supply chain aggregator **MOSIS** to help customers develop complete, high-performance ASIC solutions while reducing the cost of early-stage ASIC development. Through the use of multi-project wafer runs for device prototyping and package development early in the design cycle, customers can cost effectively improve the time to first packaged ASIC, rather than developing their own complete mask set prior to first silicon tape-out.

Lime Microsystems has announced a partnership agreement with the strategic investment firm **In-Q-Tel**, an independent, non-profit organization that identifies innovative technology solutions to support the missions of the U.S. Intelligence Community. The partnership will enable advances in transceiver technology to be deployed in commercial and government markets, and the creation of state of the art systems that can be used across many applications.

Autotalks and **Altis Semiconductor** announced that they have reached a cooperative agreement on the development of Autotalks' PLUTON automotive grade vehicle-to-vehicle RF transceiver to be manufactured by Altis Semiconductor. Together with Autotalks' CRATON integrated communication controller, they form a comprehensive, automotive grade, VLSI solution enabling OEMs' deployment of vehicle-to-vehicle in 2015 model year. Autotalks has further selected to partner, for circuit and system design, with **Catena Holding Bv**, a leader in high performance RF IP, with a proven track record in design for automotive applications and high performance IEEE802.11p RF.

Aeris® Communications, the only cellular carrier built exclusively for machines, announced it has partnered with **Novotech Technologies**, a leading global distributor of wireless, machine-to-machine (M2M) products, services and solutions, to deliver M2M connectivity services. With this partnership, Novotech will begin distributing products connected by Aeris' intelligent machine framework. Aeris' network will optimize performance and provide the deepest level of visibility for every Novotech device on its network.

Peregrine Semiconductor Corp. announced the pricing of its initial public offering of 5,500,000 shares of common stock at a price to the public of $14 per share. Of the 5,500,000 shares being offered, 5,340,780 are being offered by Peregrine and 159,220 shares are being offered by certain selling stockholders. The company will not receive any proceeds from the sale of shares by the selling stockholders. Peregrine has also granted the underwriters a 30-day option to purchase up to 825,000 additional shares of common stock from Peregrine.

CTIA - The Wireless Association® and **Global Certification Forum** (GCF) have agreed to a common process for evaluating the over-the-air performance of new wireless devices. The agreement allows GCF to incorporate CTIA's Test Plan for Wireless Device Over-the-Air Performance into its Performance Measurement process. The agreement also allows the organizations to work together on future updates of the test plan to ensure that the needs of network operators and device vendors throughout the world are being addressed.

RF Micro Devices Inc. announced it received "Product of the Year" awards from **Cable Spotlight** for three of its broadband cable television (CATV) products. The award winning products – the RFAM2790 integrated EDGE QAM amplifier, the RFCM2680 GaAs/GaN power doubler and the RFPP2870 push-pull amplifier – highlight RFMD's product and technology leadership and the company's ability to improve performance and enhance functionality of global CATV access networks.

For up-to-date news briefs, visit mwjournal.com

HIGH POWER PRODUCTS

POWER DIVIDERS

Model #	Frequency (MHz)	Insertion Loss (dB) [Typ./Max.] ◊	Amplitude Unbalance (dB) [Typ./Max.]	Phase Unbalance (Deg.) [Typ./Max.]	Isolation (dB) [Typ./Min.]	VSWR (Typ)	Input Power (Watts) [Max.] ◦	Package
2-WAY								
CSBK260S	20 - 600	0.28 / 0.4	0.05 / 0.4	0.8 / 3	25 / 20	1.15:1	50	377
DSK-729S	800 - 2200	0.5 / 0.8	0.05 / 0.4	1 / 2	25 / 20	1.3:1	10	215
DSK-H3N	800 - 2400	0.5 / 0.8	0.25 / 0.5	1 / 4	23 / 18	1.5:1	30	220
P2D100800	1000 - 8000	0.6 / 1.1	0.05 / 0.2	1 / 2	28 / 22	1.2:1	5	329
DSK100800	1000 - 8000	0.6 / 1.1	0.05 / 0.2	1 / 2	28 / 22	1.2:1	20	330
DHK-H1N	1700 - 2200	0.3 / 0.4	0.1 / 0.3	1 / 3	20 / 18	1.3:1	100	220
P2D180900L	1800 - 9000	0.4 / 0.8	0.05 / 0.2	1 / 2	27 / 23	1.2:1	5	331
DSK180900	1800 - 9000	0.4 / 0.8	0.05 / 0.2	1 / 2	27 / 23	1.2:1	20	330
3-WAY								
S3D1723	1700 - 2300	0.2 / 0.35	0.3 / 0.6	2 / 3	22 / 16	1.3:1	5	316

◊ In excess of theoretical split loss of 3.0 dB
◦ With matched operating conditions

HYBRIDS

Model #	Frequency (MHz)	Insertion Loss (dB) [Typ./Max.] ◊	Amplitude Unbalance (dB) [Typ./Max.]	Phase Unbalance (Deg.) [Typ./Max.]	Isolation (dB) [Typ./Min.]	VSWR (Typ)	Input Power (Watts) [Max.]	Package
90°								
DQS-30-90	30 - 90	0.3 / 0.6	0.8 / 1.2	1 / 3	23 / 18	1.35:1	25	102SLF
DQS-3-11-10	30 - 110	0.5 / 0.8	0.6 / 0.9	1 / 3	30 / 20	1.30:1	10	102SLF
DQS-30-450	30 - 450	1.2 / 1.7	1 / 1.5	4 / 6	23 / 18	1.40:1	5	102SLF
CSDK3100S	30 - 1000	0.8 / 1.2	0.05 / 0.2	0.2 / 3	25 / 18	1.15:1	50	378
DQS-118-174	118 - 174	0.3 / 0.6	0.4 / 1	1 / 3	23 / 18	1.35:1	25	102SLF
DQK80300	800 - 3000	0.2 / 0.4	0.5 / 0.8	2 / 5	20 / 18	1.30:1	40	113LF
MSQ80300	800 - 3000	0.2 / 0.4	0.5 / 0.8	2 / 5	20 / 18	1.30:1	40	325
DQK100800	1000 - 8000	0.8 / 1.6	1 / 1.6	1 / 4	22 / 20	1.20:1	40	326
MSQ100800	1000 - 8000	0.8 / 1.6	1 / 1.6	1 / 4	22 / 20	1.20:1	40	346
MSQ-8012	800 - 1200	0.2 / 0.3	0.2 / 0.4	2 / 3	22 / 18	1.20:1	50	226
180° (4-PORTS)								
DJS-345	30 - 450	0.75 / 1.2	0.3 / 0.8	2.5 / 4	23 / 18	1.25:1	5	301LF-1

◊ In excess of theoretical coupling loss of 3.0 dB

COUPLERS

Model #	Frequency (MHz)	Coupling (dB) [Nom]	Coupling Flatness (dB)	Mainline Loss (dB) [Typ./Max.]	Directivity (dB) [Typ./Min.]	Input Power (Watts) [Max.] ◦	Package
KDS-30-30	30 - 512	27.5 ±0.8	±0.75	0.2 / 0.28	23 / 15	50	255 *
KFK-10-1200	10 - 1200	40 ±0.75	±1.0	0.4 / 0.5	22 / 15	150	376
KBS-10-225	225 - 400	10.5 ±1.0	±0.5	0.6 / 0.7	25 / 18	50	255 *
KDS-20-225	225 - 400	20 ±1.0	±0.5	0.2 / 0.4	25 / 18	50	255 *
KBK-10-225N	225 - 400	10.5 ±1.0	±0.5	0.6 / 0.7	25 / 18	50	110N *
KDK-20-225N	225 - 400	20 ±1.0	±0.5	0.2 / 0.4	25 / 18	50	110N *
KEK-704H	850 - 960	30 ±0.75	±0.25	0.08 / 0.2	38 / 30	500	207
SCS100800-10	1000 - 8000	10.5 ±1.5	±2.0	1.2 / 1.8	8 / 5	25	361
KBK100800-10	1000 - 8000	10.5 ±1.5	±2.0	1.2 / 1.8	8 / 5	25	322
SCS100800-16	1000 - 7800	16.8 ±1.5	±2.8	0.7 / 1	14 / 5	25	321
KDK100800-16	1000 - 7800	16.8 ±1.5	±2.8	0.7 / 1	14 / 5	25	322
SCS100800-20	1000 - 7800	20.5 ±2.0	±2.0	0.45 / 0.75	12 / 5	25	321
KDK100800-20	1000 - 7800	20.5 ±2.0	±2.0	0.45 / 0.75	14 / 5	25	322

* Add suffix - LF to the part number for RoHS compliant version.
◦ With matched operating conditions

Unless noted, products are RoHS compliant.

SYNERGY® MICROWAVE CORPORATION

Phone: (973) 881-8800 | Fax: (973) 881-8361
E-mail: sales@synergymwave.com
Web: WWW.SYNERGYMWAVE.COM
Mail: 201 McLean Boulevard, Paterson, NJ 07504

Around the Circuit

CONTRACTS

Anaren Inc. has received three contracts totaling in excess of $11.5 million in follow-on orders for passive ranging subsystems to be deployed in airborne applications. These orders from a defense OEM customer are related to a continuing long-term supply agreement for both domestic and international applications of Anaren's proprietary electronic warfare technology. Deliveries are expected to be completed over a 26 month timeframe beginning in the first quarter of calendar 2013.

Cobham Antenna Systems has been awarded a contract from **Embraer S.A.** to design and manufacture nose radomes for the KC-390 military transport aircraft being developed for the **Brazilian Air Force**. The company has also been awarded orders totaling more than £13.8 million during the second quarter of 2012 to supply European customers with hand-held Improvised Explosive Device (IED) detection equipment incorporating the group's leading-edge Ground-Penetrating Radar (GPR) systems. These orders will be delivered during the second half of 2012 from the Cobham Antenna Systems site in Leatherhead, UK.

LadyBug Technologies has been awarded a contract from a branch of the **U.S. Armed Forces** for the company's power meter/sensor products. The contract covers LadyBug's model LB479A PowerSensor+™, a 10 MHz to 10 GHz wide dynamic range average power sensor capable of measuring CW, pulse and other signals.

PERSONNEL

▲ *Bob Ferrante*

Crane Aerospace & Electronics appointed **Bob Ferrante** as VP of the microwave solution of its electronics group. In his role, Ferrante is responsible for operations of all electronics group microwave solutions locations, including those in MA, AZ, NJ and Costa Rica. He will be located in West Caldwell, NJ. He has over 30 years of experience in the defense electronics industry and holds a BS in Political Science from Catholic University of America Washington, DC.

American Microwave Corp. welcomes **Pete Schramm** as its new director of sales and marketing. Schramm's focus will be on finding new growth opportunities while building stronger relations with the current customer base in conjunction with AMC's Rep Organization. Schramm brings a wealth of knowledge to AMC in sales and channel management with over 30 years of experience in the communications, optical and RF/microwave, and test and measurement marketplaces. Schramm will be based out of the company's Frederick, MD facility.

John Dimech joined **TRM Microwave** as business development manager. Dimech has a technical background and 20+ years of experience supporting products including

Around the Circuit

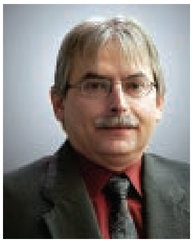

▲ John Dimech

components, multi-functional modules, test equipment, sub-assemblies and box level manufacturing and test. He will focus on expanding the company's reach into existing key accounts while cultivating new business development in support of TRM's strategic growth plan. Prior to joining TRM, Dimech was director of sales for Plansee-TMS, director of business development at Natel Engineering and has held a number of sales positions at Merrimac Industries.

▲ Brian Landy

Microwave Journal has appointed **Brian Landy** as the new sales manager covering the Pacific and Mountain U.S. time zones. Landy has extensive electronics-industry focused marketing experience, providing integrated media solutions to companies on the west coast over the past 15 years, while representing brands such as *EDN*, *ECN* and *Electronic News*. Landy lives in Santa Cruz, CA with his wife and two daughters. He can be reached at blandy@mwjournal.com.

REP APPOINTMENTS

Custom MMIC announced the appointments of **MHz Marketing**, **Southeastern Sales RF** and **Allegiance Sales** as its technical sales representatives. MHz Marketing will represent Custom MMIC in the mid-Atlantic, Southeastern will cover FL, and Allegiance Sales will cover TX.

Delta Microwave announced the appointment of **Spectrant** as the company's exclusive sales representative in southern CA.

Digi-Key Corp. announced the signing of a global distribution agreement with the RF Solutions Division of **API Technologies Corp.** The global distribution agreement includes products from API's Spectrum Control and Spectrum Sensors line of products, as well as antenna products from the API's Spectrum Microwave line.

Hesse & Knipps Inc. has appointed **Prospect Technical Sales** to support the company's family of wedge bonders in NV, OR, WA, MT, UT, CO, northern CA and the Canadian provinces of British Columbia and Alberta. Hesse & Knipps Inc. has also appointed **CWI Technical Sales** as its representative along the United States east coast (states of CT, MA, RI, VT, ME, NH, NY, NJ, DE, MD, PA, WV, VA, NC, SC, GA and FL) as well as the Canadian provinces of Quebec and Ontario.

Prober.com has entered a multi-year cooperative agreement with **ERS America LLC** as exclusive representative of its wafer level heating and cooling chuck systems in the Pacific Northwest states of OR, WA, CA, ID and UT.

Maximizing Receiver Dynamic Range for Spectrum Monitoring

As consumers continue to demand more data wirelessly through mobile devices, the increased bandwidth to support these applications has considerable implications on the usage of the RF spectrum. Currently, 75 percent of wireless devices in the U.S. are broadband capable.[1] In his keynote speech to the International CTIA Wireless 2012 Conference, FCC Chairman, Julius Genachowski talked of the "looming spectrum crunch" and made the statement that "… it is becoming increasingly harder to find free and clear blocks of spectrum." Estimates are that between 2010 and 2015, the mobile data traffic will increase at a compound annual growth rate of 92 percent.[2] This near insatiable need for more bandwidth drives the requirement for specialized equipment to monitor the RF spectrum.

Spectrum analyzers often come to mind as the receiver solution for making over-the-air spectrum monitoring measurements. Modern RF signal analyzer designs such as the vector signal analyzer (VSA) add useful features for digital signal demodulation. However, since both instruments are optimized for cabled measurements, they are subject to dynamic range limitations in spectrum monitoring applications. For this reason, a specialized receiver optimized for over-the-air measurements should be considered.

OVER-THE-AIR SIGNAL ENVIRONMENT

In many ways, the "over-the-air" signal environment is drastically different from the signal environment of a typical cabled measurement where the number of large amplitude signals is limited and whose frequencies are generally known. A quick scan of the RF spectrum would reveal signal content at a wide range of frequencies, including higher power FM radio around 100 MHz to cellular base stations at frequencies of 900 MHz and beyond. Often, the requirement is to observe a low amplitude signal in the presence of interfering large amplitude signals.

Consider the case when a signal of interest is at a low amplitude level, forcing the operator

Brian Avenell
National Instruments Corp., Austin, TX

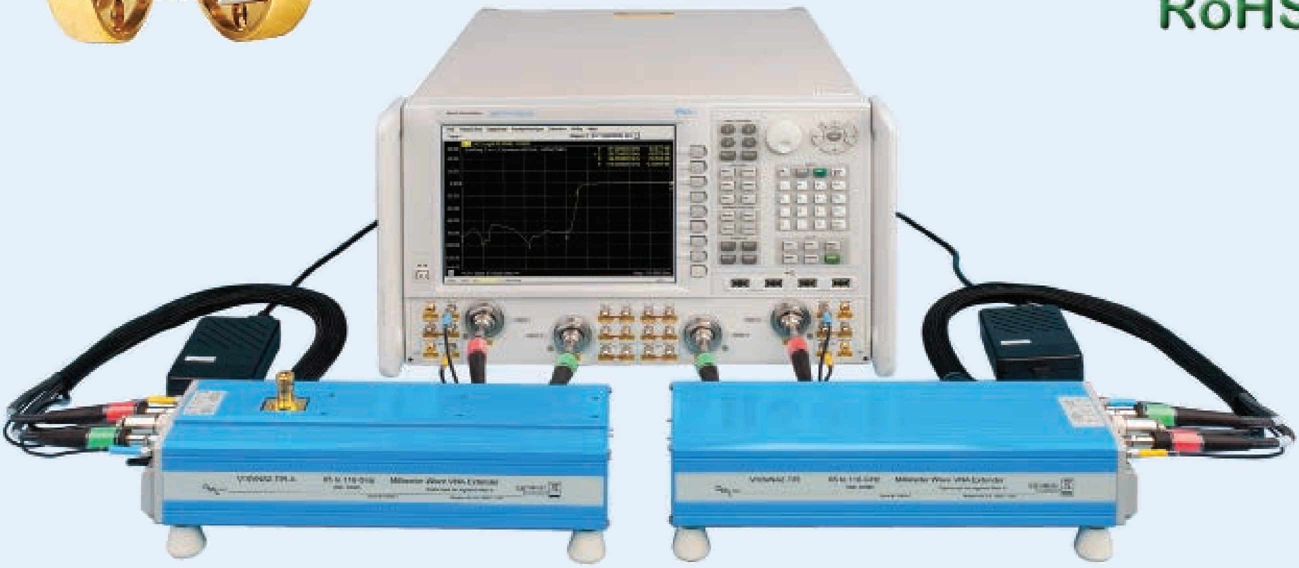

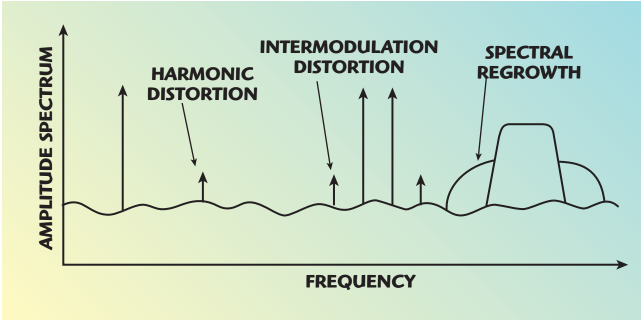

▲ *Fig. 1 Distortions in the RF spectrum.*

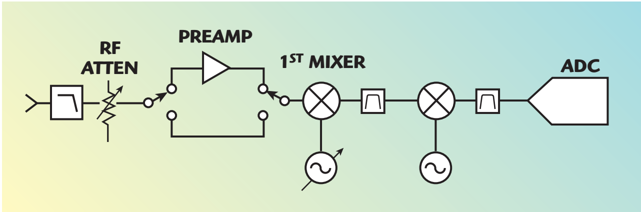

▲ *Fig. 2 Spectrum analyzer lowband path block diagram.*

to increase the receiver gain in order to improve the receiver's sensitivity. With higher gain, the receiver is more vulnerable to large amplitude interfering tones producing distortion in receiver front end components. If the distortion signal falls on or near a signal of interest, deciphering the distortion signal from the actual signal can be difficult, as shown in ***Figure 1***.

Especially when analyzing low-power over-the-air signals, both harmonic distortion and intermodulation distortion introduced in nonlinear components of the signal chain can obscure the signal of interest. Harmonic distortion, which results from a single carrier, is generated in the receiver's first mixer and any nonlinear component in front of the first mixer. Intermodulation distortion (IMD) results from two or more carriers mixing in any nonlinear component. These closely spaced carriers can all progress through the entire receiver chain resulting in IMD from both the RF and IF sections. Spectral regrowth is distortion associated with digitally modulated signals and is a problem when this distortion leaks into adjacent channels.

In addition to distortion masking the signals of interest, broadband noise due to the measurement antenna or the measurement receiver itself can mask the low amplitude signals of interest. Using the receiver's gain adjustment results in a tradeoff between the receiver's noise and distortion performance. Simultaneously achieving low distortion and low noise is often a conflicting requirement.

MEASUREMENT RECEIVER LIMITATIONS

Most spectrum analyzers rely on a dual RF path architecture: lowband and highband. The highband path normally uses a YIG Tuned Filter (YTF) as a preselector in front of the

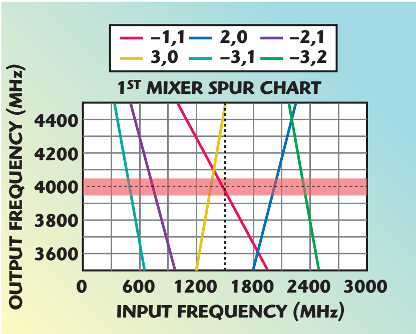

▲ *Fig. 3 Mixer spur chart.*

rest of the signal chain. However, in the lowband path, below the operating frequency of the YTF, the RF path is most often not preselected. The typical spectrum analyzer's lowband path is shown in ***Figure 2***.

Mixer spurious responses are governed by:

$$mf_{RF} + nf_{LO} = f_{IF} \qquad (1)$$

where m,n are integer values representing harmonics of the RF and LO signals. At any given LO frequency, all possible combinations of the harmonics of the RF and LO signals that satisfy Equation 1 will generate an IF response and will be visible on the receiver's display.

A graphical representation of the mixer spur equation is shown in the spur chart. ***Figure 3*** shows the mixer spur chart for a typical spectrum analyzer lowband path. The x-axis represents the RF port signal frequency and the y-axis represents the IF port


AWR
A National Instruments Company™
Achieve hyper speed simulations on complex multi-tone circuits.
Stop waiting and waiting and waiting for your complex multi-tone designs to simulate. AWR users don't wait. They simulate at turbo speeds thanks to multi-rate harmonic balance (MRHB) technology. With simulation times that are typically 10x faster, designs with 2, 3, 4 or even more tones converge quickly — and nail the performance, too! Fewer mouse clicks and novel MRHB technology mean shorter process times, right-the-first-time designs, and less stress for you. Don't you deserve that? Grab a test copy at awrcorp.com/MWO.
Stop waiting and start designing™
MICROWAVE OFFICE™
© 2012 AWR Corporation. All rights reserved.

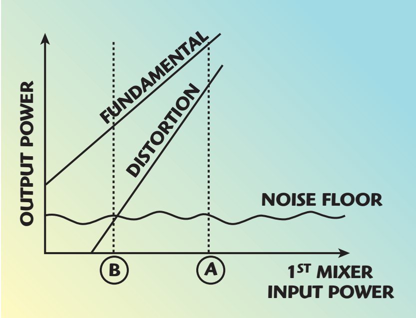

▲ *Fig. 4 Power out vs. power in for receiver fundamental and distortion tones.*

frequency. In this example, the spectrum analyzer is tuned to a frequency of 1.5 GHz with an IF of 4 GHz. The LO frequency needed to support this configuration is 5.5 GHz.

The m = –1, n = 1 response is the desired mixing product. An RF signal present at the tune frequency of 1.5 GHz will produce the wanted displayed response. All other lines on the chart represent spurious responses. When a spur line crosses the horizontal center band, which represents the IF port bandwidth, this signifies that the mf_{RF} and nf_{LO} combination produces an unwanted signal at f_{IF}. Once this undesired signal falls on the IF frequency of the first mixer, the IF signal progresses through the rest of the receiver chain. In this example, if an RF signal is present at 1.33 GHz, the (3,0) mixer spur response generates an unwanted response even though the receiver is tuned to 1.5 GHz. Deciphering a true signal response at 1.5 GHz from the spurious response generated by the 1.33 GHz RF signal becomes a challenge. Because the lowband path of the typical spectrum analyzer normally contains only a single lowpass filter, the first mixer is vulnerable to spurious responses generated by signals whose frequency is anywhere within the lowband frequency range.

Another form of spurious responses is due to intermodulation distortion resulting from two or more signals present at the input of the receiver. If two signals are present at RF frequencies of f_1 and f_2 then third-order IMD products fall at frequencies of $2 \times f_2 - f_1$ and $2 \times f_1 - f_2$. If there is a signal of interest whose frequency is located near one of the distortion products, it is possible to confuse the signal for the receiver-generated distortion product. One technique to minimize the receiver generated distortion amplitudes is to reduce the power levels of the fundamental tones before they reach the first mixer. In the spectrum analyzer, the RF attenuator accomplishes this task. However, reducing the fundamental signal power at the first mixer also decreases the receiver's sensitivity. ***Figure 4*** illustrates the concept of improved distortion performance at the expense of degraded sensitivity as a function of first mixer power level.

At point 'A,' the RF attenuation is relatively low, allowing the high power fundamental tone to reach the first mixer. This results in a relatively high signal-to-noise ratio (SNR) at the expense of relatively large distortion levels. At point 'B,' the RF attenuation has been increased to lower the fundamental tone power incident on the first mixer. While this reduces distortion signal amplitude, the consequence is degraded receiver SNR.

The temptation to overcome degraded receiver sensitivity is to employ a preamplifier that is either part of the spectrum analyzer as shown in Figure 2 or is external to the spectrum analyzer. The improvement in SNR by switching in the preamplifier usually coincides with much worse distortion performance. The end result is worse receiver dynamic range by using the preamplifier over the dynamic range when the preamplifier is bypassed.

Vector signal analyzers are characterized by having IF bandwidths at least as wide as the signal's modulation bandwidth. Measurements such as error vector magnitude (EVM) require sampling of the entire signal. With a wide bandwidth final IF in the receiver chain, the analog-to-digital converter (ADC) can easily be overdriven by unwanted signals when trying to maximize the SNR. Especially if the low amplitude signal of interest is close in frequency to a stronger interfering signal, the ADC may introduce harmonics and intermodulation distortion products and mask the signal of interest.

Additionally, the noise figure of the ADC is normally higher than the noise figure of the front end. Increasing the front end gain is required to minimize the noise impact of the ADC to the overall noise figure of the receiver.

RFMD.

High-Power GaN Power ICs

RFMD's GaN Power ICs (PICs) are wideband power amplifiers designed for continuous wave and pulsed applications such as military communications, electronic warfare, wireless infrastructure, radar, two-way radios, and general purpose amplification. Using an advanced high power density Gallium Nitride (GaN) semiconductor process, these high-performance amplifiers achieve high efficiency, flat gain, and power over a large instantaneous bandwidth in a single amplifier design. These GaN discrete amplifiers are 50Ω input-matched, packaged in a small form factor 5 x 6mm SOIC-8 outline air cavity ceramic package that provides excellent thermal stability through the use of advanced heat-sink and power-dissipation technologies. Ease of integration is accomplished through the incorporation of optimized input matching network within the package that provides wideband gain and power performance in a single amplifier.
An external output match offers the flexibility of further optimizing power and efficiency for any sub-band within the overall bandwidth.

SPECIFICATIONS

Freq Range (Min) (MHz)	*Freq Range (Max) (MHz)*	*Gain (dB)*	*OP3dB (dBm)*	*Power Added Efficiency (%)*	*V_D (V)*	*I_D (mA)*	*Package*	*Part Number*
30	2500	11.0	39.0	40.0	28	55	AIN SOIC-8	RF3826
50	1000	16.0	41.3	53.0	28	88	AIN SOIC-8	RFHA1000
30	512	18.5	39.5	70.0	28	55	AIN SOIC-8	RFHA1003
225	1215	16.6	39.4	62.5	28	88	AIN SOIC-8	RFHA1006

FEATURES

- Advanced GaN HEMT technology
- Advanced heat-sink technology
- Input internally matched to 50Ω
- High power added efficiency
- -40ºC to 85ºC operating temperature
- Wide instantaneous bandwidth
- Large signal models available

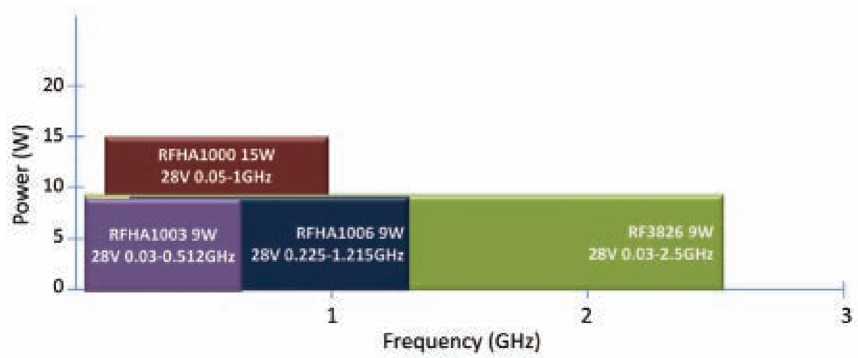

Mobility. Connectivity. Energy.

With strong interfering tones within the bandwidth of the IF, increasing front end gain to improve receiver sensitivity can lead to additional distortion in the final amplifier stages of the receiver.

SPECTRUM MONITORING RECEIVER

The spectrum monitoring receiver builds upon the spectrum analyzer by adding a preselection filter at the RF input and analog IF filters, termed roofing filters, in the final IF. ***Figure 5*** shows where these additional elements are added to the basic spectrum analyzer structure.

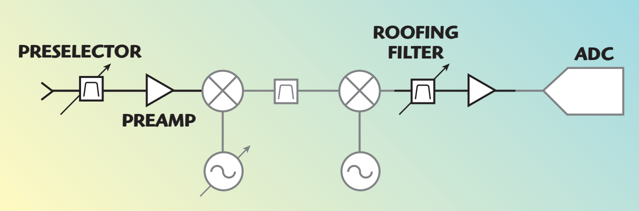

▲ *Fig. 5 Spectrum monitoring receiver block diagram.*

The preselector filter can either be a bank of fixed tuned filters or a tunable filter. In either case, the bandwidths of the filters should be less than one octave in order to effectively block harmonics of strong interfering signals. In ***Figure 6***, the signal of interest is located at a frequency of f_2. The preselector filter tunes to allow f_2 to pass. If a large amplitude interfering signal located at a frequency of f_1, such that $f_1 = f_2/2$, is present, the preselector filter prevents the receiver's first mixer from generating 2nd harmonic distortion that would potentially mask the signal of interest.

The location of the preamplifier is crucial. It is purposely located after the preselector filter. Preamplifiers require large gain and low noise figure to overcome the noise figure of the down-stream receiver. By locating the preamplifier after the preselector filter, large amplitude interfering signals are attenuated before they reach the preamplifier. The result is both good distortion and good noise figure for the receiver. For this reason, noise performance does not need to be traded off for distortion performance in the spectrum monitoring receiver as it is when using a spectrum analyzer.

At RF frequencies, the low quality factor (Q) of the preselector filters prevents sufficiently narrow enough bandwidth to block all interfering signals. If the signal of interest is located at a frequency close to the interfering signal, both signals can progress through the receiver chain. The roofing filters, located at one of the IF stages, provide further suppression of interfering signals before they can reach the final IF stages or the ADC. These analog filters are a set of fixed frequency bandpass filters whose bandwidths are variable.

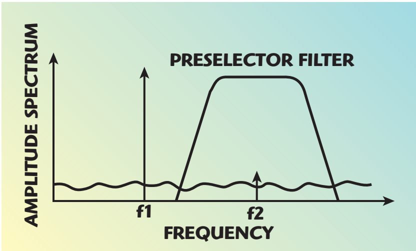

▲ *Fig. 6 Preselector filter blocks interfering signals.*


H100N
A30X4
Anaren

These filters can either be configured as a bank of filters or a single filter with tunable bandwidth.

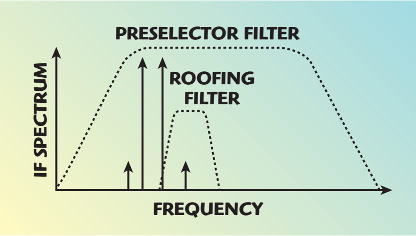

▲ *Fig. 7 Roofing filter suppresses distortion in final IF stages.*

Figure 7 shows how the roofing filter is used in the spectrum monitoring system. In this figure, two large amplitude signals are close enough in frequency that the preselector filter at the RF input cannot remove both tones. The roofing filter, due to operating at a lower frequency has a Q sufficiently large enough to allow for narrow bandwidths. Roofing filters are effective when a signal of interest is located at a frequency that would fall near an IMD product generated by the two large interfering signals. When measuring the weaker signal of interest, the large amplitude interfering signals fall outside the roofing filter bandwidth. With the interfering tones attenuated by the roofing filter, the amplifier stages that follow the roofing filters no longer create significant distortion which allows the gain of these final stages to be increased. Two important results occur: one is that the increased gain helps overcome the noise figure of the ADC and the other is that the higher signal level at the ADC input improves the ADC's spurious-free dynamic range performance.

PXI SPECTRUM MONITORING RECEIVER

As demonstrated here, spectrum monitoring receivers generally apply a few important modifications to the traditional vector signal analyzer architecture to provide sufficient dynamic range performance for over-the-air signals. Especially in PXI, these solutions can be provided simply with "add-on" modules to existing RF signal analyzers. For example, the NI spectrum monitoring receiver (PXIe-5667) was built upon the NI RF vector signal analyzer by using two additional modules: one module contains preselection filters and the other contains the roofing filters.

In addition, the software-defined nature of the spectrum monitoring receiver can be just as important as the hardware. In a typical application, an operator might want to observe just the power and frequency of a tone; or one might want to perform demodulation of the signal. In some cases, the signal is demodulated without any knowledge of the modulation scheme, a process known as blind detection. PXI spectrum monitoring receivers are often used with software such as NI LabVIEW system design software to execute these types of signal processing routines. For more computationally intense signal processing operations, the PXI spectrum monitoring receiver can even be combined with user programmable FPGA modules such as NI FlexRIO. These modules allow the FPGA to be programmed, enabling real-time spectrum monitoring measurements with increased spectrum scanning speeds.

VERY LOW DISTORTION

MIXERS

+36 dBm IP3   2 to 3100 MHz   from $9.95 ea. qty. 1000

Mini-Circuits shielded LAVI frequency mixers deliver the breakthrough combination of very high IP3 and IP2, ultra-wideband operation, and outstanding electrical performance. By combining our advanced ceramic, core & wire, and semi-conductor technologies, we've created these evolutionary patented broadband mixers that are specially designed to help improve overall dynamic range.

With a wide selection of models, you'll find a LAVI mixer optimized for your down converter and up converter requirements. Visit the Mini-Circuits website at www.minicircuits.com for comprehensive performance data, circuit layouts, and environmental specifications. Price & availability for on-line ordering is provided for your convenience.

Check these LAVI Mixer outstanding features!

- Very wide band, 2 to 3100 MHz
- Ultra high IP2 (+60 dBm) and IP3 (+36 dBm)
- -73 dBc harmonic rejection 2LO-2RF, 2RF-LO
- Super high isolation, up to 52 dB
- High 1dB compression, up to +23 dBm
- Extremely low conversion loss, from 6.3 dB

RoHS compliant **U.S. Patent Number 6,807,407**

Mini-Circuits…we're redefining what VALUE is all about!

Mini-Circuits®
ISO 9001 ISO 14001 AS 9100

P.O. Box 350166, Brooklyn, New York 11235-0003 (718) 934-4500 Fax (718) 332-4661

YONI2® ***The Design Engineers Search Engine*** *finds the model you need, Instantly* • For detailed performance specs & shopping online see **minicircuits.com**

U.S. Patents
7739260, 7761442

IF/RF MICROWAVE COMPONENTS

451 Rev J

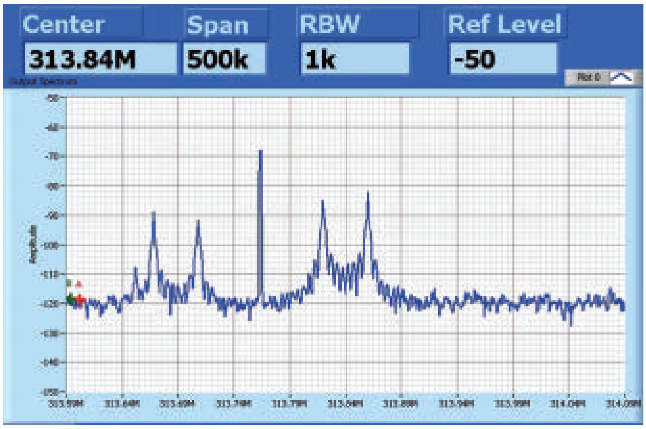

▲ *Fig. 8 FSK modulated signal without roofing filter.*

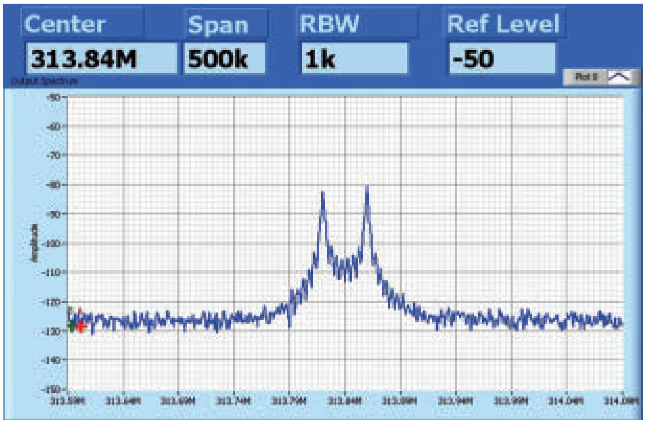

▲ *Fig. 9 FSK modulated signal with roofing filter.*

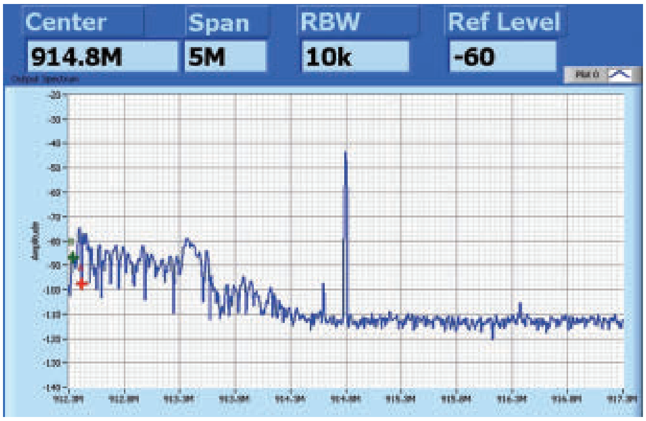

▲ *Fig. 10 Second harmonic distortion with preselector bypassed.*

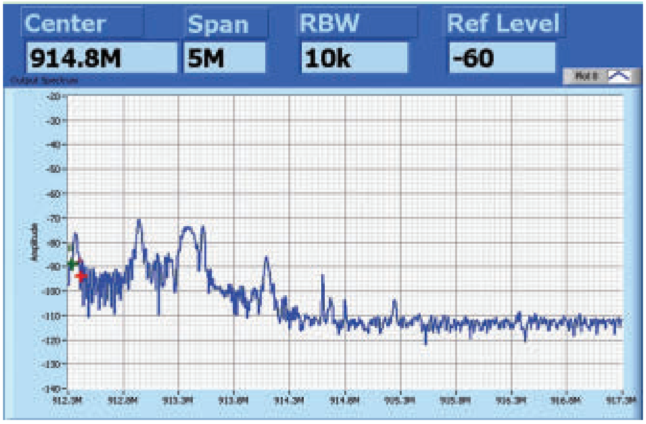

▲ *Fig. 11 Second harmonic distortion with preselector module included.*

MEASUREMENT EXAMPLES

1. Roofing Filter Example

Using a spectrum monitoring receiver, the following measurement example shows how the roofing filters improve the receiver's dynamic range when measuring an FSK modulated signal. A large amplitude interfering signal is injected such that it falls within the bandwidth of the final IF. To view the lower level FSK signal shown at the center of the spectrum in ***Figure 8***, the receiver gain must be increased. This causes the final IF amplifiers and the ADC at the end of the IF chain to distort. This distortion manifests itself as a CW spur and with the FSK signal being mirrored about the CW spur. A user would not be able to decipher the true FSK signal and the receiver-generated distortion product from Figure 8.

In ***Figure 9***, a roofing filter has been selected such that the large amplitude interfering signal is blocked from progressing on to the final IF stages and the ADC. The result is improved receiver distortion performance. The true FSK signal can now clearly be seen.

2. Preselector Filter Example

In this example, a large amplitude signal whose frequency is at one-half the center frequency of the spectrum monitoring receiver is injected. When the preselector module is bypassed, as shown in ***Figure 10***, the second harmonic generated in the receiver is clearly visible above the level of other signals in the ISM band.

In ***Figure 11***, the preselector module is included in the receiver chain. The receiver-generated second harmonic is now greatly suppressed, allowing the other signals in the ISM band to be clearly separated from the receiver distortion products.

CONCLUSION

Over-the-air measurements of the RF spectrum are subject to unknown and unwanted interfering signals. As we have seen, traditional receiver architectures that feature a wide bandwidth RF section as well as a wide bandwidth IF section are prone to receiver-generated distortion that could mask the signal of interest. Also, simply lowering the receiver gain to improve receiver distortion performance can adversely affect the receiver's sensitivity performance. A spectrum monitoring receiver, on the other hand, is uniquely designed to analyze over-the-air signals. By combining strategic preamplification and filtering at both the RF and the IF, a spectrum monitoring receiver provides maximum dynamic range when measuring a low level signal even in the presence of large interferes. ■

References

1. www.4gamericas.org, "4G Americas Report Addresses the Impact of Applications, Devices and End User Behavior on Mobile Network Congestion", May 15, 2012.
2. "Repurpose Spectrum For Wireless Broadband Use," *Microwaves and RF*, May 2011, ED Online ID #23501.

New Tile Structure for Microwave Modules Using Solderless Vertical Interconnections

This article proposes a new form of three-dimensional (3D) structure that can be easily constructed at a low cost. The proposed structure creates a set by combining a component attached layer-board using a frame-board as a spacer. Another element of the proposed structure stacks these sets to realize a tile structure similar to how a container house is built. Each set is connected through vertical interconnections by a solderless-method, using fuzz buttons. A tile structure active Transmit/Receive module is created, based on the proposed structure and is applied to an active phased array radar, operating in the 18 GHz frequency range. The fabricated module and its test results confirm that the proposed structure is cost efficient and easy to realize.

Present and future microwave products are gradually transitioning into more cost effective and smaller sized models. Reflecting this trend, microwave module structures are also changing from 2D to 3D structures. A 3D structure, from a design engineer's perspective, has some issues concerning spatial restrictions around signal line routing or component placements. However, compared to a 2D structure, a 3D structure can be miniaturized and its weight reduced as the volume and weight of the module are reduced.[1] A 3D structure also requires fewer components for constructing the module; thus, it can be cost effective.[2] Therefore, the 3D structure is of interest for these reasons.

Studies on 3D structures have developed rapidly in the area of transmit/receive modules (T/R modules) used in radar systems. In particular, an active phased array radar is composed of hundreds or thousands of T/R modules. The weight, volume and cost of each T/R module become important parameters in determining overall performance of the radar. Active phased array radars used in missile or airborne systems

Ju-Young Moon and Sang-Won Yun
Sogang University, Seoul, Korea
Chang-Soo Ahn and Seon-Joo Kim
Agency for Defense Development, Taejon, Korea

especially have tighter physical restrictions; thus, T/R modules used in these types of radars are gradually changing from brick (2D) to tile (3D) structures.[3]

This article proposes a new tile structure that can be easily constructed at a low cost. This proposal also includes a vertical interconnection structure that is necessary for realizing the tile. The design and fabrication of a tile structure active T/R module that can be applied to active phased array radar is presented and, finally, the possibility of the proposed tile structure is validated.

THE PROPOSED TILE STRUCTURE

The key points that determine the structure of the tile type modules can be summarized into two topics: how the stacking is arranged and how its vertical interconnections are realized. These points can be resolved through the proper choice of the spacer. The role of the spacer is to create room between the neighboring layer-boards within the tile structure, thereby protecting components attached on the layer-board. It also works as the medium for vertical interconnection. The spacer, therefore, is a critical factor for the tile structure. Previous studies showed that many issues of the stacking and vertical interconnection were resolved by the use of metallic spacers. Metallic spacers are particularly useful for securing ground levels for stacked boards. However, the signal line and ground plane have to be isolated in the spacer to create a vertical interconnection. In other words, a vertical interconnection is created by inserting a dielectric element into the spacer so that signal lines of the vertical interconnection are created within that dielectric element.[4-6]

This article proposes a new tile structure that uses a non-metallic spacer, which provides trades-offs for the pros and cons of using a metallic spacer. Unlike the spacers used in previous studies, this new tile structure uses a non-metallic spacer and creates a solderless vertical interconnection method using fuzz buttons. The non-metallic spacer was created using the same laminate used to fabricate the layer-boards, which makes it insensitive to external influences such as pressure or temperature. The proposed tile structure is shown in ***Figure 1***.

The core of the proposed structure is the way that the frame-board, which is used as layer-board, is combined. As shown in ***Figure 2***, the ground planes of both the layer-board and the frame-board are soldered with solder balls. Here, the layer-board is considered as the “Floor” while the frame-board is the “Wall.” Therefore, the structure’s “Floor-Wall set” (F-W SET) is obtained. The F-W SET is soldered between ground planes of both the layer-board and frame-board and can thus secure ground level related problems, arising from the use of a non-metallic spacer.

The F-W SET stacking of the proposed tile structure is shown in ***Figure 3***. This structure connects

Fig. 1 The proposed tile structure.

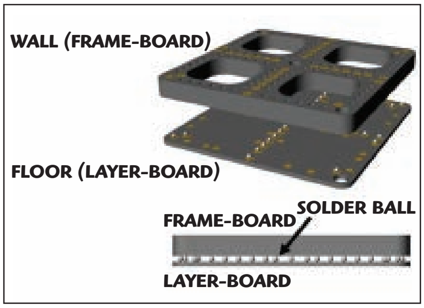

Fig. 2 Floor-wall set.

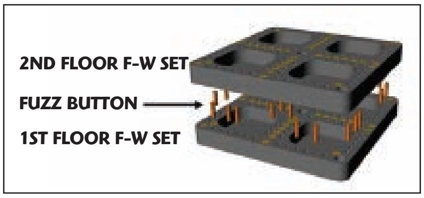

Fig. 3 Stack of F-W SETs using fuzz buttons.

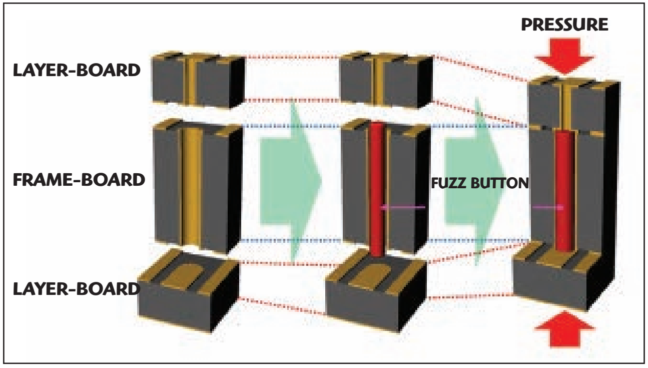

Fig. 4 Structure of the proposed vertical interconnections.

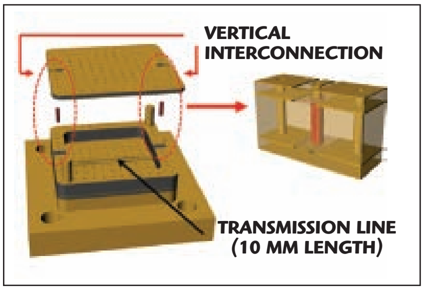

Fig. 5 Structure of the test fixture for the vertical interconnection.

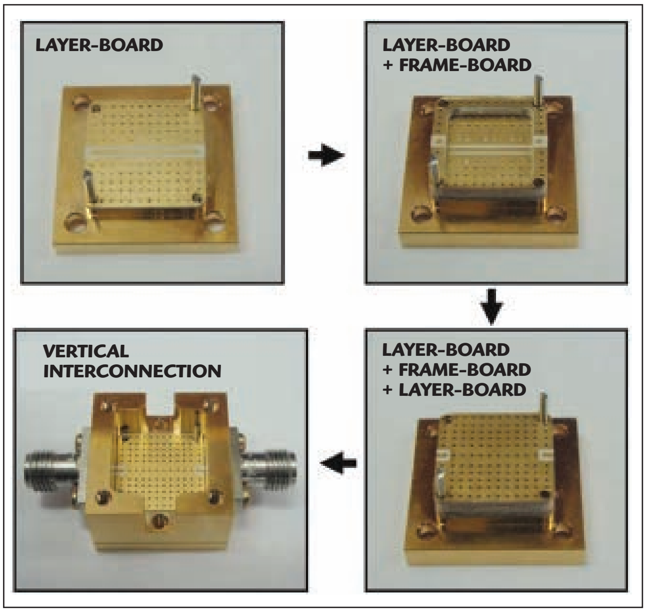

Fig. 6 Test-fixture for the vertical interconnection.

both the lower and upper F-W SET through vertical interconnections using fuzz buttons. The vertical interconnection that assembles each F-W SET is formed by a solderless-method. This allows users to conveniently repair, rework or replace the module, should any problem arise after module fabrication.

DESCRIPTION OF THE PROPOSED VERTICAL INTERCONNECTION

The proposed vertical interconnection uses the elasticity of the fuzz button to contact the neighboring layer-boards without soldering. This vertical interconnection structure is shown in ***Figure 4***. The fuzz button is inserted into a signal via hole in the frame board so that the via hole and fuzz button together form a filled via. This signal filled via part and the neighboring layer-board's signal line parts are in contact, thereby creating a vertical interconnection. The fuzz button, inserted into the frame-board, is contacted by pressure coming from the neighboring layer-boards.

The fuzz button used in the vertical interconnection is manufactured from a gold-plated nickel chromium alloy wire. It has a cylindrical shape with a diameter of 10 mils and a length of 70 mils and was manufactured by Custom Interconnects. The fuzz button has an insertion loss of approximately 0.5 dB and a return loss greater than 15 dB in the 18 GHz frequency range. For more convenient testing, the test fixture of the vertical interconnection consisted of two vertical interconnections and a transmission line that connected the two, as shown in ***Figure 5***. The loss of the inserted transmission line is 0.03 dB/mm and the return loss is greater than 20 dB. The design goal of this test fixture was set based on the loss of the transmission line that connects the external connector and the vertical interconnection. Therefore, a single vertical interconnection was designed to generate less than 0.6 ± 0.05 dB of insertion loss and over

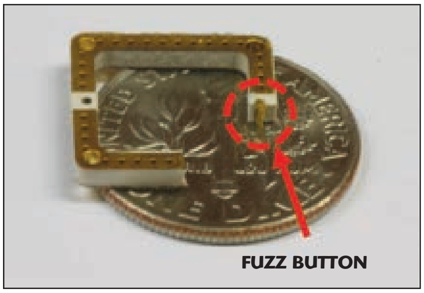

Fig. 7 *Fuzz button on the frame-board.*

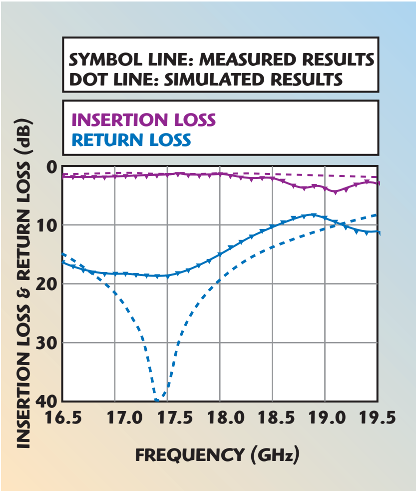

Fig. 8 *Characteristics of the test fixture for the vertical interconnection.*

15 dB of return loss. This test fixture was designed to satisfy a 10 percent bandwidth at the center frequency. The simulation was done using HFSS V.11 from Ansoft.

A test fixture was created, using a RO3003 series laminate from ROGERS to fabricate the layer-board and frame-board. The thickness of the layer-board is 15 mils and that of frame-board is 60 mils. Super SMA series connectors (214-521SF) by Southwest Microwave were used as an external connector. ***Figure 6*** shows the test fixture for vertical interconnection and ***Figure 7*** shows how the fuzz button is inserted into the frame-board.

The fabricated test fixture was tested using a 8510C vector network analyzer from Agilent. ***Figure 8*** shows the comparison of results from test fixture measurement and simulation. The test showed that the test fixture has an 11 percent bandwidth at a 17 to 18 GHz range and has an insertion loss of 1.6 dB and a return loss greater than 14 dB. By removing the characteristics of the 10 mm transmission line from

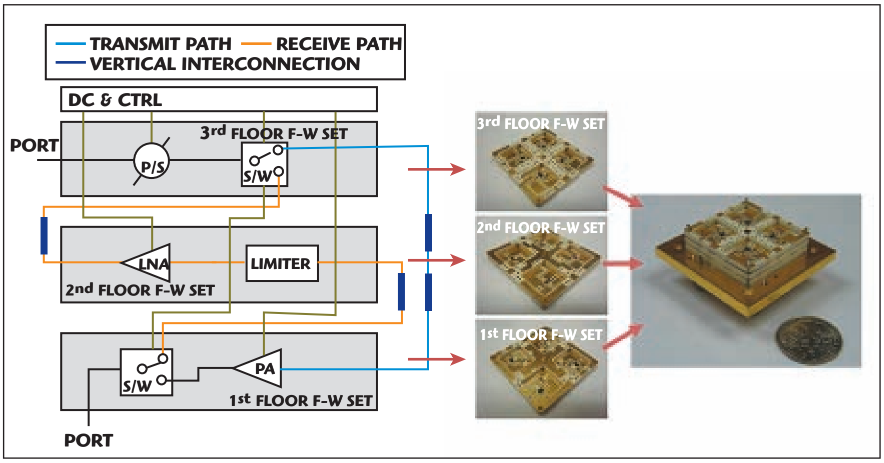

Fig. 9 *Proposed active transmit/receive module tile structure.*

the measured result, each vertical interconnection shows an insertion loss of approximately 0.65 dB. This test allowed us to confirm that the characteristics of the vertical interconnection satisfy the design goals.

DESIGN OF THE PROPOSED ACTIVE TRANSMIT/RECEIVE MODULE TILE STRUCTURE

Based on the proposed tile structure, an active T/R module was designed that can be applied to an 18 GHz frequency range. The proposed structure was validated by eliminating functional components such as the attenuator and driving amplifiers and the structure was simplified by only maintaining the key components needed for the T/R module. A hypothetical active phased array radar was considered and the specifications of the T/R module were calculated, using the radar equation so that it can be applied to the supposed radar system.[7] The design specifications were set so that the transmit path would have more than 13 dB of gain, more than 10 dB of output return loss and an output power more than 26 dBm. The receive path was set to attain more than 8 dB gain, more than 10 dB input return loss and to satisfy a less than 8 dB noise figure. The simulation was performed using the HFSS V.11 from Ansoft and ADS 2008 from Agilent.

The active T/R module that was fabricated based on the proposed tile structure is shown in ***Figure 9***. The proposed T/R module tile structure has a 2 × 2 array form; thus, it consists of four layer-boards and three frame-boards. One layer-board is a bias

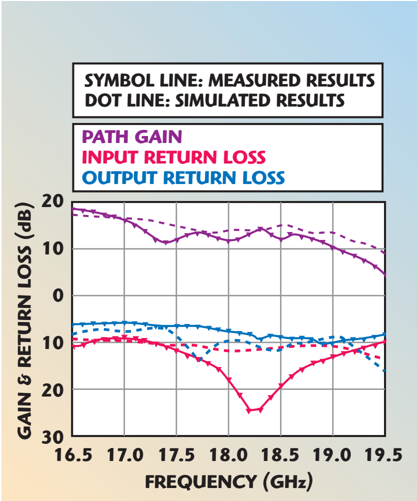

Fig. 10 *Characteristics of the transmit path (gain and return loss).*

board which is positioned to transfer the T/R module's DC bias and control bits from the outside. The proposed T/R module shown eliminates the bias board and thus consists of three floors of F-W SETs. Each of these three floors is structured as shown in the schematic diagram on the left of the figure. The first floor F-W SET is connected to the radiation element and is installed with a power amplifier in the transmit path and a switch that separates the transmit and receive paths. The second floor F-W SET is installed with a limiter and a low noise amplifier in the receive path. Lastly, the third floor F-W SET is installed with a switch that separates the transmit and receive paths and the phase shifter that is connected to the control circuit. Vertical interconnections between each floor were connected with a solderless-method, using fuzz

Electronic Assembly Manufacturing, Inc.
126 Merrimack St.
Methuen, MA 01844
P: 978-374-6840
F: 978-374-6375
www.eamcableassemblies.com

ISO 9001:2000 *Registered* | **ROHS** *Compliant* buttons in the RF path, DC bias and control bits.

Figure 10 shows the gain characteristics of the transmit path, which was confirmed as 13±1.5 dB, as well as the return loss characteristics of the transmit path, which were confirmed as more than 10 dB as specified. ***Figure 11*** shows the output power characteristics, confirmed to be over 25 dBm. ***Figure 12*** shows the characteristics of the receive path, with a gain of approximately 9 dB and a return loss greater than 10 dB. ***Figure 13*** shows the noise figure of the receive path, which is approximately 8 dB. The fabricated active T/R tile structure module resulted in characteristics that almost satisfied the design specifications.

The fluctuations of the test results are thought to be created by the possible occurrence of an imperfect ground between the stacked F-W SETs. The possible imperfect ground could be secured by a thin film gasket.[8]

This new tile structure, created by stacking the boards (F-W SET) through vertical interconnection using fuzz buttons, was built and

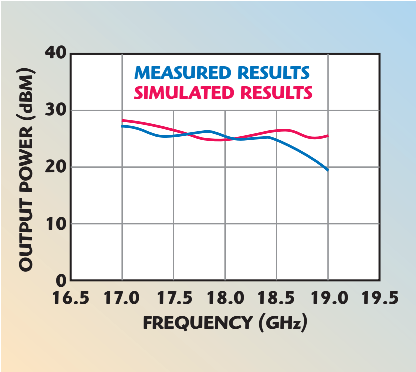

▲ *Fig. 11 Characteristics of the transmit path (output power).*

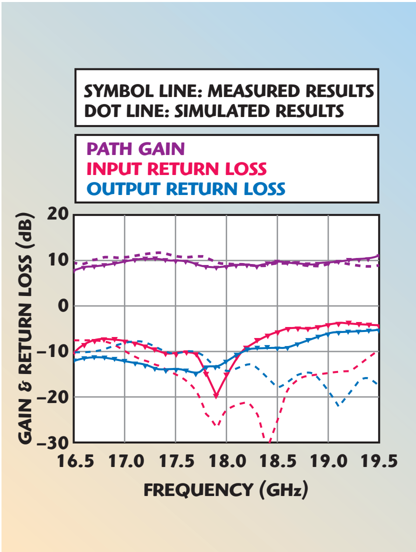

▲ *Fig. 12 Characteristics of the receive path (gain and return loss).*

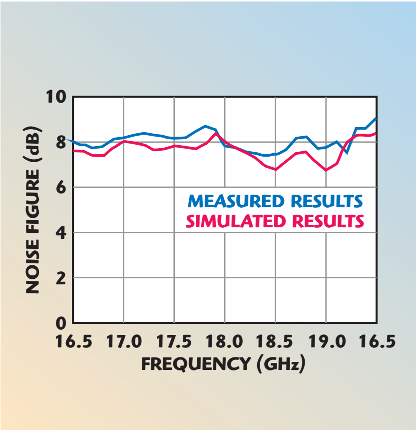

▲ *Fig. 13 Noise figure of the receive path.*

tested. Some aspects require further resolution; however, the feasibility of the proposed structure was confirmed.

CONCLUSION

This article proposes a new type of tile structure that is unlike those proposed in previous studies and can be applied more conveniently and easily. The proposed tile structure was constructed using a spacer made out of the same laminate material used to make the layer-board. Creation of both the layer-board and frame-board from the same laminate material made the F-W SET less sensitive to external influences than when they are formed using different materials. This article also shows a solderless method to realize the vertical interconnecting using fuzz buttons. The module was constructed by stacking F-W SETs using the solderless-method so that any identified problems after fabrication could be easily fixed. The proposed tile structure is more cost-effective and easier to fabricate, compared to other structures proposed in previous studies. Therefore, the proposed tile structure can be easily duplicated by other engineers and other tile structures with better performances can be realized through further studies. ■

ACKNOWLEDGMENT

This research was supported by the Agency for Defense Development Korea, through the Radiowave Detection Research Center at Korea Advanced Institute of Science & Technology.

References

1. M.S. Hauhe and J.J. Wooldridge, "High Density Packaging of X-Band Active Array Modules," *IEEE Transactions on Components, Packaging and Manufacturing Technology – Part B*, Vol. 20, No. 3, August 1997, pp. 279-291.
2. J.J. Wooldridge, "High Density Microwave Packaging for T/R Modules," *2005 IEEE MTT-S International Microwave Symposium Digest*, Vol. 1, pp. 181-184.
3. K. Axelsson, "Generic Packaging Technologies for T/R-modules," *2005 European Microwave Conference Digest*, Vol. 2.
4. J.J. Wooldridge, "High Density Interconnect (HDI) Packaging for Microwave and Millimeter Wave Circuits," *1998 IEEE Aerospace Conference Proceedings*, Vol. 1, pp. 369-376.
5. T. Barbier, F. Mazel, B. Reig and P. Monfraix, "A 3D Wideband Package Solution Using MCM-D BCB Technology for Tile TR Module," *2005 13th European GaAs and Other Semiconductors Applications Symposium Digest*, pp. 549-552.
6. Y. Mancuso, "Thales Components and Technologies for T/R Modules," *2008 IEEE Radar Conference Digest*, pp. 1-5.
7. M.I. Skolnik, "Introduction to RADAR Systems," Third Edition, McGraw-Hill, New York, NY, 2001, pp. 30-97.
8. TECKNIT Homepage, www.tecknit.com.

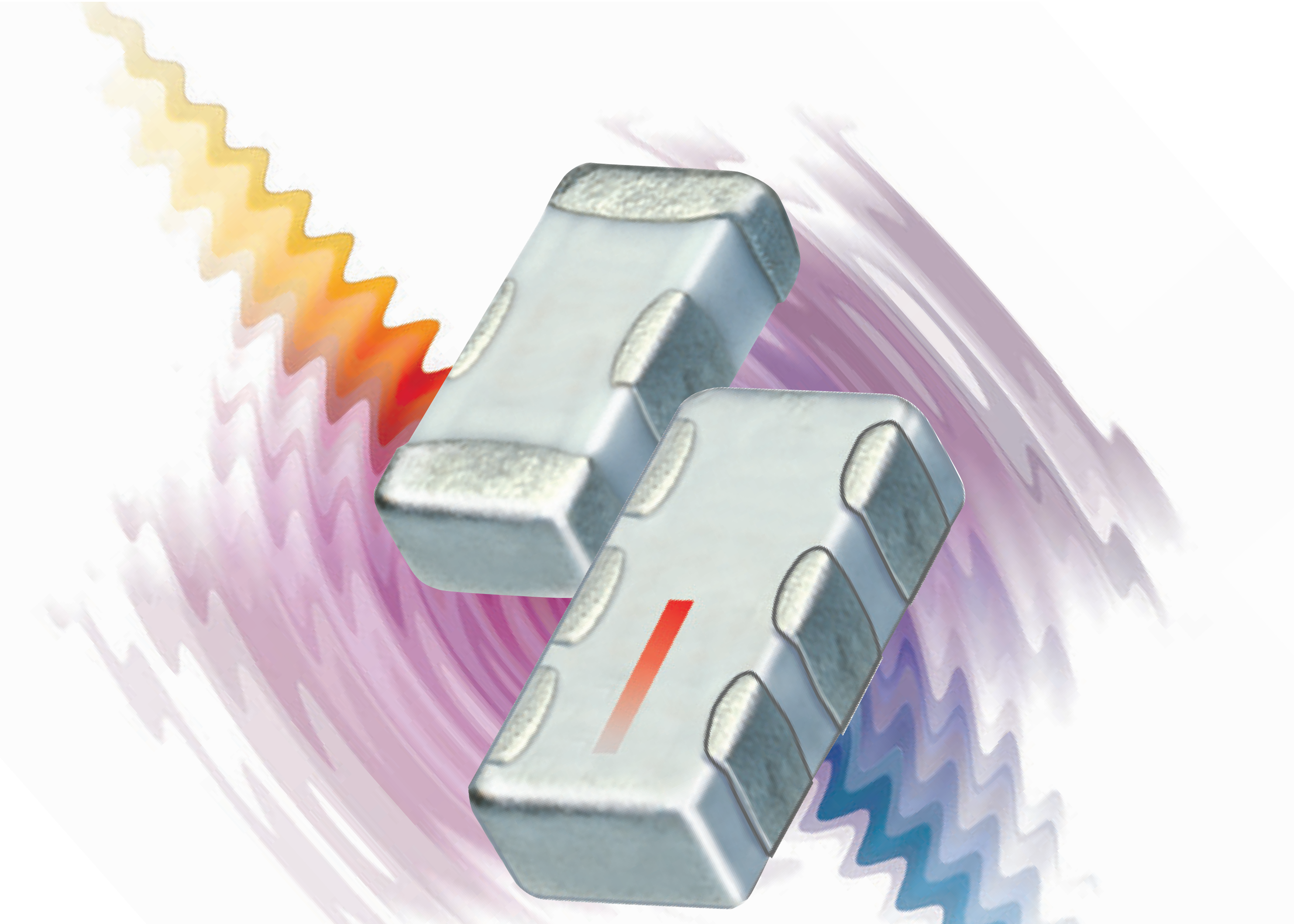

CERAMIC FILTERS

LOW PASS BANDPASS HIGH PASS

45 MHz to 13 GHz from **99¢** *ea. qty.3000*

Over ~~167~~ 179 models…only 0.12 x 0.06" These tiny hermetically sealed filters utilize our advanced Low Temperature Co-fired Ceramic **(LTCC)** technology to offer superior thermal stability, high reliability, and very low cost, making them a must for your system requirements. Visit our website to choose and view comprehensive performance curves, data sheets, pcb layouts, and everything you need to make your choice. You can even order direct from our web store and have units in your hands as early as tomorrow!

Wild Card KWC-LHP LTCC Filter Kits *only $98*

Choose any 8 LFCN or HFCN models
Receive 5 of ea. model, for a total of 40 filters
Order your KWC-LHP FILTER KIT TODAY!

RoHS compliant U.S. Patents 7,760,485 and 6,943,646

Now available in small-quantity reels at *no extra charge:*
Standard counts of 20, 50, 100, 200, 500, 1000 or 2000. Save time, money, and inventory space!

Mini-Circuits…we're redefining what VALUE is all about!

Mini-Circuits®
ISO 9001 ISO 14001 AS9100

P.O. Box 350166, Brooklyn, New York 11235-0003 (718) 934-4500 Fax (718) 332-4661

YONI2® ***The Design Engineers Search Engine*** *finds the model you need, Instantly* • For detailed performance specs & shopping online see **minicircuits.com**
U.S. Patents 7739260, 7761442

IF/RF MICROWAVE COMPONENTS

Design of a Passive, Broadband Equalizer for a SLED

Wavelength Division Multiplexing Passive Optical Networks (WDM PON) have recently been commercialized by vendors including LG, Nortel and Alcatel-Lucent, and are considered by many to be higher performance than Time Division Multiplexing (TDM) PON systems, which are widely deployed today. Adding broadcast service to TDM PON is relatively simple, as it requires the addition of a single downstream wavelength. For WDM PON, it is more complex, since the 1:N Arrayed Waveguide Grating (AWG) used at the remote node requires a broadband light source to broadcast to N users. AT&T Labs Research and Development in Middletown, NJ, has investigated the possibility of overlaying video and Gigabit Ethernet (GbE) through the direct modulation of a super luminescent light emitting diode (SLED), that acts as a broadband source (similar to an LED) with high power (similar to a laser source), which when coupled with an optical bandpass filter to eliminate wavelength interference with other channels, can excite the wavelengths of a 1:32 AWG. A high level block diagram of their proposed system, from central office to user, is shown in ***Figure 1***.

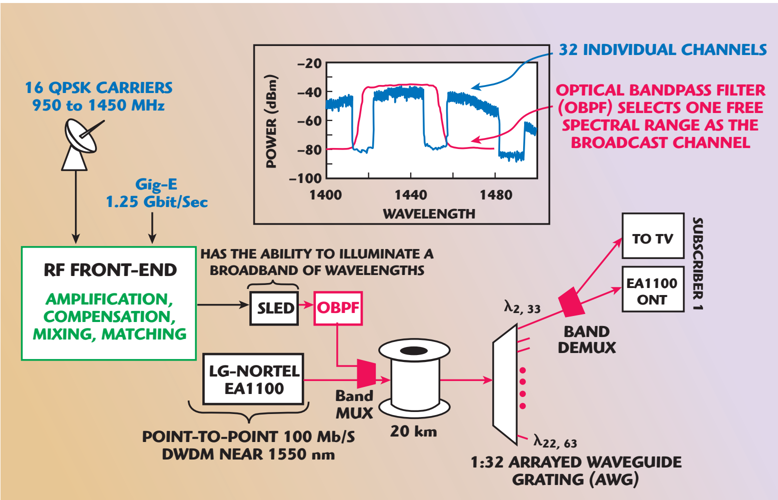

▲ *Fig. 1 Broadcast service addition to a WDM PON network showing the necessary RF front-end circuitry before the SLED.*

One shortcoming of this technique is that the SLED has a poor modulation response. To this end, a small scale, passive gain equalizer implemented on a printed circuit board (PCB) was designed and measured, which shall be referred to as a compensator. Throughout this article, the simulations rely solely on AWR's Microwave Office.

Chris Brinton, Matthew Wharton and Allen Katz
Princeton University, Princeton, NJ


EWT
Where Performance Counts
Bandpass • Bandreject • Highpass • Lowpass • Transmit • Receive • Duplexers • Multiplexers
Military • Commercial
Wireless • Space
Eastern Wireless TeleComm understands just how much is on the line with each and every product we make. We continually provide the highest quality filter products, design support, and service to our customers each and every time. Where Performance Counts, Count on EWT.
Specializing in custom design and manufacturing of RF and Microwave filters and filter based products to 50 GHz.
www.ewtfilters.com
Eastern Wireless TeleComm, Inc.
Tel: 410.749.3800 Fax: 410.749.4852
sales@ewtfilters.com

COMPENSATOR DESIGN

In order to design the compensator, the electrical characteristics of the SLED are considered. By modeling it as a two-port network, as shown in ***Figure 2***, the S-parameters can be measured to obtain its gain response. With a_1 and a_2 representing the incident waves and b_1 and b_2 representing the reflected waves on ports 1 and 2, respectively, S-parameter theory shows that

$$\begin{bmatrix} b_1 \\ b_2 \end{bmatrix} = \begin{bmatrix} S_{11} & S_{12} \\ S_{21} & S_{22} \end{bmatrix} \begin{bmatrix} a_1 \\ a_2 \end{bmatrix}, \quad (1)$$

and thus

$$\frac{b_2}{a_1}\Big|_{a_2=0} = S_{21}, \quad (2)$$

which is a measure of the two-port network gain in a system that has input and output impedances matched to the characteristic impedance Z_0 = 50 V.

The two-port S-parameters of SLED were measured using a vector network analyzer (VNA). A bias of 5 V and 142 mA was applied to the device through a bias tee to obtain the recommended operating conditions. The magnitude and phase response measurements of the SLED are shown in ***Figure 3***. The gain response shows a 3 dB bandwidth of 340 MHz and over 30 dB loss in magnitude over the bandwidth of interest. The phase response has a linear regression correlation coefficient of roughly unity, corresponding to the almost constant group delay $\tau_g(f) \approx 35$ ns of the SLED. With the responses shown, it was concluded that only the magnitude response of the SLED required alteration. Therefore, a passive compensator should, through attenuation at lower frequencies, emulate the following response:

$$G_{comp}(f) = \begin{cases} \dfrac{A}{|G|_{SLED}(f)} e^{-j2\pi f t_0}, \sim \text{DC} < f < 650 \text{ MHz} \\ \dfrac{A}{\left(\dfrac{f}{650 \times 10^6}\right)|G|_{SLED}(f)} e^{-j2\pi f t_0}, \ 650 \text{ MHz} < f < 1.25 \text{ GHz} \end{cases} \quad (3)$$

In Equation 3, A is a variable gain constant. The condition that the resultant response of the filter roll off exactly as a single pole lowpass filter after 650 MHz is an approximate specification – the results were deemed to be satisfactory as long as the overall response begins to consistently decrease in magnitude after reaching approximately 650 MHz at a rate of no greater than 50 dB/decade.

Given the necessity of obtaining sharp responses within the 650 to 850 MHz range, highpass characteristics were required. Simultaneously, in order to pass components at DC without the use of active circuitry, another parallel section was needed that was capable of providing the necessary low frequency attenuation, without completely blocking the signal within these ranges. Finally, frequency selective band-attenuation sections were needed at the onset of the circuit to gain additional control over the sharpness of the highpass response. Excluding the effects of loading between each stage, a block diagram of the network is shown in ***Figure 4***.

Development of the necessary components in the circuit was accomplished using a seventh-order LC highpass filter, in parallel with a divider between a resistance and a resistance in series with an inductance. At the onset of the network, three RLC attenuation sections and a tee attenuator were placed for additional shaping of the highpass response. The resulting circuit, with ideal component values, is shown in ***Figure 5***. The simulated response as compared to the ideal compensator response can be seen in ***Figure 6***. There is less than 1 dB of difference between the ideal gain response and the response shown up to ~ 940 MHz. The response begins to deviate by greater than 1 dB after 960 MHz, with a maxi-

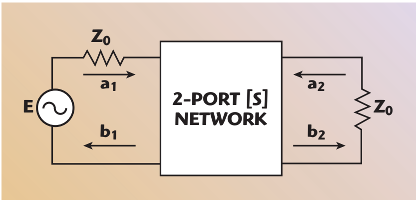

▲ *Fig. 2 Two port network represented by its S-matrix.*

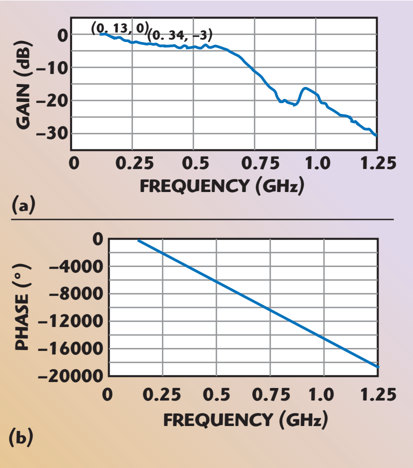

▲ *Fig. 3 SLED $|S_{21}|$ magnitude (a) and phase (b).*

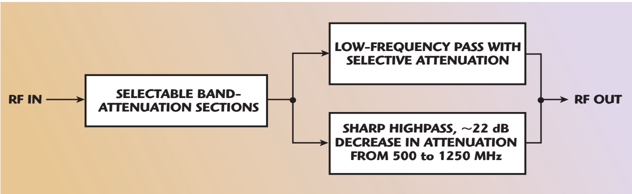

▲ *Fig. 4 Block diagram showing the overall logic used in developing the compensator stage.*

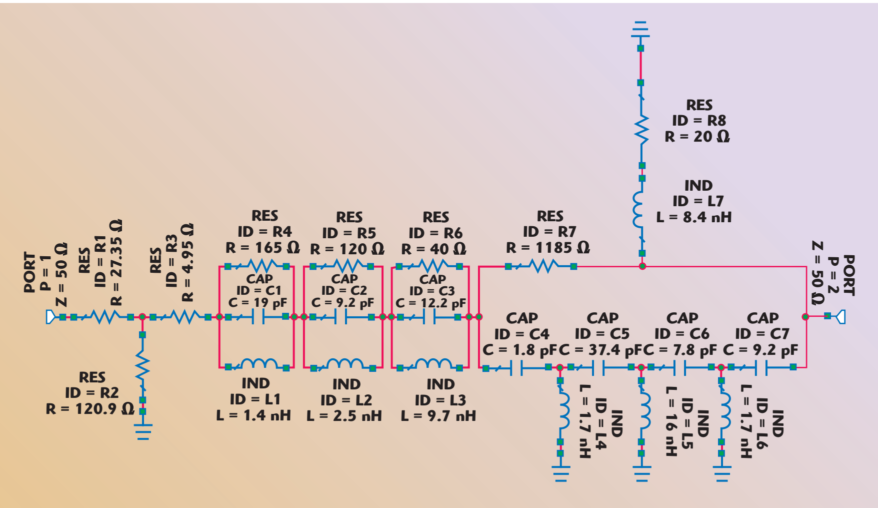

▲ *Fig. 5 Compensator design using ideal circuit components.*

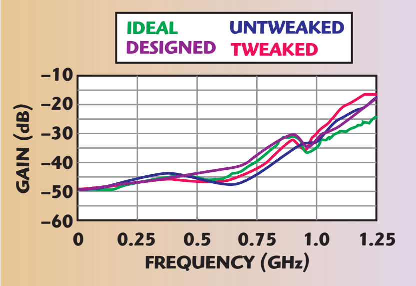

▲ *Fig. 6 Comparison between the ideal, designed, untweaked, and tweaked compensator.*

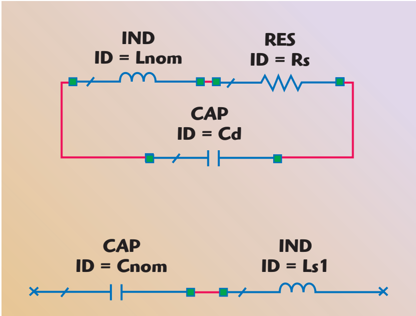

▲ *Fig. 7 Inductor (a) and capacitor (b) models, factoring in f_{res} and ESR.*

mum deviation of ~2.8 dB at 1.25 GHz.

Before fabricating the compensator, it was necessary to develop a sophisticated model of the circuit to determine possible variation in the output response. First, commercially available SMT inductors were chosen from Digi-Key Corp., since generally SMT inductors have less options and are more prone to self-resonance (f_{res}) and equivalent series resistance (ESR) than SMT capacitors. The corresponding models used to simulate the effects of

TABLE I

INDUCTORS AND CAPACITORS SELECTED FROM DIGI-KEY CORP. WITH L_s AN C_d CALCULATIONS

Component	L (nH) or C (pF)	Tolerance (±nH or ±pF)	Q (X_L/R_S)	F_r(MHz)	F_{RES} (GHz)	R_s @ F_r	L_s (nH) or C_d (pF)
L1	1.5	0.3	8	100	15	0.1178	0.0751
L2	2.4	0.3			10	0.1885	0.1055
L3	10	0.5			3.7	0.7854	0.1850
L4,L6	1.8	0.3			14	0.1414	0.0718
L5	15	0.75			3.1	1.1781	0.1757
L7	8.2	0.41			4.6	0.6440	0.1460
C1	18	0.18	-	-	4	-	87.95
C3	12	0.12			4		131.9
C4	1.8	0.05			9		173.7
C5	27	0.27			2.5		150.1
C6	7.5	0.1			4		211.1
C2, C7	9.1	0.1			4		174.0

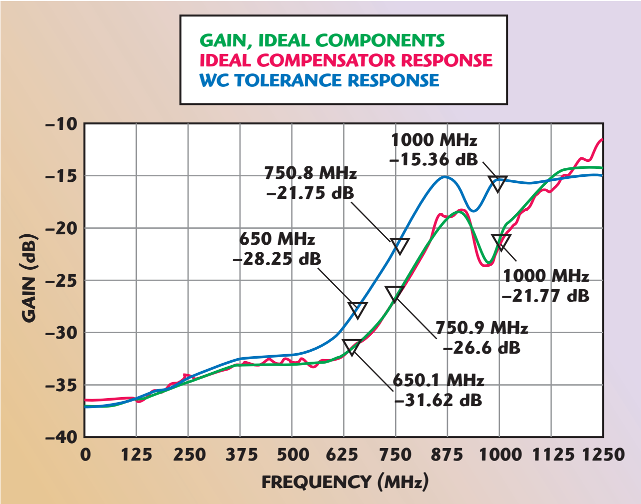

▲ *Fig. 8 Response factoring the worst case tolerances on the inductors.*

f_{res} and ESR are shown in ***Figure 7***. The calculations of C_d and R_s for the inductors employed the following equations:

$$C_d = \frac{1}{(2\pi f_{res})^2 L_{nom}} \tag{4}$$

$$R_s = \frac{X_L(f)}{Q(f)} \tag{5}$$

using the data provided in ***Table 1*** for the chosen inductors. Similarly, Equation 4 can be rearranged to calculate L_s from C_{nom}.

From the quality factor (Q) data given graphically as function of frequency (not shown), it was determined that for each of the inductors chosen, the value of R_s would have insignificant effects on the compensator response above 100 MHz, since the reactance was at least eight times as large. Near DC, the value of R_s became so small that it provided an approximate short circuit relative to the generally large resistances surrounding the inductors. Even so, the inductor model in Figure 7 was implemented in Microwave Office, using a frequency-dependent resistance for R_s based upon the values of Q supplied by the manufacturer. The resultant circuit was simulated and plotted against the model with ideal component values (not shown). While the ESR and self-resonant characteristics were not seen to affect the designed response by more than a few dB, the inductor tolerances were seen to affect the compensator response by as much as 7 dB, as shown in ***Figure 8***. Therefore, it was determined that measuring their actual values on a VNA was necessary in order to emulate the ideal response.

Once the inductors were received, they were soldered onto female flange SMA connectors, and their S_{11} characteristics were measured and displayed on a VNA's Smith Chart. The resistive and reactive components of the inductors were measured as a function of frequency from 300 kHz to 1.25 GHz. The reactance plot is shown in ***Figure 9***, and linear regression was run on the reactive data for each inductor, all of which gave a correlation coefficient of $R^2 \geq 0.99$, with the exception of the 15 nH which had $R^2 = 0.98$. From the plots, the equivalent inductances can be

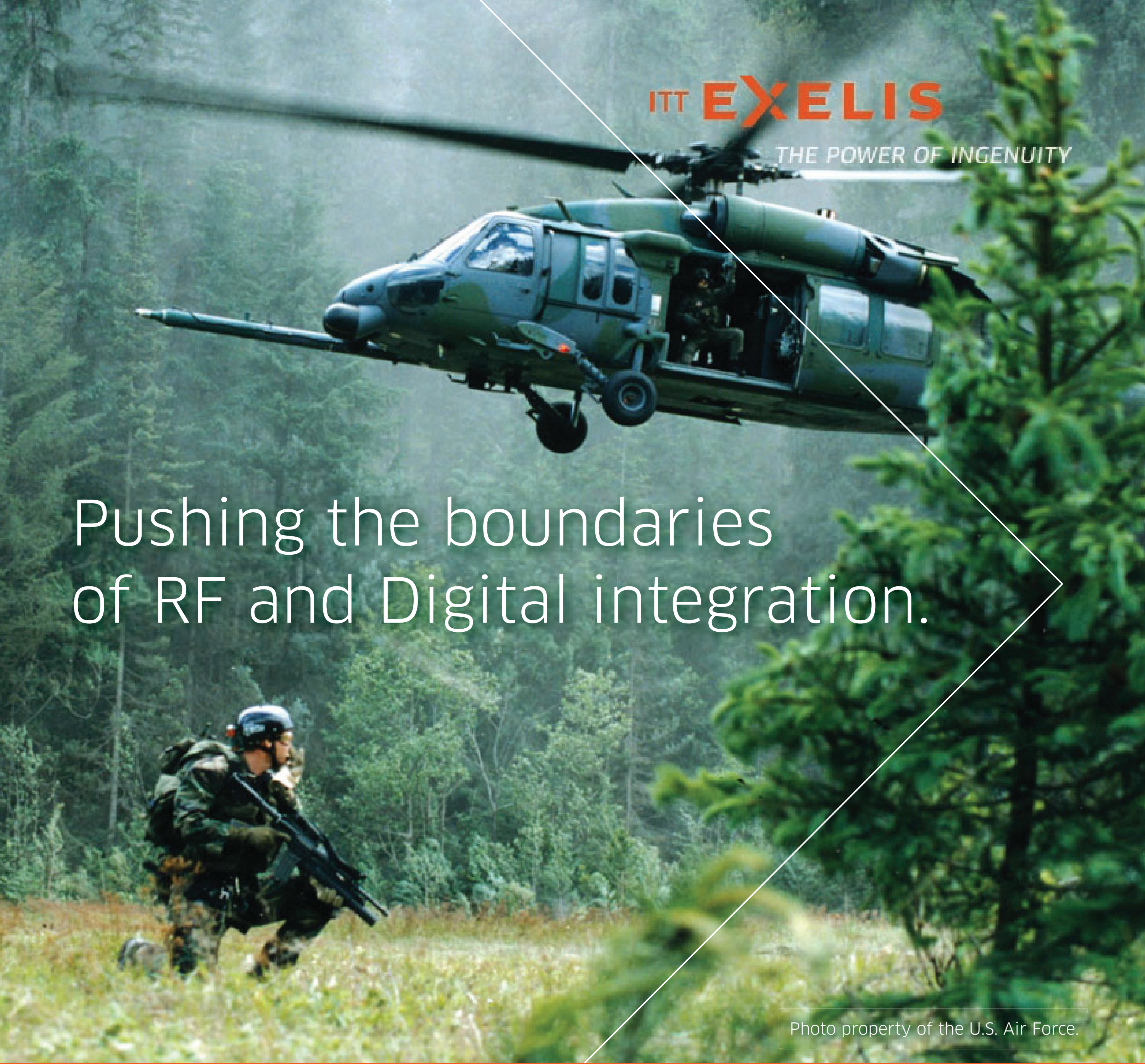
ITT EXELIS
THE POWER OF INGENUITY
Pushing the boundaries of RF and Digital integration.
Photo property of the U.S. Air Force.


EXELIS
EXELIS

calculated from

$$L = \frac{1}{2\pi}\left(\frac{X(f)}{f(MHz)}\right)10^{-6}\,H \qquad (6)$$

The values calculated from Equation 6 are shown in ***Table 2***. It is important to note that despite the linearity of the reactance, each inductor is significantly larger than its nominal value.

The measured inductance values were imported into Microwave Office, using the element ZFREQ, which allows for arbitrary definitions of resistance and reactance at specified frequencies and uses a linear interpolation model at all points between. At this point, it was necessary to retune much of the circuit, due to the non-idealities and deviation in nominal values of the inductors. To accomplish this, the compensator was cascaded with the SLED's two-port model in Microwave Office and the real-time tuning feature was used to tweak the components of the circuit, while monitoring the resulting $|S_{21}|$ response. For instance, it was necessary to place an 8.2 nH nominal (measured 9.34 nH) in parallel with each of the 1.5 and 1.8 nH inductors in order to bring them closer to the specified values.

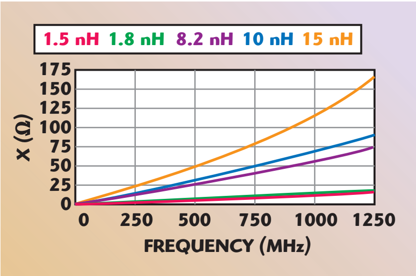

▲ *Fig. 9 Measured inductance plots.*

TABLE II

MEASURED INDUCTANCES VERSUS NOMINAL INDUCTOR VALUES

L (nH)	*Measured Inductance (nH)*
1.5	2.10
1.8	2.18
8.2	9.34
10	10.89
15	20.2

C5 and L6 were noticed to have had little effect on the frequency response and were eliminated from the circuit. The updated compensator schematic is shown in ***Figure 10***. The expectation is that the compensator will yield a passband ripple of less than 1 dB.

COMPENSATOR FABRICATION AND TESTING

After completing the simulations, the compensator was fabricated and tested. Eagle was used to generate the necessary Gerber files for the etching of the board. The geometry used was coplanar waveguide (CPW) with ground. The substrate chosen was industry standard 62 mil-thick FR-4, which has little variation in its dielectric constant ε_r of 4.7 over the frequency range of interest and a loss tangent δ = 0.017. The copper signal traces used were 1 oz (1.4 mil), 35 mil wide with 7 mil isolation between the conductor and ground, guaranteeing approximately 50 Ω (50.6 exact) traces. Twelve mil diameter, round vias were placed around the components

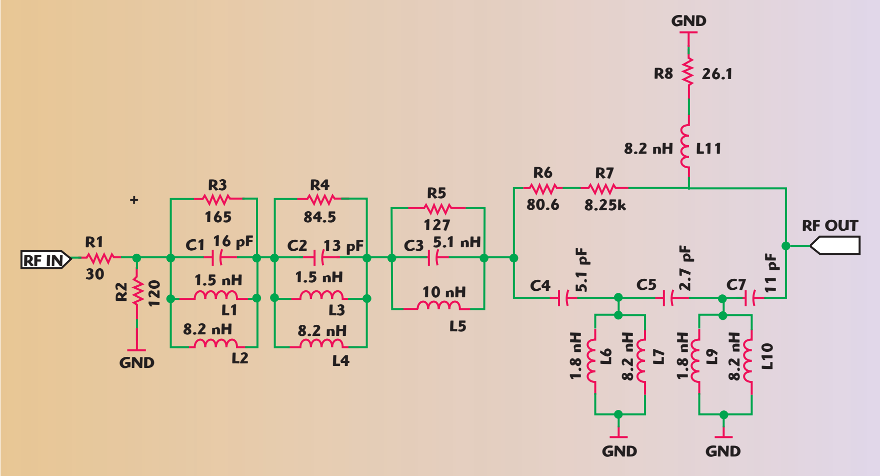

▲ *Fig. 10 Eagle board layout of the compensator.*

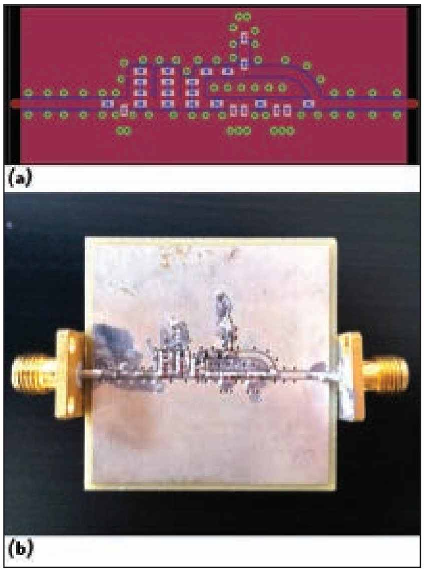

▲ *Fig. 11 Eagle board layout (a) fabricated compensator (b).*

of the board (farther than 7 mil away). The input and output ports were reached through ~50 Ω traces extended to the edge of the board for side-mount SMA connectors. For convenience of shape, and to leave enough room for additional SMT components if needed, a 2" × 2" board was chosen. The routed Eagle board file and the fabricated compensator (built at Linearizer Technology in Hamilton, NJ) are shown in the top and bottom of ***Figure 11***, respectively.

The measured compensator response, as compared to the designed and ideal responses, is shown in ***Figure 12***. In the critical frequency range, from 0 to 650 MHz, the difference between the maximum and minimum deviations between the ideal and measured responses gives the passband ripple. This value was determined to be approximately 6.7

DC Power Conditioning

Lowest Noise Linear Voltage Regulators for 64-QAM Modulation Applications!

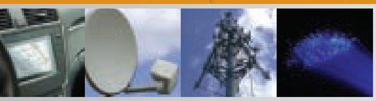

Analog, Digital & Mixed-Signal
ICs, Modules, Subsystems & Instrumentation

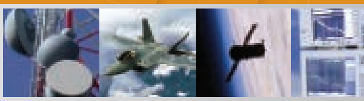

HMC1060LP3E Quad Output Low Noise High PSRR Linear Voltage Regulator

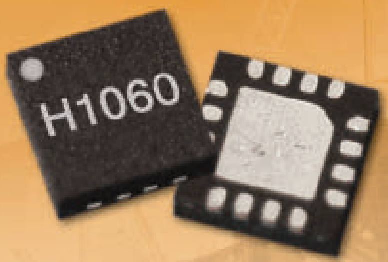

Less than 1 μA Power Down Current

- ***Ultra Low Noise Density:***
  3 nV/√Hz at 10 kHz, 7 nV/√Hz at 1 kHz
- ***High Power Supply Rejection Ratio (PSRR):***
  80 dB at 1 kHz, 60 dB at 1 MHz
- ***Four Adjustable Voltage Outputs:***
  VR1: 100 mA at 1.8V to 5.2V
  VR2 & VR3: 50 mA at 1.8V to 5.2V
  VR4: 300 mA at 1.8V to 5.2V

Output Noise Density vs. Frequency

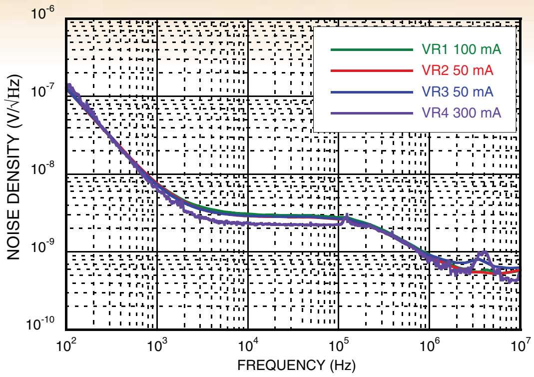

Power Supply Rejection Ratio vs. Frequency

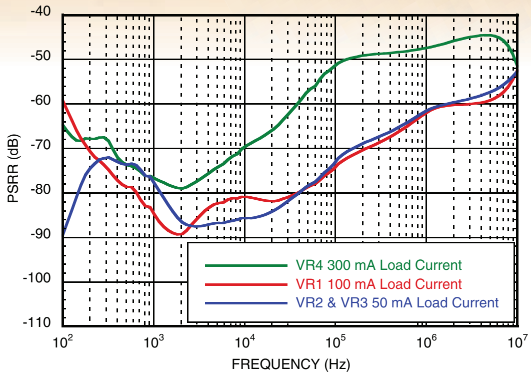

	Input Voltage (V)	Function	Output Voltage (V)	Output Current (mA)	Power Supply Rejection Ratio (PSRR) (dB)		Output Noise Spectral Density (nV/√Hz)		Regulated Outputs	Part Number
					1 kHz	1 MHz	1 kHz	10 kHz		
	3.3 - 5.6	Low Noise, High PSRR	1.8 to 5.1	400	60	30	6	3	1	**HMC976LP3E**
	3.35 - 5.6	Quad High PSRR	2.5 - 5.2	240	80	60	7	3	4	**HMC860LP3E**
NEW!	3.35 - 5.6	Low Noise, High PSRR	1.8 - 5.2	500	80	60	7	3	4	**HMC1060LP3E**

Ideal for Powering Hittite's Broad Line of Low Noise VCOs, Wideband PLLs and PLL + VCOs!

Hittite MICROWAVE CORPORATION

2 Elizabeth Drive • Chelmsford, MA 01824
978-250-3343 tel • 978-250-3373 fax • sales@hittite.com

Order On-Line at: www.hittite.com
Receive the latest product releases - click on "My Subscription"

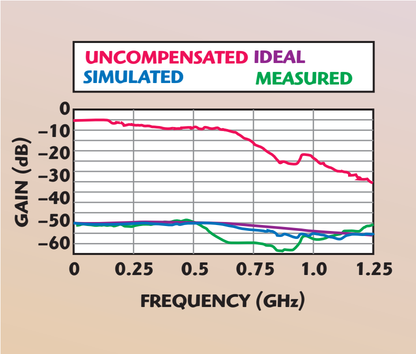

▲ *Fig. 12 Comparison between the uncompensated, ideal, simulated and measured compensations responses.*

dB, taking the difference between the deviation at 250 MHz and at 650 MHz, which was ~4 dB higher than desired. In addition, although the flatness of the high frequency response is not as critical, the measurements were between 5 and 6 dB lower than the expected response of the compensator from 590 to 885 MHz. This will cause the overall system to have this amount of additional roll-off when operating within this frequency range.

COMPENSATOR ERROR ANALYSIS AND TUNING

As a result of the poor correlation between the designed and measured responses (which, even as is, would significantly improve the high frequency response of the SLED), the next step was taken to determine possible causes for the deviations. Feasible explanations are that incorrect component values were shipped, or that incorrect components were drawn from the packages when soldering. The sharp decrease in response from ~400 to 600 MHz is controlled by the value of C6 in Figure 9. Changing this value to 5.1 pF makes the measured and simulated responses agree over this band. At the highest frequencies, the value of C2 in the R2-L2-C2 band-attenuation section controls the sharpness of the response. Reducing this value to 5.1 pF makes the frequency responses from 1 to 1.25 GHz almost identical. In addition, the response drop that is expected to occur from 900 to 1010 MHz, a result of the R2-C2-L2 band-attenuation section, was not present in the measurements. This can be eliminated from the design by changing the value of R2 to 84.5 Ω (which is the nominal value of R1).

Another explanation for the lack of agreement between the responses is the tolerances on the component values. Most likely, at least some error was caused by deviation of the inductors from their nominal values, since the specific ones measured were seen to deviate largely, as shown in Table 2.

To correct the measured response, the compensator was tuned. Increasing C1 by adding a 2.7 pF capacitor in parallel had the desirable effect of bringing the frequency dip present from 950 to 1000 MHz in Figure 6 to a lower frequency range while simultaneously increasing its sharpness. R8 provided control over the low frequency attenuation, and therefore the ripple shown in this range was reduced by increasing its value to 39 Ω. The sharpness of the highpass response was improved by placing a 1 pF capacitor in parallel with C5. Finally, the reduction in the sharpness of the dip, now located

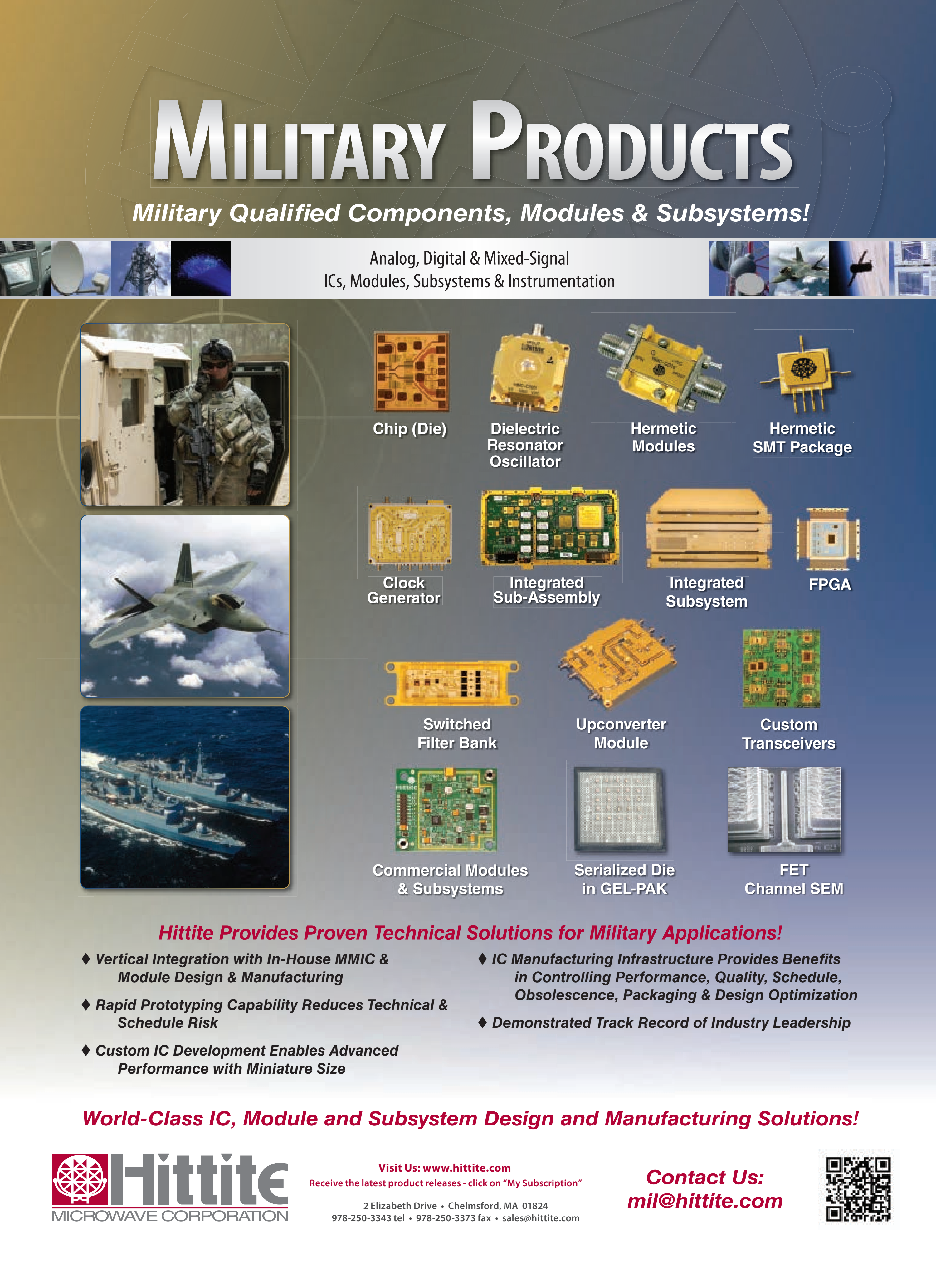
MILITARY PRODUCTS
Military Qualified Components, Modules & Subsystems!
Analog, Digital & Mixed-Signal
ICs, Modules, Subsystems & Instrumentation
Chip (Die)
Dielectric Resonator Oscillator
Hermetic Modules
Hermetic SMT Package
Clock Generator
Integrated Sub-Assembly
Integrated Subsystem
FPGA
Switched Filter Bank
Upconverter Module
Custom Transceivers
Commercial Modules & Subsystems
Serialized Die in GEL-PAK
FET Channel SEM
Hittite Provides Proven Technical Solutions for Military Applications!
♦ Vertical Integration with In-House MMIC & Module Design & Manufacturing
♦ Rapid Prototyping Capability Reduces Technical & Schedule Risk
♦ Custom IC Development Enables Advanced Performance with Miniature Size
♦ IC Manufacturing Infrastructure Provides Benefits in Controlling Performance, Quality, Schedule, Obsolescence, Packaging & Design Optimization
♦ Demonstrated Track Record of Industry Leadership
World-Class IC, Module and Subsystem Design and Manufacturing Solutions!
Hittite MICROWAVE CORPORATION
Visit Us: www.hittite.com
Receive the latest product releases - click on "My Subscription"
2 Elizabeth Drive • Chelmsford, MA 01824
978-250-3343 tel • 978-250-3373 fax • sales@hittite.com
Contact Us: mil@hittite.com

at ~955 MHz, was accomplished by completely removing R3 from the circuit. The resulting response, as compared with the untweaked, designed, and ideal responses, is also shown in Figure 6. The difference between the maximum and minimum deviations, when comparing the tweaked and ideal responses, yields a ripple for frequencies below 650 MHz of only 2.75 dB.

NET RESULT

To observe the overall compensation, the measured two-port parameters of the compensator was imported into Microwave Office, placed in cascade with the SLED and the resultant $|S_{21}|$ response was measured. A graphical comparison of the uncompensated, ideal, simulated, and measured compensation is shown in Figure 12. It indicates that the 3 dB point of the SLED was increased from 340 to 550 MHz, and the overall response dip was decreased from over 30 dB to less than 12 dB, which constitutes significant improvement. It is also important to note that the phase response of the compensator had an insignificant slope as compared to the phase of the SLED, and thus the compensator preserves phase linearity. Even without the additional tuning, the compensator would have improved the SLED response significantly. Overall, the compensator shows a small-scale, cost-effective means of correcting for the poor modulation response of the SLED, which is of much utility when attempting to broadcast over WDM PON networks. ■

Chris Brinton *is a first year PhD student at Princeton University, and received his BSEE (valedictorian and summa cum laude) in 2011 from The College of New Jersey. He holds various publications (current and pending) in the fields of power systems optimization, RF and microwave, fiber optics communications and digital signal processing. He has worked internships at AT&T Labs Research, Linearizer Technology and AT&T. His current research interests are in developing optimization algorithms to find and analyze minimum cost placements of renewable energy generators in congested electric transmission systems.*

FILTER SOLUTIONS

DC to 15 GHz

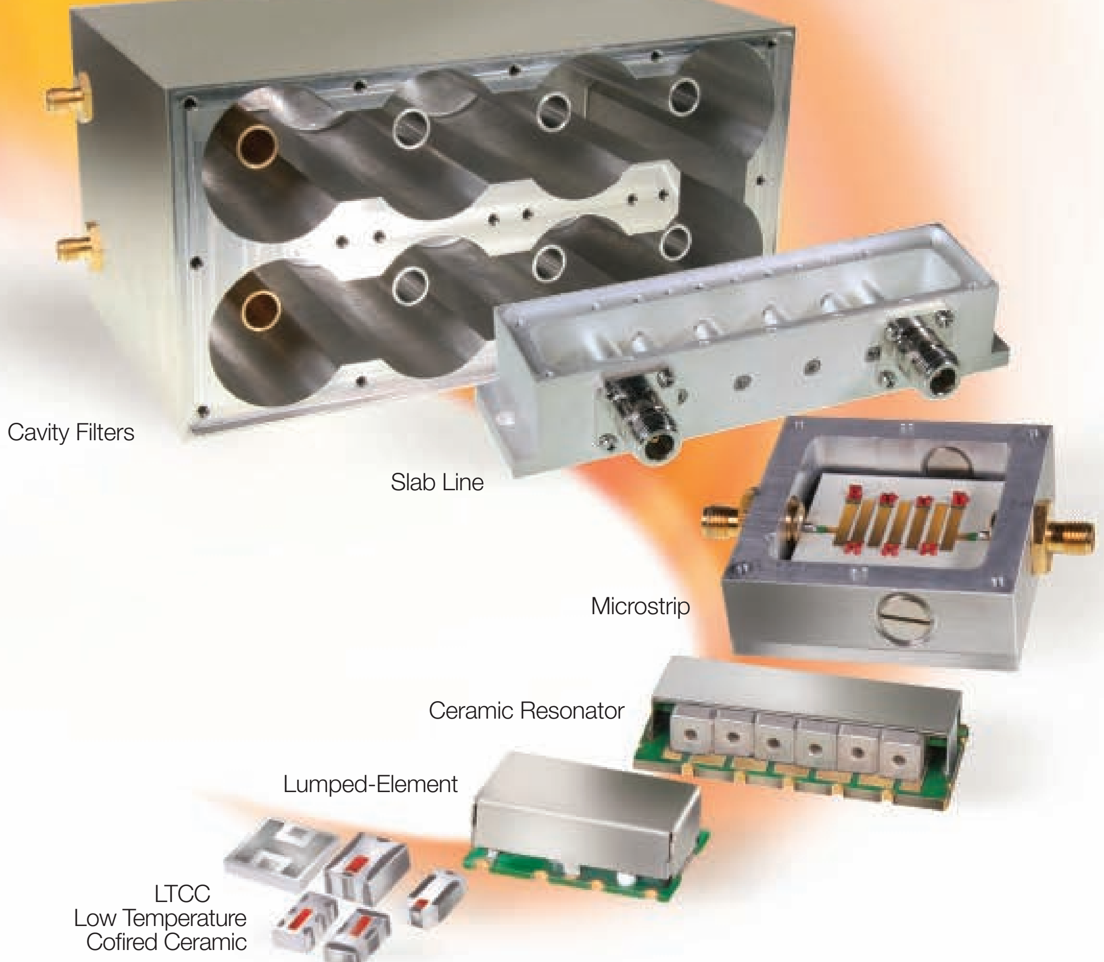

Over 300 Models IN STOCK ...Immediate Delivery! *from* $1.99 *ea. 10-49*

Different needs demand different technologies, and the Mini-Circuits RF/microwave filter lineup delivers. Over 300 proven solutions, from DC to 15 GHz, are standing by, ready to ship. High-pass or low-pass, band-pass or band-stop, in coaxial, surface-mount, or plug-in packages. Across the board, our filters achieve low insertion loss and low VSWR in the passband and high attenuation in the rejection band. Just go to minicircuits.com for more information. If you need a specific performance and want to search our entire model database, including engineering models, click on Yoni2, our exclusive search engine.

In Yoni2, you can enter the response type, connection option, frequency, insertion loss, or any other specifications you have. If a model cannot be found, we understand the sense of urgency. So contact us, and our engineers will find a quick, cost-effective, custom solution and deliver simulation results within a few days.

Yoni2® ***The Design Engineers Search Engine...*** *finds the model you need, Instantly.*
U.S. Patent 7739260, 7761442

Mini-Circuits...we're redefining what VALUE is all about!

Mini-Circuits®
ISO 9001 ISO 14001 AS 9100

P.O. Box 350166, Brooklyn, New York 11235-0003 (718) 934-4500 Fax (718) 332-4661

Yoni2® ***The Design Engineers Search Engine*** *finds the model you need, Instantly* • For detailed performance specs & shopping online see **minicircuits.com**
U.S. Patents 7739260, 7761442

IF/RF MICROWAVE COMPONENTS

484 Rev B

A Low-Power Multi-Channel UWB Single Chip Transceiver with Pulse Detectors

A single chip transceiver for ultra-wideband (UWB) impulse radio is described in this article. The UWB transmitter implements a low power Gaussian shaping filter to reduce the side lobes in the frequency domain, and a simple pulse amplitude modulation (PAM) is employed to maintain the low power consumption. The proposed architecture features a simple design, low-power operation and enables the pulse-shape generation for a multi-channel UWB radio. A low power UWB receiver was implemented with a pulse detector for the demodulation. This receiver is for the three lower bands of the UWB from 3.1 to 5 GHz. The IC is implemented using a 0.18 μm RF CMOS technology with a 1.8 V power supply. The total current consumption of the transceiver is 17 mA.

Impulse radio ultra-wideband communication (IR-UWB), using impulse signals that have an ultra wide bandwidth, is a specific form of UWB where the data bits modulate the short pulses in the time domain. An IR-UWB transmitter must comply with Federal Communications Commission (FCC) regulations.[1] To avoid interference with the wireless local area network (WLAN) band at 5 GHz, the UWB transmitters often operate in either the 3 to 5 GHz band or the 6 to 10 GHz band. In the selected 3 to 5 GHz band of this transceiver, the bandwidth of the impulse signals is restricted to a few hundred megahertz for the multi-channel operation. The idea behind the multi-channel operation is to efficiently utilize the UWB spectrum by facilitating the frequency division multiple access operation, and to ease the demands in the hardware implementation in CMOS. The channel selection is accomplished by setting the required carrier of the UWB impulse. The carrier frequency determines the center frequency of the channel, while the impulse shape and the duration control the bandwidth and minimize the interference of adjacent channels. The Gaussian pulse shape is often used for the multi-channel UWB signals because of its low side lobes. In this article, a simple CMOS Gaussian shaping filter is proposed and a simple modulation scheme is described. For the conventional transmitter, the baseband signal is up-converted by the mixer and amplified before being fed to the antenna. To keep the power consumption low for the proposed design, simple switches are employed to perform the up-conversion and its output is directly fed to the 50 Ω antenna.

Caixia Chen, Manh Anh Do, Kiat Seng Yeo, Chirn Chye Boon and Wei Meng Lim
Nanyang Technological University, Singapore

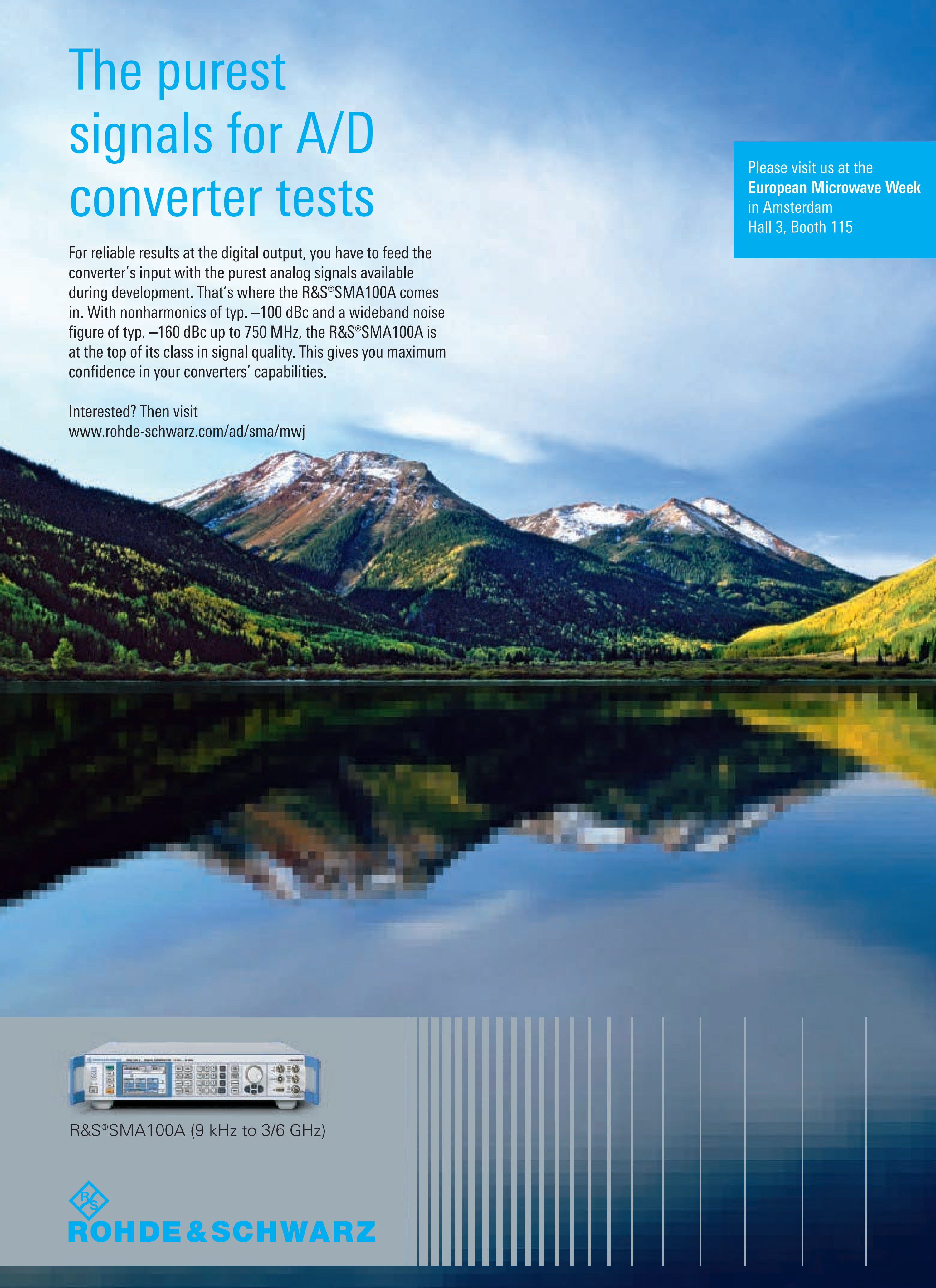
The purest signals for A/D converter tests
For reliable results at the digital output, you have to feed the converter's input with the purest analog signals available during development. That's where the R&S®SMA100A comes in. With nonharmonics of typ. –100 dBc and a wideband noise figure of typ. –160 dBc up to 750 MHz, the R&S®SMA100A is at the top of its class in signal quality. This gives you maximum confidence in your converters' capabilities.
Interested? Then visit
www.rohde-schwarz.com/ad/sma/mwj
Please visit us at the
European Microwave Week
in Amsterdam
Hall 3, Booth 115
R&S®SMA100A (9 kHz to 3/6 GHz)
ROHDE&SCHWARZ

The architecture of the UWB receiver is more complicated than that of the transmitter and consumes more power than the transmitter. Lowering the power consumption of the receiver is one of the key challenges for research in UWB. Most receivers have been designed using a direct conversion architecture[2] because of many advantages over the conventional heterodyne receiver, such as smaller size, lower cost and reduced power consumption. However, many publications[3,4] only show the front-end of the receivers, without explanation of how the down-converted UWB signal is demodulated. As the bandwidth of the baseband signal is extremely wide, it is not practical to use a digital demodulation. In this article, an impulse radio receiver including the baseband pulse detector is proposed.

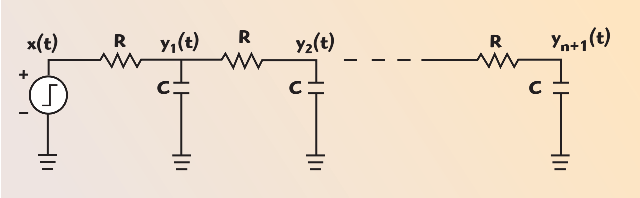

▲ *Fig. 1 Lowpass section of the $(RC)^{n+1}$ filter.*

THE PULSE GENERATION METHOD

The shape of a UWB pulse should be designed to achieve low side lobes and compliance to FCC regulation on transmitted power. Pulse shaping is important for the UWB transmission, as it minimizes both adjacent channel interference and inter-symbol interference. Pulse shaping determines the primary characteristic of the distribution of energy within the frequency domain. It concentrates most energy in the main lobe of the pulse spectrum and reduces the side lobe energy, hence reducing the adjacent band interference.[5]

The most common wideband pulse shape is the Gaussian pulse. Thus, the first attention is directed to the approximated shape of the Gaussian pulse in the CMOS process. The desired step response of the pulse-shaping filter is a Gaussian-shaped pulse and the corresponding frequency response. A well-known technique for approximating a delayed Gaussian waveform is to use a CR-$(RC)^n$ filter.[6] The Gaussian pulse can be approximated by a realizable CR-$(RC)^n$ quasi-Gaussian filter of the form,[7]

$$y(t) = \left[t^n / n!\right] e^{-t} \tag{1}$$

The $(RC)^{n+1}$ filter shown in ***Figure 1*** has a transfer function given by:

$$H(f) = \frac{1}{\left(1 + j\omega RC\right)^{n+1}} \tag{2}$$

where n+1 is the number of the RC sections and $\omega = 2\pi f$.

Its step response is given by

$$y(t) = \frac{1}{n!} \frac{(t)^n}{(RC)^{n+1}} e^{-(t/RC)} = K\left[t^n / n!\right] e^{-t} \tag{3}$$

where $K = e^{-(1/RC)}/(RC)^{n+1}$ is constant. Equation 3 is similar to Equation 1, so the Gaussian pulse can be approximated by a realizable $(RC)^{n+1}$ filter.

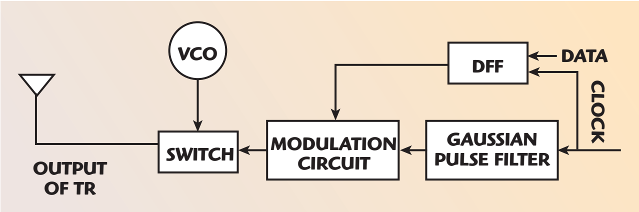

▲ *Fig. 2 Block diagram of the proposed UWB transmitter.*

TRANSMITTER ARCHITECTURE

The proposed UWB transmitter block diagram is shown in ***Figure 2***. The Gaussian shaping filter produces a pulse train. In this pulse train, the pulse width is inversely proportional to the bandwidth of the required signal. The clock and data inputs are synchronized by the D-flip-flop (DFF). The output of the DFF Q is the synchronized data input. The output P of the Gaussian shaping filter is modulated by the synchronized data to produce the impulse trains S. The switches perform a multiplication between the impulse train S and the carrier signal generated by the voltage control oscillator (VCO). The output can be directly fed to a 50 Ω antenna.

Gaussian Shaping Filter

The proposed Gaussian shaping filter, shown in ***Figure 3***, is used to approximate a Gaussian pulse and smooth the sharp edge of the clock pulse as explained previously. A CMOS transistor can be modeled as a switch with infinite off-resistance and finite on-resistance. The on-resistance and the capacitance of the transistor determine the transient behavior of an inverter. The additional capacitors of the transistor drains reduce the slope of the rising edge and falling edge of the clock (rectangular) pulse further. The clock pulse is the rectangular pulse

$$x(t) = A\,\mathrm{rect}(t/T_o) \tag{4}$$

where A is the amplitude and $T_o/2$ is the width of the rectangular pulse. Its step response is given by:

$$X(f) = AT_o\,\mathrm{sinc}(fT_o) \tag{5}$$

where A is the amplitude of the clock pulse and T_o is the width of the clock pulse. The step response of the output is

$$Y(f) = X(f)H(f) = \frac{AT_o\,\mathrm{sinc}(fT_o)}{(1+j\omega RC)^{n+1}} \tag{6}$$

Equation 6 shows that in the frequency domain, the output of the Gaussian shaping filter has very small side lobes as the number n increases.

Modulation Scheme Selection and Modulator

Figure 4 shows the arrangement for the selectable modulation schemes including PAM. P is the output of the Gaussian shaping filter. C and R are used to filter the DC values of the LO signal from the VCO. The switches facilitate the modulation of the carrier by the Gaussian pulse trains S.

As shown in the figure, P is transferred to S when Q is high, but it is isolated and S is grounded when Q is low. So P is modulated by Q to form S. M_2 is used to reduce the noise when

M_1 is turned off. And I_O shifts the pulses of S into the desired frequency. C_L and the antenna load (50 Ω) form a high pass filter. For this modulation scheme, the pulses are only produced at the output only when Q = 1.

THE PROPOSED UWB RECEIVER

In this article, the receiver is designed for the lower band UWB system, with multi-channel applications. ***Figure 5*** shows the proposed direct conversion receiver (DCR). The architecture of DCR is simple and few external components are needed. It is thus suitable for various multi-band, wideband, and multi-standard applications. A wideband LNA operating from 3 to 5 GHz was designed to amplify the received radio frequency signal. This variable gain LNA has a 50 Ω input impedance for antenna matching and filtering of out-of-band interferers. The passive mixers down-convert the RF signal from the LNA to the baseband I and Q signals by the quadrature LO signals. The passive mixers are selected for their zero power consumption. The RC low pass filter (LPF) removes the high frequency components of the down-converted signals. The full wave rectifiers align the polarities of the pulses in the I and Q paths before the summation. And the comparator, with the inverters, is used after the rectifiers to convert the analog pulse to a digital pulse.

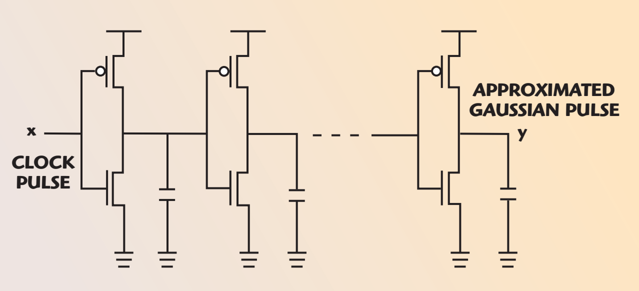

▲ *Fig. 3 The Gaussian shaping filter.*

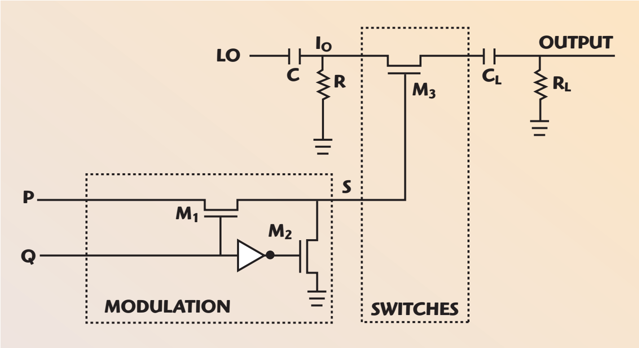

▲ *Fig. 4 Modulation scheme for PAM.*

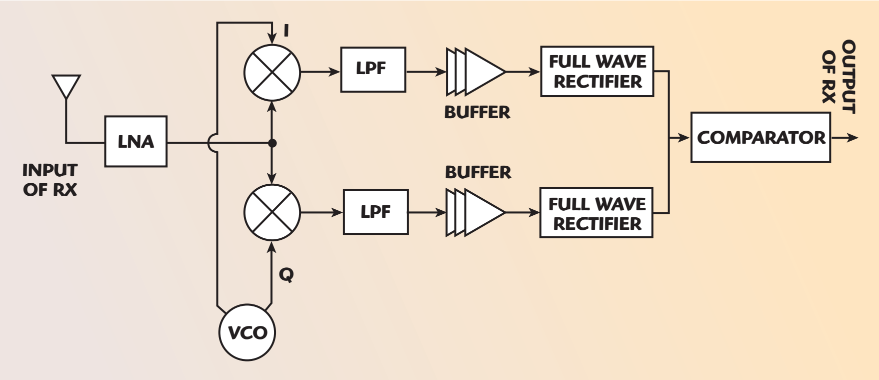

▲ *Fig. 5 Proposed receiver structure.*

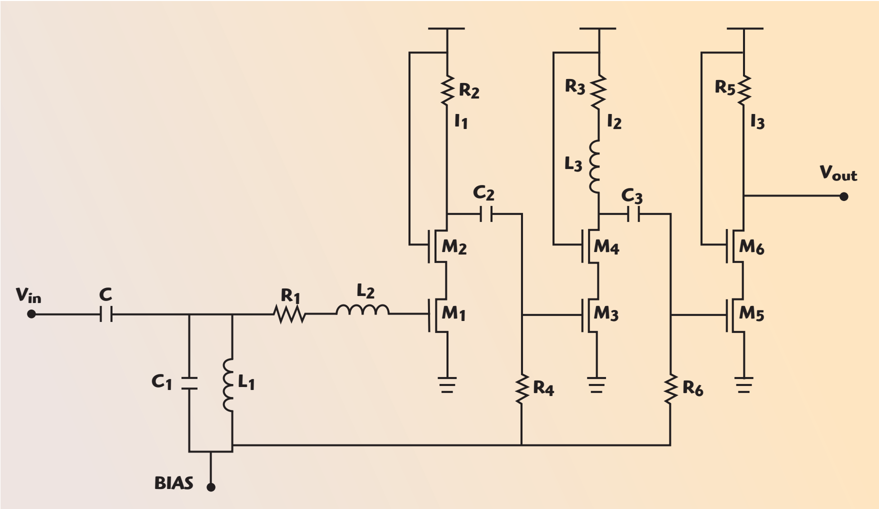

▲ *Fig. 6 Proposed low power variable gain LNA.*

Low Power Variable Gain LNA

The proposed low power variable gain LNA is shown in ***Figure 6***. The first requirement of the LNA is to provide a 50 Ω input impedance for matching the antenna or band select filter to the amplifier. The input matching network of the LNA assists in filtering out the interferers and optimizing the noise performance. The LNA should amplify the radio signal to a desired amplitude that is not too high to affect the linearity or too low to affect the receiver noise figure. A variable gain LNA can be used to optimize the receiver performance.

For the proposed common source LNA, the gain can be adjusted while maintaining low noise figure (NF) and power consumption. The variable gain LNA has three stages. The conventional source inductive degeneration input architecture is not selected, due to its low gain and extra chip area of the source inductor.[8] The input impedance of the proposed LNA can be described [8] by:

$$Z_{in} = \left[j\omega L_2 - j\frac{1}{\omega C_{gs}} \right] + \left(R_1 + R_g + R_i \right) \qquad (7)$$

where R_i is the channel charging resistance,[9] R_g is the sum of the intrinsic and extrinsic gate resistance and C_{gs} is the gate-source capacitor of M_1. The additional parallel resonator L_1 and C_1 to the series resonator form a wideband bandpass filter, which gives flat response to the LNA.[10] The gain of LNA can be tuned by the bias voltage. The current of M_1, M_3 and M_5 and the overall gain of the LNA are

Aethercomm
We make hardware that saves lives.™

HIGH POWER RF SWITCHES

Aethercomm has been designing and manufacturing solid state high power RF switches for over 12 years for our own high power systems. We are now offering them to the industry as stand alone modules.

Custom Modules Available:

- Different Frequency Ranges
- Smaller Volumes
- Higher Isolation
- Higher Power Levels
- Faster Switching Speeds
- Lower Insertion Loss

Standard Product Offerings Available:

Model Number	Frequency Range	CW Power Rates	Peak Power Handling	Insertion Loss	Isolation	VSWR	Switching Speed	Size
SSHPS 0.96-1.22-3000	960-1220 MHz	250 Watts	3000 Watts	0.8 dB	60 dB	2.0:1	4 µsec	4.5 x 3.5 x 1.0 inches
SSHPS 1.2-1.4-4000	1200-1400 MHz	200 Watts	4000 Watts	0.7 dB	60 dB	1.6:1	4 µsec	4.5 x 3.5 x 1.0 inches
SSHPS 2.7-2.9-1000	2.7-2.9 GHz	100 Watts	1000 Watts	0.8 dB	40 dB	1.7:1	4 µsec	3.5 x 3.5 x 1.0 inches
SSHPS 2.9-3.1-1000	2.9-3.1 GHz	100 Watts	1000 Watts	0.8 dB	40 dB	1.8:1	4 µsec	3.5 x 3.5 x 1.0 inches
SSHPS 2.7-3.5-1000	2.7-3.5 Ghz	50 Watts	1000 Watts	0.9 dB	40 dB	2.0:1	4 µsec	3.5 x 3.5 x 1.0 inches
SSHPS 0.020-1.000-200	20-1000 MHz	200 Watts	1500 Watts	0.7 dB	25 dB	2.0:1	5 µsec	3.0 x 3.0 x 1.0 inches
SSHPS 0.225-0.450-400	225-450 MHz	400 Watts	2000 Watts	0.7 dB	40 dB	2.0:1	5 µsec	3.0 x 3.0 x 1.0 inches
SSHPS 1.0-2.5-200	1000-2500 MHz	200 Watts	1000 Watts	0.9 dB	25 dB	1.5:1	4 µsec	4.0 x 6.0 x 1.3 inches

SSHPS 1.03-1.09-5000 Typical Data

- Operation from 1030-1090 MHz
- Peak Power Handling of 5000 Watts
- Insertion Loss = 0.4 dB nominal
- Isolation = 58 dB typical
- Operation into an Infinite VSWR
- -40C to +70C Operation
- Internal BIT
- < 5µSec Switching Speed
- Return Loss, All Ports = -14 dB nominal
- 4.5" wide x 3.5" long x 1.0" high
- All switches High Power Tested & ESS Screened

SSHPS 1.03-1.09-5000

Tel 760.208.6002
sales@aethercomm.com

BSI REGISTERED
ISO 9001:2008
FM 09366

BSI
AS 9100
FM 551035

12 YEARS IN BUSINESS 12 1999-2011

www.aethercomm.com

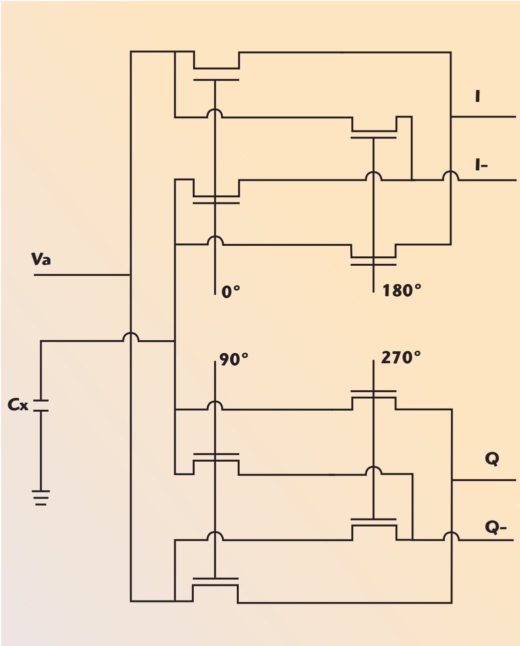

▲ *Fig. 7 The passive mixer.*

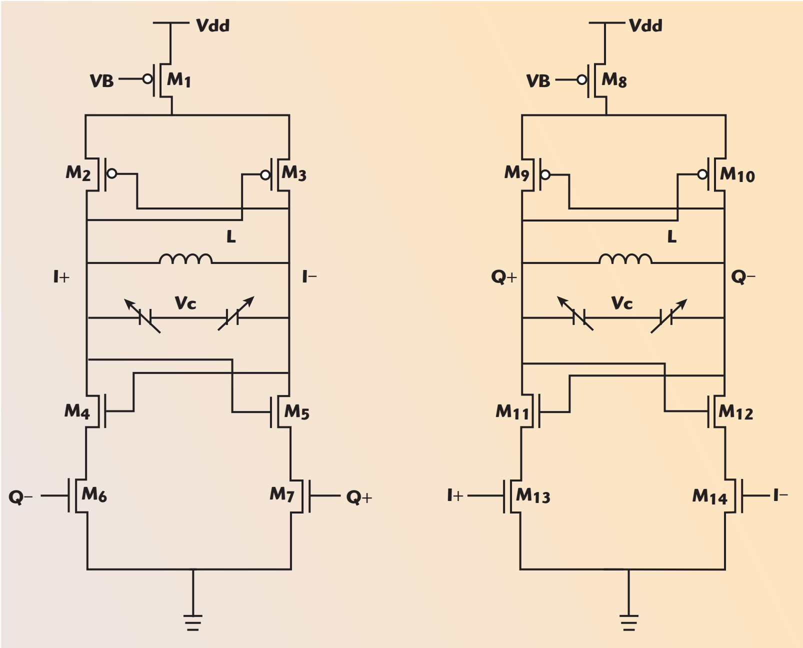

▲ *Fig. 8 Schematic of the S-QVCO.*

controlled by the bias voltage. The first and third stages have a high gain at low frequencies, and the second stage has a high gain at high frequencies. The size of M_1 is designed for proper input matching. The value R_2 is critical as it determines the gain of the first stage. The second stage is a cascode common source stage, which provides high frequency gain and better isolation. A series peaking inductor L_3 is resonant with the total parasitic capacitance at the drain of M_4 and C_3.

Mixer and S-QVCO

After the LNA, a passive mixer is used due to its low power and high linearity. A passive mixer dissipates no DC current. In ***Figure 7***, the output Va of the LNA is connected to one of RF terminals of the passive mixer, while the other RF terminal of the mixer is connected to AC ground through the bypass capacitor Cx (5 pF). During the operation of the passive mixer, the transistors act as switches to down-convert the frequency of the signal. In this switching process, the transistors' on-resistance plays an important role in contributing to the noise figure. In order to turn on and off the transistor, the gate voltage can be described as[11]

$$V_G = V_{CM} + V_{TH} \tag{8}$$

where the source drain terminals are biased at V_{CM} and V_{TH} is the threshold voltage of transistors. The higher aspect ratio of the transistors leads to the better noise performance. In contrast, the small aspect ratio and zero drain-source voltage (V_{CM}) of transis-

Since 1990 Dielectric Laboratories Inc. has been manufacturing Space qualified parts to MIL Standards.

In late 2012 QPL will be launched.

EARTH TESTED, SPACE PROVEN.

Our Capacitors, Hi-K Ceramics, and Custom Thin Film Components have over

200,000,000

LIFE TEST HOURS*

WITH NO FAILURES!

When failure is not an option, reliability means everything. You can turn to DLI with confidence for Space rated components.

With ***nearly 40 years of experience*** DLI is the pre-eminent ceramic component manufacturer in the industry.

*Between 1990 and 1995 over 92 million hours of life test data (MIL-C-49464) was accumulated with zero failures. Between 1997 and 2003 DLI collected an accelerated amount of life test hours of > 71 million hours with zero failures, performed per the requirements of MIL-C-49464. Between 2005 and 2010 DLI collected an accelerated amount of life test hours of > 74 million hours with zero failures, performed per the requirements of MIL-PRF-49464. Testing is in progress for the 2011 – 2016 period.

There Is No Substitute For Experience

DLI DIELECTRIC LABORATORIES
A DOVER COMPANY
CMP

www.dilabs.com

CERAMIC & MICROWAVE PRODUCTS
Electronic Components & Microwave Solutions
A DOVER COMPANY
CMP

BCS FILTERS • DOW-KEY MICROWAVE • NOVACAP • SYFER TECHNOLOGY
DIELECTRIC LABORTORIES • K&L MICROWAVE • POLE/ZERO • VOLTRONICS

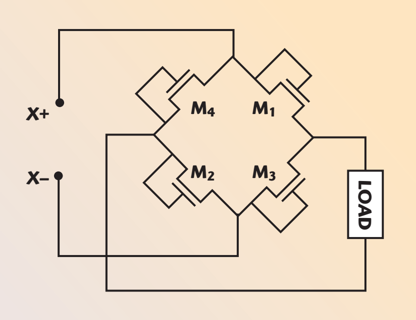

▲ *Fig. 9 Full wave rectifier with CMOS diodes.*

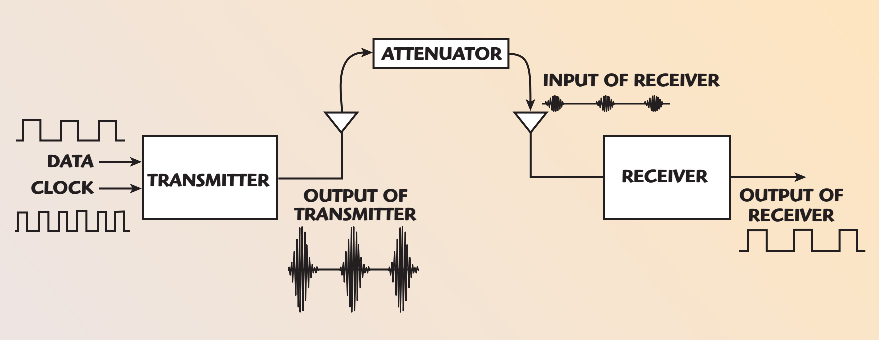

▲ *Fig. 11 Setup of simulation measurement for the complete transceiver.*

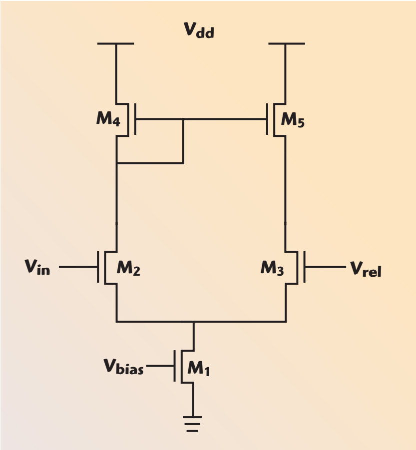

▲ *Fig. 10 One bit comparator.*

tors in the passive mixer core can improve the LO-to-RF isolation.[12] V_{CM} is very small and negligible, so the gate voltage is closed to the threshold voltage. To keep the NF of the receiver low, the gain of the LNA must be reasonably high. Thus, smaller aspect ratio transistors are used to give high load impedance to the LNA, and the size of the transistors is optimized against the NF of receiver.

The output of the LNA is down-converted by the passive mixer and the series quadrature VCO (S-QVCO) shown in ***Figure 8***. The architecture of the S-QVCO has a low power consumption.[13] Due to the low power criterion, the S-QVCO is used for quadrature signal generation and connected with the passive mixer. For this receiver, the required frequency is 4 GHz. A PMOS transistor has a lower flicker noise than an NMOS counterpart, and a p-tail np-core structure is often used in LC VCO. As shown, the circuit has been improved. Here L is 3.5 nH.

The Pulse Detector

After the LPF and the buffer, the outputs of the buffer are not of the same polarity. Detectors that consist of a squarer and an integrator have been published.[14,15] The squarer and the integrator are used to produce the same polarity pulses in the UWB receiver. In this article, CMOS full wave rectifiers used as the pulse detector are chosen for such purposes and are shown in ***Figure 9***. The signal goes through M_1 and M_2 for the positive half cycle and passes the other two transistors for the negative cycle. The low power full wave rectifiers are used to synchronize the polarities of the pulses in the pulse trains. The full wave rectifiers are used to synchronize the polarities of the pulses in the pulse trains and make the same polarity of the pulses when data is "1." This is new for a UWB receiver. This can be implemented for both the pulse amplitude demodulation and pulse position demodulation.

Comparator

The comparator is a circuit that compares an analog signal with another analog signal or reference and

Available for shipment within 24 hours from receipt of your order.

AS 9100 & ISO 9001:2001 CERTIFIED

On-Demand
minibend®
CABLE ASSEMBLIES

minibend® SMA plug to SMA plug cable assemblies (3” to 16”) are now available for shipment within 24 hours from receipt of your order. Astrolab’s expedited shipping is available for all orders up to 100 cable assemblies. Varying lengths can be ordered in any combination to achieve the best quantity discount.

Astrolab’s patented minibend® cable assemblies provide an excellent commercial-off-the-shelf (COTS) solution for your cable assembly needs. The perfect low profile design solution for making point-to-point interconnections between RF modules. minibend® cable assemblies are readily integrated into virtually any commercial, military, or space application.

minibend® cable assemblies are engineered to meet or exceed applicable industry and military standards. They’re triple shielded, bend-to-the-end and easily outperform competitive semi-rigid or semi-flex cable. All minibend® assemblies are 100% tested and are superior replacements for custom pre-formed semi-rigid cables.

If your company uses RF cables, you need to talk to us. We’ll work with you to supply a minibend® solution that will deliver proven superior performance. Contact our customer service department to experience the minibend® difference.

ASTROLAB® INC.
Tel: 732.560.3800
Email: sales@astrolab.com
www.astrolab.com

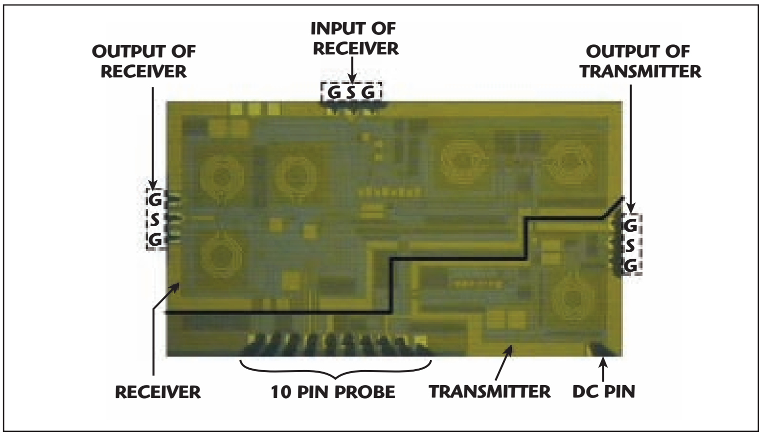

▲ *Fig. 12 Photograph of the fabricated single chip transceiver.*

outputs a binary signal based on the comparison. The quantum voltage comparator consists of two cascade differential pairs with current mirror load.[16] Here, the second differential pair of the comparator is replaced by the CMOS inverters. The inverter works as a gain booster to improve the gain of the comparator. ***Figure 10*** shows a one bit comparator that consists of one comparator pair with current mirror load. This comparator with the inverters is used after the rectifiers to convert the analog pulse to digital pulse. The transistor M_1 is the switching current source. The differential pair (M_2 and M_3) of the comparator boosts the input difference voltage in order to provide the voltage difference needed.

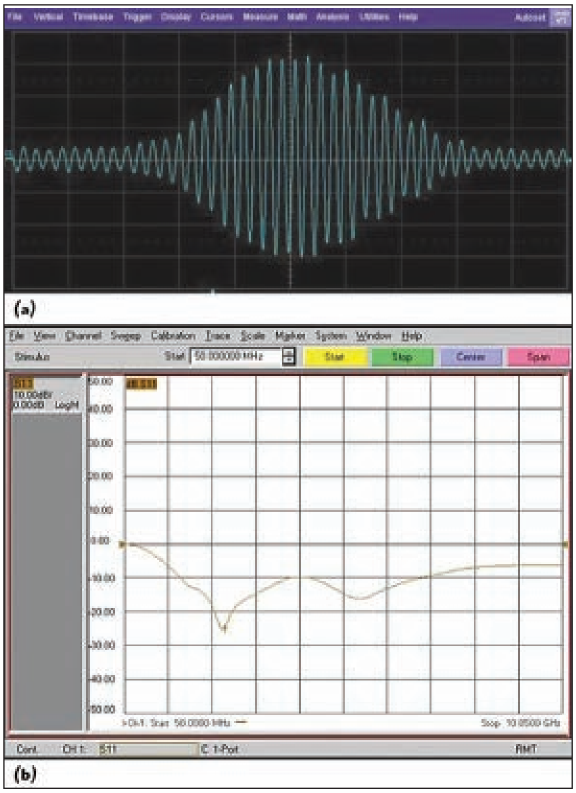

▲ *Fig. 13 Single pulse at the output of the transmitter (a), S_{11} of the LNA at the input of the receiver (b).*

MEASUREMENT RESULTS

The measurement setup for the transceiver is shown in ***Figure 11***. The data input and clock input were sent to the transmitter and the Gaussian pulse train was measured at the output of the transmitter. The output of the transmitter was connected to the receiver through an attenuator, which accounts for the power propagation loss in the air in a wireless connection. The received power can be determined by the emitted power from the transmitter and the distance between the transmitter and the receiver if the antenna gain is negligible. The receiver demodulates the attenuated signal and produces detected data at the output of the receiver. The die photograph of the whole transceiver is shown in ***Figure 12***. The chip size is 2.4 × 1.3 mm.

The approximate single Gaussian pulse shown in ***Figure 13*** is measured at the output of the transmitter. The Vpp of the transmitter is 125 mV and the center frequency is 4 GHz. The figure also shows the input return loss of the receiver. The measured S_{11} is less than –10 dB from 2 to 6 GHz. For a 1.8 V power supply, the current consumptions of the transmitter and re-

TABLE I SUMMARY OF MEASURED TRANSCEIVER PERFORMANCE

	This Work	[15]	[14]	[17]
Tech	0.18 μm CMOS	0.18 μm CMOS	0.09 μm CMOS	0.18 μm CMOS
Status	Measured	Measured	Measured	Measured
Max V_{DD}	1.8 V	1.8 V	1.2 V	1.8 V
Modulation	PAM/PPM	MD-OFDM	PAM	FSK
Receiver Gain	39 dB	25.3 to 84 dB	22.6 dB	31 to 40 dB
Receiver P. Cons	25.2 mW	285 mW	156 mW	54 mW
Transmitter P. Cons	5.4 mW	139 mW	125 mW	15.4 mW
NF	8 dB	6.5 to 8.25 dB	~	10 to 7.5 dB
Bandwidth	3 to 5 GHz	3.1 to 8 GHz	3.1 to 9.5 GHz	3 to 8 GHz
Die Area	3.1 mm^2	15.6 mm^2	1.5 mm^2	6.8 mm^2

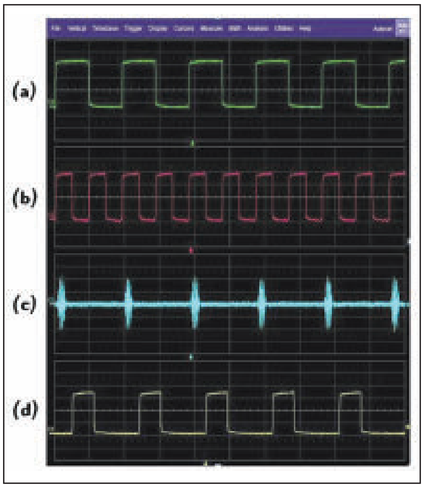

▲ *Fig. 14 Data input of the transmitter (a), clock input of the transmitter (b), received pulse train at the receiver (c), output of the receiver (d).*

ceiver are 3 and 14 mA, respectively.

As the measurements were performed on wafer, the output of the transmitter is passed through an attenuator to account for the propagation loss then looped back to the receiver. In ***Figure 14***, the data input (a) and the clock input (b) of the transmitter are shown, as well as the time-domain response of the proposed transmitter (c) with a pulse repetition frequency of 52 MHz input at a 1.8 V supply voltage, while (d) is the demodulated output of the receiver. The whole receiver achieves a 39 dBm gain. The tuning range of the center frequency of S-QVCO in the receiver is 1 GHz. The noise figure of the whole transceiver is 8 dB.

The proposed transceiver is compared with other receivers in ***Table 1***. As shown, the proposed transceiver has the lowest power consumption. Although the area of Zhang's transceiver[14] is half of the proposed transceiver, its power consumption is five times the power consumption of the proposed transceiver and its transmitter power consumption is twenty-three times that of the proposed transmitter. Additionally, the gain of the proposed receiver is higher by 16.4 dB. The several nanosecond narrow pulse train was demodulated in the proposed receiver. The small narrow analog pulse has been demodulated into the rectangular digital in the proposed receiver. This is an additional contribution of this proposed transceiver. The demodulation of the short pulse is usually not dealt with in other publications. This receiver

can be used for both pulse amplitude modulation and pulse position modulation.

CONCLUSION

In this article, a new design of a single chip transceiver is presented. The proposed transceiver can operate at various frequencies, determined by the S-QVCO. The design frequency is from 3 to 5 GHz of the lower band of the UWB system. This transceiver can be used for the multi-band UWB system, consumes a low power and occupies a small size for both transmitter and receiver. A new proposed Gaussian pulse filter is used in the transmitters. It consumes low power and can obtain the approximate Gaussian pulses. A simple and low power modulation scheme was also designed for transmitter.

The main advantage of the proposed receiver is that both the size and the power consumption are small, while maintaining sufficient gain. The rectifiers are used to polarize the pulse polarity in the UWB receiver for the first time. The pulses can be demodulated by using the CMOS full wave rectifiers that consume a low power and occupy a small area in the chip. This is the first innovation point in the receiver. The variable gain LNA has been investigated also. The gain of these three stages LNA could be tuned by the bias voltage in the LNA. The LNA offers sufficient gain to keep a low noise figure for the whole receiver. ■

References

1. "Revision of Part 15 of the Commission's Rules Regarding Ultra-wide-band Transmission Systems," FCC, Washington, DC, 2002, FCC report and order, adopted February 14, 2002, released July 15, 2002.
2. A.A. Abidi, "The Path to the Software-Defined Radio Receiver," *IEEE Journal of Solid-State Circuits*, Vol. 42, No. 5, May 2007, pp. 954-966.
3. G. Cusmai et al., "A 0.18-μm CMOS Selective Receiver Front-end for UWB Application," *IEEE Journal of Solid-State Circuits*, Vol. 41, No. 8. August 2006, pp. 1764-1771.
4. F.S. Lee and A.P. Chandradasan, "A BiCMOS Ultra-Wideband 3.1 to 10.6 GHz Front-end," *IEEE Journal of Solid-State Circuits*, Vol. 41, No. 8, August 2006, pp. 1784-1791.
5. M. Ghavami, L.B. Michael and R. Kohno, "Ultra Wideband Signals and Systems in Communication Engineering," John Wiley & Sons Ltd, Chichester, UK, 2007.
6. Z.Y. Chang and W.M.C. Sansen, "Low-Noise Wide-Band Amplifiers in Bipolar and CMOS Technologies," Ch. 5, Kluwer, Norwell, MA, 1991.
7. E. Fairstein, "Linear Unipolar Pulse-Shaping Networks: Current Technology," IEEE Transaction on Nuclear Science, Vol. 37, No. 2, Pt. 1, April 1990, pp. 382-397.
8. M. Shouxian, M. Jian-Guo, Y.K. Seng and D. Manh Anh, "A Modified Architecture Used for Input Matching in CMOS Low Noise Amplifiers," *IEEE Transactions on Circuits and Systems*, Vol. 52, No. 11, November 2005, pp. 784-788.
9. T. Manku, "Microwave CMOS-device Physics and Design," *IEEE Journal of Solid-State Circuits*, Vol. 34, No. 3, March 1999, pp. 277-285.
10. A. Ismail and A.A. Abidi, "A 3-10 GHz Low Noise Amplifier with Wideband LC-Ladder Matching Network," *IEEE Journal of Solid-State Circuits*, Vol. 39, No. 12, December 2004, pp. 2269-2277.
11. T.K. Nguyen et al., " A Low-Power RF

Direct-Conversion Receiver/Transmitter for 2.1-GHz-Band IEEE 802.15.4 Standard in 0.18-μm CMOS Technology," *IEEE Transactions on Microwave Theory and Techniques*, Vol. 54, No. 12, December 2006, pp. 4062-4071.
12. C.G. Tan, "A High-performance Low-power CMOS Double-balanced IQ Down-conversion Mixer for 2.45 GHz ISM Band Application," *2003 IEEE Radio Frequency Integrated Circuits Symposium Digest*, pp. 457-460.
13. V. Krishna et al., "A Low Power Fully Programmable 1 MHz Resolution 2.4 GHz CMOS PLL Frequency Synthesizer," *2007 IEEE Biomedical Circuits and Systems Conference Digest*, pp. 187-190.
14. F. Zhang, A. Jha, R. Gharpurey and P. Kinget, "An Agile, Ultra-wideband Pulse Radio Transceiver with Discrete-time Wideband-IF," *IEEE Journal of Solid-State Circuits*, Vol. 44, No. 5, May 2009, pp. 1336-1351.
15. H. Zheng, S. Luo, D. Lu, C. Shen, T. Chan and H.C. Luong, "A 3.1 GHz-8.0 GHz Single-Chip Transceiver for MB-OFDM UWB in 0.18-μm CMOS Process," *IEEE Journal of Solid-State Circuits*, Vol. 44, No. 23, February 2009, pp. 414-425.
16. J. Yoo, K. Cho and J. Ghaznavi, "Quantum Voltage Comparator for 0.7 μm CMOS Flash A/D Converters," *2003 IEEE Annual Symposium on VLSI Digest*, pp. 280-281.
17. M.U. Nair, Y. Zheng, C.W. Ang, Y. Lian, Xiaojun Yuan and Chun Huat Heng, "A Low SIR Impulse UWB Transceiver Utilizing Chirp FSK in 0.18 μm CMOS," *IEEE Journal of Solid-State Circuits*, Vol. 45, No. 11, November 2010, pp. 2388-2403.

Caixia Chen *received her B.Eng. (1st Honors) from Nanyang Technological University (NTU), Singapore, in 2006. She is expected to get her Ph.D. degree in 2012 from Nanyang Technological University. Since October 2010, she has been working at Avago Technologies as an R&D engineer. Her research interests include design and implementation of the ultra-wideband transmitter and receiver based on CMOS for wireless communication.*

Manh Anh Do *received his B.E. (Honors) degree and a Ph.D. degree in electrical engineering from the University of Canterbury, Christchurch, New Zealand, in 1973 and 1977, respectively. Between 1977 and 1989, he held various positions, including as a design engineer, production manager, and research scientist in New Zealand and a senior lecturer with the National University of Singapore, Singapore. He joined the School of Electrical and Electronic Engineering, Nanyang Technological University (NTU), Singapore, as a senior lecturer in 1989 and obtained the Associate Professorship in 1996 and Professorship in 2001. Between 1995 and 2005, he was head of the division of circuits and systems, NTU. He was the director of center for integrated circuits and systems from 2007 to 2010. He is currently a member of the NTU Research Council. His current research interests include mobile communications, RFIC design and mixed-signal circuits.*

Kiat Seng Yeo *received his B.Eng. (Honors) (Elect) in 1993 and Ph.D. (Elect. Eng.) in 1996, both from Nanyang Technological University, Singapore. In 1996, he joined the School of Electrical and Electronic Engineering, Nanyang Technological University, Singapore, as a lecturer and became an assistant professor in 1999 and an associate professor in 2002. He has been appointed head of circuits and Systems for a period of six years from 1 July 2005.*

Chirn Chye Boon *received his B.E. (Honors.) (Elect.) in 2000 and his Ph.D. (Elect. Eng.) in 2004 from Nanyang Technological University (NTU), Singapore. In 2005, he joined NTU as a Research Fellow and became an assistant professor in the same year. Before that, he was with Advanced RFIC, where he worked as a senior engineer. He specializes in the areas of radio frequency (RF) and mm-wave circuits and systems design for biomedical and communications applications.*

Wei Meng Lim *received his B.E. (Honors) and M.E. degrees from Nanyang Technological University (NTU), Singapore, in 2002 and 2004 respectively. Upon his graduation, he joined the School of Electrical and Electronic Engineering, NTU, as a research staff. His research interests include RF circuit designs, RF devices characterization and modeling.*

We've Pushed The Technology Envelope.

Our New Hybrid Power Modules Now Provide High Output Power Levels Across An Instantaneous BW From 4-18 GHz.

AR's new line of Hybrid Power Modules (HPM's) are small, compact and lightweight, but they're big on power and performance. Our standard products deliver up to 5 watts of output power with excellent linearity, gain flatness and the ability to withstand infinite output mismatches.

Ultra Wide Bandwidth and High Power – A Great Combination

Our rugged modular products utilize the latest microelectronic technologies to achieve outstanding performance and small size for demanding applications. Thin film processes using chip and wire devices are used for the higher frequency 4-18 GHz frequency bands, whereas thick film lower cost custom design approaches using chip or packaged transistors can be used in the lower frequency regions.

Regardless of the techniques used, we can supply our HPM's in true hermetic housings to meet both fine and gross leak testing to military specifications.

AR Has The Capabilities To Produce Cost-Effective, Custom-Designed HPM's To Your Specs

Both military and commercial solutions can be provided to meet your specific need for high performance in a compact size. Connectorized or pallet type custom designs, which can be integrated into higher order assemblies, can also be provided, giving you alternate solutions for even your most demanding applications. These modular amplifiers can also be supplied as a complete self contained air cooled assembly including power supplies, a digital control panel, gain control and input overdrive protection.

Applications For Our HPM's Are Limited Only By Your Imagination but a small sampling are:
Jammers, Radars, ECM, ECCM, Data links, TWTA replacements and drivers, and Communications.
To learn more, call AR RF/Microwave Instrumentation at 215-723-8181.

www.arworld.us/hpm

RoHS

ISO 9001:2008 Certified

rf/microwave instrumentation

Other ar divisions: modular rf • receiver systems • ar europe

USA 215-723-8181. For an applications engineer, call 800-933-8181.
In Europe, call ar United Kingdom 441-908-282766 • ar France 33-1-47-91-75-30 • ar Benelux 31-172-423-000

www.arworld.us

Design of a Compact Bandpass Filter with Capacity Loaded Ridged Waveguide

A K-Band bandpass filter, using a single ridge waveguide and capacity-loading posts, is presented in this article. It is based on transmission line and ridged waveguide theories. In contrast to the traditional evanescent-mode ridged waveguide filters, the width of both ridge and capacitor-loading post of the proposed new type of the ridged waveguide bandpass filter are the same. A filter is designed, simulated and fabricated at 22.3 GHz, demonstrating a fractional bandwidth of 42.2 percent, from 17.6 to 27 GHz, a VSWR less than 1.5 and an out-of-band rejection of –60 dB at 15 and 30 GHz, respectively. Based upon these good performances, the proposed ridged waveguide filter can be used in microwave and millimeter wave communication systems.

Waveguide bandpass filters are playing an increasingly important role in modern communication systems and other microwave fields. With the rapid development of modern microwave and millimeter wave communication systems, the requirement for filters with high performance, wide bandwidth and small size is growing.

To make the waveguide filter more compact, a traditional resonator is modified in order to obtain multiple resonant frequencies. Hence, one resonator can be treated as the equivalent of multiple resonators. The dual-mode filter is one of the most widely used in multiple-mode filters that have been developed.[1-3] However, the limitation for such a filter is that the width of a dual-mode filter is greater than that of traditional rectangular waveguide filters.

Evanescent-mode filters have been proposed by Graven to reduce the width of the waveguide filter and the technology had been applied for years.[3-6] Besides, the evanescent-mode filters perform well in out-of-band rejection. And they have small size and light weight, making such filters more widely used in microwave and millimeter wave systems.

Evanescent-mode ridged waveguide bandpass filters have been developed[7-9] where various configurations of ridge are used and wide spurious-free out-of-band responses are achieved. However, the disadvantage of this technology is that the different cross sections of the cavity make the fabrication difficult for building a wideband filter.

Cohn has reported the ridge waveguide and analyzed its properties.[10] Because of its high power capacity, low insertion loss and good frequency selectiveness, the ridged waveguide filter has attracted attention, followed by many reports on the subject, to reduce the size of

Xianrong Zhang, Qingyuan Wang, Jinhua Cao and AnJ Peng
University of Electronic Science and Technology of China, Chengdu, China

the filters.[11-12] Compared to rectangular waveguides, ridged waveguides have the advantages of wide fundamental-mode operating bandwidth, low cutoff frequency and low wave impedance.[10-11] Fundamental-mode operating bandwidth of four to one or more is easily obtainable with ridged waveguides. The low cutoff frequency yields a small cross section and hence, a compact size ridged waveguide component can be achieved. The low wave impedance allows an easy transition to planar transmission lines such as strip lines or microstrip lines. Therefore, ridged waveguide bandpass filters are the ideal components for these applications.

In this article, a new type of 10-order, wideband bandpass filter, employing ridged waveguide and capacitor-loading is proposed. It is noticed that the widths of the ridge and posts are identical, making the manufacturing process convenient. The design specifications for the filter are a 22.3 GHz center frequency, demonstrating a fractional bandwidth of 42.2 percent, from 17.6 to 27 GHz, with a VSWR less than 1.5, an out-of-band rejection at 15 and 30 GHz less than –60 dB, respectively. The bandpass filter was fabricated and measured. Both the simulated and measured results are presented.

THEORY AND ANALYSIS

For the cross section of the single ridged waveguide shown in ***Figure 1***, the width and height of the single ridged waveguide are a_1 and b_1. The width of the ridge is a_2 and b_2 is the distance from the top of the ridge to the top of the waveguide. The equivalent circuit is also shown, where C_s is the electrostatic capacitance originating between the ridge and ground, while C_d denotes the capacitance formed from the discontinuity of the ridge. L is the equivalent inductance of the waveguide from the two sides of the ridge.

The capacitance C_s is given by:

$$C_s = \frac{\varepsilon_1 a_2}{b_2} \tag{1}$$

where ε_1 is the dielectric constant of the medium. The capacitance C_d depends on the b_2/b_1 ratio. Using a conformal transformation, C_d can be expressed as follows[13]

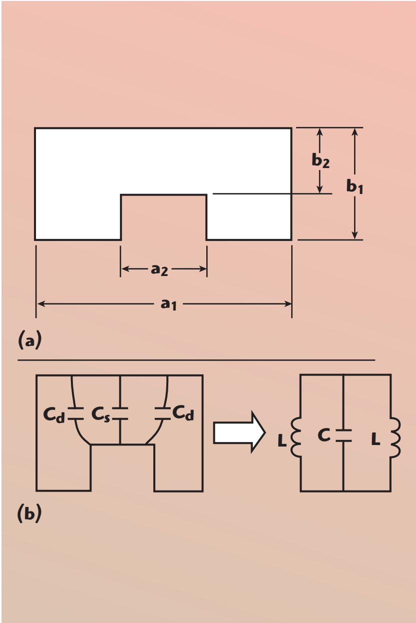

▲ *Fig. 1 Single ridged waveguide (a) cross section, (b) equivalent circuit.*

$$C_d = \frac{\varepsilon_1}{\pi} \cdot \left[\frac{x^2+1}{x} \cosh^{-1}\left(\frac{1+x^2}{1-x^2} - 2\ln\frac{4x}{1-x^2} \right) \right] \tag{2}$$

where x represents b_2/b_1. Hence, the total capacitance per unit length can be expressed as

$$C_1 = \frac{\varepsilon_1 a_2}{b_2} + 2C_d \tag{3}$$

The equivalent inductance per unit length is expressed as

$$L_1 = \frac{\mu_1 (a_1 - a_2)}{2} b_1 \tag{4}$$

where μ_1 is the permeability of the medium. The cutoff frequency of the ridged waveguide f'_c can be expressed using Equations 3 and 4 as follows:

$$f'_c = \frac{1}{2\pi\sqrt{\frac{L_1}{2} C_1}} = \frac{1}{\pi\sqrt{\mu_1 \varepsilon_1}\sqrt{\left(\frac{a_2}{b_2} + \frac{2C_d}{\varepsilon_1}\right)(a_1 - a_2) b_1}} \tag{5}$$

The cut off wavelength of the ridged waveguide can be expressed as

Radar, Wireless Communications, SATCOM, and Space

High-Reliability GaN Power Where You Need It

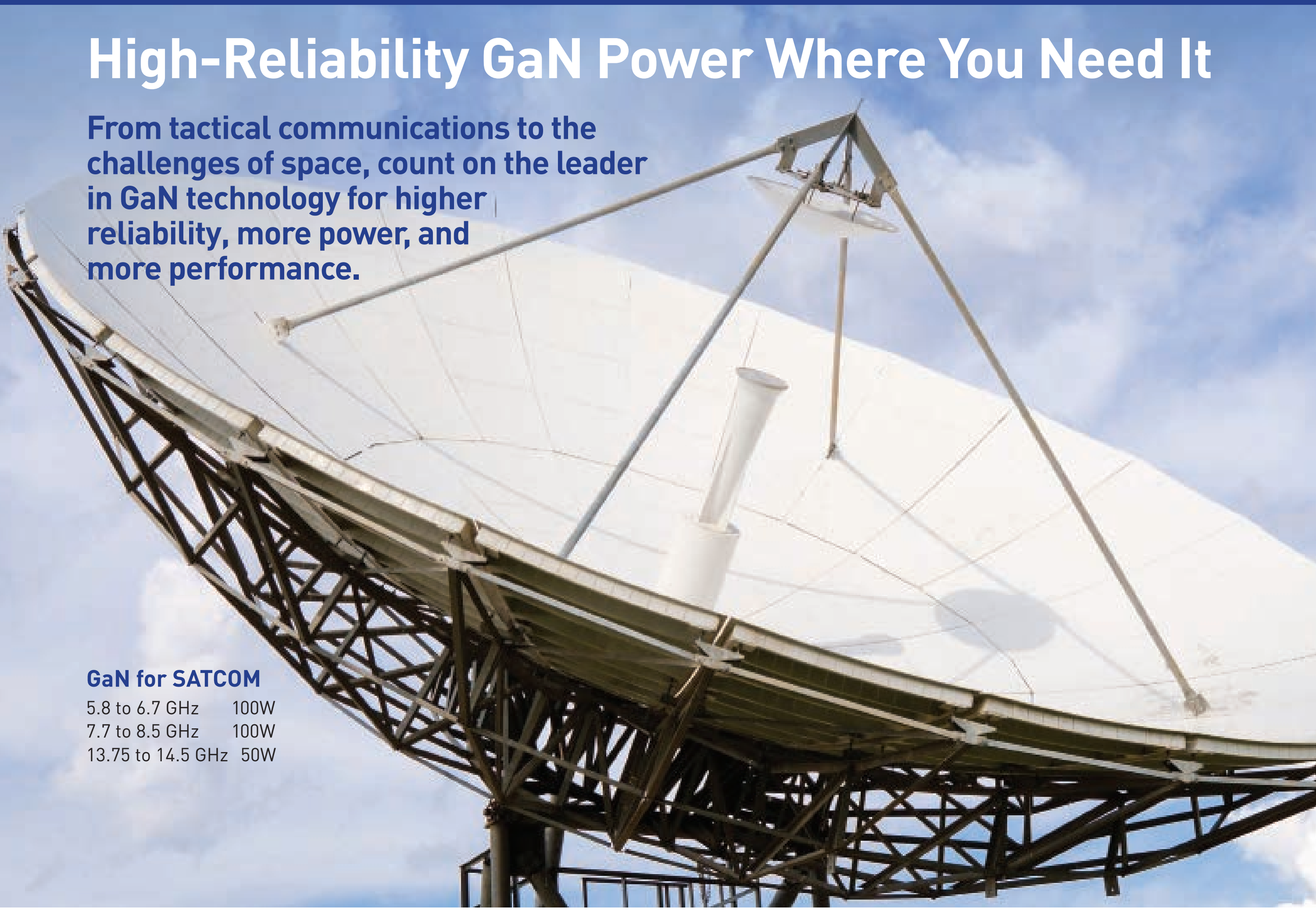

From tactical communications to the challenges of space, count on the leader in GaN technology for higher reliability, more power, and more performance.

GaN for SATCOM

5.8 to 6.7 GHz	100W
7.7 to 8.5 GHz	100W
13.75 to 14.5 GHz	50W

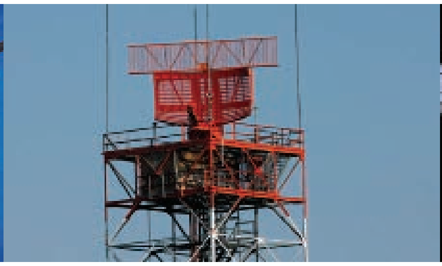

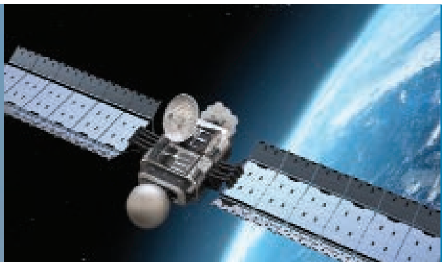

GaN for Mobile

UHF to 3.5 GHz
10/30/90/100W

SPDT Switch
VHF to 3.5 GHz 30W
VHF to 2.5 GHz 60W

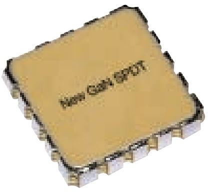

To learn more, contact usacomm@sei-device.com

GaN for Radar

S-Band

2.9 to 3.3 GHz	600W	Discrete & Pallet
3.1 to 3.5 GHz	600W	Discrete & Pallet

X-Band
9.2 to 10 GHz

60W	Discrete
120W	Discrete

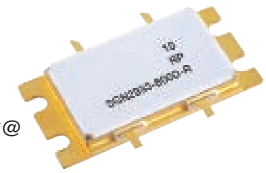

To learn more, contact usaradar@sei-device.com

GaN for Space

UHF to 2.5 GHz
4/8/20/50/100W

To learn more, contact usaspace@sei-device.com

www.sei-device.com

SUMITOMO ELECTRIC
Ingenious Dynamics

$$\lambda_c' = \frac{1}{f_c'\sqrt{\mu_1\varepsilon_1}} = \pi\sqrt{\left(\frac{a_2}{b_2}+\frac{2C_d}{\varepsilon_1}\right)(a_1-a_2)\,b_1} \quad (6)$$

Then, $\frac{\lambda_c'}{\lambda_c}$ can be given by

$$\frac{\lambda_c'}{\lambda_c} = \frac{\pi}{2}\sqrt{\left(\frac{a_2}{b_2}+\frac{2C_d}{\varepsilon_1}\right)\left(\frac{b_1}{a_1}\right)\left(1-\frac{a_2}{a_1}\right)} \quad (7)$$

where λ_c is the cutoff wavelength of the dominant mode of the rectangular waveguide. Here a = 4.5 mm, then

$$\lambda c = 2a = 9 \text{ mm} \quad (8)$$

Substituting $b = b_1 = 2.9$ mm yields,[11]

$$\frac{\lambda_{c10}'}{a} = \frac{\lambda_{c10}}{a} + F_{10}\left(\frac{b}{a} - 0.45\right) = 3.8 \quad (9)$$

Here, the λ'_{c10} is the fundamental-mode cutoff wavelength of the ridged waveguide. Thus, $\lambda'_{c10} = 3.8 \times 4.5 = 17.1$ mm, far longer than the cutoff wavelength of the traditional waveguide.

It is noted that the conventional single ridged waveguide structure shown in ***Figure 2*** can be regarded as a specific case of transmission line. From transmission line theory, the capacity-loaded ridged waveguide equivalent circuit is also shown. The conventional ridged waveguide transmission line has the impedance Z_0 and electrical length βL, while its corresponding capacity-loaded transmission line is made up of two symmetric sections of transmission lines with the impedance Z_1, electrical length $\beta_1 l$ and capacitance represented by the susceptance jβ. Discussed from the point of transmission line, the network functions are:

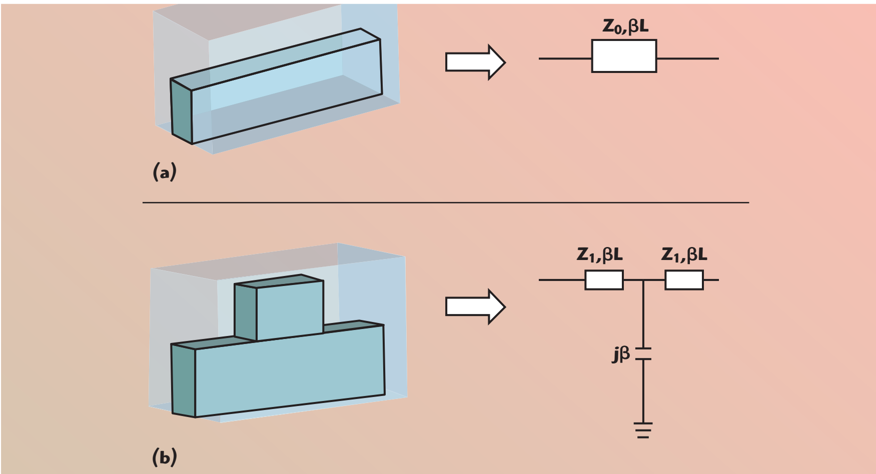

Fig. 2 Ridge waveguide and equivalent circuit, (a) single ridge, (b) capacity loaded ridge.

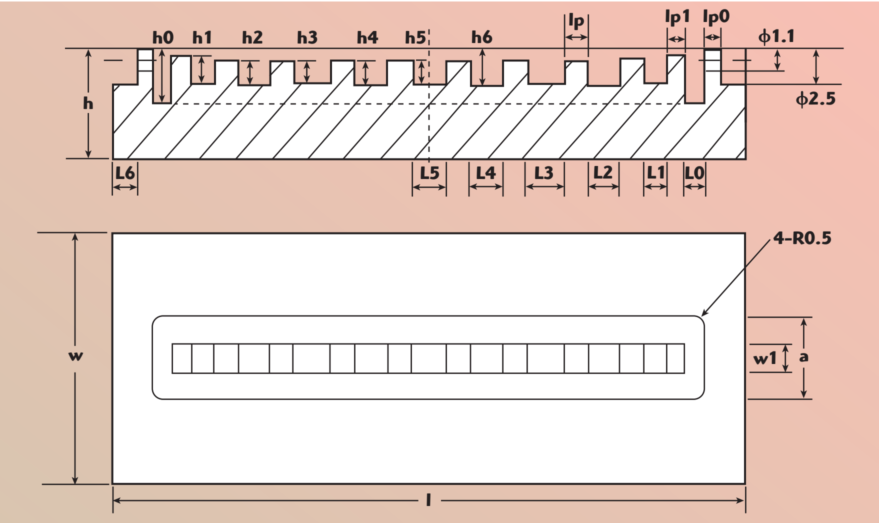

Fig. 3 Schematic of a compact capacitor loaded ridged waveguide filter.

$$A = \begin{bmatrix} \cos(\beta L) & jZ_0 \sin(\beta L) \\ j\sin(\beta L)/Z_0 & \cos(\beta L) \end{bmatrix} \quad (10)$$

$$A_1 = \begin{bmatrix} \cos(\beta_1 l) & jZ_1 \sin(\beta_1 l) \\ j\sin(\beta_1 l)/Z_1 & \cos(\beta_1 l) \end{bmatrix} \cdot \begin{bmatrix} 1 & 0 \\ jB & 1 \end{bmatrix} \begin{bmatrix} \cos(\beta_1 l) & jZ_1 \sin(\beta_1 l) \\ j\sin(\beta_1 l)/Z_1 & \cos(\beta_1 l) \end{bmatrix}$$

$$= \begin{bmatrix} \cos(2\beta_1 l) - \frac{BZ_1 \sin(2\beta_1 l)}{2} & jZ_1 \sin(2\beta_1 l) - jBZ_1^2 \frac{1-\cos(2\beta_1 l)}{2} \\ \frac{j\sin(2\beta_1 l)}{2Z_1} + jB\frac{1+\cos(2\beta_1 l)}{2} & \cos(2\beta_1 l) - \frac{BZ_1 \sin(2\beta_1 l)}{2} \end{bmatrix} \quad (11)$$

where matrix A means the network function of the traditional ridged waveguide transmission line and matrix A1 represents the network function of the equivalent compounded capacity-loaded transmission line. If the two matrix have the relation that A = A1, from Equations 10 and 11, one obtains,

$$Z_0 = Z_1 \sqrt{\frac{2\sin(2\beta_1 l) - BZ_1 + BZ_1 \cos(2\beta_1 l)}{2\sin(2\beta_1 l) + BZ_1 + BZ_1 \cos(2\beta_1 l)}} \quad (12)$$

$$\tan(\beta L) = \frac{Z_1}{Z_0} \frac{\left[2\sin(2\beta_1 l) - BZ_1\left(1-\cos(2\beta_1 l)\right)\right]}{2\cos(2\beta_1 l) - BZ_1 \sin(2\beta_1 l)} \quad (13)$$

and from Equation 12, $Z_0 \geq Z_1$. From Equation 13, if $\beta L = \pi/2$, implying that

$$2\beta_1 l = \tan^{-1}(2/BZ_1) \quad (14)$$

when BZ_1 is large enough, $2\beta_1 l$ can be considerably smaller than $\pi/2$, that is, the total length of the compound transmission line is much shorter than the length of its equivalent conventional transmission line.

Therefore, the length of the cavity can be reduced by capacitor-loading. On the other hand, the ridged waveguide serves as a way to obtain wide bandwidth, since its dominant mode frequency is lower compared to a conventional waveguide and the frequency of first higher-order mode (TE_{20}) is higher than that of a conventional waveguide. Hence, by using capacitor-loading in ridged waveguide, good performance with small size and wide bandwidth can be realized.

DESIGN, SIMULATION AND MEASURED RESULTS

The design specification is to build a filter whose center frequency is 22.3 GHz, demonstrating a fractional bandwidth of 42.2 percent, from 17.6 to 27 GHz, with a VSWR less than 1.5 and out band rejection at 15 and 30 GHz less than –60 dB, respectively.

A mode-matching technique is used to build exact numerical models of the rectangular-to-ridged waveguide junction as filter key elements. The full-wave-matrix of a rectangular waveguide bifurcation was calculated in accordance with the technique described by Vasilyeva et al.[14] The generalized scattering matrix of the discontinuity is obtained using the mode-matching method.[15] The analysis of combined filter components, as well as the analysis of a filter as a whole, was performed by the generalized-matrix technique. The improved procedure of the prototype filter synthesis was used to obtain an initial filter configuration needed to feed the optimization procedure.[16] The latter was based on the multi-parametric gradient approach and worked in some stages with different goal functions. At the first stage, a special emphasis was put on the filter response to satisfy the specified skirt selectivity and width of the passband. At other stages, the required level of passband return loss was reached.

The configuration of the 10 order capacity-loaded compact ridged waveguide filter is shown in ***Figure 3***. It is made up of ridges with ten posts symmetrically placed in cavities. It is noticed that the width w1 of the ridge and posts is identical, making it convenient in the manufacturing process. The frequency of the passband can be adjusted by tuning the height of post hi (i = 1, 2…5). The coupling is determined by the distance of adjacent length Li (i = 1, 2…5), which can be tuned easily. Besides, two removable 2.92 mm-type coaxial connectors are used to connect with the outside. By changing the length (L0) and height of post (h0), the coupling between the cavity and the outside can be adjusted.

To meet the design requirements, a wideband waveguide filter has been designed using CST Microwave Studio. Its dimensions are as follows: L0 = 1.08 mm, L1 = 1.31 mm, L2 = 1.80 mm, L3 = 2.18 mm, L4 = 2.08 mm, L5 = 2.14 mm, L6 = 1.6 mm, lp0 = 0.92 mm, lp1 = 1.15 mm, lp = 1.5 mm, h0 = 2.9 mm, h1 = 1.48 mm, h2 = 1.45 mm, h3 = 1.27 mm, h4 = 1.34 mm, h5 = 1.30 mm, h6 = 1.73 mm, a = 4.5 mm, w = 1.5 mm.

Depending on the discussions above, a new type of ridged waveguide bandpass filter made of aluminum has been manufactured, according to the dimensions obtained from the simulation data. ***Figure 4*** shows photographs of the fabricated filter. This type of filter is compact, with outside dimensions of 58 × 13.36 × 9.8 mm.

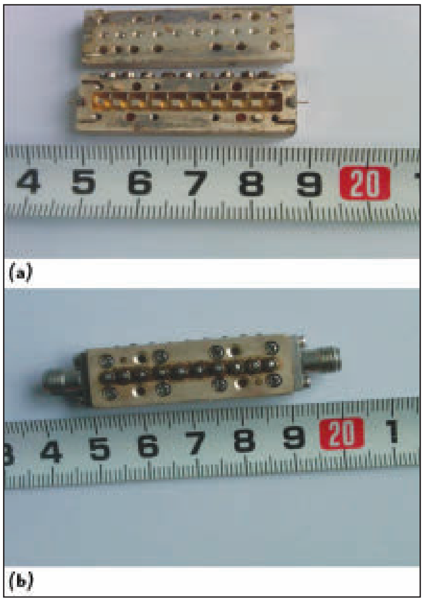

▲ *Fig. 4 Photographs of the filter (a) inner configuration, (b) with 2.92 mm connectors.*

The broadside of the compact ridged waveguide filter is only 4.5 mm, a decrease of 57.9 percent, compared to the traditional waveguide whose broadside is 10.688 mm, allowing its more widely application in the design of microwave and communication systems.

In order to compensate for the fabricating errors, tuning screws are added in the cover

plate of the filter and side of the cavity to tune the frequency and coupling error in the process of manufacturing. Also, in order to reduce the insertion loss, the filter is made of aluminum, with its inner surface plated with silver. The filter cavity and its cover were soldered.

The filter was measured at room temperature with an Agilent 8722ES vector network analyzer over the frequency range from 50 MHz to 40 GHz. A 50 Ω matching load was used in the measurement. Two 2.92 mm-type connectors were used for testing. The simulated and measured results of the proposed filter are shown in ***Figure 5***. The results show that the proposed filter has a wide bandwidth from 17.6 to 27 GHz with a fractional bandwidth (FBW) of 42.2 percent at a center frequency of 22.3 GHz. The minimum insertion loss measured is found to be less than 0.6 dB, except at the lower and upper edges of the passband, where the loss is less than 0.8 dB. The measured return loss is better than 15 dB over the whole passband.

Meanwhile, the implemented filter exhibits a flat group delay response, which is below 0.6 ns. The group delay variation is less than 0.3 ns at the lower and upper passband edges. At 3 GHz away from the passband, the out-of-band rejections are less than –61 and –63 dB, respectively. The measured results and simulations agree well in both magnitude and trend. Hence, these results verify this design method.

CONCLUSION

In this article, a new type of ridged bandpass filter with capacitor-loading has been designed, fabricated and measured. When compared with typical evanescent-mode ridge waveguide filters, the proposed new type of ridged waveguide bandpass filter is easier to fabricate, with the same width of the ridge and capacitor-loading post. The resonant frequencies can be easily adjusted by tuning the height of the posts. The coupling is determined by the distance of adjacent length, making it convenient in the process of designing and manufacturing. It provides a convenient method of designing a compact wideband ridged waveguide filter. Both the simulated and measured results are presented and discussed. The superior features of designing this kind of filter indi-

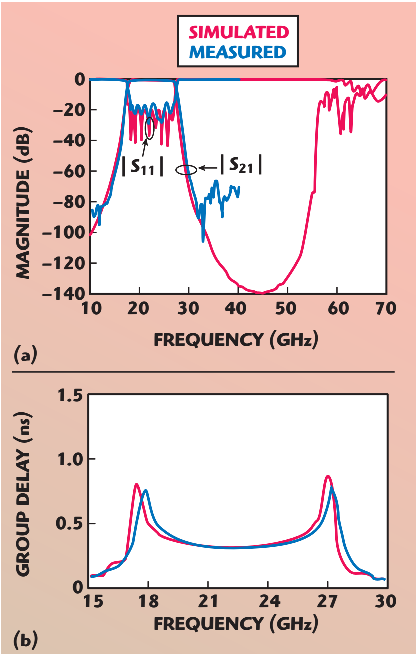

▲ *Fig. 5 Simulated and measured performance of the filter (a) S-parameters, (b) group delay.*

LOW NOISE AMPLIFIERS & LIMITING AMPLIFIERS

Offering a complete line of Amplifiers and Limiting Amplifiers up to 40 GHz

- Amplifiers
- Attenuators - Variable
- DLVA & ERDLVA & SDLVA's
- DTO's
- Filters
- Form, Fit & Function Products
- Hybrids, Dividers & Couplers
- IFM's & Frequency Discriminators
- Integrated MIC/MMIC Modules
- I/Q Vector Modulators
- Limiters & Detectors
- Log Amplifiers
- Pulse & Bi-Phase Modulators
- Phase Shifters
- Rack & Chassis Mount Products
- Receiver Front Ends
- Single Sideband Modulators
- SMT & QFN Products
- Solid-State Switches
- Switch Matrices
- Switch Filter Banks
- Threshold Detectors
- USB Products

NARROW BAND, OCTAVE BAND, BROADBAND

ULTRA WIDEBAND 10 MHz TO 40 GHz

LOW NOISE AMPLIFIERS

LINEAR AMPLIFIERS

LIMITING AMPLIFIERS

LABORATORY TEST BENCH AMPLIFIERS

USB AMPLIFIERS

OPTIONS AVAILABLE:

- VARIABLE GAIN (DIGITAL & ANALOG CONTROL)
- POSITIVE GAIN SLOPE
- TEMPERATURE COMPENSATION
- HERMETIC SEALING
- GAIN AND PHASE MATCHING
- CUSTOM DESIGNS & HOUSINGS
- CONNECTORIZED & SMT / QFN PACKAGING

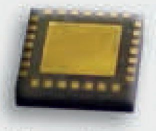

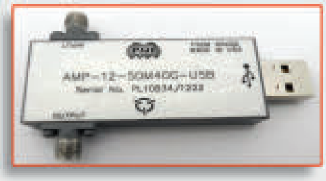

Limiting Amplifiers :

Model Number	Frequency Range (GHz)	Input Power (dBm, CW)	Limited Output Power (dBm)	Output Power Variation vs. Input Power (dB)	Noise Figure (dB)	Harmonic Rejection (dBc)	VSWR	DC Current @ +12 to +15VDC
PEC2-2G18G-2DBM-LM-SFF	2.0 - 18.0	-50 to +30	+2dBm	±2.0dB	10dB	-10dBc	2.0:1	460mA
PEC2-2G18G-21DBM-LM-SFF	2.0 - 18.0	-45 to +10	+21dBm	±2.0dB	10dB	-8dBc	2.0:1	700mA
PEC3-40-2G6G-15-LM-SFF-HS	1.85 - 6.25	-15 to +17	+15dBm	±2.0dB	5.5dB	-15dBc	2.0:1	350mA

OTHER MODELS AVAILABLE, PLEASE CONTACT US WITH YOUR REQUIREMENTS

HIGH POWER RF LIMITERS AVAILABLE

PMI

PLANAR MONOLITHICS INDUSTRIES, INC.

7311-F Grove Road, Frederick, Maryland 21704 USA
Tel: 301-662-5019 | Fax: 301-662-1731
Email: sales@pmi-rf.com | www.pmi-rf.com

ISO9001:2008 Certified

cates that it has the potential to be utilized in microwave and millimeter wave communication systems. ■

ACKNOWLEDGMENT

This project was supported by the Science and Technology Bureau of Sichuan Province, China (No. M110104012008 HH0013/2008FX0023/2009GZ0006) and Chengdu Science and Technology Bureau of Sichuan Province, China (No. M1701040110YTYB022G).

References

1. J.F. Liang, X.P. Liang, K.A. Zaki and A.E. Atia, "Dual-Mode Dielectric or Air-Filled Rectangular Waveguide Filters," *IEEE Transactions on Microwave Theory and Techniques*, Vol. 42, No. 7, July 1994, pp. 1330-1336.
2. S. Amari and M. Bekheit, "A New Class of Dual-Mode Dual-Band Waveguide Filters," *IEEE Transactions on Microwave Theory and Techniques*, Vol. 56, No. 8, August 2008, pp. 1938-1944.
3. S. Bastioli, C. Tomassoni and R. Sorrentino, "A New Class of Waveguide Dual-Mode Filters Using TM and Nonresonating Modes," *IEEE Transactions on Microwave Theory and Techniques*, Vol. 58, No. 12, December 2010, pp. 3909-3917.
4. G. Craven, "Waveguide Bandpass Filters Using Evanescent Modes," *Electronics Letters*, Vol. 2, No. 7, July 1966, pp. 251-252.
5. Q. Zhang and T. Itoh, "Computer-aided Design of Evanescent-mode Waveguide Filter with Nontouching E-plane Fins," *IEEE Transactions on Microwave Theory and Techniques*, Vol. 36, No. 2, February 1988, pp. 404-412.
6. L.S. Wu, X.L. Zhou and W.Y. Yin, "Evanescent-Mode Bandpass Filters Using Folded and Ridge Substrate Integrated Waveguides (SIW)," *IEEE Microwave and Wireless Components*, Vol. 19, No. 3, March 2009, pp. 161-163.
7. A. Kirilenko, L. Rud, V. Tkachenko and D. Kulik, "Evanescent-mode Ridged Waveguide Bandpass Filters With Improved Performance," *IEEE Transactions on Microwave Theory and Techniques*, Vol. 50, No. 5, May 2002, pp. 1324-1327.
8. T. Shen and K.A. Zaki, "Length Reduction of Evanescent-Mode Ridge Waveguide Bandpass Filters," *Progress In Electromagnetics Research*, Vol. 40, 2003, pp. 71-90.
9. C. Rauscher and S.W. Kirchoefer, "Miniature Ridge-waveguide Filter Module Employing Moldable Dielectric Material," *IEEE Transactions on Microwave Theory and Techniques*, Vol. 54, No. 3, March 2006, pp. 1190-1196.
10. S.B. Cohn, "Properties of Ridge Waveguide," *Proceedings of the IRE*, Vol. 35, No. 8, August 1947, pp. 783-788.
11. S. Hopfer, "The Design of Ridged Waveguides," *IRE Transactions on Microwave Theory and Techniques*, Vol. 5, No. 5, October 1955, pp. 20-29.
12. M.M. Fahmi, J.A. Ruiz-Cruz, R.R. Mansour and K. . Zaki, "Compact Ridge Waveguide Filters With Arbitrarily Placed Transmission Zeros Using Nonresonating Nodes," *IEEE Transactions on Microwave Theory and Techniques*, Vol. 57, No. 12, December 2009, pp. 3354-3361.
13. R.E. Collin, *Foundations for Microwave Engineering*, 2nd Ed., McGraw-Hill, New York, N.Y., 1992.
14. T. Vasilyeva, A. Kirilenko, L. Rud and V. Tkachenko, "Calculation of Full-wave S-matrices of Monoaxially Uniform (2D) Elements In Rectangular Waveguides," *Proceedings of the 7th international Conference on Mathematical Methods in Electromagnetic Theory*, Vol. 1, 1998, pp. 399-401.
15. C. Wang and K.A. Zaki, "Full-wave Modeling of Generalized Double Ridge Waveguide T-junctions," *IEEE Transactions on Microwave Theory and Techniques*, Vol. 44, No. 12, December 1996, pp. 2536-2542.
16. A. Kirilenko, L. Rud, V. Tkachenko and D. Kulik, "Design of Bandpass and Lowpass Evanescent-mode Filters on Ridged Waveguides," *Proceedings of the 29th European Microwave Conference*, Vol. 3, 1999, pp. 239-242.


SIZE MATTERS
1 kW in
20 to 500 MHz
500 to 1000 MHz
20 to 1000 MHz
5U
chassis
NEXT GENERATION
POWER AMPLIFIERS
COTS modules * rack mount amplifiers * multi-function PA solutions
1163 20-520 MHz, 125 Watt
1193 20-1000 MHz, 125 Watt
1189 500-2500 MHz, 100 Watt
1178 2000-6000 MHz, 35 Watt
Certified to ISO 9001:2008
TÜVRheinland
Precisely Right.
www.EmpowerRF.com
EMPOWER
RF SYSTEMS, INC.
316 West Florence Ave., Inglewood, CA 90301 USA, Phone: +1(310)412-8100, Fax: +1(310)412-9232

Technical Feature

LTE Downlink Transmitter Simulation Using MATLAB

Long Term Evolution (LTE) is a state-of-the-art standard for wireless communication, currently in technical implementation.[1-5] The standard has been defined by the 3GPP organization and is publicly available – every engineer, researcher or student can download the official specification from www.3gpp.org. The 3GPP organization manages an international project called Evolved Packet System (EPS), which is widely known as "the 4th generation of mobile telecommunication systems (4G)." The Evolved Packet System includes the entire architecture of the 4G mobile systems, both packet network and radio interface. LTE is a part of the EPS project, which refers to a 4G air interface standard. Currently many companies in the world, as well as many universities, conduct research and development on this technology.

The authors of this article are involved in research on signal processing for LTE systems and they found that there is a lack of free software able to generate LTE signals. Although open source advanced LTE system simulators exist, no easy-to-use public domain signal generators exist to be used in signal processing research and development.

This article presents a MATLAB toolbox to fill this gap. Functions able to generate the downlink LTE signals are the main part of the toolbox. Together with the functions, a module named "LTE Professor" is presented. LTE Professor is a Graphical User Interface (GUI), which is able to generate LTE signals, analyze these signals and visualize LTE time/frequency resources utilization. The whole source code is GPL licensed and is publicly available at the authors' website.[6]

The present article is divided into two main parts. The first part is an introduction to the LTE downlink Physical Layer. Here the basics of the LTE downlink time/frequency resources and signal generation are discussed. The second part of the article presents usage and architecture of the software, together with some examples of generated LTE signals.

LTE DOWNLINK INTRODUCTION

The 4th generation of mobile telecommunication systems has, at least in theory, very good performance parameters in comparison to the previous generations.[3] Unfortunately, this gain came at a price of significant complication of the whole system. The LTE protocol stack is divided into several layers. Additionally, there is a distinction between the downlink and uplink protocol stacks, since there are significant asymmetries between the different directions of data transmission. Description of the entire LTE system would exceed the limitations of a single article. Therefore, this work is focused on a MATLAB toolbox which emulates the

Jacek Pierzchlewski and Torben Larsen
Aalborg University, Aalborg, Denmark

LTE downlink transmitter. This transmitter translates code words, which are the input to the transmitter, into the LTE radio signal. The software is dedicated to engineers and scientists who are involved in research on modern communication signals and systems. In particular, this toolbox is useful in simulation of the LTE base station (BTS) transmission circuits, antenna systems and User Equipment (UE) receiver front ends. It can also be practical in the investigation of the LTE and Orthogonal Frequency Division Modulation (OFDM) channel models. In addition, this software can cooperate with models of higher LTE downlink layers.

During the downlink, data is passed from a BTS to a number of UEs, which are currently within range of the BTS. To provide downlink data transmission service for multiple users, LTE systems use OFDMA. The baseband signal is created using OFDM. In OFDMA, resources are represented in a time/frequency plane (see ***Figure 1***) – one Resource Element (RE) is an atomic unit in the plane. The LTE standard fully supports multi antenna technology, so there may be up to eight time/frequency planes.

The accessible bandwidth is divided into a number of subcarriers.[7] In the LTE standard, the separation between subcarriers is 15 kHz during regular transmission. Subcarriers are gathered in Resource Blocks (RB), where one RB consists of 12 subcarriers. The number of subcarriers depends on the size of the baseband. However, there is always an integer number of resource blocks in the baseband. There are six possible bandwidths in the LTE standard: 1.4, 3, 5, 10, 15 and 20 MHz.

The time organization is a bit more complicated.[1,3,7] One symbol is an atomic unit of the time/frequency plane. The base length of a symbol (t_s) is equal to a multiplicative inverse of the subcarriers' separation, so t_s = $(15\ \text{kHz})^{-1}$ = 66.7 µs. The Inverse Fast Fourier Transform (IFFT) operation is used to generate a downlink signal. To ensure reliable transmission, a copy of the last part of a symbol is copied to the beginning of every symbol, this copy is called 'Cyclic Prefix' (CP). Cyclic Prefix has a length t_{CP} and this length may differ, depending on the current CP settings. There are two basic CP settings: normal CP and extended CP.

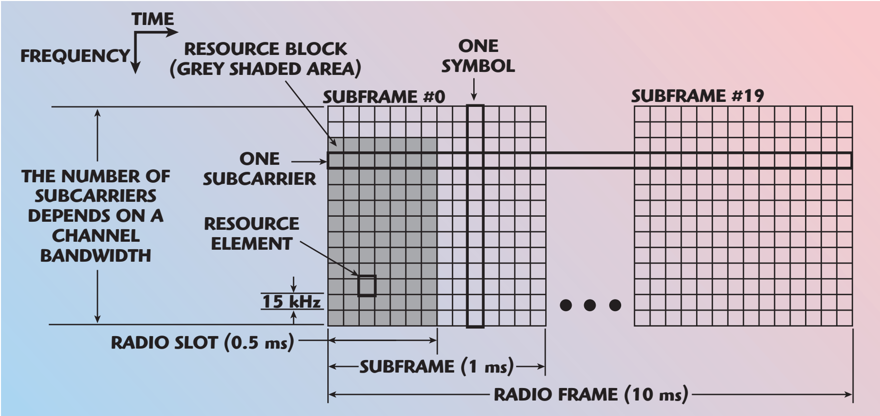

▲ *Fig. 1 Time/frequency resources organization in the LTE.*

The symbols are grouped in Radio Slots (RS). The duration of a single RS is always 500 µs. The number of symbols in one RS depends on the cyclic prefix type currently in use. There are six symbols in one RS in the case of the extended cyclic prefix. In the case of the normal cyclic prefix, there are seven symbols in one RS. Additionally, in the latter case, every first symbol in an RS has a longer cyclic prefix.

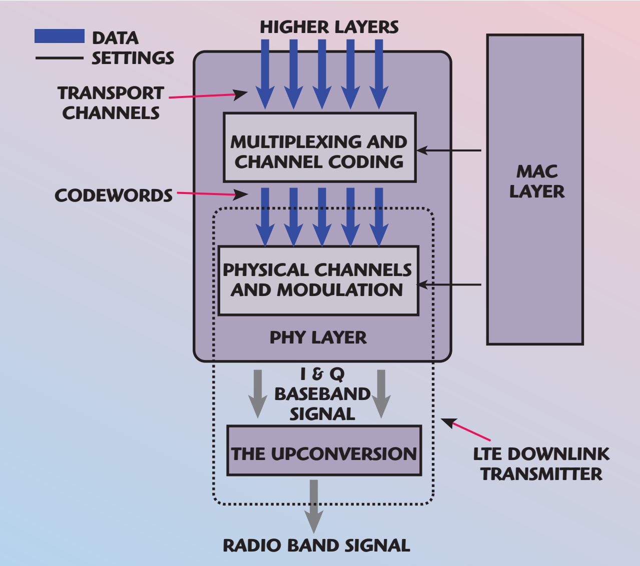

▲ *Fig. 2 The LTE downlink transmitter in the LTE stack.*

A longer LTE time unit is a Subframe (SF). The subframe has a time length of 1 ms and consists of two Radio Slots. A group of consecutive ten Subframes constructs a Radio Frame (RF). The RF is the longest time unit in the LTE standard. The duration of one RF is 10 ms (see Figure 1). In the LTE downlink, bandwidth resources are granted to a specific UE as a group of resource blocks. The resource assignment is renewed in every SF and cannot be changed until the end of an SF.

THE MATLAB MODELS OF THE LTE TRANSMITTER

LTE Downlink Transmitter

Figure 2 shows the position of the LTE downlink transmitter in the LTE protocol stack. There are two main parts of the LTE Physical Layer responsible for processing data from the higher layers. The upper part is responsible for multiplexing and channel coding.[8] The bottom part is responsible for physical channels modulation and mapping to the resource elements.[7] The MAC layer controls the entire physical layer. [1,3,7,8] The presented MATLAB model emulates the bottom part of the Physical Layer.

The resource planes, in which signals and channels are mapped, are given to the OFDM modulator. The modulator generates the baseband signal. The baseband signal is then up-converted to the LTE radio signal. The presented software emulates both the baseband signal generator and the radio frequency generator. The baseband in-phase and quadrature signals (I and Q signals), as well as the radio frequency signal are the output from the presented model. Additionally, users have access to the resource planes and modulation symbols mapped to all physical signals and channels.

Downlink data comes to the transmitter in the form of code words. Code words are mapped to physical channels. Different physical channels can be in use depending on the current type of transmission. In the LTE standard, different types of transmission are used on different Antenna Ports (AP). The implemented MATLAB model supports the most common type, the transmission with Cell Specific Reference (CSR) signals.[7] The multi antenna transmission is supported. In the current software version, the first and the second transmission modes are implemented.

The LTE Transmitter Model and Supplementary Software

The presented MATLAB model is available in the form of a toolbox. The detailed description of the toolbox can be found in ref. 6. The 'LTE scenario' structure must be passed as an argument to the main generator function. This structure is necessary to run the generator. It groups user settings and settings coming from the MAC layer. The toolbox contains examples of LTE scenario files to be used by users as a base for their own LTE scenario.

The second data structure passed to the generator is a structure with code words data. In general, this structure is not required since in the case of no input data, the LTE generator sends random bits. Additionally, it is possible to include code words only for a few physical channels – the missing data will be randomly generated.

The generator returns one structure. Obviously, this structure contains the baseband and radio band signals. Beside these signals, there are resource matrices that indicate signals/channels mapping and modulation mapping, matrices with symbols mapped to particular channels and structures with LTE Physical Layer specific parameters. The detailed description of this structure can be found in ref. 6.

The next essential part of the presented toolbox is the 'LTE Professor' module. This module consists of two main parts. The first part is dedicated to be a graphical interface for the developed MATLAB LTE model functions. With this part, users are able to set all parameters of the LTE scenario used by the LTE transmitter function. It is possible to get information about

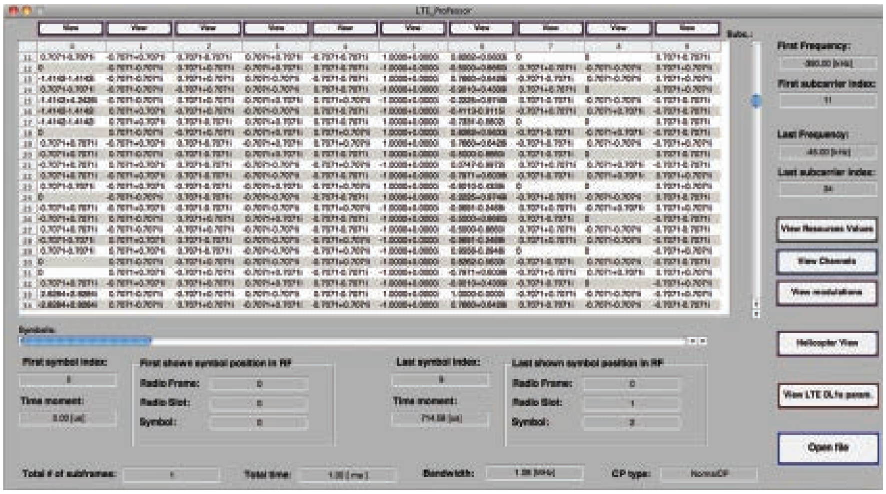

Fig. 3 Screen shot of the LTE Professor.

time and frequency parameters of the signal, which corresponds to the adjusted scenario settings. Finally the user is able to generate the LTE downlink signal and store it in the chosen file.

The second part of the LTE Professor is able to analyze and visualize generated signals. Users can observe the detailed view of the signals and channels mapping. This view gives information about modulation schemes and values mapped to all Resource Elements used in the analyzed LTE signal (see ***Figure 3***). It is possible to generate the indicative 'helicopter view' of the entire resources plane (see ***Figure 4***). Moreover, the entire LTE signal, as well as every particular LTE symbol in the generated transmission, can be viewed and analyzed in the frequency and time domains (see ***Figures 5*** and ***6***). The extensive description of the LTE Professor is available.[6]

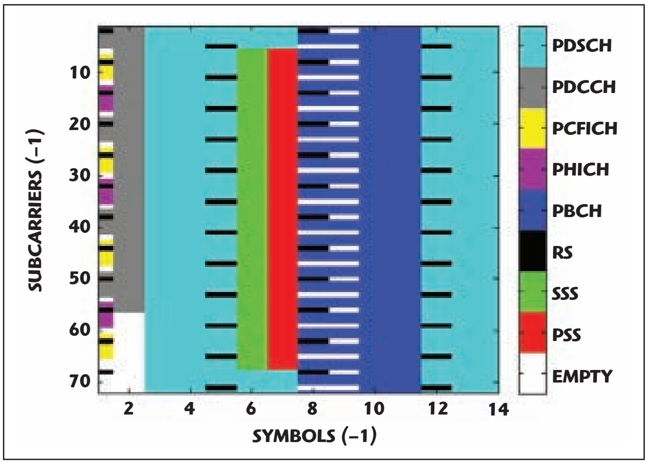

Fig. 4 LTE signals and physical channels map made by the software (1.4 bandwidth).

The validation of the software was performed in a few different ways. The LTE Professor module, which is also a

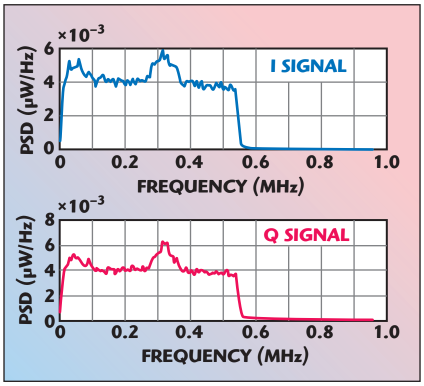

Fig. 5 Power spectral density of the baseband signals (1.4 MHz bandwidth).

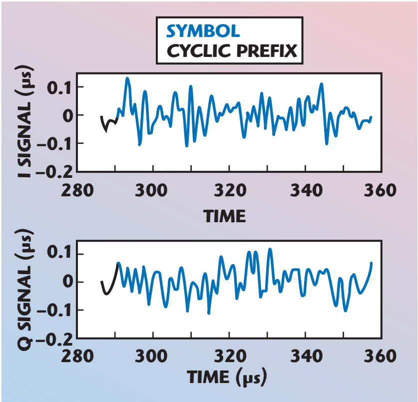

Fig. 6 Baseband signals in the time domain (1.4 MHz bandwidth).

Integrated Microwave Assemblies

Advanced Technology - Extensive Experience - Superior Performance

CPI
Communications & Power Industries

Communications & Power Industries' Beverly Microwave Division (BMD) offers product technology that includes Integrated Microwave Assemblies and Control Components. BMD's broad experience and extensive capabilities in the areas of high power microwave component design for military and non-military radar, satellite, communications, and EW systems makes it uniquely suited to design and manufacture a wide range of components and multi-function assemblies in small, lightweight packages. Coupling that with our experience in other transmission lines and technologies gives us a technical capability that is unparalleled in the microwave industry.

* Multi-function components
* RF front ends
* Switches & attenuators
* High level assemblies & modules
* Design capability up to 40 GHz
* Power handling to 1 MW+ peak
* Integral driver & associated electronics
* The industry's most extensive high power test facility

Communications & Power Industries
Beverly Microwave Division

150 Sohier Road
Beverly, MA 01915
Phone: (978) 922-6000
Fax: (978) 922-2736

marketing@bmd.cpii.com
www.cpii.com/bmd

part of the presented toolbox, was originally dedicated to validate the generator. The generated signals were analyzed with the LTE Professor. Mapping of LTE signals into time/frequency resources were compared with the maps that can be found in the literature. Additionally, the peak-to-average power ratio of the generated LTE bandwidth signals was measured to ensure that the generated signals are correct.

The Software Internals

Figure 7 shows the architecture of the implemented MATLAB models. The main 'LTE_DL1a' script controls the whole process. The LTE Resource Parameters Calculation (RPC) unit is run as the first sub module. This unit generates three structures: 'sP,' 'sF' and 'sT,' which contain LTE system parameters, LTE bandwidth parameters and LTE time parameters, respectively. These three structures are used in all later steps of the LTE signal generation. After running the RPC unit, three identical matrices are allocated in the Resources Allocation (RA) unit. These matrices reflect the time/frequency resources. The number of rows in the matrices is equal to the number of subcarriers and the number of columns is equal to the number of symbols in the entire LTE transmission. The reference and synchronization signals are added in the Signals Mapping (SM) unit. The channels are mapped to the time/frequency resources in the Channel Mapping (CM) unit.

When all signals and channels are mapped to the LTE resources, the IFFT module generates the pure OFDM signal (without CPs). Adding cyclic prefixes to the pure OFDM signal generates the final baseband signal. Afterward, the signal is up-converted to the radio frequency.

Example of Signals Generated by the Software

Figure 5 shows the power spectrum density of the example baseband signal generated by the software. The signal on this figure is a 1.4 MHz LTE baseband signal. It appears that the power is not uniformly distributed, which is due to the nonuniform channels and signals mapping. In the LTE standard, not all resource elements are in use during transmission. Rules of the channel and signal mapping can vary due to the current bandwidth settings.

In Figure 6, the above LTE baseband signals are shown in the time domain. The time length of the shown signals is equal to the time length of one symbol with a cyclic prefix. The cyclic prefix, marked in black, is exactly the same as the last part of the symbol – it is correct according to the LTE standard. The presented plots are generated automatically using the LTE Professor software. A screenshot of this software, with a view on the resource elements with mapped signals and channels, is presented in Figure 3. Figure 4 shows the LTE signal in the time/frequency domain. The resource elements, in which the LTE signals and channels are mapped, are depicted. This map is generated by the 'helicopter view' option in the LTE Professor. The map presents the first Subframe in the Radio Frame.

The signal presented is just an example of the LTE signal that can be generated by the software. Hence, due to the GUI interface and predefined scenarios delivered with the software, it is easy to generate signals that correspond to the demands of the user. With relevance to reproducible research, the authors prepared MATLAB scripts that can be used to generate the presented signals. The scripts are available on the project website.[6]

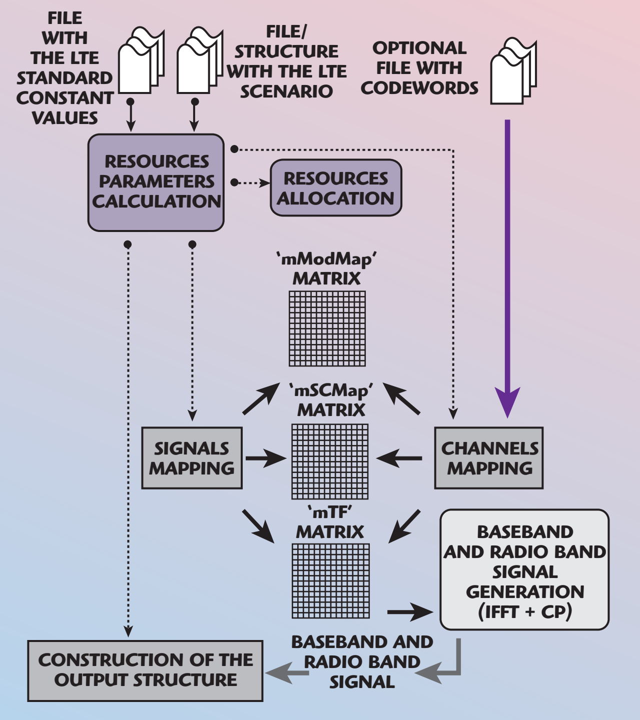

▲ *Fig. 7 The LTE transmitter model architecture.*

CONCLUSION

The MATLAB toolbox, which is able to generate LTE downlink signals, has been presented. This program is published under the GPL open source license. The authors have prepared a website where the code is available for users. The website also contains a blog about the MATLAB LTE signal generator and a message board for information and comments exchange. The signals generated by the software are also included. ■

ACKNOWLEDGMENTS

The work of Jacek Pierzchlewski is financed by The Danish National Advanced Technology Foundation under grant number 035-2009-2. T. Larsen was supported by The Danish Council for Strategic Research under grant number 09-067056, as well as The Danish National Advanced Technology Foundation under grant number 035-2009-2.

References

1. S. Sesia, I. Toufik and M. Baker, *LTE - The UMTS Long Term Evolution: From Theory to Practice*, John Wiley & Sons Ltd., 2009. ISBN: 978-0-470-69-716-0.
2. V. Tarokh, *New Directions in Wireless Communications Research*, Springer Science+Business Media LLC, 2009, ISBN 978-1-4419-0674-4.
3. E. Dahlman, S. Parkvall, J. Skold and P. Beming, *3G Evolution: HSPA and LTE for Mobile Broadband*, Elsevier Ltd., 2007, ISBN: 978-0-1237-2533-2.
4. F. Khan, *LTE for 4G Mobile Broadband*, Cambridge University Press, 2009, ISBN: 978-0-521-88.
5. H. Holma and A. Toskala, *LTE for UMTS - OFDMA and SC-FDMA Based Radio Access*, John Wiley & Sons Ltd., 2009, ISBN: 978-0-470-99401-6.
6. Author's website with code repository and blog dedicated for the presented software: http:/sparsesampling.com/lte.htm.
7. 3GPP TS 36.211 v10.0.0 Technical Specification, "3rd Generation Partnership Project; Technical Specification Group Radio Access Network; Evolved Universal Terrestrial Radio Access (E-UTRA); Physical Channels and Modulation." (c) 3GPP Project 2010, available on the 3GPP website: www.3gpp.org.
8. 3GPP TS 36.212 v10.0.0 Technical Specification, "3rd Generation Partnership Project; Technical Specification Group Radio Access Network; Evolved Universal Terrestrial Radio Access (E-UTRA); Multiplexing and Channel Coding." (c) 3GPP Project 2010, available on the 3GPP website: www.3gpp.org.

HIGH POWER

100 MHz to 20 GHz

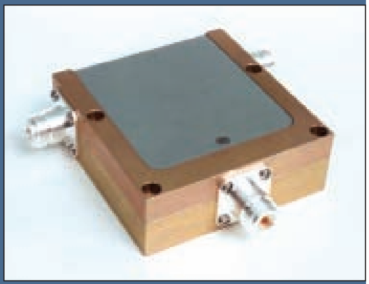

For Military / Radar Applications.

Isolators/Circulators

As one of the leading suppliers of ferrite components in the industry, UTE Microwave has pioneered innovative designs, quality craftsmanship and exceptionally high quality products. Custom designs, standards...many of them off-the-shelf, are the result of over 35 years of experience in the industry. UTE Microwave continues this tradition with new products for ever changing applications. Our broad line of HIGH POWER, low loss circulators and isolators spans the spectrum from below 100 MHz in coax/stripline units to waveguide devices at 18 GHz for both peak and average powers.

100 MHz HIGH POWER Circulator for Medical, Scientific and Industrial applications

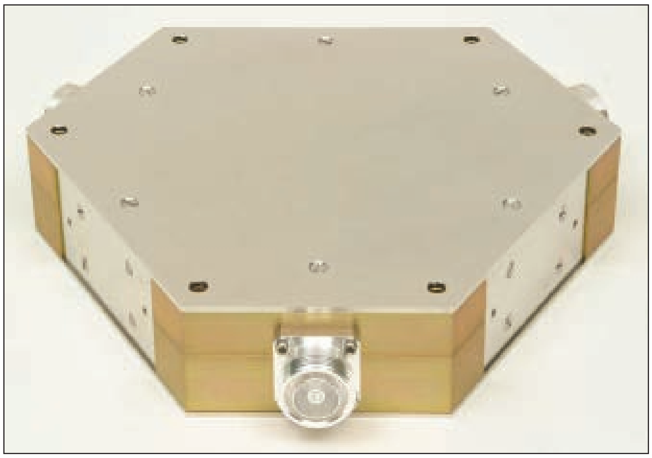

A new HIGH POWER Circulator suitable for FM Broadcast, Scientific and Medical applications is now available. The unit provides 10 MHz bandwidth in the 85–110 MHz spectrum.

Specifications are 20 dB min. isolation, 0.3 dB max. loss and 1.25 max. VSWR. Operating power is 1 kW average and 25 kW peak. The 8-1/2" hex x 2" thick unit operates over a 15°–50° C temperature range. DIN 7/16 connectors are standard. Other units are available at higher frequencies.

HIGH POWER Drop-in Series

A broad line of low loss HIGH POWER Drop-in circulators are available from VHF to Ku band including Kilowatt average power levels at VHF thru S band. L and S band radar are a specialty. A few of these are shown here.

A) 2.7–3.1 GHZ 1 kW pk, 100 W av

B) 1.2–1.4 GHZ 3 kW pk, 300 W av

C) UHF TV Band 5 kW pk, 500 W av

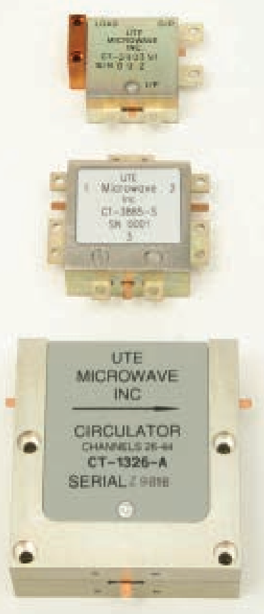

A.

B.

C.

Our "POWER-LINE" serves the COMMUNICATIONS, TELECOM, MEDICAL, SCIENTIFIC, TV, PCS and INDUSTRIAL markets.

The following models are examples of our High Power units

Model No.	Power	Connectors	Freq. Range
CT-1542-D	10 Kw Pk 1 Kw Av	DIN 7/16	420–470 MHz
CT-2608-S	3 Kw Pk 300 W Av	"Drop-in"	1.2–1.4 GHz
CT-3877-S	2.5 Kw Pk 250 W Av	"Drop-in"	2.7–3.1 GHz
CT-3838-N	5 Kw Pk 500 W Av	N Conn.	2.7–3.1 GHz
CT-1645-N	250 W Satcom	N Conn.	240–320 MHz
CT-1739-D	20 Kw Pk 1 Kw Av	DIN 7/16	128 MHz Medical

FEATURES:

- Power levels to 5 KW CW, 75 KW Pk.
- Low Intermod Units
- Low Loss Options
- Extended Octave Bandwidths
- Power Monitors and DC Blocks
- Iso Filter-Monitor Assemblies

Broadband Units • Common Band Devices • High Isolation Units • Multiport Devices • Drop-In Devices • Wireless/PCN Devices • High-Power Industrial/Medical Iso Adaptors Waveguide Junctions • High-Power TV Units • VHF and UHF Devices

sales@utemicrowave.com

UTE MICROWAVE INC.
3500 Sunset Ave., Asbury Park, NJ 07712
Tel: 732-922-1009 Fax: 732-922-1848
E-mail: info@utemicrowave.com

Contact us for more information on our extensive product line and current catalog. We accept Visa, MC, Amex

Silicon-on-Sapphire Process Technology Enables Low-Power RF Designs

Whether in the space, military, industrial, consumer or other markets, today's electronic designers are challenged to create low-power designs that maximize battery life while minimizing overall design size. This article will discuss how ICs built on a silicon-on-sapphire (SOS), technology process with integrated power-management functions can enable smaller, low-power RF applications.

SOS technology has long been used to minimize power consumption in many applications—from micro-power charge pumps embedded in RF switches, to integrated regulation within RF power amplifiers, to power-management/bias-control chips in transmit/receive (T/R) modules, and even DC-to-DC converter products for space applications. In addition to power consumption, another key factor that SOS technology addresses in RF applications is noise. SOS-based ICs feature an insulating sapphire substrate that provides high isolation.

As a result, it eliminates a lot of the noise issues associated with ICs that are not created in a SOS process. A specialized version of SOS ICs is UltraCMOS® technology (Peregrine Semiconductor). UltraCMOS is a technology where sapphire is the insulator. UltraCMOS technology differs from other silicon-on-insulator (SOI) technologies in that it has no conductive underlayer — meaning, this source of noise generation and coupling is eliminated. Additionally, the high level of isolation that UltraCMOS technology provides enables the integration of RF and power-management circuitry on a single chip.

POWER MANAGEMENT IN RF PRODUCTS

Engineers often find it difficult to address on-chip power conversion in RFICs. For example, there may be a need for more supply voltages than one battery can provide. When the required supply voltages are greater than (or outside of) the battery rail voltages, some form of power conversion is needed. SOS technology can be used to improve power management in numerous RF devices. Examples include

James Swonger, Peter Bacon and Gary Wu
Peregrine Semiconductor, San Diego, CA

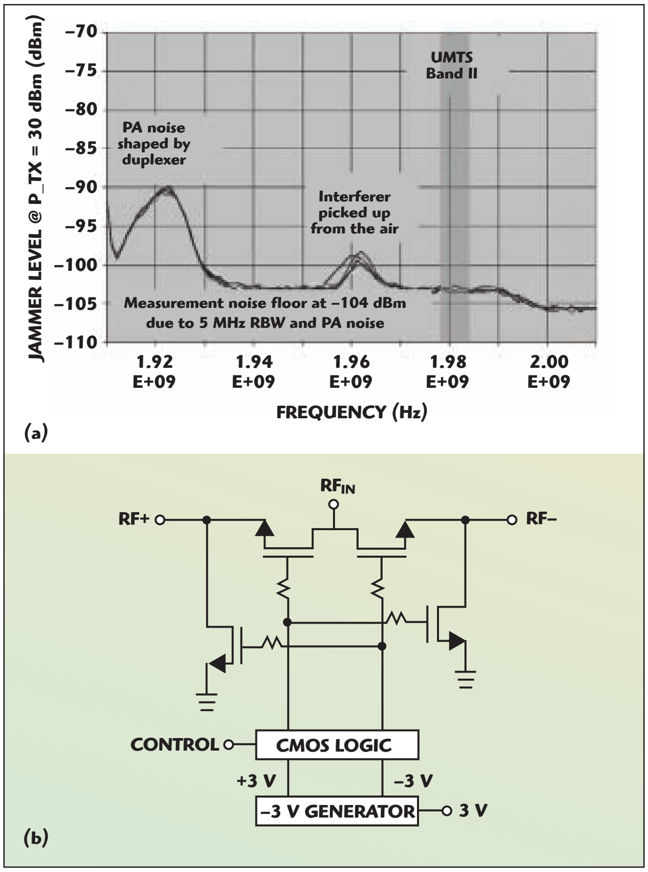

▲ *Fig. 1 UltraCMOS technology-based RF switch with on-chip charge-pump negative-voltage generator (a) noise performance and (b) block diagram.*

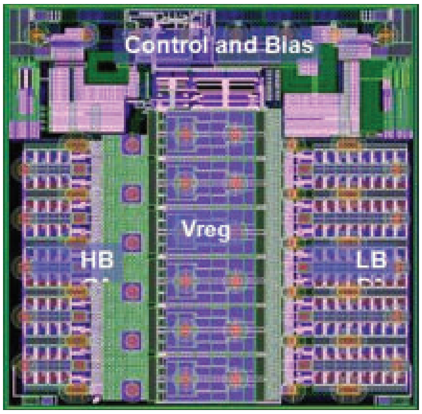

▲ *Fig. 2 Dual-band RF power amplifier in CMOS-on-sapphire technology, with on-chip low dropout regulator (LDO).*

switches, T/R modules, and DC-to-DC converters, for end-use applications such as cellular telephones and satellite systems.

RF switches based upon SOS technology enable higher performance, due primarily to the use of stacked low-threshold FETs on the fully-insulating sapphire substrate. These switches require a negative control voltage. If the negative voltage comes from an off-chip supply, it could lead to a power-consumption penalty in single-supply systems, and also act as a path for potential noise injection. Generating the negative voltage on-chip prevents these issues. The challenge for the switch designer, then, is to bring the negative voltage supply on chip without degrading noise performance (see ***Figure 1***).

The RF PA in cellular phones, military radios, and portable data appliances is often the single largest power drain in the system. High-performance RF circuits are often designed with FETs that perform well at high frequencies, but are poor at turning off, and have relatively low voltage tolerance. Power-management circuitry and techniques should be employed to control the power level within the system, to ensure that the devices are not damaged by voltage extremes (such as in high VSWR and overcharge scenarios), and to maximize the circuit's power efficiency.

Dual-band constant-envelope PAs built using UltraCMOS technology typically include embedded low dropout (LDO) regulators to optimize power-management functions (see ***Figure 2***). The on-chip LDOs allow a 3 V CMOS technology to operate across a 2:1 battery voltage range, which allows the RF PA to remain at its ideal operating point for performance and reliability.

T/R MODULE POWER MANAGEMENT AND BIAS CONTROL

T/R modules for space-borne radar present an unusually large power-management problem. These systems feature up to tens of thousands of radiating elements that can draw hundreds of milliamps each when active, so it is necessary to carefully control power draw. The radar performance, particularly the uniformity of element power that affects beam quality, also requires tight control of each element's bias point across process, temperature and aging. Unfortunately, the III-V MMICs used at common radar frequencies cannot effectively throttle power by themselves. This complex set of needs can be addressed using custom UltraCMOS element-control devices for radar systems (see ***Figure 3***).

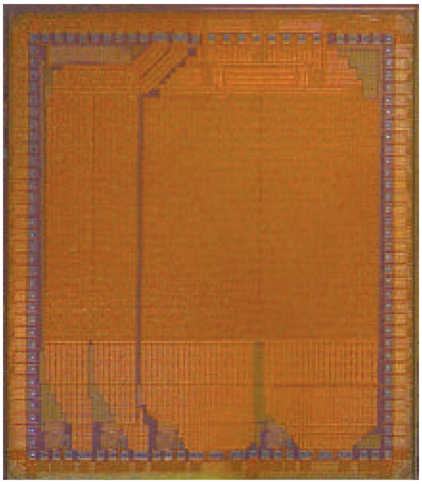

▲ *Fig. 3 An UltraCMOS T/R module element control chip with four drain switches and active-bias control channels, 48-level shifting attenuator/phase shifter control I/Os and serial interface.*

Raw power control in T/R modules requires drain switches that handle high current and have low on resistance. For example, in systems using 3.5 V PHEMT/MHEMT technology, a single or stacked PMOS FET can handle 1 A of current at under 100 mΩ. Two- and four-channel versions are available. The drain switches incorporate fault protection via cross lockout and gate control under-voltage. This is relatively easy to achieve in an integrated approach, but it is less practical with discrete devices. In the case of the UltraCMOS technology switch, a serial control channel with numerous level-shifter outputs translates the positive CMOS control signals from the host system to the –3 V gate-control voltages required by the MMIC. The insulating sapphire substrate enables the design of a chip with four separate power domains in

software included

This tiny peak power sensor will make a giant impact on your productivity.

In your job, there's no time for downtime. And there's less tolerance for error. That's why we created Agilent U2020 X-Series USB peak power sensors. They're the world's fastest USB power sensors, so you'll spend less time in testing. Plus you'll save cost and complexity with built-in trigger in/out. Now you'll always be ready to achieve your peak performance.

U2020 X-Series Peak Power Sensors
3,500 readings/sec measurement speed
2 models: up to 40 GHz
–30 to +20 dBm peak power range
Internal zero and calibration

Scan the QR code or visit goo.gl/AcGQv to see a video demo

Agilent and our Distributor Network
Right Instrument.
Right Expertise.
Delivered Right Now.

Buy from an Authorized Distributor
www.agilent.com/find/distributors

Make faster and more accurate pulse measurements. Download our app note at
www.agilent.com/find/USBpowersensor

Anticipate __Accelerate __Achieve

Agilent Technologies

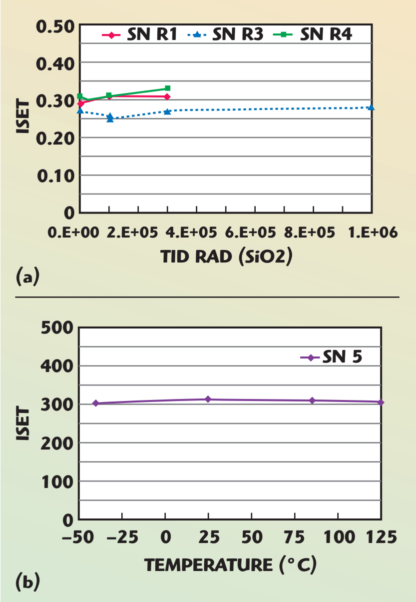

▲ *Fig. 4 TX active bias set point vs. total ionizing dose (TID) (a) and vs. temperature (b).*

close proximity—CMOS VDD, TX, RX, and the –3 V VSS gate control voltage.

UltraCMOS technology can be used to integrate custom operational transconductance amplifiers (OTA) and reference ladders to accurately control bias points. Closed-loop power control maintains bias set-point accuracy across 100 Krad, and it is insensitive to supply and temperature (see ***Figure 4***). Settling time (inclusive of drain switch turn on) is under 500 ns worst case, enabling agile radar power cycling.

The use of high-performance IC technology in space systems is limited by the availability of qualified, low-voltage power-supply solutions. In fact, the majority of available pulse-width-modulation (PWM) and linear-regulator ICs are unusable at modern low power supply voltages for a number of reasons, one having to do with maintaining stable reference voltages, and the fact that high step-down ratios are unachievable, such as those required to reduce a 40 V bus to a 1 V logic supply. However, many space systems use a 5 V rail for high-current capacity, so a distributed power approach using this resource with point-of-load (POL) converters makes sense.

POL DC-to-DC buck regulators with integrated power FETs have been designed and manufactured in UltraCMOS technology and are being used to power advanced logic devices such as SiRF FPGAs (a hardened version of Xilinx V5). Advanced FPGAs typically draw more than 10 A from a 1 V supply (as well as I/O and AUX supplies at 2.5 V), and they feature continuous current ratings of 2, 6 and 10 A that handle most applications. For higher currents, load-sharing and polyphase operation can be supported on the UltraCMOS DC-to-DC POL buck regulators using simple pin strapping (see ***Figure 5***).

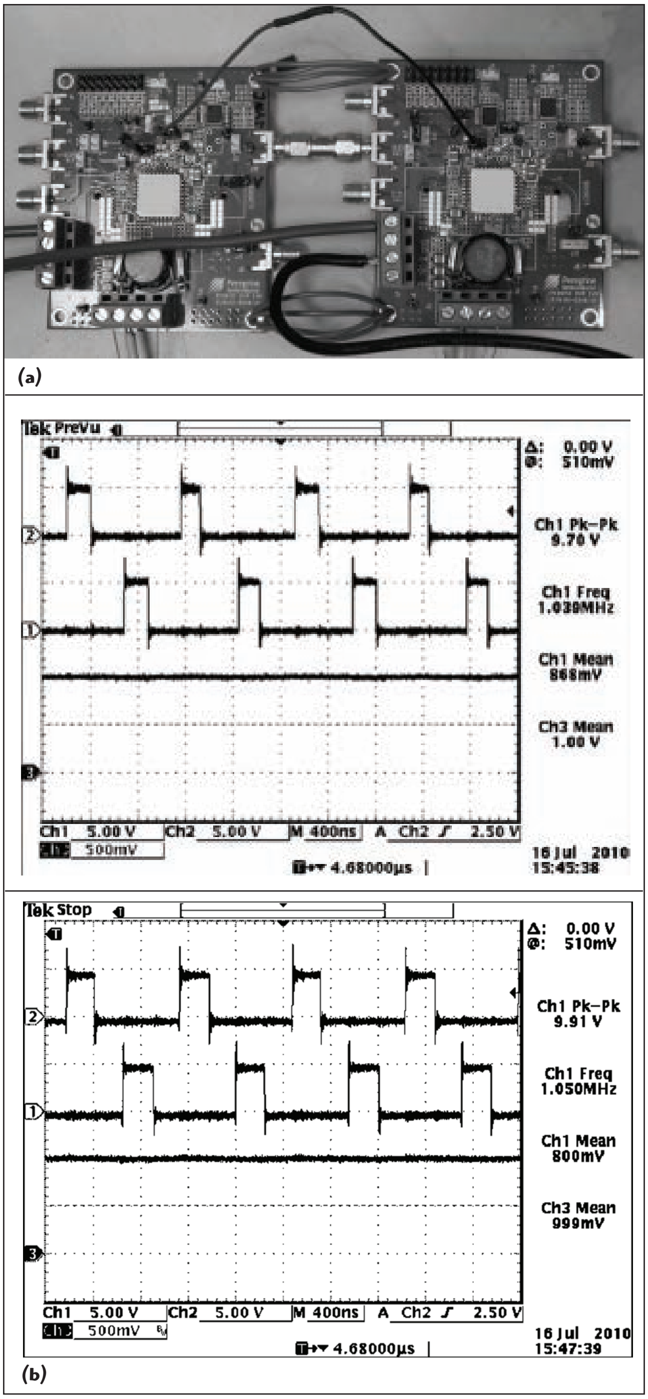

▲ *Fig. 5 A 20A 2-phase DC-to-DC buck regulator (converter), using two wires (no load) (a) and 14A waveforms, 1 mV load regulation 0-14A, and a negligible voltage ripple (b).*

The high speed of UltraCMOS technology allows these converters to run up to 5 MHz SYNC (provided that suitable passives can be obtained) and minimizes switching losses. ***Figure 6*** shows that peak measured efficiency is more than 92 percent at 800 KHz for a 10 A integrated POL DC-to-DC buck regulator.

The UltraCMOS-based integrated DC-to-DC POL buck regulator requires only small passive components that were deliberately left off-chip to allow easy access to set point voltage, loop dynamics, etc. (See ***Figure 7*** and note that the power inductor is actually larger than the DC-to-DC buck regulator device.)

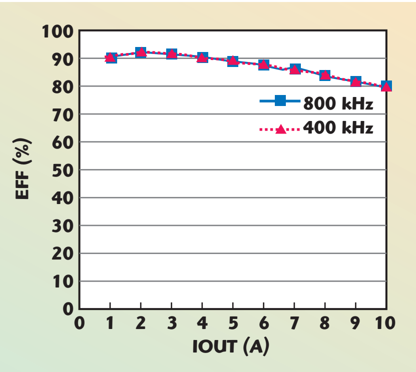

▲ *Fig. 6 Measured 10A integrated POL DC-to-DC buck regulator "wallplug" efficiency vs. load current.*

Another challenge for many power-management products used in space applications is a high single-event transient amplitude and duration. These may be tolerable in a higher voltage, low/constant current application where filtering can be used to ride out the overshoot or undershoot. Modern logic ICs, however, are much more demanding in terms of DC and step currents, meaning that passive filtering alone cannot suffice. Today's logic ICs are also much less tolerant of overstress (as little as 200 mV overshoot is outside absolute maximum ratings) and 30 percent undershoot could erase the configuration memory or at least make its contents unreliable (see ***Figure 8***).

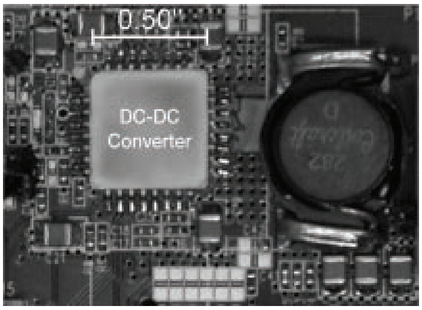

▲ *Fig. 7 DC-to-DC buck regulator evaluation kit photo with scale.*

The UltraCMOS process is able to address issues in power hungry RF applications, and is a viable approach for systems used in space. With more than one billion RFICs shipped into a variety of markets, including space, UltraCMOS technology has achieved volume manufacturing, high functional density, and high-performance, high-speed operation in a variety of RF integrated circuits. Over the years, UltraCMOS has been used to integrate RF, digital, analog and power functions for commercial high-volume applications, as well as specialized high-reliability military and space products.

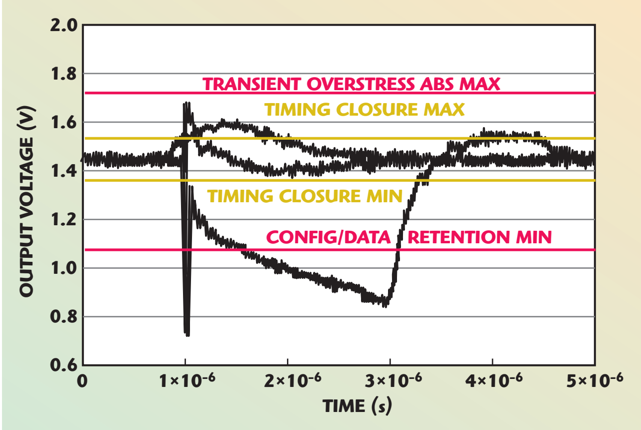

▲ *Fig. 8 Linear LDO single-event transients and LV logic IC performance/reliability voltage limits, as compiled by NASA.*

References

1. Customer-furnished data from EVK sample.
2. M.V. O'Bryan et al, "Compendium of Single Event Effects Results for Candidate Spacecraft Electronic for NASA," *IEEE NSREC 2006 W-4.*

SSPA Technology Achieves 10 kW CW at S-Band

This special report discusses the present state-of-the-art in S-Band high power amplifier design. A 10 kW CW solid state power amplifier (SSPA) has been designed using solid state technology at 2 GHz. The SSPA utilizes the latest GaN HEMT device technology to meet the needs of high power S-Band Satcom amplifiers to replace current traveling wave tube amplifier (TWTA) systems.

Solid state power amplifiers (SSPA) have been dramatically evolving over the past thirty years. Microwave amplifiers have been a driving force in EW and radar systems, terrestrial communication, wireless infrastructure, instrumentation and EMC applications as well as satellite communications. Satellite communication (Satcom) amplifiers are used in base station — earth station installations and have some of the most stringent requirements of all amplifier applications. Satcom amplifiers are required to operate continuously and must provide linear power amplification. This presents a challenge to the amplifier engineer in that both efficiency and power density are of paramount importance in the design of Satcom amplifiers. The requirement for linear output power means that the amplifier must be operated at an output power level far below its maximum saturated output power capability. Often a Satcom amplifier is operating in a multicarrier environment carrying anywhere from ten to over fifty carriers.

SATCOM AMPLIFIER TECHNOLOGY

Due to the very high linear output power levels required to transmit multicarrier signals to a satellite, Satcom earth station amplifiers have been dominated by klystron and traveling wave tube amplifiers in the past. Because of the continuous operation requirement and extremely high collector operating temperatures, tube-based amplifiers have experienced some reliability problems. Since the emergence of GaAs power transistors in the late 1970s, solid state amplifiers gradually began to replace klystron and traveling wave tube amplifiers (TWTA) in applications where sufficient linear power could be produced. Over the past two decades, GaAs devices have evolved such that SSPAs have become the preferred choice for earth station amplifier installations. Output power levels up to 1 kW have been achieved at S-Band, 4 kW at C-Band, 1 kW at X-Band and Ku-Band and 50 W at Ka-Band, using GaAs FET technology. A combination of innovative power combining techniques and redun-

Stephen D. Turner
Teledyne Paradise Datacom, State College, PA
Tom Dekker
Cree, Inc., Durham, NC

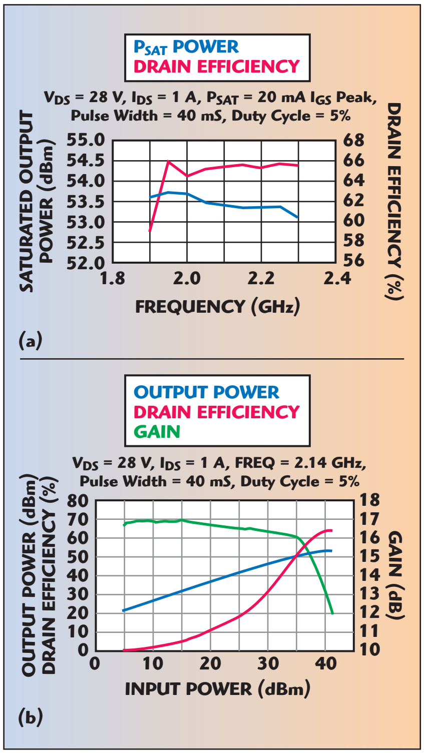

▲ *Fig. 1 CGH21240F typical device power vs. frequency (a) and typical swept power performance (b).*

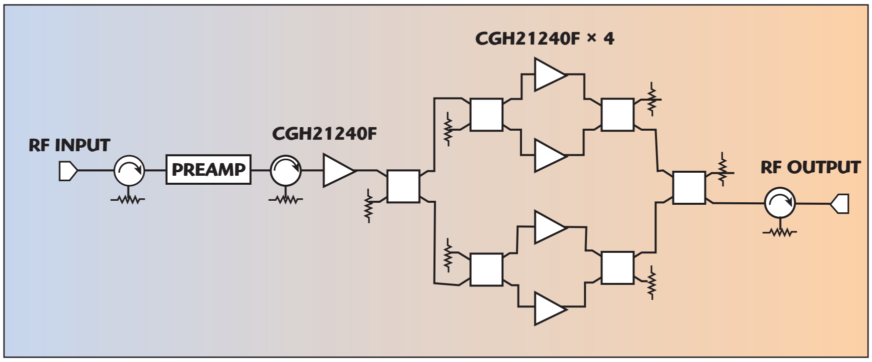

▲ *Fig. 2 800 W S-Band SSPA module block diagram.*

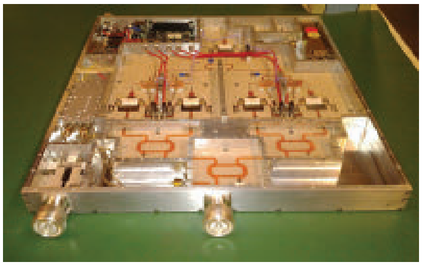

▲ *Fig. 3 800 W S-Band SSPA module assembly.*

dant, soft-fail architectures have given SSPAs a dominant position in the market. Despite this evolution, there remain applications that require even greater linear output power levels that until recently have still required the use of traveling wave tube amplifiers. As the available output power levels from GaAs FET devices have reached their limit, amplifier designers have been in need of solid state devices with greater power density along with higher channel temperature operation. The advent of GaN solid state device technology gives amplifier designers the ability to take SSPA power levels three to five times higher than what is presently possible with GaAs technology.

GALLIUM NITRIDE DEVICE TECHNOLOGY

Cree has recently released 40 V, 0.25 µm and 50 V, 0.4 µm GaN HEMT processes that extend the frequency range of the previous 28 V, 0.4 µm through Ku-Band and support larger power requirements, allowing the best fit to the application. These include multi-octave, high power pulsed and CW, linear applications for markets such as point-point radio, satellite communications, cellular, instrumentation, medical and military. The Teledyne application is an example of an innovative approach to achieving the power and efficiency advantages of GaN HEMT for S-Band applications.

The market adoption for GaN HEMT devices has accelerated in recent years for high power, high frequency SSPAs. GaN HEMT technology has proven itself to be reliable and rugged with companies such as Cree fielding over 2 billion GaN HEMT devices hours with a field FIT rate of less than 10. The technology is thermally rugged and supports operational junction temperatures of 225°C at excellent mean time to failure (MTTF) exceeding 2 million hours.

S-BAND SSPA MODULE DESIGN

The 10 kW S-Band SSPA system is designed around an internally input matched 28 V, 240 W GaN HEMT transistor, optimized for operation in the 1.8 to 2.2 GHz range. The transistor offers greater than 16 dB power gain, greater than 53 dBm output power and greater than 64 percent drain efficiency under pulsed conditions (see ***Figure 1***).

The amplifier system is designed using an array of phase combined SSPA modules. The SSPA module uses one device driving four phase combined devices as shown in ***Figure 2***. This results in a module that produces a minimum output power of 800 W in the 2 GHz range. The devices are then driven by a preamplifier section. The preamplifier contains additional GaN and GaAs FET driver stages along with a variable attenuator for amplifier gain adjustment. Also included in the preamplifier section is an analog predistortion linearizer. The linearizer serves to shape the GaN HEMT's power transfer curve shown in Figure 1b to behave similar to a GaAs FET's hard limiting characteristic. This increases the 1 dB compression point of the amplifier and improves the overall intermodulation distortion performance.

The device is biased in mid-Class AB mode. The initial impedance matching was performed using the large signal device impedance.[1] The matching networks are then optimized using the nonlinear device model in a Harmonic Balance simulator. The nonlinear modeling allows the designer to optimize the tradeoffs among output power, efficiency and intermodulation performance. The module is physically realized using softboard microstrip techniques. The 800 W module along with preamplifier and linearization circuitry is shown in ***Figure 3***.

SSPA SYSTEM DESIGN

The amplifier system is a modular soft-fail architecture based on Teledyne Paradise Datacom's patented PowerMAX technology.[2] Eight discrete (800 W) SSPA modules are phase combined to produce over 5 kW of saturated CW output power after the RF combining losses. The eight modules are arranged in a single

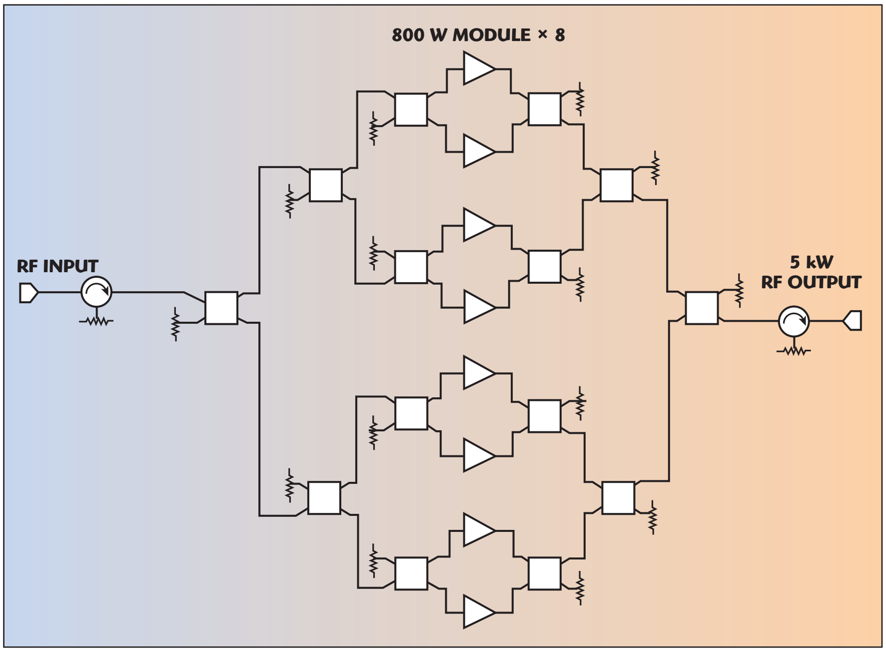

▲ *Fig. 4 5 kW, S-Band SSPA block diagram.*

▲ *Fig. 5 10 kW S-Band phase combined amplifier system.*

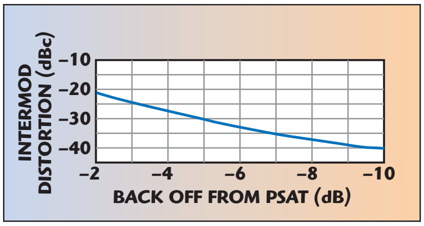

▲ *Fig. 6 10 kW two-tone intermod distortion performance.*

cabinet and are powered by n+1 redundant (28 VDC) power supplies. The eight SSPA modules are phase combined using specially designed spatial and waveguide combiner arrays integrated in the amplifier cabinet. The 5 kW SSPA cabinet block diagram is shown in ***Figure 4***.

The architecture is considered a self-redundant system. The failure of one entire SSPA module results in a reduction of 1.2 dB in output power capability from the cabinet. The architecture allows modular amplifier systems to achieve very high output power levels. The sophisticated embedded control circuitry allows the system to be operated as a 'single-box' amplifier.

The SSPA modules as well as the power supply modules are removable from the front panel of the equipment chassis. This facilitates very easy maintenance and replacement of the modules. Forced convection air cooling is used for the heat transfer through the cabinet. The thermal design maintains device flange temperatures at less than 50°C. The low-loss passive combining array provides a robust, soft-fail architecture.

Two identical 5 kW SSPA cabinets (see ***Figure 5***) are then phase combined using a waveguide hybrid combiner in WR430. This creates a system comprised of 16 parallel combined 800 W SSPA modules. The PowerMAX system architecture enables system configurations up to 16 modules. In a 16 module system, the failure of one SSPA module results in a reduction of 0.6 dB in output power capability.[3]

CONCLUSION

There has been much published about very high power SSPAs in the pulsed and radar genre. Many have held the position that solid-state power amplifiers are not able to achieve multi-kilowatt CW power levels. The maturation of GaN technology now dispels this myth with amplifier systems, such as the 10 kW S-Band HPA described in this article. The marriage of GaN HEMT technology and the redundant system architecture described here produces a high performance HPA system for demanding Satcom earth station installations. The combination of mid-Class AB bias and analog predistortion enable the GaN HEMT SSPA to have a similar intermodulation characteristic as its GaAs FET counterpart. The two-tone intermodulation versus back off plot is shown in ***Figure 6***.

The soft-fail characteristics and hot-swap field replaceable modules achieve system reliability figures that TWTA systems cannot achieve. GaN technology enables this system to approach similar prime power to linear RF output power efficiency as TWTAs. As device manufacturers continue to push the envelope of GaN technology, SSPA systems will become more versatile, covering wider bandwidths and higher frequency bands. GaN-based PowerMAX systems have already been manufactured in all of the major Satcom frequency bands ranging from 1 kW at Ka-Band to 10 kW at S-Band. ■

ACKNOWLEDGMENTS

The authors would like to acknowledge the contributions of the amplifier design team members: Craig Harris, Oleg Karpenko, Sithorn Prak, Dave Johnson and Jason Fetters.

References

1. A.A. Behagi and S.D. Turner, "An Electronic Design Automation Approach," *Microwave and RF Engineering*, Vol. 1, BT Microwave LLC, 2011.
2. Paradise Datacom LLC, "Power Amplifier System" U.S. Patent 8,189,338 B2, May 29, 2012.
3. S.D. Turner, "Concepts in Communication Amplifier Redundancy Systems," *Armed Forces International*, December 2004.

UP TO **100 Watt**

AMPLIFIERS

NOW! **100 kHz to 18 GHz**

from $945 ea. qty. (1-9)

High-powered performance, across wide frequency ranges. These class A linear amplifiers have set a standard throughout the RF & microwave industry. Rugged and reliable, they feature over-voltage and over-temperature protection, including the ability to withstand opens and shorts! And they're all in stock, whether with a heat sink/fan (for design labs and test benches), or without (for quick integration into customer assemblies). Go to minicircuits.com, and it's easy to select the models that meet your needs, including new features like TTL-controlled RF output. Place an order today, and you can have them in your hands as soon as tomorrow—or if you need a custom model, just give us a call for an engineer-to-engineer discussion of your requirements!

Mini-Circuits…we're redefining what VALUE is all about!

Model (with heat sink/fan*)	Frequency (MHz)	Gain (dB)	Pout @ Comp. 1 dB (W)	Pout @ Comp. 3 dB (W)	$ Price (Qty. 1-9) *with* heat sink	$ Price (Qty. 1-9) *without** heat sink
LZY-22+	0.1-200	43	16	32	1495	1470
ZHL-5W-1	5-500	44	8	11	995	970
• ZHL-100W-GAN+	20-500	42	79	100	2395	2320
• ZHL-50W-52	50-500	50	40	63	1395	1320
• ZHL-100W-52	50-500	50	63	79	1995	1920
LZY-1+	20-512	43	37	50	1995	1895
• ZHL-20W-13+	20-1000	50	13	20	1395	1320
• ZHL-20W-13SW+	20-1000	50	13	20	1445	1370
LZY-2+	500-1000	46	32	38	1995	1895
NEW ZHL-100W-13+	800-1000	50	79	100	2195	2095
ZHL-5W-2G+	800-2000	45	5	6	995	945
ZHL-10W-2G	800-2000	43	10	13	1295	1220
ZHL-30W-252+	700-2500	50	25	40	2995	2920
ZHL-30W-262+	2300-2550	50	20	32	1995	1920
ZHL-16W-43+	1800-4000	45	13	16	1595	1545
ZVE-3W-83+	2000-8000	36	2	3	1295	1220
ZVE-3W-183+	5900-18000	35	2	3	1295	1220

Listed performance data typical, see minicircuits.com for more details.

** To order **without** heat sink, add **X** suffix to model number (example: LZY-22X+).*

• Protected under U.S. Patent 7,348,854

Mini-Circuits®

ISO 9001 ISO 14001 AS 9100

P.O. Box 350166, Brooklyn, New York 11235-0003 (718) 934-4500 Fax (718) 332-4661

YONI2® ***The Design Engineers Search Engine*** *finds the model you need, Instantly* • For detailed performance specs & shopping online see **minicircuits.com**

U.S. Patents 7739260, 7761442

IF/RF MICROWAVE COMPONENTS

416 rev Z

Rugged High-Performance VNA Cable Assemblies

For VNA test applications with frequencies through 67 GHz, GORE® VNA Microwave/RF Test Assemblies offer extremely precise phase and amplitude stability when flexed and provide the highest accuracy and longest time interval between recalibrations. These test assemblies are designed to improve Vector Network Analyzer (VNA) performance in applications where precision, stability and repeatability are key requirements. These include testing antenna and radar systems going into aircraft, electronic warfare self-protection systems, amplifiers and other active devices – anything that operates at microwave frequencies.

Gore's VNA assemblies are supplied with most original equipment VNAs because manufacturers recognize the improved performance that they provide to high-end, extremely precise and very expensive ($100,000 range) test instruments. The exceptional phase and amplitude stability of the test assemblies ensures accurate and repeatable measurements, exceeding specifications for phase and amplitude stability, with additional testing performed to guarantee their phase and amplitude performance with flexure (see ***Figure 1***).

Unlike conventionally designed RF test assemblies, GORE VNA Microwave/RF Test Assemblies provide the most reliable phase and amplitude stability with flexure. They remain electrically stable when flexed – easily withstanding the rigors of typical bench testing procedures – while maintaining excellent insertion loss and VSWR. These assemblies can withstand 40 lbs (18 kg) of accidental pull without permanent degradation of electrical characteristics and up to seven lbs. (3 kg) of pull during normal use without exceeding electrical stability specifications. With a minimum bend radius of 2.25 in (57.2 mm), their unique armor construction provides a high degree of flexibility for long flex life. They have an auto-limiting bend radius of 2.25 in (57.2 mm), and the spring-back is virtually zero.

W. L. Gore & Associates Inc.
Landenberg, PA

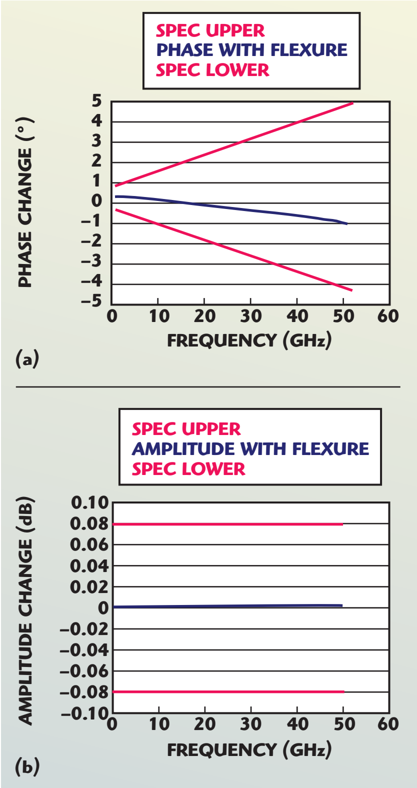

▲ *Fig. 1 Typical phase (a) and amplitude (b) stability with flexure for Gore part number FE0BN0BM025.0.*

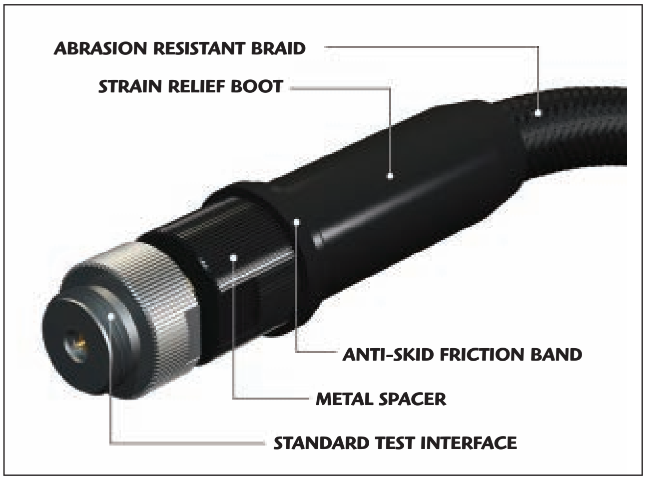

▲ *Fig. 2 Assembly features.*

In addition to providing high-precision measurements, GORE VNA Microwave/RF Test Assemblies offer maximum reliability with a rugged, lightweight construction that enables longer service life, reduced downtime and lower operating costs over the life of the equipment. They feature exceptionally rugged cable construction and NMD-style connectors that withstand repetitive mating, flexure, crushing, twisting and kinking. Crush resistance is greater than 800 lbs/linear inch, and the cable is capable of up to 100,000 flexures at minimum bend radius, depending on the configuration. An abrasion-resistant polymer braid covers a flexible armor casing, while a strain-relief boot protects against forces affecting the internal cable-to-connector termination (see ***Figure 2***).

Ruggedized, test-port style connectors are utilized for direct attachment to the VNA test ports, allowing use of adapters compatible with the test ports for optimum durability and stability. The test assemblies are available in the following standard lengths: 25 inch (0.64 meter), 38 inch (0.97 meter), and 48 inch (1.22 meter).

The NMD connectors are specifically engineered to optimize the performance of the assembly. These connectors mate with standard VNA systems, allowing mode-free broadband coaxial measurements from DC to maximum frequency. They have an auxiliary, large thread and bearing surface for mating with conventional connectors of the same type and for attaching either pin or socket adapters. They maintain a high center conductor, which yields better performance and reduces the frequency of recalibration.

The combination of this ruggedized construction and NMD-style connector ensures longer flex life with consistently durable and stable performance. GORE VNA Microwave/RF Test Assemblies offer the optimum level of electrical and mechanical performance for high-precision test applications.

W. L. Gore & Associates Inc., Landenberg, PA, www.gore.com/microwave.

NOW

PRECISION TEST Cables DC to 40 GHz!

from $68.95 ea. (qty.1-9)

Different cables for different needs—and all built to last. For almost 40 years we searched for reliable, high-performance cables that could stand up to the heavy use our 100% testing policy demands. Finally, we were able to acheive our goal, and we're proud to make these cables available to the rest of the industry, backed with our unprecedented 6-month guarantee.* Just go to minicircuits.com and order some for yourself! You'll quickly find that consistent long-term performance, less retesting, and fewer false rejects really add up to bottom-line savings, test after test!

Model Family	Freq. (GHz)	Connectors (male)	Lengths† (ft)	Temp (°C)
Performance Test (CBL)	DC-18	SMA‡, N	1.6-25	-55/+105
Quick Lock (QBL)	DC-18	SMA	1.0-6.6	-55/+105
Armored (APC)	DC-18	N	6.0-15	-55/+105
Low Loss (KBL-xx-LOW)	DC-40	2.92	1.5-6.6	-55/+85
Phase Stable (KBL-xx-PHS)	DC-40	2.92	1.5-6.6	-55/+85

**Mini-Circuits will repair or replace your test cable at its option if the connector attachment fails within six months of shipment. This guarantee excludes cable or connector interface damage from misuse or abuse.*

† Custom lengths available by special order.

‡ SMA female connectors featured on some models, or via special order.

K-Connector is a registered trademark of Anritsu Company.

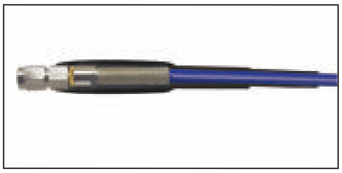

Full solder wick protected by stainless collar and three different layers of strain relief.

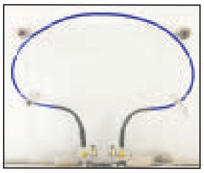

Flex Test™ setup shows triple strain relief, effective through 20,000 flex cycles for all models.

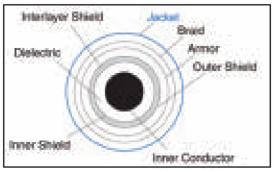

Armored Test Cables: rugged, triple shielded construction, flexible enough to pass 20,000+ Flex-Test cycles.

40 GHz cables compatible with SMA, K®, 2.9 & 3.5 connectors.

See minicircuits.com for cable lengths, specifications, performance data, and surprisingly low prices!

Mini-Circuits...we're redefining what VALUE is all about!

Mini-Circuits®

ISO 9001 ISO 14001 AS 9100

P.O. Box 350166, Brooklyn, New York 11235-0003 (718) 934-4500 Fax (718) 332-4661

Yoni2® **The Design Engineers Search Engine** finds the model you need, Instantly • For detailed performance specs & shopping online see minicircuits.com

U.S. Patents 7739260, 7761442

IF/RF MICROWAVE COMPONENTS

Ultra-Low Noise 200 MHz to 3 GHz Signal Sources

VHF OCXOs are widely used as 'master oscillators' in signal sources and frequency synthesizers, where the output frequencies are derived by techniques including multiplication, PLL, DDS, etc. In low-noise sources, the phase noise floor is typically limited by the multiplied OCXO.

Pascall's XMN (crystal multiplied by N) series combines an OCXO with frequency multipliers, bandpass filters and amplifiers to provide a fixed-frequency output with low phase noise, in the range of 200 MHz to 3 GHz. The XMNP adds a phase-locked loop to enable the OCXO to be locked to an external reference.

DESIGN

It is well known that multiplying frequency by N increases phase noise by 20 log(N) dB. However, achieving this theoretical ideal is easier said than done, particularly when the fundamental signal has a very low noise floor.

Active multipliers almost inevitably have a high noise figure and therefore degrade the phase noise floor at the input frequency. With passive multiplication, the added noise is mostly determined by the signal level at the output frequency and the noise figure of the following amplifier. An inappropriate choice of multiplier or amplifier devices can also increase the flicker noise.

In the XMN, the nonlinear resistance of Schottky diodes is used to generate harmonics, with the multiplier tuned for the required input and output frequencies. The conversion loss varies relatively little with temperature and input power, and the circuit is easily tuned to different frequencies.

Two multiplier configurations are used to produce odd and even harmonics, respectively. All multiples up to 10 can be generated – typically up to 1.3 GHz, depending on the fundamental frequency. The first stage is followed, if necessary, by a further doubler or tripler, to generate frequencies up to 3 GHz.

The XMN is available with either electrical tuning (0 to +10 V, positive or negative slope) or mechanical tuning by means of a multi-turn potentiometer. The XMNP phase-locked variant includes RF and reference dividers. This provides flexibility in the choice of customer-specified reference frequency, which may be as high as the oscillator frequency. If a reference signal is detected, the XMNP automatically locks to it. In the absence of a reference it behaves as an XMN, with the frequency set by a multi-turn potentiometer.

All variants provide a supplementary output at the fundamental frequency. This may typically be used to generate intermediate frequencies in a synthesizer, or to lock the XMN in a customer-designed PLL.

The design allows customers to specify the oscillator frequency (up to 160 MHz) as well as the multiplied frequency. For example,

Pascall Electronics Ltd.
Ryde, Isle of Wight, UK

Phase Critical PERFORMANCE

Phase Optimized Interconnects from TIMES Microwave Systems

- **Leading Edge phase Performance**
- **Eliminate Phase/Temperature "PTFE knee"**
- **Absolute Phase and Tracking Applications**
- **Wide Temerature Range**
- **Range of Styles and Sizes**

Phasetrack™ flexible cable assemblies

- PT130, PT180, PT210, PT318
- Proven, Rugged Flexible Construction
- TF4 Dielectric Phase Performance
- Triple Shielding Technology
- -55C to +125C Temperature Range

Phasetrack P-Flex™ cable assemblies

- PF130, PF402
- Flexible "In-the-Box" Cable Assemblies
- TF4 for Absolute and Tracking Phase Applications
- Easy Installation, Proven Reliability
- -55C to +150C Temperature Range

Phasetrack™ Low Smoke cable assemblies

- PT400-LS, PT600-LS
- Support Low Smoke Applications
- Absolute and Tracking Phase Applications
- Sized for Rugged, Low Loss Performance
- -40C to +85C Temperature Range

PhaseTrack™ Semi-Rigid cable assemblies

- PT110-SR, PT141-SR
- Classic Semi-Rigid Style now with TF4
- New Designs or Drop-In Replacements
- -55C to +125C Temperature Range

SiO2 (Silicon Dioxide) Cable Assemblies

- SiO2-090, SiO2-141, SiO2-200, SiO2-270
- Semi-Rigid Style Assemblies
- Ultimate Phase Tracking Performance
- Extreme Temperatures, Harsh Environments
- -273C to +600C Temperature Range

For Performance, Quality and Reliability you can count on, count on Times Microwave Systems - The Leader

TIMES MICROWAVE SYSTEMS
An Amphenol Company

AS9100 / ISO 9001:2008 Registered

World Headquarters: 358 Hall Avenue, Wallingford, CT 06492 • Tel: 203-949-8400, 1-800-867-2629 Fax: 203-949-8423
International Sales: 4 School Brae, Dysart, Kirkcaldy, Fife, Scotland KY1 2XB UK • Tel: +44(0)1592655428
China Sales: No. 318 Yuan Shan Road • Shanghai, China 201108 • Tel: 86-21-51761234 Fax: 86-21-64424098
www.timesmicrowave.com

1 GHz can be generated from 100 MHz × 10, 111.111 MHz × 9, 125 MHz × 8 or 142.857 MHz × 7. This flexibility can facilitate frequency planning for a particular application, or alternatively can be used to optimize the phase noise. Lower multiplication ratios give lower noise floor. On the other hand, choosing a lower oscillator frequency will reduce the close-in phase noise.

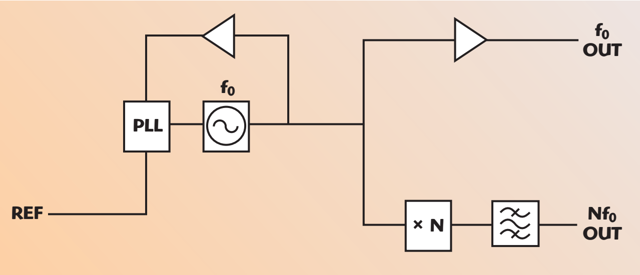

▲ *Fig. 1 Simplified block diagram of XMNP.*

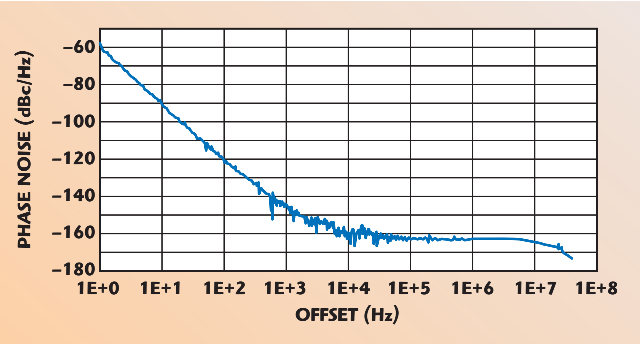

▲ *Fig. 2 1.2 GHz XM10 phase noise.*

The basic package size is 101.6 × 57.2 × 20.3 mm for the XMN and 101.6 × 87.5 × 20.3 mm for the XMNP. This typically allows for all multiples up to 10. If an extra multiplication stage is needed, for 3 GHz output for example, the width increases to 81.5 mm or 111.8 mm for the XMN and XMNP, respectively. The standard supply voltage is +12 V, with +15 V available as an option. ***Figure 1*** shows a simplified block diagram of the XMNP phase-locked signal source.

PERFORMANCE

The main criterion when developing the XMN was that the phase noise should be as low as possible. In this regard, integrating oscillator, multiplier, amplifiers and filters into a single unit can give better performance than a building-block approach, as the individual sections can be optimized to work with each other.

The phase noise floor at the multiplied output is typically equivalent to –183 dBc/Hz at the oscillator's frequency. For example, the phase noise floor of an 840 MHz output derived from 120 MHz is typically –166 dBc/Hz.

Close-to-carrier phase noise is similar to that of Pascall's OCXO and OCXOF oscillators. Internal regulators are used to reduce the effect of supply noise and ripple. Particular care has been taken to minimize low-frequency noise on the oscillator supply, ensuring that even at 1 Hz offset, the full performance offered by low-noise crystals is realized.

Figure 2 shows the phase noise at the 1.2 GHz output of an XM10 (120 MHz × 10), measured with an Agilent E5052B signal source analyzer. Output power at both fundamental and multiplied frequencies is 13 dBm, with sub-harmonics and spurious products <–80 dBc.

The XMNP operates with reference input levels from –3 to +16 dBm, which makes it very easy to incorporate into customers' applications. The PLL bandwidth is ≤1 Hz, giving it high rejection of noise and spurs on the reference signal.

APPLICATIONS

The low phase noise and spurious outputs of the XMN and XMNP make them ideal building blocks for high performance synthesizer designs. Other uses include satellite ground stations, phase noise test systems, and EW systems and scientific research. In certain applications, the XMN/XMNP may provide a practical alternative to a SAW oscillator, offering improved close-to-carrier phase noise and flexibility of output frequency without incurring the development cost of a non-standard SAW resonator.

Pascall Electronics Ltd.,
Ryde, Isle of Wight, UK
+44 (0)1983 817300,
enquiries@pascall.co.uk.,
www.pascall.co.uk.

Rugged Connectors for Harsh Environments

Amphenol RF
Danbury, CT

Amphenol® RF has developed a new line of rugged connectors (ARC) for transportation, military, mining and construction, public safety, wireless, smart energy, industrial control and other outdoor harsh environment applications. The ARC line of rugged connectors is IP67-rated in both mated and unmated conditions. These connectors are designed to withstand extreme conditions in harsh environments where they will be subject to intense shock, vibration and heavy mechanical loads. Amphenol RF strengthened the plating of the new ARC line connectors for increased mating cycles and improved chemical resistance. The addition of seals and an improved geometry design has made the new ARC line submersion resistance beyond the level of IP-67 per IEC 529. The line's superior design and manufacturing techniques allow these cable jacks and plugs to be fully submersible and impenetrable to fluids in mated and unmated conditions, even when subjected to extreme changes in temperature and humidity. The ARC line is engineered to reduce the total cost of ownership of outdoor installation maintenance.

The ARC line utilizes a single-piece body design in Amphenol's straight connectors instead of conventional, multi-piece modular designs. This provides for greater load capability and mechanical shock survival. The environmental specifications are shown in ***Table 1***.

The ARC line is available in TNC and Type N cable interfaces with standard and reverse polarity options (electrical performance is shown in ***Table 2***). Cable jacks and plugs are

TABLE I
ENVIRONMENTAL SPECIFICATIONS FOR ARC PRODUCT LINE

	TNC	*Type N*
Temp. Range	-65° to +165°C*	-65° to +165°C*
Thermal Shock	MIL-STD-202, method 107, cond. B	MIL-STD-202, method 107, cond. B
Vibration	MIL-STD-202, method 204, cond. B	MIL-STD-202, method 204, cond. B
Shock	MIL-STD-202, method 213, cond. G	MIL-STD-202, method 213, cond. 1
Sealing	IEC 529, IP67	IEC 529, IP67

*With heat shrink wrap tubing temperature range up to 85°C

TABLE II
ELECTRICAL SPECIFICATIONS FOR ARC PRODUCT LINE

	TNC	*Type N*
Impedance	50 ohm	50 ohm
Frequency Range	DC to 6 GHz	DC to 6 GHz
Performance Spec Standard Polarity STR: DC to 3 GHz STR: 3 to 6 GHz R/A: DC to 3 GHz R/A: 3 to 6 GHz	 1.2 Max. 1.3 Max. 1.3 Max. 1.3 Max.	 1.1 Max. 1.2 Max. 1.15 Max. 1.2 Max.
Insulation Resistance	5000 MΩ Min.	5000 MΩ Min.
Contact Resistance	Center Contact: ≤=1.5 mΩ, Outer Contact: ≤=0.2 mΩ	Center Contact: ≤=1 mΩ, Outer Contact: ≤=0.2 mΩ
Dielectric Withstanding Voltage	1000 VRMS	1000 VRMS

available in straight, right angle and bulkhead configurations to fit to various outdoor installation requirements. Since the ARC line's introduction in June 2012, Amphenol RF has been enhancing its product offering by including more cable groups to the product lineup.

To complement the connector line, Amphenol RF offers ruggedized cable assemblies with various integrated armor to limit the effects of abrasion and impact. Conduit style armor is available to aid with chemical resistance.

Amphenol RF will be expanding its ARC line in the upcoming months to include IP-67 rated PCB jacks and between series adapters.

Amphenol RF,
Danbury, CT
(800) 627-7200,
arc.amphenolrf.com.

Tech Brief

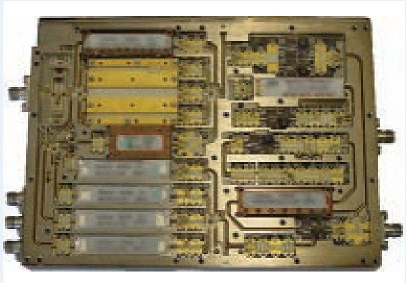

High Performance Broadband Converter and Receiver

Norden Millimeter has developed an 18 to 40 GHz down converter with an integrated 0.5 to 18 GHz bypass path for combining both into a single 0.5 to 18 GHz IF output. Conversion gain is 12 dB (± 3 dB) typical, noise figure is 14 dB typical and VSWR IF/LO/RF is 2.5:1 typical. Norden uses a variety of technologies to miniaturize multiple functions into a single small housing running off a single power supply voltage to minimize size, weight and power. These are designed for the ELINT and EW markets.

In addition, Norden Millimeter has developed a 0.5 to 18 GHz receiver for the ELINT market. The frequency range of this receiver can also be extended by using Norden's 18 to 26.5 GHz and 26.5 to 40 GHz block down converters. The noise figure is 14 dB typical with an IF of 1 GHz ± 250 MHz. Image rejection is 85 dBc typical, IF rejection is greater than 100 dBc typical and spurs/harmonics at –15 dBm input are 60 dBc typical. The receiver is highly channelized for increased interference immunity. To minimize the power consumption of the receiver, the unselected bands are turned off. Norden uses the latest MMIC and packaging technology to bring this design to manufacturing in an extremely small package size.

Norden Millimeter has extensive experience in design and manufacturing of frequency converter products for both the commercial and military markets. Norden understands that the vast majority of requirements for converter products involve custom design and packaging, custom LO and IF frequency selection, conversion gain and linearity requirements. To this extent, it is difficult to develop a useful line of "standard" converter products. Consequently, Norden recognizes that the majority of requirements for these products will be per individual customer specifications.

Norden Millimeter,
Placerville, CA
(530) 642-9123,
www.nordengroup.com.

Your Source for Military Interconnect Solutions

With **over 30 years experience** providing solutions for challenging defense applications, **Teledyne Storm's heritage is your heritage.**

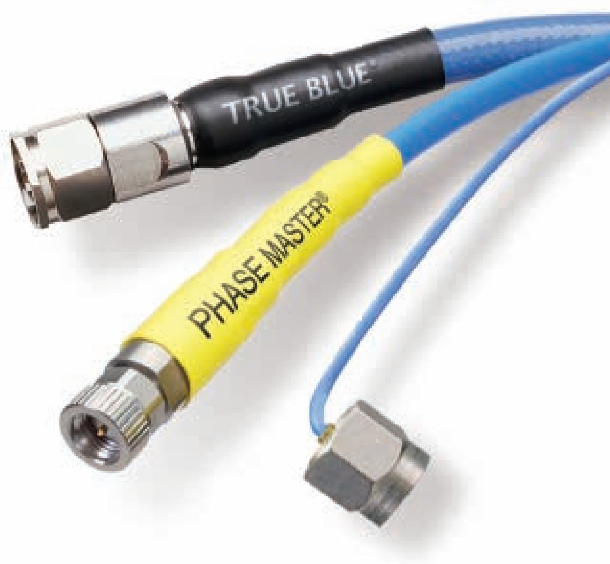

We understand your needs for high performance microwave assemblies specifically engineered for military radar and EW applications and offer a product line that includes:

- ***True Blue®*** *low loss flexible assemblies*
- ***Phase Master®*** *phase stable flexible assemblies—superior phase stability, exceptional value*
- ***Storm Flex®*** *assemblies—durable, compact, superior electrical performance*
- ***Maximizer Gold™*** *phase stable semi-rigid assemblies*
- *Miniature blindmate assemblies*

Put our reputation for **technical expertise and outstanding customer service** to the test.

Contact us today to discuss how Teledyne Storm Products can combine **high quality, performance, & value** in a product solution that works for you.

TELEDYNE
STORM MICROWAVE
Everywhere**you**look™

10221 Werch Drive ▪ Woodridge, Illinois 60517
Tel 630.754.3300 ▪ Fax 630.754.3500
Toll Free 888.347.8676
storm_microwave@teledyne.com

www.teledynestorm.com/mj1012

Compact 1 kW Power Amplifiers

The first models of Empower's 'Size Matters' high power PA product family are packaged in a 5U, air cooled chassis and deliver over 1 kW of output power in the frequency ranges of 20 to 500 MHz, 500 to 1000 MHz and 20 to 1000 MHz. All models are suitable for octave bandwidth high power CW, modulated and pulse applications.

The 1 kW solid-state amplifiers utilize high power LDMOS devices that provide wide frequency response, high gain, high peak power capability and low intermodulation distortion. Exceptional performance, long-term reliability and high efficiency are achieved by employing advanced broadband RF matching networks and low-loss combining techniques, all qualified components and EMI/RFI filters. This is particularly important due to the prevalence of wireless transmitters in the modern urban environment, where Empower's amplifiers permit verifying products for hardness compliance against EM/RF interference.

The amplifiers include a built-in control and monitoring system, with protection functions that preserve high availability. Remote management and diagnostics are via an embedded web server, allowing network managed site status and control simply by connecting the unit's Ethernet port to a LAN. Using a web browser and the unit's IP address allows ease of access with the benefit of multilevel security.

The system core supports software and firmware encryption, uses an embedded real-time OS (Linux), has a built-in non-volatile memory for event recording, storage of control parameters, event logs and factory protected setup recovery features. The extended memory option allows for enhanced internal diagnostics and troubleshooting – basically, there is a flight recorder in the amplifier.

The 1 kW family features a 'minimal touch' design, which eliminates a number of manual manufacturing process steps – design margin evaluation (DME) analysis and a full set of factory acceptance tests are integral to the product. Detailed thermal analysis and demonstrated heat spreading techniques, including device management, have all contributed to high system reliability.

VENDORVIEW

Empower RF Systems Inc., Los Angeles, CA (310) 412-8100, www.empowerrf.com.

Turnkey EMC Reverberation Chambers

Reverberation chambers (RVC) are modern EMC test environments that provide an alternative to semi or full anechoic rooms (SAR/FAR), open area test sites (OATS) or Gigahertz Transverse Electromagnetic (GTEM) cells. The new RVC XS and 2XS models expand Teseq's extensive chamber portfolio.

RVCs consist of a shielded room and a 'stirrer,' which changes the resonant electromagnetic field distribution inside the chamber, producing a statistically uniform field. The two new RVC models are designed specifically to accommodate small Equipment Under Test (EUT), eliminating the need for a larger, more expensive, traditional chamber. Both models are fully assembled and tested in the factory and no on-site assembly is required as the chambers are delivered ready to use.

The 2XS, the smaller of the two chambers, has an internal size of 1.5 × 0.8 × 1.0 m, providing a test volume of 0.5 × 0.3 × 0.5 m at a start frequency of about 800 MHz. The larger model, the XS, has an internal size of 2.7 × 1.5 × 1.3 m, resulting in a test volume of 1.2 × 1.0 × 0.8 m and a start frequency of about 500 MHz.

Optimal mechanical stability of the two RVCs is achieved using a rigid construction and an outside reinforced frame. Furthermore, the inside of the chamber has a completely flat surface (no connective elements are used for pan type or sandwich construction), which is made of aluminium for optimal power and field performance. Field strengths of more than 100 V/m are easy to achieve with 1 W applied to the antenna and with an empty chamber.

Both chambers are fully equipped with a stirrer — designed and optimized for the intended frequency range in accordance with the requirements of the basic standards. The stirrer commands are provided in the user manual and enable easy implementation of the stirrer controller within any measurement software. Drivers and RVC application packages for Teseq's Compliance 5 EMC software are available.

Teseq AG, Luterbach, Switzerland +41 32 681 4075, www.teseq.com.

Catalog Update

Wireless Connectivity Brochure

VENDORVIEW

Gain greater insight into wireless design and test with Agilent's new brochure *Test Solutions for Greater Insight into Wireless Connectivity*. This brochure focuses on test solutions for technologies such as WLAN, WiMAX™, RFID, NFC, Bluetooth®, UWB and ZigBee. The brochure is available now at www.agilent.com/find/wirelessconnectivity, in the What's New section. There is no cost and no registration required.

Agilent Technologies Inc.,
www.agilent.com.

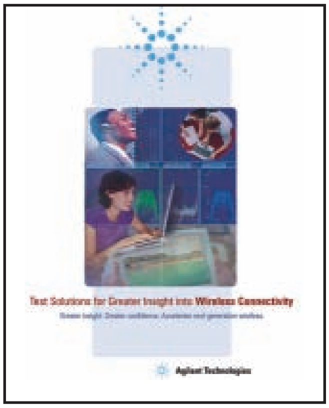

EMC & RF Testing Catalog

VENDORVIEW

AR's new product catalog is now available from the company's local AR sales associate. The catalog is easy to use, with "find-it-fast" charts and color coding to help get right to whatever you need for RF and EMC testing. It is also available for free download, either in full or by section at www.arworld.us.

AR RF/Microwave Instrumentation,
www.arworld.us.

Connector Catalog

Astrolab Inc. announces the publication of its new RF and microwave connector catalog. The catalog is a resource for system and component engineers to identify solutions that maximize system performance while minimizing its mass, volume and footprint. The catalog includes connectors with BMA, BMZ, MCX, MMCX, SMP, SMPM and the company's space qualified SMPM-T interfaces, and RF contacts that include size 12, 16 and 20 interfaces. The catalog introduces the new "gigablock" connection system with 16 microwave connections in one connector that can be used up to 40 GHz.

Astrolab Inc.,
www.astrolab.com.

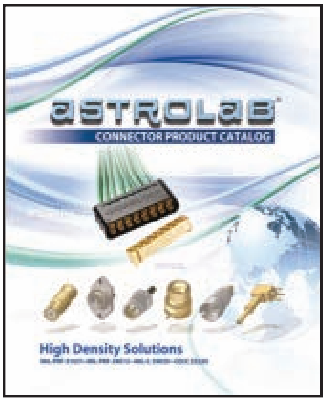

Microwave Capabilities Catalog

Crane Aerospace & Electronics Microwave Solutions launches the new microwave capabilities catalog that features a wide range of product solutions from component level devices to complex, advanced integrated microwave assemblies. Products are illustrated from major product areas and represent the breadth of technical capability of Crane. The company's microwave brands include Merrimac, Signal Technology and Polyflon. For more information on Crane Microwave Solutions, please visit www.craneae.com/mw.

Crane Aerospace & Electronics Microwave Solutions,
www.craneae.com.

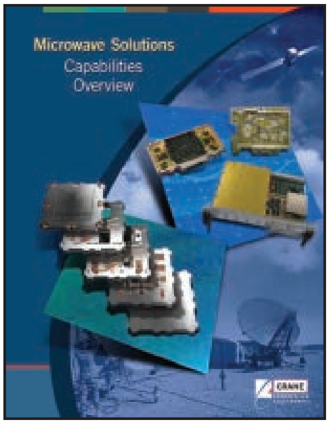

Supplier Line Card

VENDORVIEW

Richardson RFPD Inc. announced the availability of its 2012 Supplier Line Card. The updated, expanded Line Card features a section of 'Suppliers by Product Category' matrix tables that offers at-a-glance reference of supplier devices. The expanded Supplier Line Card reflects Richardson RFPD's best-in-class New Product Introduction program that provides supplier partners with maximum exposure to design engineers developing the next generation of products for applications in aerospace and defense, broadcast transmission, machine-to-machine (M2M), renewable energy, and wireless infrastructure.

Richardson RFPD Inc.,
www.richardsonrfpd.com.

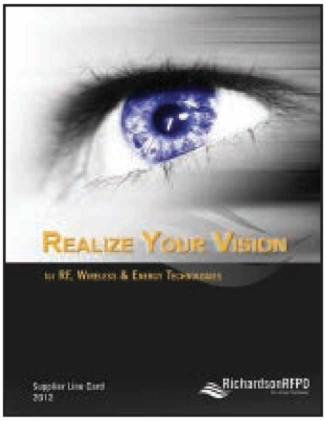

USB Products Brochure

RFMW announced its latest short form brochure highlighting the Telemakus family of USB-controlled test devices and software applications. This interactive brochure provides an overview of Telemakus low-cost devices including synthesized signal generators, true RMS power detectors, vector modulators, phase shifters, variable step attenuators, switches, multipliers and amplifiers. An application library reviews 2-tone analyzer measurements, functional pulse modulators, pulse power analyzers, a low-cost scalar analyzer system and data logging functions. A copy of the interactive brochure may be downloaded at: www.rfmw.com/data/Telemakus_2012_Short_Form.pdf.

RFMW,
www.rfmw.com.

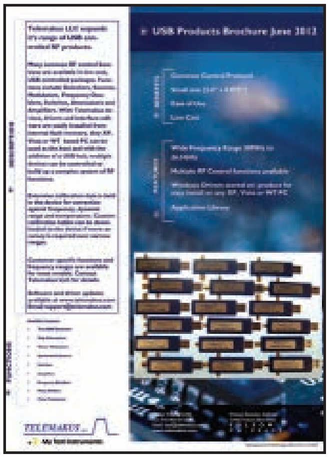


The World Leader in tactical
communications doesn't compromise.

Catalog Update

Legacy Pro Brochure

VENDORVIEW

Do you need to replace discontinued instrumentation in your ATE? Rohde & Schwarz offers signal generators as well as spectrum and network analyzers that understand the existing code written for your test system. Retain your current test system software. Benefit from the company's experience in code emulation. Rely on its long-term support. Find out more in the R&S Legacy Pro brochure (order number: PD 5214.5603.62) or online: www.rohde-schwarz.com/ad/legacypro.
Rohde & Schwarz GmbH & Co. KG, www.rohde-schwarz.com.

Radar & Satellite Catalog

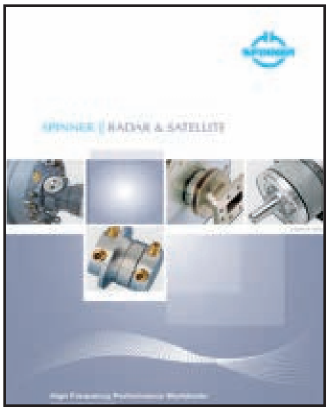

SPINNER's new radar and satellite catalog presents its product portfolio, which includes several kinds of rotary joints such as single and multi channel fiber optic, coax and waveguide solutions. The special benefits of these include compact design, excellent electrical and mechanical performance and longest life time. SPINNER's innovations, technical know-how and top quality made the company one of the leading rotary joint manufacturers for off-the-shelf and custom-made solutions.
SPINNER GmbH, www.spinner.group.com.

Cables, Connectors & Assemblies Brochure

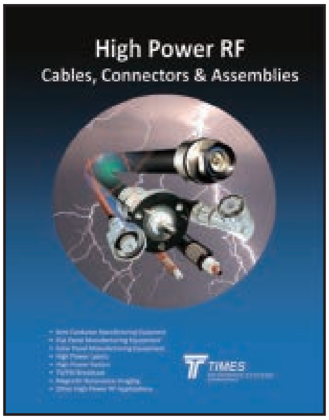

Times Microwave Systems introduced *High Power RF Coaxial Cables, Connectors & Assemblies* covering 50 Ω flexible cables for use in demanding high power applications such as high power radar and lasers, pulse power, medical equipment (MRI), semiconductor, flat panel and solar panel manufacturing, and particle physics. Cables are available for use at continuous operating temperatures up to 200°C. The product range includes MIL-C-17 cables, special Times-designed high power cables such as SFT®, HP, FBT®, LMR-LLPL® and LMR®-FR cables.
Times Microwave Systems, www.timesmicrowave.com.

Ultra Low Phase Noise OCXO

Wireline | Wireless | Military & Space | Industrial

The OX-204 is an Ultra Low Noise OCXO designed for applications that have a need for uncompromised phase noise performance. The OX-204 achieves a noise floor of <-175dBc, without compromising the close-in phase noise at 1 and 10 Hz. The OX-204 is the latest addition to Vectron's family of low phase noise products.

75% reduction in area while maintaining Ultra Low Phase Performance

Key Features

- -135 dBc / Hz at 10 Hz offset
- -175 dBc / Hz at 10 kHz offset
- 10 MHz standard, other frequencies available
- Compact 1" x 1" hermetic enclosure
- Low Power Consumption:
  4 Watts during warm-up
  1.5 Watts during steady state
- Temperature Stability:
  +/-10ppb at -20 to 70°C
  +/-20ppb at -40 to 85°C

Phase Noise Performance

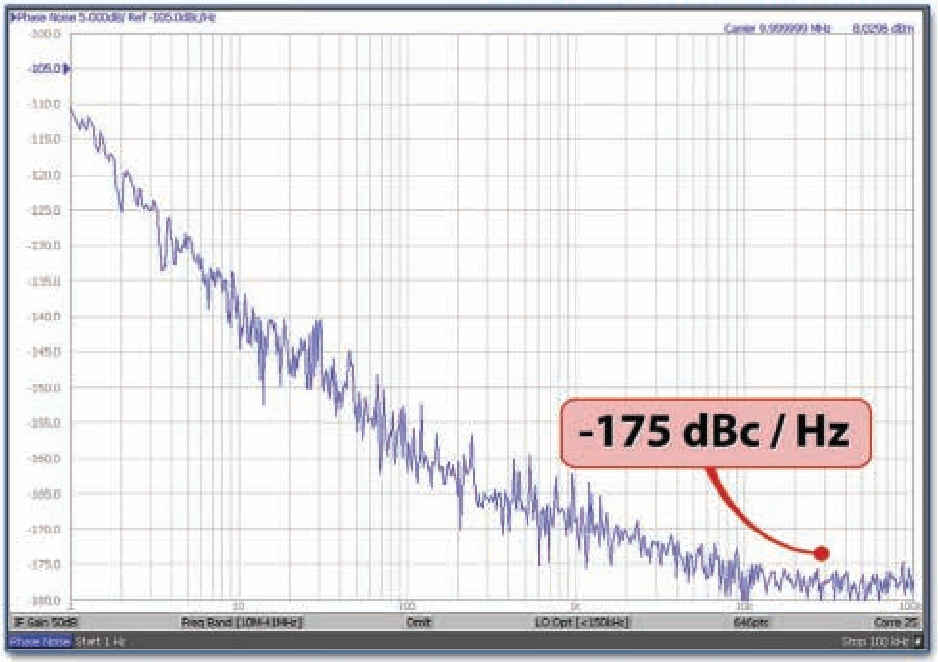

Applications

- Radar
- Satellite Communications
- Military Communications
- Test & Measurement Equipment
- DRO & Synthesizer references

OCXO/EMXO | TCXO | VCSO | VCXO | Jitter Attenuation | SAW Filter | Clocks/XO | Crystals | Timing Solutions | High-Temp Electronics

For more information on these product visit www.vectron/products/ocxo/ox-204.htm or contact a customer service representative at 1-88-VECTRON-1

Select from **Our Precision Portfolio** that supports your performance requirements, ensuring **Stability , Synchronization and Timing.**

Helping Customers Innovate, Improve & Grow

VECTRON INTERNATIONAL

A DOVER COMPANY

Components

Micro-Miniature Connectors

Amphenol Aerospace offers a series of rugged, micro-miniature connectors that provide more power throughput and consistent coupling by incorporating more electrical connections in compact form factor. Available in shell sizes from 5 to 23, the new high-density 2M Series weighs 72 percent less and is 52 percent smaller than standard MIL-DTL-38999 connectors. The connectors are intermateable and intermountable with existing micro-miniature high-density connectors typically used in aerospace and defense applications. The 2M Series maximizes SWaP (size, weight and power) in a variety of high-reliability, harsh environments.

Amphenol Aerospace,
www.amphenol-aerospace.com.

Multiplexers

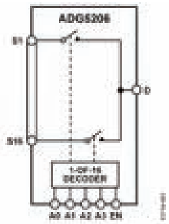

ADI introduced two multiplexers, ADG5206 and ADG5207, able to guarantee latch-up prevention in high-voltage industrial applications operating up to ±22 V. The low leakage (20 pA) feature ensures high accuracy and resolution. They operate from ±9 to ±22 V in applications where the analog signal is bipolar and from +9 to +40 V in applications where the analog signal is unipolar. They feature 3.5 pF off-source capacitance, 60 MHz –3 dB bandwidth, ultra-low charge injection (0.35 pC at 0 V) and source off leakage (400 pA at 125°C) performance.
Analog Devices Inc.,
www.analog.com.

Connector and Cable Harness

Astrolab Inc. announced the release of a new 65 GHz multiple mate PCB connector and cable harness system. This system, Gigablock, was developed using the company's rugged and patented micro-bend® cable assemblies that can be terminated with SMA, SMPM, SMP, 2.9mm (K) and 1.85mm connectors. This high density cable and connector solution maximizes system performance while minimizing its mass, volume and footprint.
Astrolab Inc.,
www.astrolab.com.

Coaxial Cable Assemblies

Crystek has introduced a line of 26.5 GHz hand-formable coaxial cable assemblies, a new addition to its low-loss RF coaxial cables. Designed to operate from DC to 26.5 GHz, the hand-formable CCSMA26.5-MM-086 cable assemblies are ideally suited for jumpers, instrumentation and high-frequency interconnects. The 50 Ω cables provide an attenuation value of 1.40 dB/ft. at 26.5 GHz, and offer shielding effectiveness of greater than 100 dB with an operating temperature range of −40° to +85°C. Electrically matched pairs are also available.
Crystek Corp.,
www.crystek.com.

Module Chips

Ethertronics unveiled EtherChip 1.0™, the first in a series of building blocks for RF front-end module chips from the Ethertronics Chip Division to provide more "smarts" to antenna and RF systems. EtherChip 1.0 leverages Ethertronics' Air InteRFace Digital Conditioning™ (AIRFDC™) technology to provide tuning capacitance, seamlessly adjusting the characteristics of a cellular antenna to its dynamic requirements – such as retuning for frequency shift, hand or head effects, or more bandwidth. EtherChip 1.0 is a silicon chip available for immediate integration by OEMs.
Ethertronics,
www.ethertronics.com.

Analog-to-Digital Converters

VENDORVIEW

The HMCAD1104 is a 10-bit octal channel ADC with low power and high performance. Operating at 65 MSPS, the HMCAD1104 delivers a signal to noise ratio (SNR) of 61.6 dB, while dissipating only 30 mW of power per channel. The HMCAD1104 is pin compatible with Hittite's family of 12-bit ADCs including the HMCAD1100, HMCAD1101 and HMCAD1102, all of which are compatible with the EasySuite™ Test and Evaluation Tool for analysis and system configuration. The HMCAD1104 is specified for operation over the industrial temperature range of –40° to +85°C.

Hittite Microwave Corp.,
www.hittite.com.

Contact Clip

The Contact Clip KK-541 offers reliable contacting with flat connectors on the outer surface. Even contacting in rough test conditions using vibrations, contaminations and long test cycles, the KK-541 proves it is the most suitable due to its double spring clip structure. The Contact Clip is designed for flat connectors of 0.5 to 0.8 mm. Depending on the fitting, for example test fixtures or test plugs, there are two different versions available: press fit or screw in.
Ingun Pruefmittelbau GmbH,
www.ingun.com.

Solid-State RF Switches

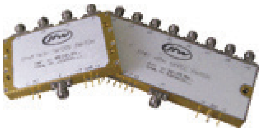

The 50S-1720 (1P2T), 50S-1721 (1P4T) and 50S-1722 (1P8T) are JFW's newest line of PIN-diode RF switches. They boast an operating frequency from 0.5 to 18 GHz, 50 dB minimum isolation at 18 GHz, and a maximum switching speed of 100 nanoseconds. Their compact, self-terminating design makes them perfect for OEM and test applications where reliability, speed or bandwidth is critical. SMA female connectors and TTL control are standard, but other configurations may be available upon request. For more information, email: sales@jfwindustries.com.
JFW Industries,
www.jfwindustries.com.

DC/DC Converter

VENDORVIEW

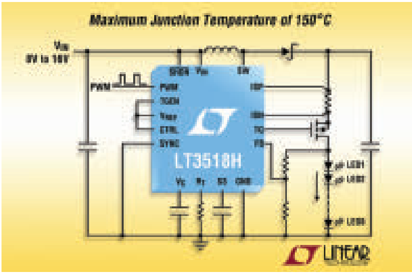

Linear Technology announces the H-grade version of the LT3518. The LT3518 is a 45 V, high-side current sense DC/DC converter designed to drive high current LEDs at constant current. It has a 3 to 30 V input voltage range with transient protection to 40 V. The H-grade version operates with a junction temperature up to 150°C, compared to the E- and I-grade versions' 125°C maximum junction temperature. The H-grade parts are tested and guaranteed to the maximum junction temperature of 150°C.
Linear Technology Corp.,
www.linear.com.

Bridge Couplers

Marki Microwave presents the highest performance bridge couplers available on the market today. The CBR16-0003 and CBR16-0006 offer outstanding typical directivity of 40 dB, which is higher than any other coupler available and enables high accuracy forward and reflected power measurements. The CBR16-0012 offers 30 dB directivity from 200 kHz to 12 GHz, the broadest bandwidth available for such a high directivity coupler.
Marki Microwave,
www.markimicrowave.com.

FLAT GAIN WIDEBAND *amplifiers*

flatness from ±0.7dB across 0.1-6 GHz   IP3 up to 38 dBm

Our new GVA-62+ and GVA-63+ amplifiers are spot-on for high performance base stations, portable wireless, LTE and cellular, CATV/DBS systems, MMDS, and wireless LANs. They make excellent gain blocks for almost any 50Ω circuit. DC power as low as 5V/69 mA delivers a typical output power of 18 dBm, unconditional stability, and built-in ESD protection, all with no external matching components required!

Just go to minicircuits.com for technical specifications, performance data, export info, pricing, ***real-time availability***, and everything else you need to make your selection today—for delivery as soon as tomorrow!

Model	Freq. Range (MHz)	Gain (dB)	P_{OUT} (dBm)	Price $ ea. (Qty. 20)
GVA-62+	10-6000	15	18	0.99
GVA-63+	10-6000	20	18	0.99

Mini-Circuits…we're redefining what VALUE is all about!

Mini-Circuits®
ISO 9001 ISO 14001 AS 9100
P.O. Box 350166, Brooklyn, New York 11235-0003 (718) 934-4500 Fax (718) 332-4661

YONI2® ***The Design Engineers Search Engine*** *finds the model you need, Instantly* • For detailed performance specs & shopping online see **minicircuits.com**

U.S. Patents 7739260, 7761442

IF/RF MICROWAVE COMPONENTS

New Products

Mixers

VENDORVIEW

Mini-Circuits MAC mixers employ a unique new design and a highly repeatable, tightly controlled, automated process that delivers industry-leading reliability at a remarkably affordable price. Schottky diode quads meeting the company's strict specifications are bonded to a multilayer integrated LTCC substrate, then hermetically sealed under a controlled atmosphere with gold-plated covers and eutectic AuSn solder. These passive, double-balanced mixers have been tested to MIL requirements for gross leak, fine leak, thermal shock, vibration, acceleration, mechanical shock, and HTOL, and are backed with a three-year guarantee.

Mini-Circuits,
www.minicircuits.com.

Four-Throw Switch

VENDORVIEW

MITEQ's ultra-broadband single-pole four-throw switch, model SW4-005400AN1NF, offers a wide frequency range of 0.5 to 40 GHz. This absorptive 40 GHz terminated switch has an insertion loss of only 7.5 dB maximum with an isolation of 60 dB minimum. This small, ultra-compact, wideband switch housing is available in both hermetic and non-hermetic packaging.

MITEQ,
www.miteq.com.

Fixed Attenuators

VENDORVIEW

Narda Microwave-East introduced the model 769A family of bidirectional coaxial fixed attenuators. All models in the 769A Series handle a maximum input power of 150 W average and 3 kW peak, have a maximum VSWR of 1.35:1 or less, weigh 3.3 lb. (1.5 kg), and have Type-N female connectors. Models with 3, 6 and 10 dB of attenuation have maximum attenuation deviation of ±0.4 dB to 2 GHz, and ±0.75 dB to 6 GHz. The 20 and 30 dB models have maximum attenuation deviation of ±0.5 dB to 2 GHz, and ±1 dB to 6 GHz.

Narda Microwave-East,
www.nardamicrowave.com/east.

Modulator/Phase Shifter

VENDORVIEW

Model PS-90-2040-SY is a miniature 0 to 180° bi-phase modulator/phase shifter with TTL control logic operating over a frequency range of 2856 MHz ±15 MHz. This model provides low loss of 1 dB maximum and offers a fast switching time of 50 nsec maximum. This model is designed to handle an input power level of 1 W. The unit measures 1.39" × 1.0" × 1.0". Other frequency ranges are available.

Planar Monolithics Industries,
www.pmi-rf.com.

Waveguide Isolator

Raditek's high power WR75 waveguide isolator is comprised of a circulator with a removable 400 W load. The load has small fins suitable for convection cooling. Standard specifications: 10.75 to 12.80 GHz, 0.3 dB insertion loss, 21 dB isolation, 1.22:1 VSWR, average power 400 W CW, peak power 2 Kilowatts, operating temperature 0 to 50°C. Circulator dimensions: 45 × 45 × 38.5 mm. Load dimensions: 180 × 75 × 75 mm.

Raditek,
www.raditek.com.

Symmetric Switch

VENDORVIEW

RFMD's new RFSW6131 is a GaAs PHEMT single-pole three-throw (SP3T) switch designed for use in cellular, 3G, LTE and other high performance communications systems. It offers a symmetric topology with excellent linearity and power handling capability, while also 3 and 5 V positive logic compatible. It features LF to 6000 MHz operation; low loss: 0.5 dB (2 GHz); isolation: 27 dB (2 GHz); high IP3: 56 dBm; P0.1 dB: 31 dBm (5 V, 2.2 GHz); and DFN, 1.5 × 1.5 mm package. It is currently available in production quantities. Pricing begins at $0.60 each for 1000 pieces.

RFMD,
www.rfmd.com.

SMA Switch

RLC Electronics' Micro Miniature SMA switch is a single-pole two-position type. The switch incorporates SMA connectors to allow high density packaging and excellent electrical performance through 26.5 GHz. The switch is available in failsafe and latching configurations with a choice of three different frequency ranges and three different coil voltages. It has a power rating of RF cold switching, an impedance of 50 Ω and an operating power of 25°C (mA nominal), 5 V DC at 310 mA, 12 V DC at 130 mA, and 28 V DC at 75 mA.

RLC Electronics Inc.,
www.rlcelectronics.com.

New Products

Receiving Coil

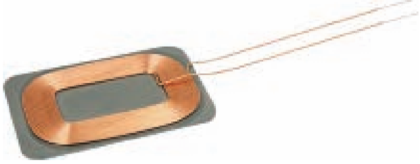

Vishay Intertechnology announced a new powdered-iron-based, WPC-compliant receiving coil for the wireless charging of 5 V portable electronics. Offering a durable construction and high permeability shielding, the new IWAS-3827EC-50 provides high efficiency greater than 70 percent for Rx applications to 10 W and is 33 percent smaller than the standard 48 × 32 mm IWAS-4832FF-50 Rx coil, with dimensions of 38 × 27 mm. As an alternative to Ferrite-based solutions the IWAS-3827EC-50 offers a magnetic saturation of 50 percent at 4000 gauss.

Vishay Intertechnology Inc.,
www.vishay.com.

USB Powered Switches

VENDORVIEW

The new Lab Brick product family has a 10 W power handling capability and offers reliable, high isolation, low power and low cost solid state switch products in both SPDT and SP4T configurations. The LSW Series Switches have manual, internal and external switch control capability and can be easily controlled and programmed directly from the included GUI or through the external control inputs. Easily programmable for ATE applications, the LSW Series Switches can also be used in WiMAX, 3G, LTE test platforms, and engineering and production test labs.

Vaunix Technology Corp.,
www.vaunix.com.

Amplifiers

GaN SSPA

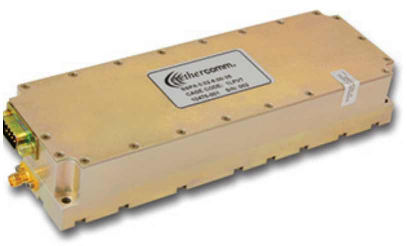

Aethercomm Inc. introduced a broadband, high power SSPA using GaN. This extremely large bandwidth operates from 20 to 6000 MHz. Model number SSPA 0.020-6.000-35 produces 20 to 80 W Psat typical across this frequency band. The amplifier design can be employed in high shock and vibration environments and is housed in a 2.5" (w) × 7.7" (l) × 1.4" (h) module. The SSPA 0.020-6.000-35 amplifier is designed for either pulsed or CW and is ideal for use in commercial and military platforms.

Aethercomm Inc.,
www.aethercomm.com.

Amplifiers

MILMEGA, a Teseq company, has introduced the new AS0728 product range. Designed, in response to customer demands, to cover the test requirements within the wireless testing frequency bands, these 700 MHz to 2.8 GHz amplifiers are available in 25, 50, 100 and 170 W P1dB power levels.

MILMEGA,
www.teseq.com.

Power Amplifier Modules

VENDORVIEW

Richardson RFPD introduced a pair of highly linear and efficient, fully-matched power amplifier modules designed for Picocell, Femtocell and Customer Premises Equipment (CPE) applications from ANADIGICS. Both devices are designed for WCDMA, HSDPA and LTE downlink air interfaces operating in the 2.11 to 2.17 GHz band. They are manufactured using an advanced InGaP HBT MMIC technology offering state-of-the-art reliability, temperature stability and ruggedness. The self-contained 7 × 7 × 1.3 mm surface mount packages incorporate RF matching networks optimized for output power, efficiency and linearity in 50 Ω systems.

Richardson RFPD Inc.,
www.richardsonrfpd.com.

Low Noise Amplifiers

VENDORVIEW

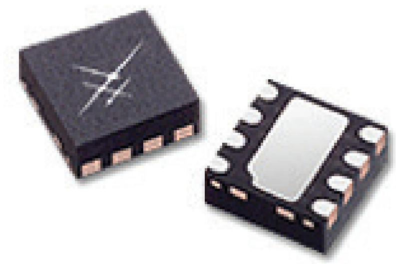

Skyworks introduces two new, enhancement mode LNAs that offer low noise figure, high linearity, and excellent return loss: The SKY67012-396LF (0.3 to 0.6 GHz) and SKY67013-396LF (0.6 to 1.5 GHz). On-die active bias design ensures consistent performance, enables unconditional stability, and simplifies external matching. These highly flexible and low power gallium arsenide PHEMT LNAs have a small form factor and very low current draw (5 mA) and wide input voltage range (1.8 to 5 V) capability.

Skyworks Solutions Inc.,
www.skyworksinc.com.

Power Amplifier Module

This wideband GaAs amplifier module is ideal for CW or pulsed applications. It is very linear and highly efficient. Due to several state-of-the-art circuits, this unit is highly immune

New Products

from damage due to any out of spec DC voltage conditions that may be applied. Its rugged construction guarantees fault-free operation in the most extreme environments. It features 5 W output power, 37 dB linear gain, rise and fall time < 1 usec, +12 V DC, 1.8 amps at 100 percent duty cycle, and is 5" × 2.5" × 0.51".

Triad RF Systems,
www.triadrf.com.

Software

RF Design Software

A new version of the LINC2 Pro RF and microwave design, synthesis and simulation software suite has recently been released by ACS. Version 2.72 release R adds many new component models to the program's extensive model library. These include more than 600 new capacitor models, 350 inductor models and a number of new active models including GaN power devices. The latest edition also offers enhanced schematic capture. Circuits can be entered manually or created automatically by a number of circuit synthesis modules.

Applied Computational Sciences (ACS),
www.appliedmicrowave.com.

Test Calibration Software

VENDORVIEW

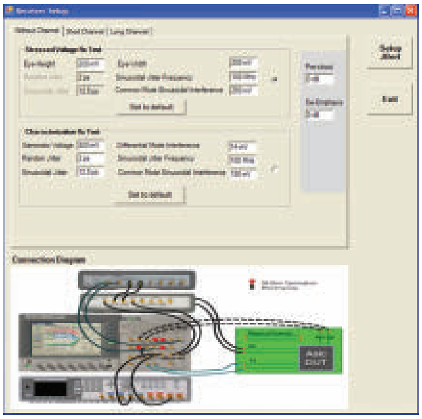

Agilent introduced its fully integrated PCI Express® (PCIe®) 3.0 receiver test calibration and transmitter test software. The software provides an integrated environment for calibrating the stressed voltage and stressed receiver eye using an Agilent J-BERT bit error-ratio tester, an Agilent 90000A-, Q- or X-Series oscilloscope, an Agilent pulse function generator and Agilent PCI Express 3.0 calibration test channels. The software provides a receiver signal calibration test suite that allows engineers to set up a J-BERT N4903B bit error-ratio tester for performing PCIe 3.0 jitter tolerance testing under the PCIe 3.0 base specification.

Agilent Technologies Inc.,
www.agilent.com.

Development Software

With TI's KeyStone-based TMS320C665x multicore digital signal processors (DSP), developers more effectively meet the specialized gateway challenges of matching voice coding techniques, processing tone and signaling messaging, distinguishing facsimile from voice, converting legacy circuit switched connections to IP and managing and reporting voice quality. The TMS320C6654 DSP at 850 MHz supports up to 64 channels of G.729AB, while the TMS320C6655 DSP at 1 GHz supports up to 128 channels of G.729AB. The TMS320C6657 DSP at 1.25 GHz provides significant head room for applications requiring added density.

Texas Instruments Inc.,
www.ti.com.

Test Equipment

Digital Radio Test System

Aeroflex introduced the 3550 digital radio test system featuring a color touch-screen. It is lightweight (8.3 lbs. including battery) for field-testing of analog, DMR, P25, NXDN, and dPMR systems, and features 4.5 hours of continuous operation with its internal battery. Uniquely, the 3550 test system allows the user to test all aspects of the radio system — the transmitter, receiver, cables, and antennas — with powerful features typically found only in bench top equipment. It has an operating range of -0 to +50°C.

Aeroflex Inc.,
www.aeroflex.com.

Simulation Models

Modelithics announced new simulation models for Coilcraft inductor families 132SM, 1812SMS, 1508/2508, 0906/1606 and 0806SQ/0807SQ/0908SQ. The highly-accurate measurement-based models are substrate and part-value scalable and support EM simulation. Datasheets give detailed information for each model, which are supported in Agilent ADS, Genesys and AWR Microwave Office. For more

New Products

information, visit: www.modelithics.com/mvp/CoilCraft/.
Modelithics Inc.,
www.modelithics.com.

Subsystems

USB Controlled Tuner

The diminuSys DWT-P909 is a compact, high dynamic range synthesized microwave tuner, spanning the 0.9 to 9 GHz band, with simple USB control, simultaneous non-inverting outputs at 900, 120 and 21.4 MHz, instantaneous bandwidth of 200 MHz and sub-octave preselection. Gain is adjustable from –40 to +20 dB with unity gain third order intercept point of +17 dBm. The DWT-P909 fulfills wideband tuning requirements for signal processors at popular IF frequencies and extends legacy receiver coverage to 9 GHz.
diminuSys,
www.diminusys.com.

Sources

Coherent Frequency Synthesizer

Elcom's UFS 18 low phase noise, coherent frequency synthesizer can now provide wideband coherent chirp waveforms at frequencies up to 18 GHz. Modulation bandwidth of

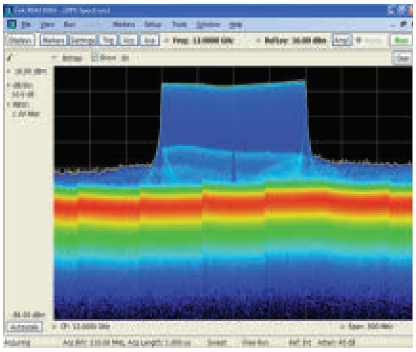

±100 MHz is possible. An IQ modulator capable of operating at a fixed frequency LO of 3 GHz and a baseband arbitrary AWG with IQ outputs is also required. With the new wideband IF Option 113A, any baseband waveform with a spectrum within DC to ±100 MHz will appear with high accuracy as modulation on the synthesizer's carrier frequency.
FEI-Elcom Tech,
www.fei-elcomtech.com.

GaAs MMIC Doubler

M/A-COM Tech introduced a GaAs MMIC doubler for VSAT applications. The XX1010-QT is an active doubler in a RoHS compliant

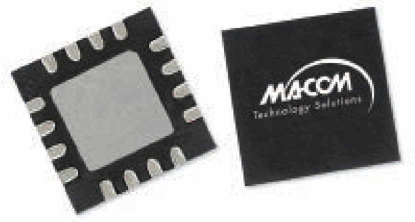

3 × 3 mm 16-lead plastic QFN package that delivers +20 dBm output saturated power (Pout) and 35 dBc fundamental suppression. Using a GaAs PHEMT process, the XX1010-QT covers the 14.625 to 15/29.25 to 30 GHz frequency bands and integrates a gain stage, doubler and driver amplifier into a single device. The device has a self-bias configuration, requiring only a positive 5 V supply.
M/A-COM Technology Solutions Inc.,
www.macomtech.com.

Signal Sources

The XMN and XMNP Series of 200 MHz to 3 GHz ultra low noise multiplied signal sources integrate an OCXOF with a low-noise frequency multiplier to give an output with a low phase noise floor – typically equivalent to –183 dBc/Hz at the oscillator's frequency. For example, the phase noise floor of a 1.2 GHz output derived from 120 MHz is typically –163 dBc/Hz.
Pascall Electronics Ltd.,
www.pascall.co.uk.

Oven Controlled Crystal Oscillator

Rakon launched a new ultra low noise crystal oscillator with unparalleled phase noise performance. The LNO 100 series at 100 MHz offers outstanding guaranteed phase noise levels of –165 dBc/Hz at 1 KHz and –178 dBc/Hz at 10 KHz. The LNO also provides rapid warm-up, excellent temperature stability and low g-sensitivity. Available in various sizes (from 51 × 51 × 25 mm down to 25 × 25 × 12 mm), in SMD or through hole packages and with SMA connectors.
Rakon,
www.rakon.com.

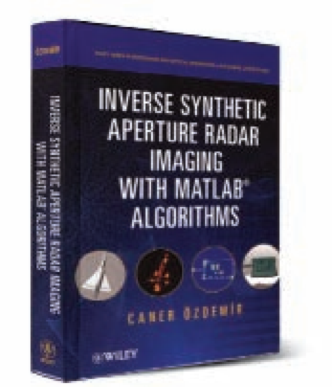

Inverse Synthetic Aperture Radar Imaging With MATLAB Algorithms

Caner Özdemir

As the author states in the preface, inverse synthetic aperture radar (ISAR) has been proven to be a powerful signal processing tool for imaging moving targets usually on the 2D down-range cross-range plane. ISAR imagery plays an important role especially in military applications such as target identification, recognition and classification. *Inverse Synthetic Aperture Radar Imaging With MATLAB* provides the conceptual description of ISAR imagery and the explanation of basic ISAR research. The book begins by covering Fourier theory, which plays an important role in radar imaging, and then covers the basics of radar and relates them to ISAR. After covering SAR, it then steps into ISAR imaging with associated MATLAB codes. Then more detailed topics related to ISAR are covered along with imaging applications at the end.

The primary audience for this book will be graduate students and other interested researchers in related fields but is also useful to engineers and scientists working in radar research and development or related industries. Examples in MATLAB are provided for the presented algorithms in order to provide a better understanding of the concepts that are covered. The MATLAB files are available on an ftp site provided in the book. This is a highly focused book and is very useful to those that are involved in this specific field of study or research and development.

To order this book, contact:

Wiley Customer Care Center – Consumer Accounts
10475 Crosspoint Blvd.
Indianapolis, IN 46256
(877) 762-2974

400 pages, $115
ISBN: 978-0-470-28484-1

ARFTG 80th Microwave Measurement Conference

Advances in Wireless Communication Test & Measurements

Hilton San Diego Bayfront Hotel, November 27th – 30th, 2012

www.arftg.org

Rusty Myers **Conference Chair**
Maury Microwave Corp.
909-204-3344
rmyers@maurymw.com

Ali Boudiaf **Technical Program Chair**
Maury Microwave Corp.
909-204-3353
aboudiaf@maurymw.com

Gayle Collins **Local Host**
MaXentric Technologies, LLC
858-605-6337
gcollins@maxentric.com

Patrick Roblin **NIST Short Course Chair**
Ohio State University
614-292-0998
roblin@ece.osu.edu

Antonio Raffo **Workshop Chair - Wireless Communications**
University of Ferrara
+39 0532 974947
antonio.raffo@unife.it

Mitch Wallis **Workshop Chair - RF Nanoelectronics**
NIST
303-497-5089
mwallis@boulder.nist.gov

Ex-Officio Members

Jim L. Taylor Executive Secretary

ARFTG Conference

ARFTG will hold its 80th Microwave Measurement Conference at the Hilton San Diego Bayfront Hotel in San Diego, CA, Nov 27th – 30th, 2012. The four-day symposium consists of the following:

- One-and-one-half day ARFTG Microwave Measurement Conference
- One-and-one-half day NIST Short Course on Microwave Measurements
- One-half day Workshop on "Design for wireless communications from transistor to system-level characterization"
- One-half day Workshop on "Measurement Techniques for RF Nanoelectronics"
- NVNA Users Forum
- Exhibits and interactive poster sessions

You can register for the conference, courses and workshops at: http://www.arftg.org

At the ARFTG Conference, there will be invited papers and submitted technical papers and posters of a high standard, describing original work on topics related to test and measurements of Wireless Communication applications, non-linear measurement and modeling techniques, calibration and measurement techniques for RF and microwave circuits and systems, as well as measurement techniques for RF Nanotechnologies.

NIST Short Course

NIST Short Course with measurement topics related to the ARFTG Conference them
Chair: Patrick Roblin – Tuesday and Wednesday, Nov 27th and Nov 28th, 2012 – Topics include:

- Principles of Power and Noise Measurements and Uncertainties
- VNA Measurements and On Wafer S-Parameter Measurements and Uncertainties
- High Speed Oscilloscope, Spectrum Analyzer and Vector Signal Analyzer Measurements
- Wireless Figures of Merit, Wireless Standards and Characterization of Envelope Tracking and Polar PAs
- Large Signal, CW and Pulsed NVNA, Broadband, Pulsed and Mixed-signal Load-pull Measurements

Workshops

Design for wireless communications: from transistor to system-level characterization
Chair: Antonio Raffo - Wednesday, November 28th, 2012 – Topics include:

- Nonlinear transistor characterization.
- Nonlinear transistor modeling based on nonlinear measurements.
- Power amplifiers design and characterization: linearity vs. efficiency trade-off.
- System-level characterization of wireless systems.

Measurement Techniques for RF Nanoelectronics
Chair: T. Mitch Wallis - Friday, November 30th, 2012 – Topics include:

- RF Nanoelectronics based on graphene and carbon nanotubes.
- Metrology of nanoscale systems for RF applications.
- Near-field scanning microwave microscopy.
- Modeling of nano-structures and nano-devices at RF frequencies.

Poster Session and Exhibits

The 80th ARFTG Conference will feature interactive posters sessions with opportunities to speak one-on-one with the authors.

The Conference also offers an outstanding exhibition with demonstrations from the leading RF & Microwave instrument and components manufacturers with an excellent opportunity to network with these industry measurement experts.

For opportunities to exhibit, please contact our Exhibits Chair (exhibits@arftg.org).

IEEE www.arftg.org MTT-S

Advertising Index

Sales Representatives

Microwave Journal
Frequency Matters.

Carl Sheffres, Publisher

Ed Kiessling, Traffic Manager

Eastern and Central Time Zones
Chuck Boyd
Northeast Reg. Sales Mgr.
(New England, New York, Eastern Canada)
685 Canton Street
Norwood, MA 02062
Tel: (781) 769-9750
FAX: (781) 769-5037
cboyd@mwjournal.com

Michael Hallman
Eastern Reg. Sales Mgr.
(Mid-Atlantic, Southeast, Midwest)
4 Valley View Court
Middletown, MD 21769
Tel: (301) 371-8830
FAX: (301) 371-8832
mhallman@mwjournal.com

Pacific and Mountain Time Zones
Brian Landy
Western Reg. Sales Mgr.
(CA, AZ, OR, WA, ID, NV, UT, NM, CO, WY, MT, ND, SD, NE & Western Canada)
144 Segre Place
Santa Cruz, CA 95060
Tel: (831) 426-4143
FAX: (831) 515-5444
blandy@mwjournal.com

International Sales
Richard Vaughan
International Sales Manager
16 Sussex Street
London SW1V 4RW, England
Tel: +44 207 596 8742
FAX: +44 207 596 8749
rvaughan@horizonhouse.co.uk

Germany, Austria, and Switzerland (German-speaking)
WMS.Werbe- und Media Service
Brigitte Beranek
Gerhart-Hauptmann-Street 33, D-72574 Bad Urach
Germany
Tel: +49 7125 407 31 18
FAX: +49 7125 407 31 08
bberanek@horizonhouse.com

Israel
Oreet Ben Yaacov
Oreet International Media
15 Kineret Street
51201 Bene-Berak, Israel
Tel: +972 3 570 6527
FAX: +972 3 570 6526
obenyaacov@horizonhouse.com

Korea
Young-Seoh Chinn
JES Media International
2nd Floor, ANA Bldg.
257-1, Myungil-Dong
Kangdong-Gu
Seoul, 134-070 Korea
Tel: +82 2 481-3411
FAX: +82 2 481-3414
yschinn@horizonhouse.com

Japan
Katsuhiro Ishii
Ace Media Service Inc.
12-6, 4-Chome,
Nishiiko, Adachi-Ku
Tokyo 121-0824, Japan
Tel: +81 3 5691 3335
FAX: +81 3 5691 3336
amskatsu@dream.com

China
Michael Tsui
ACT International
Tel: 86-755-25988571
Tel: 86-21-62511200
FAX: 86-10-58607751
michaelT@actintl.com.hk

Hong Kong
Mark Mak
ACT International
Tel: 852-28386298
markm@actintl.com.hk

MWJ Puzzler

Government and Military Electronics

ANSWERS AVAILABLE ONLINE AT MWJOURNAL.COM

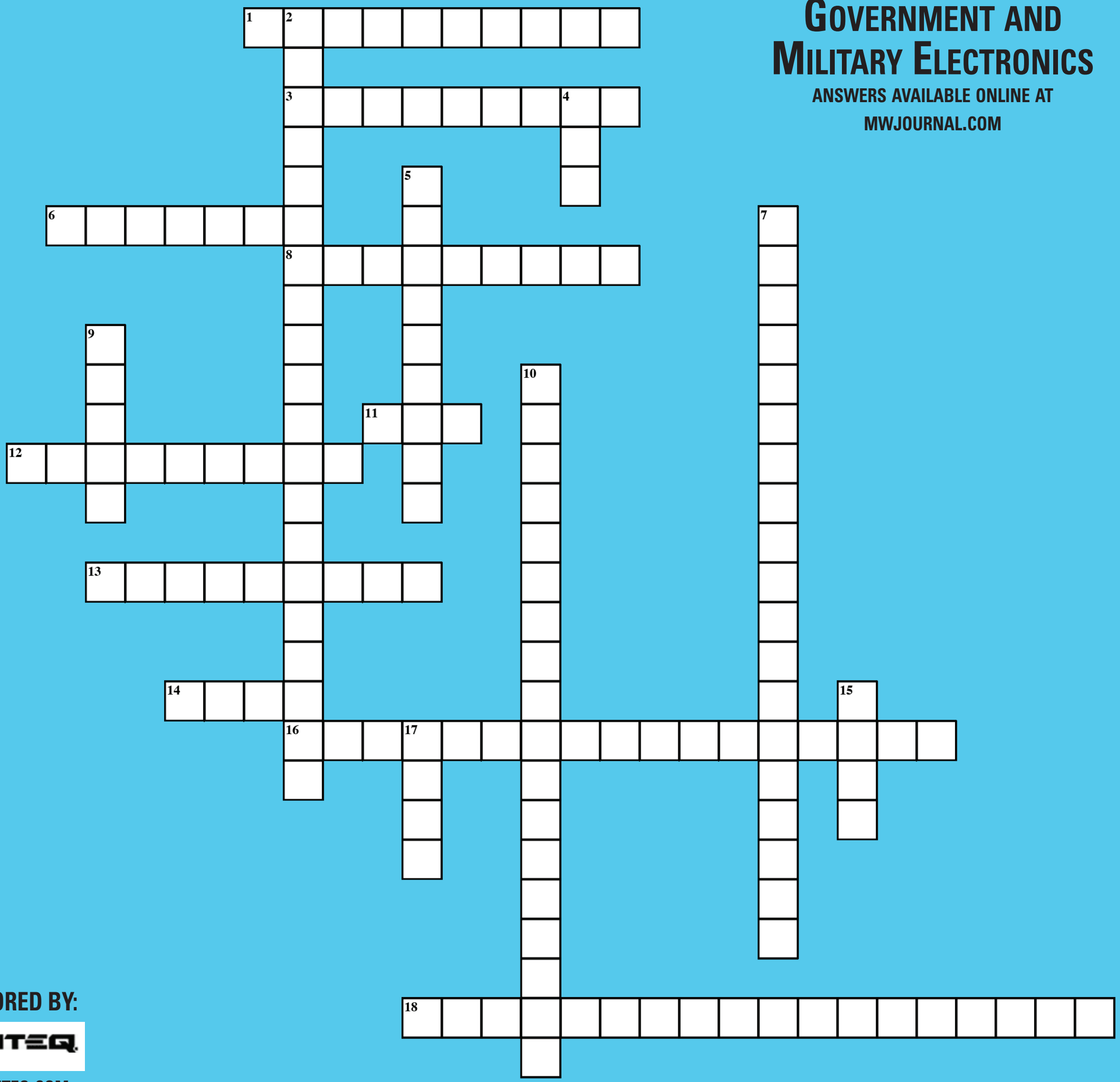

Across

1 OTA (3 words)

3 Type of interference resulting from another transmitter operating in the same spectrum as the victim receiver (2 words)

6 Type of device typically used to protect a receiver from high power signals

8 A graphical representation of the mixer spur equation is shown in a ________ __________ (2 words)

11 Short for passive intermodulation

12 Short for transmit/receive modules (2 words)

13 Short for active electronically scanned array radar (2 words)

14 Vertical interconnections by a solderless-method can by made using _____ buttons

16 EW (2 words)

18 SIGINT (2 words)

Down

2 VSA (3 words)

4 Error Vector Magnitude

5 Signals whose frequencies are an integral multiple of the frequency of the transmitted signal

7 Linking individual hardware and software test modules together to emulate standard instruments in a compact form factor (2 words)

9 Signals created by a transmitter that are outside of the frequency intended

10 The _______ _______ receiver builds upon the spectrum analyzer by adding a preselection filter at the RF input and analog IF filters, in the final IF (2 words)

15 Short for displayed average noise level

17 Commercial Off The Shelf

Mixer Solutions

IMAGE REJECTION MIXERS

3 YEAR WARRANTY

Model Number	RF/LO Frequency (GHz)	Conversion Loss (dB) Max.	Image Rejection (dB) Min.	LO-to-RF Isolation (dB) Min.
IMAGE REJECTION MIXERS				
IRM0204(*)C2(**)	2 - 4	7.5	18	20
IRM0408(*)C2(**)	4 - 8	8	18	20
IRM0812(*)C2(**)	8 - 12	8	18	20
IRM1218(*)C2(**)	12 - 18	10	18	20
IRM0208(*)C2(**)	2 - 8	9	18	18
IRM0618(*)C2(**)	6 - 18	10	18	18
IR1826NI7(**)	18 - 26	10.5	18	20
IR2640NI7(**)	26 - 40	12	18	20

Model Number	RF/LO Frequency (GHz)	Conversion Loss (dB) Max.	Balance Phase (±Deg.) Typ./Max.	Balance Amplitude (±dB) Typ./Max.	LO-to-RF Isolation (dB) Min.
I/Q DEMODULATORS					
IRM0204(*)C2Q	2 - 4	10.5	7.5/10	1.0/1.5	20
IRM0408(*)C2Q	4 - 8	11	7.5/10	1.0/1.5	20
IRM0812(*)C2Q	8 - 12	11	5/7.5	.75/1.0	20
IRM1218(*)C2Q	12 - 18	13	10/15	1.0/1.5	20
IRM0208(*)C2Q	2 - 8	12	7.5/10	1.0/1.5	18
IRM0618(*)C2Q	6 - 18	13	10/15	1.0/1.5	18
IR1826NI7Q	18 - 26	13.5	10/15	1.0/1.5	20
IR2640NI7Q	26 - 40	15	10/15	1.0/1.5	20

Over 1500 Models!

SSB UPCONVERTERS OR I/Q MODULATORS

Model Number	RF Frequency (GHz)	Conversion Loss (dB) Max.	Carrier Suppression (dBc) Min.	Carrier Suppression Carrier - Fundamental IF (dBc) Min.
IF DRIVEN MODULATORS				
SSM0204(*)C2MD(**)	2 - 4	9	20	20
SSM0408(*)C2MD(**)	4 - 8	9	20	18
SSM0812(*)C2MD(**)	8 - 12	9	20	20
SSM1218(*)C2MD(**)	12 - 18	10	20	18
SSM0208(*)C2MD(**)	2 - 8	9	20	18
SSM0618(*)C2MD(**)	6 - 18	12	20	18

Over 1000 Models!

For Carrier Driven Modulators, please contact MITEQ.

MODEL NUMBER OPTION TABLE

(*) Add Letter	LO/IF Power Range	P1 dB C.P. (dBm) (Typ.)	(**) Add Letter	IF FREQUENCY OPTION (MHz)
L	10 - 13 dBm	+6	A	20 - 40
M	13 - 16 dBm	+10	B	40 - 80
H	17 - 20 dBm	+15	C	100 - 200
			Q	DC - 500 (I/Q)

ISO 9001 Registered ANAB AS9100 Registered

RoHS compliant Available

For additional information or technical support, please contact our Sales Department at (631) 439-9220 or e-mail components@miteq.com

MITEQ

100 Davids Drive, Hauppauge, NY 11788
(631) 436-7400 FAX: (631) 436-7430
www.miteq.com

FieldFox Microwave Combination Analyzers

Agilent Technologies

FieldFox Microwave Spectrum Analyzers

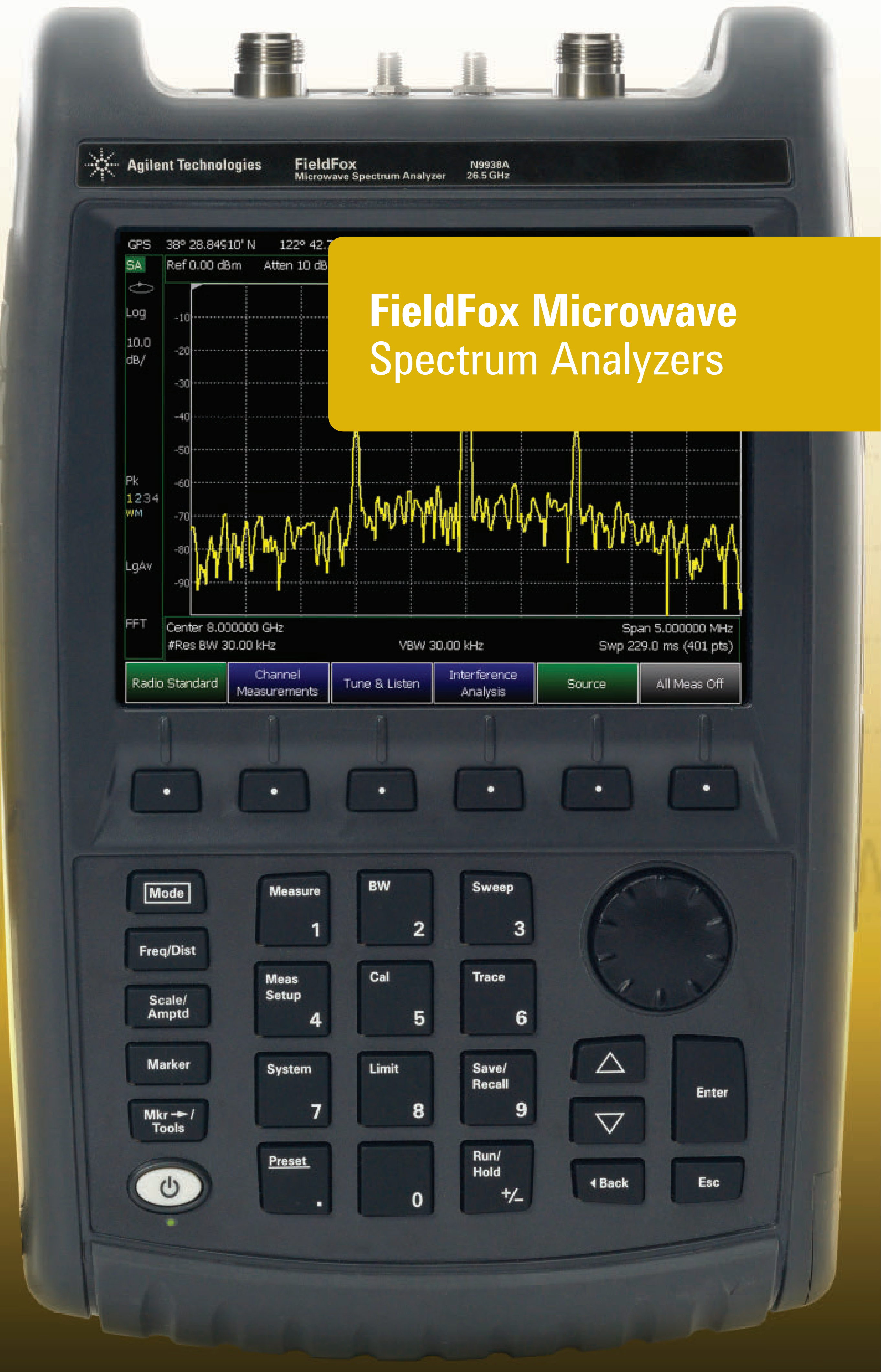

Add the world's most precise handheld microwave analyzer to your kit

Cable and antenna analyzer

- Distance-to-fault, return loss, and cable loss
- Integrated QuickCal for calibration – no cal kit required
- Immediate distance-to-fault measurements with CalReady
- 30 kHz to 26.5 GHz

Vector network analyzer

- S11, S21, S12, S22, magnitude and phase
- Guided Calibration Wizard, full 2-port cal, waveguide calibration
- Superior dynamic range of 94 dB and ± 0.004 dB of trace noise
- 30 kHz to 26.5 GHz

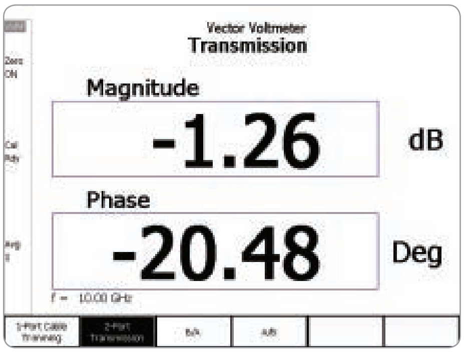

Vector voltmeter

- Cable trimming
- Phase shift and electrical length measurements
- A/B and B/A ratio measurements
- 30 kHz to 26.5 GHz

Designed for the toughest working conditions

Rugged & reliable

- Dust-free design with no fans or vents provides measurement stability in harsh environments
- All FieldFox analyzers come standard with a 3-year warranty

Field-proof

- Bright, low-reflective display, and backlit keys for easy viewing in direct sunlight or darkness
- Water-resistant; withstands salty, humid environments

MIL-spec durability

- MIL-PRF-28800F Class 2
- MIL-STD-810G, Method 511.5, Procedure I, operation in explosive environments (type tested)

Portable

- Compact and light weight (3.0 kg or 6.6 lbs.), long battery life (3.5 hrs)
- Wide operating temperature (-10 to +55 °C, 14 to 131 °F)

FieldFox	RF & microwave combination analyzers	Microwave vector network analyzers	Microwave spectrum analyzers
Model number	N9913/4/5/6/7/8A	N9925/6/7/8A	N9935/6/7/8A
Maximum frequency range	4, 6.5, 9, 14, 18, 26.5 GHz	9, 14, 18, 26.5 GHz	9, 14, 18, 26.5 GHz
Cable and antenna analyzer	✔	✔	VSWR and reflection
Vector network analyzer	✔	✔	
Spectrum analyzer, interference analyzer	✔		✔
Tracking generator, independent source	✔		✔
Vector voltmeter	✔	✔	
Built-in power meter	✔	✔	✔
Power meter with USB sensor	✔	✔	✔

Get Agilent-quality microwave measurements in the field

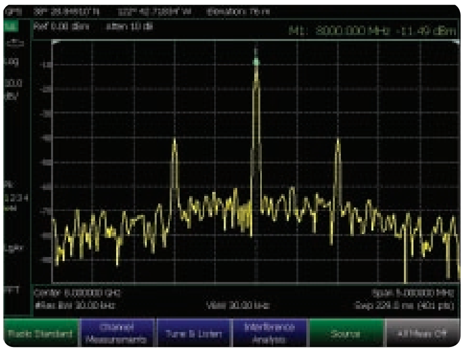

Spectrum analyzer

- Unprecedented ± 0.5 dB amplitude accuracy (full band) with InstAlign – no warm up required
- Interference analysis with spectrogram, waterfall display, record and playback
- Full-band tracking generator and preamplifier
- 5 kHz to 26.5 GHz

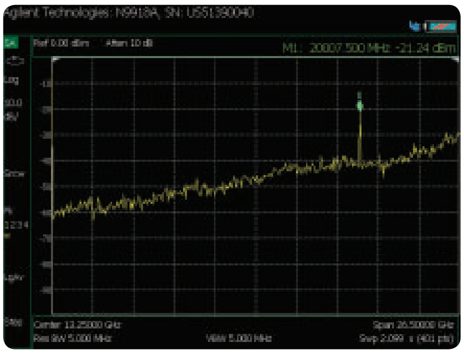

Tracking generator/independent source

- CW and swept signal source
- Output power: -45 dBm to +2 dBm, in 1 dB steps
- 5 kHz to 26.5 GHz

Built-in power meter

- Easy to view analog and digital display
- ± 0.5 dB accuracy with InstAlign
- 100 kHz to 26.5 GHz

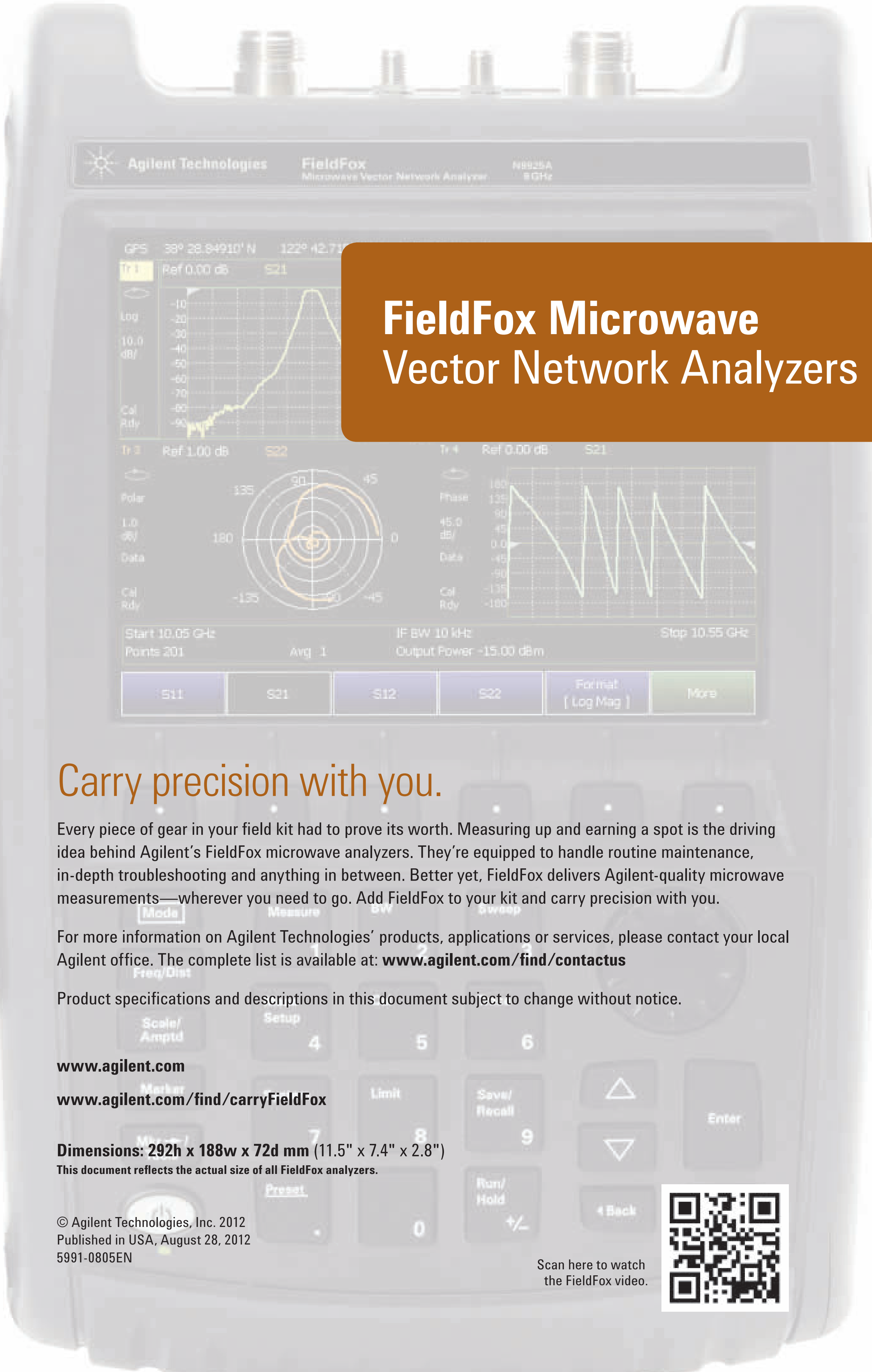

FieldFox Microwave
Vector Network Analyzers

Carry precision with you.

Every piece of gear in your field kit had to prove its worth. Measuring up and earning a spot is the driving idea behind Agilent's FieldFox microwave analyzers. They're equipped to handle routine maintenance, in-depth troubleshooting and anything in between. Better yet, FieldFox delivers Agilent-quality microwave measurements—wherever you need to go. Add FieldFox to your kit and carry precision with you.

For more information on Agilent Technologies' products, applications or services, please contact your local Agilent office. The complete list is available at: **www.agilent.com/find/contactus**

Product specifications and descriptions in this document subject to change without notice.

www.agilent.com

www.agilent.com/find/carryFieldFox

Dimensions: 292h x 188w x 72d mm (11.5" x 7.4" x 2.8")
This document reflects the actual size of all FieldFox analyzers.

Published in USA, August 28, 2012
5991-0805EN

Scan here to watch
the FieldFox video.